Novel Role and Regulation of the WASP protein

By Clelia Amato

BSc (Hons), MSc

Submitted in fulfilment of the requirements
for the degree of Doctor of Philosophy

CRUK Beatson Institute
College of Medical, Veterinary and Life Sciences
University of Glasgow

March 2018

“I willed,
I always willed,
and I passionately willed.”

“Volli,
e volli sempre,
e fortissimamente volli.”

- Vittorio Alfieri -

To Natalia,

for teaching us that it's never too late to make happy memories.

A Natalia,

per averci insegnato che non é mai troppo tardi per creare ricordi felici.

Abstract

WASP is a conserved actin nucleation-promoting factor (NPF) that drives the internalisation of clathrin-coated pits (CCPs) in *Dictyostelium*. This role has been maintained throughout evolution, as suggested by the fact that WASP orthologues in yeasts, *Drosophila* and mammals are also involved in clathrin-mediated endocytosis (CME). Whether WASP is crucial for other cellular functions is unclear. Similarly, the molecular details of WASP regulation are not fully clarified. Pioneering studies utilised *in vitro* approaches and proposed that Rho GTPases (Rac or Cdc42), phospholipids and SH3 domain containing-proteins play a role in the activation of its mammalian orthologue. However, whether their contribution is conserved across evolution and determining in living cells remains to be addressed.

Our lab has recently generated a *Dictyostelium* WASP knockout strain and uncovered a role for WASP in maintenance of cell polarity. Indeed, WASP knockout cells fail to restrict active Rac at the leading edge and aberrantly accumulate it at the rear. Furthermore, it was revealed that WASP is required for *Dictyostelium* to proliferate in suboptimal growth conditions. We have extended these observations and aimed to determine the underlying molecular mechanisms. Furthermore, we have sought to clarify the details of WASP regulation in living cells, starting by addressing the importance of Rho GTPases for its functionality.

Here we provide evidence suggesting that WASP requires a direct interaction with active Rac to spatially confine the GTPase and maintain cell polarity. Indeed, mutations in the WASP CRIB (Cdc42 and Rac interacting/binding) motif that prevent WASP/Rac interaction cause cells to retain active Rac at the rear during migration and at the cleavage furrow during cytokinesis.

The generation of WASP CRIB mutants allowed us to test whether Rho GTPases play a central role in WASP activation. We report here that the presence of a functional CRIB motif is not required for WASP to localise on CCPs and to trigger the formation of actin filaments. This result suggests that Rho GTPases do not represent the major (or the only) route for WASP activations in living cells.

Lastly, we have started to explore the role of WASP in starvation survival. We demonstrate that WASP is required for *Dictyostelium* survival under amino acid-depleted conditions, and provide a number of evidence suggesting that it may have a role in autophagy. For instance, we show here that WASP co-localises

with known autophagosomal markers within large multilobate structures. Moreover, we point out that WASP harbours a putative LIR (LC3-interacting) region, and may therefore be able to interact with core components of the autophagic machinery.

Table of contents

List of figures

List of movies

Movie 1: Localisation of GFP-Rac1A in wild type *Dictyostelium* cells (AD7_6) migrating towards a source of chemoattractant. Cells were visualised by super-resolution microscopy. This movie refers to figure 3.2.

Movie 2: Localisation of clathrin (clathrin light chain-mRFPmars) and Rac (GFP-Rac1A) in migrating wild type *Dictyostelium* cells (AD7_6). Cells were visualised by TIRF microscopy. This movie refers to figure 3.3.

Movie 3: Localisation of the active Rac marker (pakB CRIB-mRFPmars2, shown in magenta) in *Dictyostelium* WASP knockout cells (*wasA*-, AD7_1) expressing GFP-WASP (left panel, green channel not shown), GFP-ΔCRIB WASP (middle panel, green channel not shown) or GFP-**CRIB WASP (right panel, green channel not shown). Migrating cells were visualised by super-resolution microscopy. The yellow asterisk indicates the trailing edge of the cells at the start of the timelapse. This movie refers to figure 3.7.

Movie 4: Effect of the expression of GFP-G12V Rac1A (dominant active) in *Dictyostelium* wild type (*wasA*+, AD7_6) left panel) and WASP knockout cells (*wasA*-, AD7_1, right panel). Cells were imaged after 8 hour from doxycycline treatment by super-resolution microscopy. This movie refers to figure 3.11.

Movie 5: Effect of the Rac inhibitor (EHT1864) on WASP dynamics. WASP knockout cells (*wasA*-, AD7_1) expressing GFP-WASP were treated with high doses of Rac inhibitor, and imaged by super-resolution microscopy. This movie refers to figure 4.4.

Movie 6: Clathrin and WASP dynamics in *Dictyostelium* WASP knockout cells (*wasA*-, AD7_1) expressing GFP-WASP (rescue) and CLC-mRFPmars. The solid white square indicates an example of clathrin-coated pit internalisation following WASP recruitment (occurring at 6 min, 36 sec). Cells were imaged by TIRF microscopy. This movie refers to figure 4.6 A.

Movie 7: Clathrin and ΔCRIB WASP dynamics in *Dictyostelium* WASP knockout cells (wasA-, AD7_1) expressing GFP- ΔCRIB WASP and CLC-mRFPmars. The solid white squares indicate two examples of clathrin-coated pits that fail to be internalised despite recruitment of the CRIB-mutated WASP (visible in both cases at 3 min, 0 sec). Cells were imaged by TIRF microscopy. This movie refers to figure 4.7 C.

Movie 8: Actin filaments formation on *puncta* enriched in wild type WASP and CRIB-mutated WASP. *Dictyostelium* WASP knockout cells (*wasA*-, AD7_1) expressing GFP-WASP and Lifeact-mRFPmars2 (top three panels) or GFP-**CRIB WASP and Lifeact-mRFPmars2 (bottom three panels) were visualised by super-resolution microscopy during chemotaxis. The white asterisk indicates the trailing edge of the cells at the beginning of the timelapse. This movie refers to figure 4.11.

Movie 9: Existence of clathrin-negative and clathrin-positive WASP *puncta*. *Dictyostelium* clathrin light chain knockout cells (*clc*-) expressing GFP-WASP and CLC-mRFPmars were imaged using TIRF microscopy. The solid white square indicates an example of clathrin-coated pit internalised after recruitment of WASP (visible at 1 min, 14 sec). The solid yellow square indicates an example of WASP *puncta* (visible at 1 min, 36 sec) that does not occur on a pre-existing clathrin spot. This movie refers to figure 5.3 A and B.

Movie 10: Localisation of GFP-Rac1A and mRFPmars-Atg18 in migrating wild type *Dictyostelium* cells (AD7_6) visualised by super-resolution microscopy. The white asterisk indicates the trailing edge of the cell at the beginning of the timelapse. This movie refers to figure 5.8 A.

Movie 11: Localisation of GFP-Rac1A and mRFPmars-Atg18 in wild type *Dictyostelium* cells (AD7_6) subjected to mechanical stress in order to induce autophagy. Cells were visualised by super-resolution microscopy. This movie refers to figure 5.8 B.

Acknowledgement

When I first met my supervisor, Robert Insall, I was a prospective student with little experience with microscopy, cloning and actin dynamics; what I really had to offer was my enthusiasm and my commitment. I want to acknowledge Robert for seeing beyond my lack of experience and for giving me the chance to learn from him. I also want to thank him for caring for my development as a scientist, for valuing my opinion even when it did not match his own, for giving me the freedom to follow my intuition and scientific curiosity. If I had to start my PhD again, I would still choose to do it in his lab.

I would like to express my most sincere gratitude to Peter Thomason for being there every step of the way, for witnessing my achievements and failures with an unceasing willingness to teach me. I wish to every young scientist the luck I have had in meeting a researcher like him.

I want to acknowledge every member of the Insall lab, current and former. A very special thank goes to Andrew Davidson and Jose Batista for welcoming me in the lab: I will always remember our long chats about science and always look forward to some more. Thanks to Luke Tweedy and Matt Neilson for making numbers easier to understand, and to Douwe Veltman and Jason King for all the cool things they have done in and for the Insall lab.

Thanks to Laura Machesky and her group for teaching me that research comes in different flavours, and that accepting other people's perspectives makes us better scientists.

Thanks To Karen Blyth for her kindness and sense of humanity, the greatest support that a PhD advisor could have possibly ever given to me.

Thanks to Dave Bryant for his help and encouragement, it meant a lot to me.

Thanks to those who work behind the scenes. Margaret O'Prey and BAIR staff for teaching me microscopy. Andrew Keith and molecular services people for all the mini and maxi preps they helped me with over the years! Central services people for making sure that it was all set for another day of work; behind every successful experiment is also their dedicated work.

Thanks to Kirsteen Campbell for dragging me into the public engagement world. I did not know how much it would have meant to me as a scientist and as a person, and how much I would have enjoyed it!

Thanks to all the amazing people I have met along the way. Evangelos Giampazolias, for the deep and rare understanding we have of one another.

Evdokia Michalopoulou, for her warm and kind heart. Emma Woodham, for all the thoughtful attentions that made me feel welcomed. Nikki Paul, for her soothing attitude. Francesca Patella, for her tireless listening skills. I want to thank Loïc Fort for facing with me every phase of this PhD, from interviewing to thesis writing, and for showing me that no difference between two people is too great to be unbridgeable.

A special thank is for Olivia Susanto, for being next to me during the happiest and most difficult moments of the past four years, and pretty much for all of those in between; her friendship is one of the greatest blessings I have ever had.

A heartfelt thank goes to Licia Di Gregorio, for teaching me what being a Friend means. I want to aknowkledge Silvia Cottone, Zara Lombardi, Lucio Riccardi and Mario Pica for all the memories we share, but most importantly for the confidence of a bond that does not fear the miles. Thanks to Giulia Coniglio, because some ties simply cannot be broken.

Thanks to Anna Maria, Vera and my entire great family for their affection and support. Thanks to those I have loved and lost.

I want to acknowledge Lilla Barbera and Michele Corsentino for gifting me with their most precious gift, and for the love and encouragement they have given us over the years.

I want to thank my Dad, Nino, and I want to do it twice: for loving me more than words could ever express, and for letting me go nevertheless.

Thanks to my Mum, Sina, for teaching me the importance of a smile, and because her love is the most powerful weapon against any fear of failure.

Thanks to my Brother, Nello, for showing me how deep love can be and how much you can care for someone’s happiness more than you care for your own.

Thanks to Kiko, my soul mate, my best buddy, my most truthful mirror, the thread that gets me out of every labyrinth. Thanks for keeping my dreams and selflessly encouraging me to pursue them.

Ringraziamenti

La prima volta in cui ho incontrato il mio supervisor, Robert Insall, ero una candidata con poca esperienza in microscopia, clonaggio molecolare e dinamiche di actina. Le uniche cose che avevo da offrire erano il mio entusiasmo e la mia dedizione. Voglio ringraziare Robert per aver guardato al di là della mia inesperienza e per avermi dato l'opportunità di imparare da lui. Voglio ringraziarlo anche per avere avuto a cuore la mia crescita come ricercatrice, per aver dato valore alle mie opinioni anche quando non le ha condivise, per avermi dato la libertà di seguire le mie intuizioni e la mia curiosità scientifica. Se dovessi ricominciare il mio dottorato da capo sceglierei di farlo ancora nel suo laboratorio.

Vorrei esprimere la mia più sincera gratitudine a Peter Thomason per essere stato a mio fianco durante l'intero percorso di dottorato, per aver assistito ad ogni mio successo e fallimento con la sua instancabile voglia di insegnare. Auguro ad ogni giovane ricercatore la fortuna che ho avuto io nell'incontrare uno scienziato come lui.

Voglio ringraziare tutti i membri del laboratorio Insall, presenti e passati. Un ringraziamento speciale va ad Andrew Davidson e Jose Batista per avermi accolto nel lab: mi ricorderò sempre delle nostre lunghe chiaccherate scientifiche, e aspetterò con ansia che ce ne siano altre. Grazie a Luke Tweedy e Matt Neilson per aver reso i numeri meno complicati, e a Douwe Veltman e Jason King per tutte le cose fantastiche che hanno fatto per il laboratorio Insall.

Grazie a Laura Machesky e al suo gruppo, per avermi insegnato che il mondo della Ricerca é diversificato e che accettare i punti di vista degli altri ci rende scienziati migliori.

Grazie a Karen Blyth per la sua bontà d'animo e il suo senso di umanità, il piu grande supporto che una advisor poteva darmi. Grazie a Dave Bryant: il suo aiuto e incoraggiamento hanno significato tanto per me.

Grazie a tutti quelli che lavorano dietro le quinte. Margaret O'Prey e gli altri membri del BAIR per avermi insegnato ad usare i microscopi. Andrew Keith e i colleghi dei servizi molecolari per tutte le mini e maxipreps con cui mi hanno aiutato nel corso degli anni. Lo staff dei servizi centrali, per aver lavorato sodo affinché tutto fosse pronto per un'altra giornata di lavoro.

Grazie a Kirsteen Campbell per avermi trascinata nel mondo del public engagement. Non avrei mai immaginato che questa esperienza potesse

significare cosí tanto per me, come scienziata e come persona, né quanto mi sarei divertita!
Grazie a tutte le persone fantastiche che ho incontrato lungo questo cammino. Evangelos Giampazolias, per la comprensione profonda che abbiamo l'uno dell'altro. Evdokia Michalopoulou, per il suo cuore buono e affettuoso. Emma Woodham, per tutte le attenzioni premurose che mi hanno fatto sentire benvenuta. Nikki Paul, per la sua attitudine rassicurante. Francesca Patella, per la sua instancabile capacitá di ascoltare. Voglio ringraziare Loïc Fort per aver condiviso con me tutte le fasi del dottorato, dal colloquio iniziale alla scrittura della tesi, e per avermi dimostrato che non c'é differenza tra due persone che sia troppo grande da risultare incolmabile.
Un grazie speciale va ad Olivia Susanto, per essermi stata vicino in tutti i momenti del dottorato, belli o difficili che siano stati; la sua amicizia è una delle più grandi benedizioni che ho ricevuto. Un grazie di cuore va a Licia Di Gregorio, per avermi insegnato cosa vuol dire essere Amico. Grazie a Silvia Cottone, Zara Lombardi, Lucio Riccardi e Mario Pica per tutti i ricordi che condividiamo, ma soprattutto per avermi dato la certezza di un'amicizia che non teme i chilometri. E grazie anche a Giulia Coniglio, perchè certi legami non si possono rompere.
Grazie ad Anna Maria, Vera, e alla mia grande famiglia per il loro affetto e supporto. Grazie a coloro che ho amato e perso.
Un ringraziamento speciale va a Lilla Barbera e Michele Corsentino, per avermi donato il loro dono piú prezioso, e per l'amore e il supporto che ci hanno dato nel corso degli anni.
Voglio ringraziare mio Papá, Nino, e voglio farlo due volte: per amarmi molto di più di quanto le parole potranno mai riuscire ad esprimere, e per lasciarmi comunque andare via ogni volta.
Grazie alla mia Mamma, Sina, per avermi insegnato l'importanza di un sorriso, e perché il suo amore é per me l'arma più potente contro la paura dei fallimenti.
Grazie a mio Fratello, Nello, per avermi dimostrato quanto profondo può essere l'amore, e quanto si possa tenere alla felicitá di qualcun altro piu di quanto ci si tiene alla propria.
Grazie a Kiko, la mia anima gemella, il mio migliore amico, il mio specchio più sincero, il filo che mi fa uscire da qualsiasi labirinto. Grazie perché custodisci i miei sogni e mi incoraggi a perseguirli sempre.

Author's declaration

I declare that, except where explicit reference is made to the contribution of others, this dissertation is the result of my own work and has not been submitted for any other degree at the University of Glasgow or any other institution.

_____

_____

List of abbreviations

Akt	RAC-alpha serine/threonine-protein kinase
ABPs	Actin binding proteins
ADP	Adenosine diphosphate
AIM	Atg8-family interacting motif
ARPs	Actin related proteins
Ash/Grb2	Abundant Src homology/Growth factor receptor-bound protein 2
ATP	Adenosine triphosphate
AX3	Axenic strain 3
B region	Basic region
C-terminus	Carboxyl terminus
cAMP	Cyclic adenosine monophosphate
CHC	Clathrin heavy chain
CCPs	Clathrin-coated pits
Cdc42	Cell division control protein 42
CDE	Caveolin-dependent endocytosis
CLC	Clathrin light chain
CME	Clathrin-mediated endocytosis
Cobl	Cordon bleu
CRIB motif	Cdc42 and Rac interacting/binding motif
DOCKs	Dedicator of cytokinesis
Dox	Doxycycline
ER	Endoplasmic reticulum
F-actin	Filamentous actin
G-actin	Globular actin
GAPs	GTPase- activating proteins
GBD	GTPase binding domain
GDIs	Guanine nucleotide dissociation inhibitors
GDP	Guanosine diphosphate
GEFs	Guanine nucleotide exchange factors
GTP	Guanosine-5'-triphosphate
GTPγS	Guanosine 5'-O-[gamma-thio] triphosphate
HSPC300	Hematopoietic stem/progenitor cell protein 300
JMY	Junction-mediating and regulatory protein
LC3	Light Chain 3

LIR	LC3-interacting region
Lmod	Leiomodin
MCCC1	Mitochondrial 3-methylcrotonyl-CoA carboxylase α
N-terminus	Amino terminus
N-WASP	Neural WASP
Nap1	Nck-associated protein 1
NBR1	Neighbor of BRCA1 gene 1
Nck	Non-catalytic region of tyrosine kinase adaptor protein 1
NF1	Neurofibromin
NPF	Nucleation promoting factor
PakB	p21 activated kinase B
PH domain	Pleckstrin homology domain
Pi	Inorganic phosphate
PI3P	Phosphatidylinositol 3-phosphate
PIP2	Phosphatidylinositol 4,5-bisphosphate
PIP3	Phosphatidylinositol 3,4,5-trisphosphate
PRD	Proline rich domain
Rac	Ras-related C3 botulinum toxin substrate
Ras	Rat sarcoma
Rho	Ras homolog gene family
SCAR	Suppressor of cAR1
SH3	Src Homology 3
Sra1	Specifically Rac binding protein 1
SUMO	Small ubiquitin-like modifier
Tiam1	T-cell lymphoma invasion and metastasis-inducing protein 1
TIRF	Total internal reflection fluorescence
VCA domain	Verprolin homology, central/connecting region and acidic region
WASH	Wiskott Aldrich syndrome protein homologue
WASP	Wiskott Aldrich syndrome protein
WAVE	WASP-family verprolin-homologous
WHAMM	WASP homolog associated with actin, membrane and microtubules
WH domain	WASP homology domain
WIP	WASP interacting protein

Chapter 1 , *Introduction*

1.1 *Dictyostelium discoideum*, a useful tool to tackle fundamental questions in cell biology

1.1.1 Introduction

Dictyostelium discoideum is the most studied among the dictyostelids, free-living amoebas with an extraordinary ability to self-organise into a multi-cellular organism in response to harsh environmental conditions. Due to their highly cooperative behaviour, which will be described later in this section, the dictyostelids are commonly referred to as *social amoebas*. Furthermore, as they were initially mistaken for fungi, the dictyostelids are also known as *slime molds* (Brefeld, 1869). It is now clear that dictyostelids and fungi constitute two separate groups, but their relative position within the evolutionary tree is still a matter of debate: initial analysis of the ribosomal RNA sequences led some to argue that the dictyostelids were the first of the eukaryotes to diverge (McCarrol et al., 1983). However, later studies on protein sequence conservation suggested that yeasts branched off earlier (Loomis and Smith, 1990).

Dictyostelium discoideum was first isolated from a forest in North Carolina (Raper, 1935), where it still populates the soil feeding mostly on bacteria, and occasionally on yeasts, through stunningly efficient phagocytosis. As mentioned, *D. discoideum* has an exceptional ability to face starvation, and the choreographic adaptation that follows nutrient deprivation has gathered the attention of scientists interested in a wide range of biological phenomena, from chemotaxis to phagocytosis, from autophagy to development.

For the sake of clarity, *Dictyostelium discoideum* will be henceforth referred to simply as *Dictyostelium*.

1.1.2 *Dictyostelium* genome

The genome of *Dictyostelium* has been entirely sequenced as a result of a joint effort between several groups (Eichinger et al., 2005). It is distributed within 6 unique chromosomes and has a size of 34 Mb, as previously estimated (Cox et al., 1990). It harbours approximately 12500 genes, which are extremely A-T rich and generally have short introns. The splicing sites are no different from those of higher eukaryotes. The haploidy of *Dictyostelium* is one of its many strengths

as a research tool, as it makes it more straightforward to investigate a protein function.

1.1.3 *Dictyostelium* life cycle: "united we stand, divided we fall"

Dictyostelium spends most of its life as a single cell, hunting and eating prey via a successful combination of chemotaxis and phagocytosis, and fighting competitors by secreting chemorepellents.

Dictyostelium has evolved a fine system to face sudden food deprivation, an event that is more than just a possibility in the unpredictable wild. It can respond to starvation in two different ways: by forming macrocysts or fruiting bodies. A macrocyst is a giant cell whose formation is triggered by the initial fusion of two mating types and supported by the engulfment of hundreds of other amoebas, which have been brought in close proximity to the giant cell via chemotaxis to cAMP (cyclic adenosine monophosphate). Eventually the macrocyst undergoes meiosis, presumably when the environmental conditions become favourable, but the details of this process are not yet fully elucidated. Fruiting body formation is by far the most spectacular as well as the best characterised of the starvation responses. During formation of a fruiting body, starving cells secrete cAMP (Bonner et al., 1969) and respond to it in a rigorously-timed fashion, generating propagating waves of warning signals that ultimately recall up to one hundred thousand cells to aggregation sites. Some of the starving cells will sacrifice themselves to generate the stalk, a stem-like structure with a supportive function. The stalk lifts up from the soil the remaining starving amoebas, which become spores organised into a sorocarp. When a more permissive environment is found, the spores germinate and disseminate individual amoebas, ensuring the continuity of the species. An example of fruiting body formation is shown in figure 1.1.

Scattering of the spores relies mostly on invertebrates (Huss, 1989), insects (Suthers, 1985) and nematodes (Kessin et al., 1996). As the site of dispersion is unpredictable, the availability of food at the new site cannot be taken for granted. It has been recently demonstrated that in order to increase the chance of spores' germination, a certain amount of bacteria is included in the sorocarp during fruiting body formation. The food carried by the dispersed spores is not enough as a long-term stockpile, but is sufficient to start a new crop at the new site. This recent finding recognises *Dictyostelium* as one of the most primitive

farmers across evolution (Brock et al., 2011). A third response to starvation, the formation of microcysts, has been observed in other *Dictyostelium* species, but not in *D. discoideum*.

1.1.4 Brief history of *Dictyostelium* as a model organism

It was because of its ability to aggregate into fruiting bodies that *Dictyostelium* first captured the attention of scientists. The earliest attempts to use it as a research tool, however, faced some challenges. To unveil the secrets of the transition between the vegetative growth and the aggregation stage, it was imperative to find the conditions for *Dictyostelium* survival and growth away from the soil. It did not take long for the researchers to discover that *Dictyostelium* is able to grow on a lawn of bacteria, preferably *Escherichia coli* or *Klebsiella aerogenes* (Raper and Smith, 1939).
Being able to observe the formation of a multi-cellular organism from individual amoebas raised important questions about cooperativity and development: why would the stalk cells die to protect the spores from the dangers of the soil, so that these could survive? What drives some amoebas to become spores and others to generate the stalk in the first place? These are just two among the many questions about altruism and multi-cellularity that *Dictyostelium* can help address. Of interest, transplant experiments have shown that cell fate is specified at the early stages of development by a group of cells collectively named *tip* (Raper, 1940).

1.1.5 *Dictyostelium* as a model organism today

Dictyostelium can be used to address many biological questions not strictly related to cooperativity and development. A non-exhaustive list of examples includes chemotaxis, phagocytosis, macropinocytosis and autophagy.
Chemotaxis, or directed cell migration, is the ability of the cells to move up an attractant gradient that they may have contributed to generate (Muinonen-Martin et al., 2014; Tweedy et al., 2016). It is implicated in physiological processes, such as wound healing and immune response, but also in pathological events like cancer spreading. In addition to chemotaxis towards cAMP during starvation, *Dictyostelium* rely on an extremely sensitive chemotactic apparatus to seek out bacteria during vegetative growth. In the laboratory, chemotaxis of

either starving or vegetative amoebas can be easily reproduced; in the latter case folic acid, which appears to be the main chemoattractant secreted by bacteria in the wild (Pan et al., 1972), is used to stimulate directed cell migration.

Dictyostelium has also been employed for studies on phagocytosis, which consists of the engulfment of solid particles for feeding or defensive purposes. Amoebas are indeed talented phagocytes (Cosson and Soldati, 2008), as they use this process to ingest bacteria, yeasts and occasionally other amoebas.

Macropinocytosis, the uptake of fluids from the extracellular environment, has been extensively studied using *Dictyostelium*. In this regard, its convenience as a tool lies at least in part upon the careful selection of laboratory-suitable strains that took place decades ago. In fact, most of the strains used for research today do not need to be co-cultured with bacteria, as they can grow in a rich medium via an increased rate of fluid-phase uptake. It has been recently demonstrated that the up-regulation of macropinocytosis results from mutations in the gene encoding Neurofibromin (NF1) (Bloomfield et al., 2015). *Dictyostelium* NF1 is a RasGAP that shows overlapping domain composition and function with human NF1, which is mutated in neurofibromatosis as well as in melanoma and other cancers (data from http://www.cbioportal.org). Since macropinocytosis has been recently demonstrated as a scavenging route for cancer cells, acting as an extracellular source of proteins to maintain their metabolism (Commisso et al., 2013), *Dictyostelium* has unintentionally become an even more valuable tool for studying this phenomenon.

Dictyostelium also represents an amenable system for the study of autophagy, the process by which cells mobilise and degrade part of their own cytosolic components. Autophagy is, however, more than just a degradation pathway. It contributes to cells' wellbeing by clearing up damaged molecules, organelles and invading pathogens, but also to the synthesis of macromolecules by supplying the cells with their building blocks. Given the multiple roles of autophagy in cellular housekeeping, it is not surprising that interfering with its basal levels has profound effects on cellular homeostasis, as demonstrated for examples in neurons (Hara et al., 2006). It is however during stressful conditions that autophagy exerts its highest impact. Examples of harmful circumstances include amino acid starvation (Onodera and Ohsumi, 2005) and mechanical stress (King et al., 2011). As mentioned in section 1.1.3, the lack of nutrients is a

challenge that *Dictyostelium* deals with by triggering a developmental process that culminates with the formation of fruiting bodies. Ironically, the formation of a multi-cellular organism is probably the most energetically demanding process that the amoebas need to accomplish. Autophagy plays a major role as as energy supplier during development, as demonstrated by the fact that *Dictyostelium* strains lacking components of the autophagy pathway are often unable to survive nutrient deprivation and to smoothly develop into multi-cellular organism. For instance, loss of Atg8, a highly conserved ubiquitin-like protein involved in the autophagosomes' expansion and orthologue of human LC3, impairs the ability of *Dictyostelium* to overcome the lack of nutrients and alters fruiting bodies' morphology (Otto et al., 2004). Importantly, a comparable role of autophagy on starvation survival and development has been observed in higher eukaryotes. Hypomorphic mutation of lgg-1, the C. elegans ortholog of *Dictyostelium* Atg8, affects the development of the quiescent larval stage termed *dauer*, ultimately compromising its ability survive in an unfavourable environment (Melendez et al., 2003).

Chemotaxis, phagocytosis, macropinocytosis, and conceivably autophagy, share a common ground: they all require a robust yet dynamic actin polymerisation machinery. Having evolved the enviable skills to sense prey and move toward them using actin-filled pseudopods, to extend actin-mediated projections to engulf them, and having been selected for its ability to uptake liquid nutrients via actin-rich macropinosomes, *Dictyostelium* represents a desirable tool to address the role of actin and actin-related proteins in different aspects of cell behaviour.

The actin cytoskeleton, and the usefulness of *Dictyostelium* to dissect its dynamics, will be discussed in the next section.

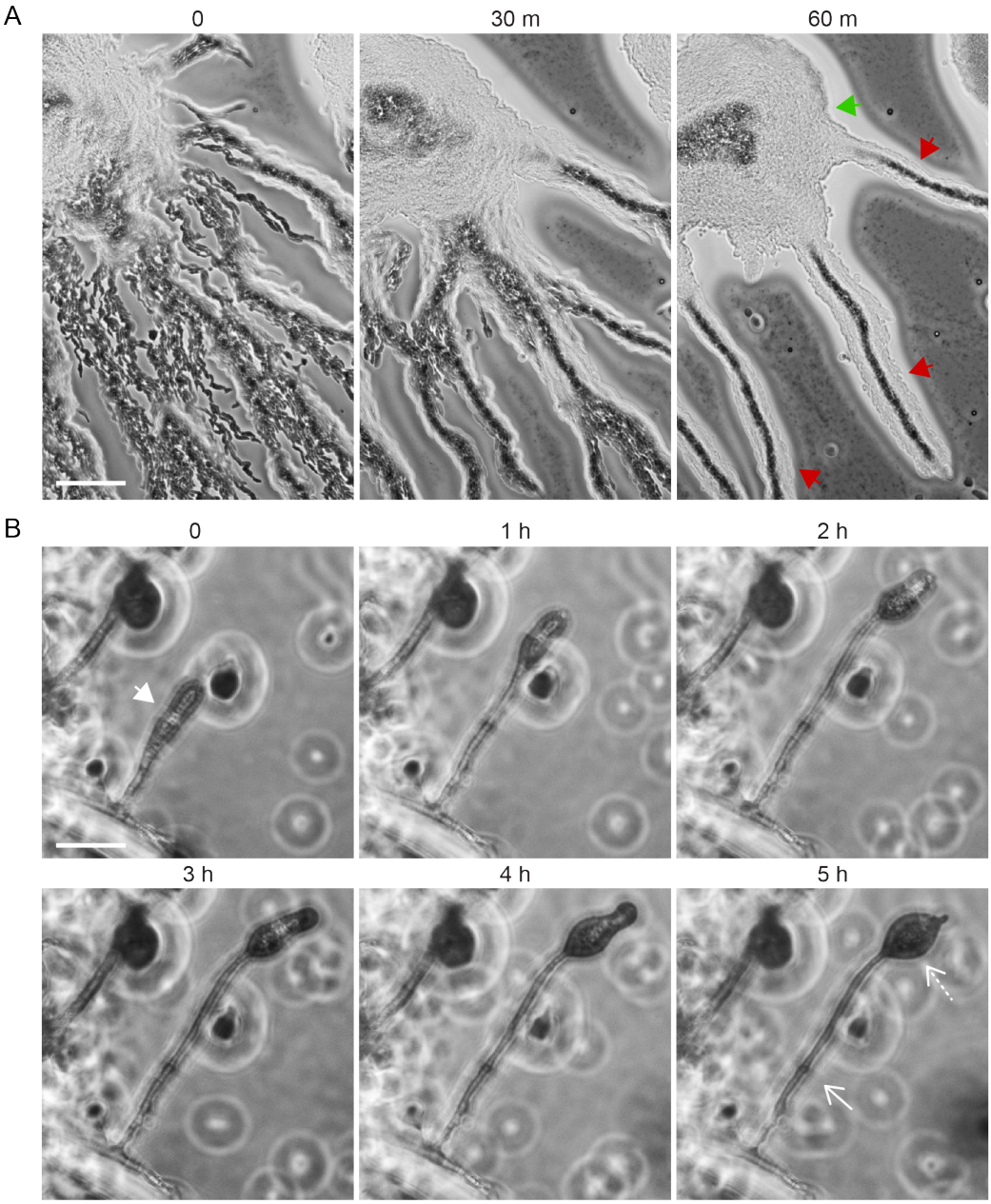

Figure 1.1 Fruiting body generation in response to starvation.

A) When deprived of nutrients, *Dictyostelium* start secreting cAMP (cyclic adenosine monophosphate) at precise time intervals. This is the warning signal that triggers aggregation: in response to it, individual amoebas chemotax toward evolving streams (red arrowheads) that will eventually flow into an aggregation centre (green arrowhead). Scale bar represents 50 um.

B) Cells gathered within an aggregation centre undergo morphogenesis to originate a fruiting body. Within the rising multi-cellular aggregate (white arrowhead) the cell fate is specified, so that a minority of amoebas will die to generate the supportive stalk (solid arrow), while most of the cells will originate the spores (dashed arrow). Scale bar represents 50 um.

1.2 Actin, actin nucleators & nucleation-promoting factors

1.2.1 Introduction

Actin is one of the most abundant proteins within cells as well as one of the most ubiquitous throughout evolution. Its expression has long been considered exclusive to the eukaryotic lineage, but proteins with similar properties and related functions are also present in bacteria, although sequence conservation is low (Doi et al., 1988; Jones et al., 2001; van den Ent et al., 2001).

Actin belongs to a large family of proteins that includes, for instance, Hsp70 and hexokinase. Despite being non-functionally related, members of this family share an ATPase domain (Bork et al., 1992). The presence of a nucleotide binding site and an intrinsic ATPase activity confer on actin the ability to cycle between a monomeric globular state, referred to as *G-actin*, and a polymeric filamentous state, termed *F-actin*. Mechanistic details of the polymerisation/depolymerisation process, and insights on the structure and functions of the two forms are described below.

1.2.2 G-actin: structure and functions

The 3D structure of the actin monomer, both ADP- and ATP-bound, has been solved at its best resolution in complex with DNase I (Kabsch et al., 1990). Co-purification is required to obtain crystals of the actin monomer, since the interaction with this enzyme prevents polymerisation. The physiological implications of the interaction between G-actin and DNase I, which has been demonstrated *in vivo*, remain to be clarified, but it has been proposed that it could shield both proteins from proteolytic cleavage (Rohr and Mannherz, 1978). The actin monomer is a parallelepiped of 55 Å in length, 55 Å in width and 35 Å in depth; it consists of two halves: a *small domain*, including subdomains 1 and 2, and a *large domain*, made out of subdomains 3 and 4 (Kabsch et al., 1990). Despite the nomenclature adopted, the two regions are almost identically-sized. Each monomer harbours a nucleotide-binding site as well as a divalent cation-binding pocket, both located in the *upper cleft*, between subdomains 2 and 4 (Kabsch et al., 1990). Each actin monomer also harbours a lower cleft, between subdomains 1 and 3. This region is involved in interactions with numerous actin-

binding proteins (ABPs) (Dominguez, 2004). A schematic representation of the actin monomer is shown in figure 1.2.

Our knowledge about localisation and roles of G-actin within cells is still unsatisfactory. Actin monomers have been detected early on within discrete cytosolic *puncta*, and this pool has been proposed to act as a reservoir from which the actin polymerisation machinery draw subunits to rapidly generate filaments (Cao et al., 1993). Cytosolic G-actin has also been indirectly linked to regulation of gene expression: actin monomers can interact with the transcription factor MKL1, retaining it in the cytosol and therefore preventing the expression of controlled genes (Miralles et al., 2003; Pawlowski et al., 2010). G-actin does not seem to localise in the nucleus of cells in interphase. Mitotic entry, however, has been shown to trigger the accumulation of actin monomers around the spindle (Meijerman et al., 1999); the implications of this finding are still largely unknown.

1.2.3 F-actin: structure and functions

F-actin has been subjected to a large number of structural studies over the decades. One of the very first attempts led to a model whereby F-actin consists of two filaments wrapped around each other, with a diameter of approximately 80 Å (Hanson, 1963). However, later studies demonstrated that F-actin consists of a single left-handed chain that harbours 13 monomers in 6 turns (Holmes et al., 1990). The twisting angle of each monomer, which is of ≈180° (166.6°), most likely accounts for the initial misinterpretation. F-actin is highly polarised. The end of the filament where monomers are bound to ATP is named the *barbed end* (or *plus end*), while the extremity of the polymer where monomers are bound to ADP is called the *pointed end* (or *minus end*). The nomenclature adopted reflects the appearance of the filament when decorated with myosin subfragment-1 (Begg et al., 1978). From a mechanistic point of view, the barbed end represents the entry site for new actin monomers, while the pointed end witnesses the detachment of G-actin from the filament, as will be discussed in the next section. Polarisation of the actin filament and key aspects af the actin polymerisation process are illustrated in figure 1.3.

The list of processes F-actin has been linked to is long and yet still growing. Many of its well-established roles and some of the emerging ones are briefly

mentioned here and discussed more extensively in the following sections of this dissertation.

Actin filaments mediate the formation of protrusions. These include locomotion-driving and adhesion-mediating protrusions, such as pseudopodia/lamellipodia (Abercrombie et al., 1971), filopodia (Lewis and Bridgman, 1992), eupodia/podosomes and invadopodia (Chen, 1989), as well as feeding tools, such as macropinosomes (Hacker et al., 1997) and phagosomes (Swanson et al., 1999). F-actin plays also a key role in different steps of trafficking. For instance, it facilitates the internalisation of coated pits during endocytosis (Aghamohammadzadeh and Ayscough, 2009; Boulant et al., 2011) and the secretion of vesicles during exocytosis (Lee and Knecht, 2002). Besides these well-established roles in trafficking, actin filaments have been more recently implicated in multiple steps of autophagy (Kast and Dominguez, 2017), as will be discussed in more details in chapter 5.

The processes mentioned so far mostly take place in the cytosol. Whether F-actin has a role in the nucleus, and whether it could be passively localised or actively generated in the nucleus in the first place has been debated for years and is now starting to be addressed. For instance, it has been recently shown that nuclear actin polymerisation in response to serum plays a major role in controlling the expression of MKL1-regulated genes (Baarlink et al., 2013; Kircher et al., 2015).

1.2.4 G-to-F transition: actin treadmilling

Actin dynamics implies three major steps: nucleation, elongation and depolymerisation. The first phase corresponds to the formation of a nucleus that contains three monomers, and has been shown to be the limiting phase (Frieden, 1983). The strategies adopted by the cells to overcome it will be discussed in the next section.

Elongation and depolymerisation of the actin filament happen simultaneously, giving rise to a highly dynamic process commonly referred to as *treadmilling*. To better understand how the actin filament undergoes treadmilling, a few concepts need to be introduced. First, actin monomers and actin filaments co-exist within cells but their relative abundance must be tightly regulated. It has been shown that the equilibrium between the two forms is estabilished when the *critical concentration* (maximum number of monomers that can co-exist with the

polymer) is maintained. When at the critical concentration, the number of monomers incorporated into the filament is equal to the number of monomers detaching from it. An excess of G-actin stimulates the formation of F-actin; conversely, levels of G-actin that fall below the critical concentration trigger disassembly of the filaments (Kasai et al., 1962). Second, the two ends of the filament are not equivalent. It has been demonstrated that they have different critical concentrations and therefore incorporate monomers at a different rate (Pollard and Mooseker, 1981; Wegner, 1976). The *fast* and the *slow ends* corresponds to the barbed and the pointed ends respectively. Third, G-actin can be bound to ADP or ATP, but ATP-actin has a lower critical concentration and is therefore added to the growing filament at a much faster rate than ADP-actin (Pollard, 1986). Fourth, once an ATP-bound actin monomer is incorporated into the barbed end of the filament, its γ-phosphate is irreversibly hydrolysed. The cleaved inorganic phosphate (Pi) remains within the nucleotide-binding pocket of the monomer without affecting its stability and without triggering its detachment from the filament. When eventually released, the phosphate group causes a dramatic destabilisation of the monomer, which is ultimately removed from the filament (Carlier et al., 1988). Altogether, these features explain why ATP-actin is preferentially incorporated at the barbed end of the filament, and why ADP-actin monomers abandon the filaments at its pointed end.

1.2.5 The Arp2/3 complex and other actin nucleators

As introduced in the previous section, the formation of an actin nucleus is the limiting step during the formation of an actin filament. This is due to the intrinsic instability of the dimer, but also to the presence of G-actin-binding proteins like thymosinβ4 that render the monomers unavailable for dimerisation (Goldschmidt-Clermont et al., 1992). It is however important to mention that other G-actin binding proteins, like profilin for instance, facilitate the exchahge of ADP for ATP, therefore creating a pool of actin monomers available for dimerisation (Goldschmidt-Clermont et al., 1992). Once the dimeric seed has been generated, the addition of a further monomer is kinetically more permissive (Frieden, 1983). Actin polymerises constantly and smoothly within cells thanks to a wide range of factors that help overcome the energetic demand of the G-to-F transition. These are collectively called *actin nucleators*.

The first described actin nucleator was the Arp2/3 complex (Machesky et al., 1994), which drives the formation of actin branches from the side of an existing polymer with a constant angle of 70° (Mullins et al., 1998). The Arp2/3 complex consists of seven stably assembled subunits. Two of them highly resemble actin in terms of sequence and 3D structure (Robinson et al., 2001), and were accordingly named *Arp* (actin-related proteins) *2* and *3*. As for the other subunits of the complex, ArpC1 harbours WD (Tryptophan-Aspartic acid) repeats while the remaining four (termed ArpC2-5) do not show any conserved motif. Some of the details of the strategy used by the Arp2/3 complex to facilitate the nucleation of actin are still unclear, but a satisfying model has been proposed. It this model, ArpC2 and ArpC4 mediate the positioning of the entire complex on an existing (*mother*) filament, while Arp2 and Arp3 trigger the elongation of a new (*daughter*) filament from its side (Beltzner and Pollard, 2004; Egile et al., 2005). To achieve this, the two actin-like proteins mimic the otherwise unfavorable dimer, therefore bypassing the kinetic burden of its formation. From there, further monomers are easily incorporated. The dual ability of the Arp2/3 complex to branch and elongate is often referred to as *dendritic nucleation*. Figure 1.4 summarises Arp2/3 complex-mediated actin filament branching and elongation.

The Arp2/3 complex is subjected to various steps of regulation, including nucleotide binding/hydrolysis and post-translational modifications; however these shall not be discussed further here. Great attention will instead be given to nucleation-promoting factors (NPFs), whose regulatory role on the Arp2/3 complex will be discussed in the next section.

Other known actin nucleators include formins and the most recently discovered Spire, Cobl (Cordon bleu) and Lmod (Leiomodin). Formins are dimeric proteins able to nucleate unbranched actin filaments and simultaneously move along the polymer to protect its barbed end from capping proteins, which would otherwise arrest the elongation of the filament. So far, formins have been shown to play a role in a wide range of cellular processes, such as maintenance of cell polarity (Zeller et al., 1989), cytokinesis (Castrillon and Wasserman, 1994), and filopodia assembly (Pellegrin and Mellor, 2005). They are characterised by two C-terminal FH (Formin Homology) domains, named FH1 and FH2. Since none of them shows any actin-binding motifs, the mechanism of action of formins must differ from that of the Arp2/3 complex. A model whereby formins stabilise spontaneously

formed actin seeds in concert with G-actin-binding proteins (Pring et al., 2003) is generally accepted. Regarding the regulation of formins, what we know so far comes from studies of the most abundant Diaphanous-related formins (DFRs). RhoGTPases have been proposed to play a role in the activation of formins by relieving their autoinhibition (Li and Higgs, 2003), but additional regulators are likely not yet identified.

Lastly, factors containing tandem actin monomer-binding motifs constitute an expanding class of nucleators. Members of this group include Spire, Cobl and Lmod. It is currently believed that these proteins stimulate actin polymerisation by gathering actin monomers (Qualmann and Kessels, 2009).

1.2.6 Nucleation-promoting factors

The intrinsic ability of the Arp2/3 complex to trigger actin nucleation is low, by far insufficient to supply the cells with the required amount of F-actin within a suitable timeframe. From a structural point of view, this is likely due to the fact that in the absence of Arp2/3 complex activators the two actin-mimicking subunits are too far apart to sufficiently resemble a dimer (Robinson et al., 2001).

The efficiency of the Arp2/3 complex is strongly boosted by a number of activators collectively termed nucleation-promoting factors (NPFs). These can be broadly sorted into two groups, class I and class II, depending on the mechanisms utilised to activate the Arp2/3 complex. This thesis shall focus on a group of class I NPFs known as the WASP (Wiskott-Aldrich Syndrome Protein) family. The mechanism of action of the WASP family members, their structure, roles and regulation will be discussed in the next section of the thesis.

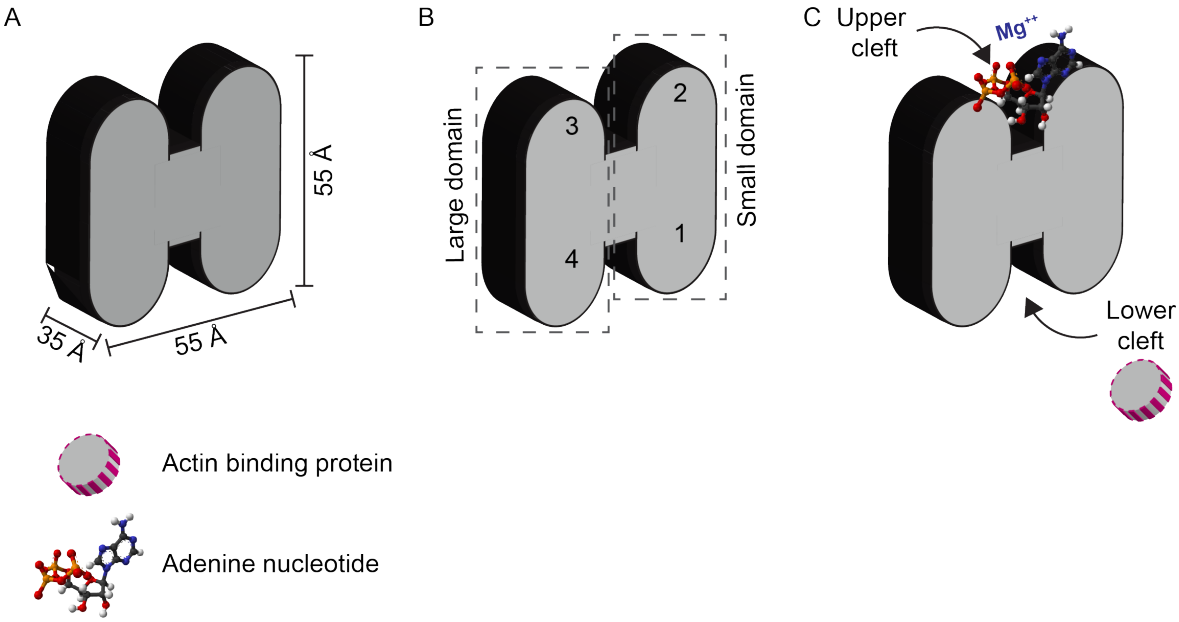

Figure 1.2 Structural details of the actin monomer.

A) Each actin monomer is a rectangular prism of 55x55x35 Å.

B) Two halves can be identified in each monomer: a large domain, comprising subdomains 3 and 4, and a small domain, consisting of subdomains 1 and 2. Large and small domains are almost identical in size.

C) The folding of the monomer generates two major pockets. The upper cleft is located between subdomains 2 and 4 and harbours the nucleotide- as well as the bivalent cation-binding site. The lower cleft is located between subdomains 1 and 3 and establishes interactions with actin-binding proteins (ABPs).

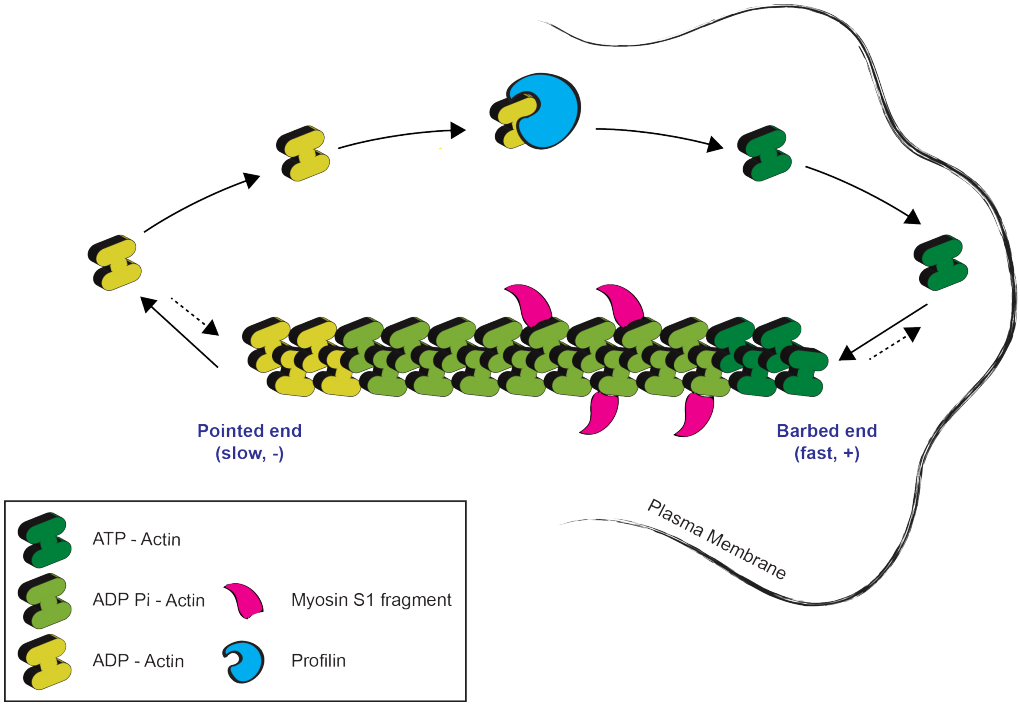

Figure 1.3 Polarisation of the actin filament and key aspects of the actin treadmilling.

The actin filament has a defined polarity. The region where actin monomers are incorporated within the growing filament is referred to as barbed end; the end where actin monomers are released from the filament is referred to as pointed end. The nomenclature reflects the orientation of myosin S1 fragments bound to the filament. ATP-bound monomers (dark green) join the filament via its barbed end (also referred to as fast or plus end). Once the monomer is incorporated, its γ-phosphate is cleaved leading to the formation of ADP Pi-Actin (pale green). The inorganic phosphate remains within the nucleotide-binding pocket and is eventually relesed. The resulting ADP-actin (yellow) abandons the filaments at the pointed end (also referred to as slow or minus end). When released, the ADP-bound monomer is targeted by G-actin-binding proteins . Among them Profilin facilitates the exchange of ADP for ATP, maintaining a pool ATP-bound actin monomers that can be re-join in the filaments via its barbed end.

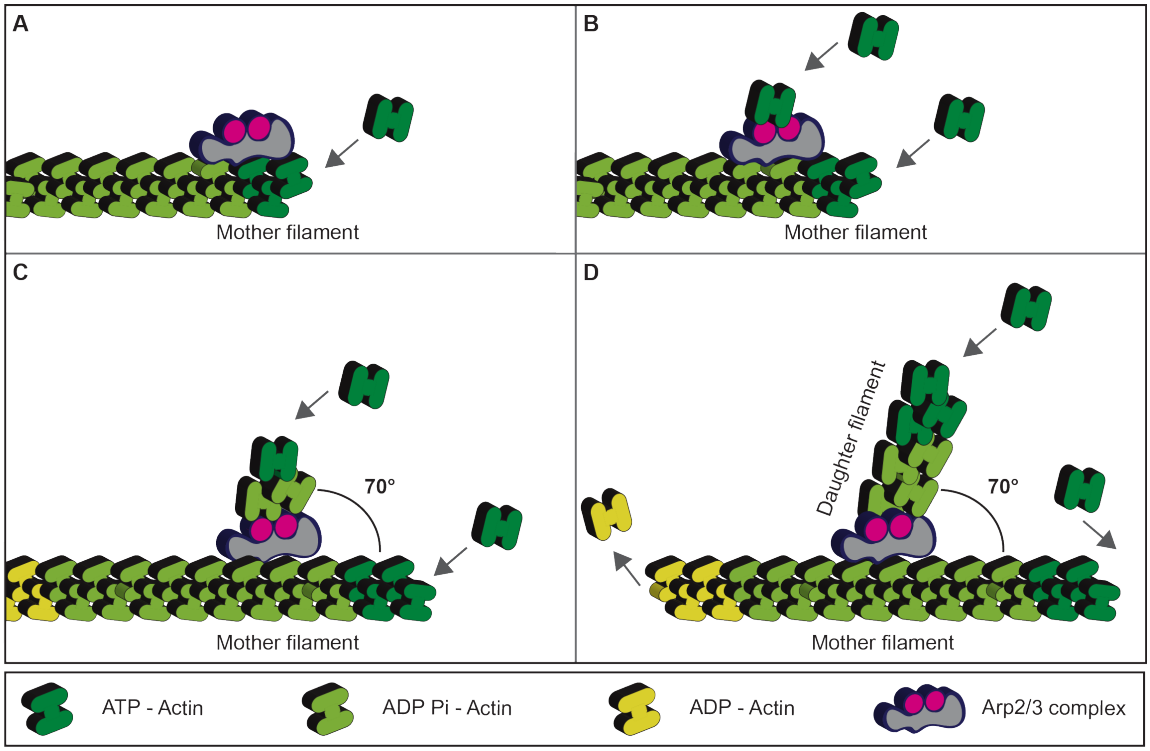

Figure 1.4 Mechanism of Arp2/3 complex-mediated branching and elongation.

A) The Arp2/3 complex (grey and pink shape) binds to the side of an existing (mother) actin filament. B) The two Actin-related subunits of the complex (Arp2 and Arp3, pink circles) mimic an actin dimer, facilitating the recruitment of ATP-G-actin (dark green). C) ATP-bound monomers are added to the newly formed filament and undergo γ-phosphate cleavage, therefore becoming ADP-Pi-Actin (pale green). The filament originated from the side of the mother filament is referred to as daughter filament and grows at the constant angle of 70°. D) Both mother and daughter filaments undergo treadmilling and eventually release ADP-bound actin monomers (yellow).

1.3 Family matters: WASP and other relatives

1.3.1 Introduction

The WASP family was the first group of class I NPFs discovered in eukaryotes. Its members activate the Arp2/3 complex via a common C-terminal VCA domain, which consists of subdomains V, C and A. These have distinct properties. The V region binds to actin monomers (Machesky and Insall, 1998) and its name reflects its homology to verproline; it is also referred to as WH2 (WASP Homology 2) domain. The C region binds to actin monomers as well as to the Arp2/3 complex (Marchand et al., 2001); initially named after its presumed homology to cofilin, it is now commonly referred to as central or connecting region. The A region interacts with the Arp2/3 complex (Machesky and Insall, 1998), and is a relatively unstructured subdomain highly enriched in acidic residues. Regarding the mechanism underlying the VCA-mediated activation of the Arp2/3 complex, it has been shown that upon direct interaction with WASP proteins the Arp2/3 complex undergoes structural rearrangements that result in the acquisition of a closed conformation. In this new layout, Arp2 and Arp3 are in close proximity and therefore capable of mimicking an actin dimer (Goley et al., 2004; Rodal et al., 2005). In addition to their bridging role between the two Arp subunits, WASP family proteins further facilitate actin polymerisation by supplying the pseudo actin dimer with the third subunit of the nucleus. Six family members have so far been described. Of these, only WHAMM and JMY are exclusively expressed in vertebrates, while at least one gene encoding a orthologue of the ancestral WASP, SCAR/WAVE and WASH is present in the genome of almost every eukaryote (Veltman and Insall, 2010). As this thesis is mostly focussed on investigating WASP using *Dictyostelium*, the following sections will thoroughly summarise our current understanding of its roles and regulation; SCAR/WAVE and other relatives will also be briefly discussed.

1.3.2 N-WASP & WASP: nomenclature and evolutionary homology

Mentioning WASP without providing information about the organism or at least the cell type it refers to can be misleading. Non metazoans and invertebrates, *Dictyostelium*, yeast and *Drosophila* for instance, possess only one copy of the ancestral gene, named Las17/Bee1 in yeast, WASP in amoebas and Wsp in *Drosophila*. On the contrary, vertebrates express two paralogues: WASP and N-

WASP. WASP is expressed exclusively in the hematopoietic lineage and is mutated in patients affected by the recessive X-linked Wiskott-Aldrich Syndrome (Derry et al., 1994). N-WASP (Neural-WASP) is instead ubiquitous (Miki et al., 1998a), despite initially thought to be selectively expressed in the brain (Miki et al., 1996). Vertebrates' WASP and N-WASP have a substantially overlapping domain composition, but N-WASP harbours an additional WH2 domain immediately upstream the canonical VCA domain. Phylogenetic analysis revealed that vertebrates' N-WASP, and not hematopoietic WASP, is the functional homologue of the unique WASP gene expressed by invertebrates and non metazoans (Veltman and Insall, 2010). For the sake of completeness it must be mentioned that the *Dictyostelium* genome harbours two genes encoding unconventional WASPs (WASP B and C), which lack the N-terminal domain. These might have a similar role to the canonical WASP (Veltman and Insall, 2010) but are expressed at very low levels (data from http://dictyexpress.biolab.si/) and have not been thoroughly investigated. Furthermore, a recent study suggests that WASP-related proteins that are devoid of a WH1 domain may constitute a separate family, which has been named WAWH (WASP without WH1 domain) (Kollmar et al., 2012).

Since vertebrates' WASP is cell-type specific and likely exerts specialised functions, it will not be discussed in detail in this thesis; when mentioned, it will be referred to as *hematopoietic WASP*. From now on, *WASP* will only be used to refer to the ubiquitous and evolutionarily conserved paralogue.

1.3.3 WASP domain composition

Dictyostelium WASP possesses an N-terminal WH1 (WASP Homology 1) domain, which interacts with WIPa (WASP interacting protein) (Myers et al., 2006). A WH1-mediated interaction with WIP has also been shown in human N-WASP, and might account for its localisation at sites of vaccinia-induced actin tails (Moreau et al., 2000). Moving towards the centre of the molecule, *Dictyostelium* WASP harbours a basic (B) region, which interacts with phospholipids, and an immediately downstream CRIB (Cdc42 and Rac interacting/binding) motif, which preferentially binds to the active form of Rho GTPases Cdc42 and Rac (Burbelo et al., 1995). The CRIB motif (and occasionally the combination of CRIB motif and B region) is often referred to as GBD (GTPase binding domain). Finally, just upstream of the VCA domain, *Dictyostelium* WASP shows a Proline-rich domain

(PRD), which binds to SH3 (Src Homology 3) domain-containing proteins. As shown in figure 1.5, human N-WASP has a remarkably similar domain composition.

1.3.4 Known functions of WASP

WASP ortuologues have mostly been linked to endocytosis (Kochubey et al., 2006; Madania et al., 1999; Merrifield et al., 2004) and, contextually, to protrusion generation (Veltman et al., 2012; Zhu et al., 2016). Intriguingly, WASP has been observed in the nucleus, where it appears to contribute to gene expression of target genes (Suetsugu and Takenawa, 2003). Although fascinating, the role of N-WASP in the nucleus shall not be discussed further here.

1.3.4.1 WASP and endocytosis

Different mechanisms of small-scale internalisation have been described. These include clathrin-mediated endocytosis (CME), caveolin-dependent endocytosis (CDE) and clathrin/caveolin-independent endocytosis.

CME is possibly the one process WASP has been consistently linked to throughout evolution. Since it is by far the best characterised of the endocytic pathways, and the most relevant for the purpose of this thesis, it will be described in more detail. CME is often referred to as *receptor-mediated endocytosis* since it drives primarily, but not exclusively, the uptake of membrane-bound receptors and their ligands. At the onset of CME, transmembrane receptors interact via their cytosolic tail with adaptor proteins bound to clathrin subunits. This triggers the assembly of a clathrin lattice and the formation of a clathrin-coated pit (CCP) that expands inward until is pinched off and released into the cytosol. Once internalised, the vesicle is uncoated and fused with endosomes, from where it can proceed to lysosomes or being recycled back to the plasma membrane (Robinson, 2015).

WASP is the main NPF to activate the Arp2/3 complex at endocytic patches in different organisms. In yeasts, for instance, loss of Las17 significantly reduces the internalisation rate of α-factor/Ste2 receptor (Madania et al., 1999). In *Dictyostelium*, WASP is recruited on a clathrin-enriched spot (Veltman et al., 2011) and its deletion dramaticaly impairs the internalisation of CCPs (Davidson, 2014). Similarly, N-WASP is transiently activated on CCPs in murine fibroblasts (Merrifield et al., 2004). The effect of N-WASP deletion in mammalian cells,

however, is less clear than in simpler organisms, since in mouse fibroblasts lacking N-WASP, internalisation of EGF still occurs although at a much lower rate (Benesch et al., 2005). Interestingly, in the same study it was shown that the requirement for the Arp2/3 complex at endocytic patches is absolute, since a total block in uptake occurs when the complex is sequestered. This suggests that some other NPFs might play a redundant role in CME, but the involvment of SCAR/WAVE has already been excluded (Benesch et al., 2005) and no further details are available. Recruitment of WASP triggers the formation of transient F-actin *puncta* in yeasts (Kaksonen et al., 2003), *Dictyostelium* (Brady et al., 2010) and mammals (Merrifield et al., 2002). Recruitment of the actin polymerisation machinery at endocytic spots is an active, temporally-regulated and evolutionarily conserved process. However, while it is mandatory in yeasts (Kaksonen et al., 2003) and *Dictyostelium* (Davidson, 2014), it does not occur in all mammalian cells (Fujimoto et al., 2000) nor even on different membranous surfaces of the same cell (Gottlieb et al., 1993). The reason behind the requirement of F-actin at endocytic spots in the first place, and its dispensability in different systems/membranes has been beautifully unveiled: actin filaments are not required to finalise the uptake of CCPs as long as the plasma membrane is suffiently plastic to undergo significant deformation; stretching, swelling, or any other mechanical stress render the plasma membrane less able to achieve invagination, and actin filaments are therefore nucleated to facilitate it (Aghamohammadzadeh and Ayscough, 2009; Boulant et al., 2011). Figure 1.6 summarises the key events of CME.

Mechanistic details of other types of small-scale endocytosis are still limited, but the involvement of actin filaments in either CDE or clathrin/caveolin-independent endocytosis has been demonstrated. The SV40 virus, for instance, penetrates the host cells throught caveolae, and its entry requires an intact actin cytoskeleton (Pelkmans et al., 2002). As for the NPFs involved in CDE, N-WASP has been proposed as a possible player mostly on the basis of its interaction with syndapin, a Caveolin-1-interactin protein (Qualmann et al., 1999). Since syndapin is also involved in CME, however, it is difficult to tease apart the role of N-WASP in CDE from its role in CME. The involvement of N-WASP in caveolin-dependent endocytosis, if any, remains therefore uncertain. N-WASP has been shown to play a role in the clathrin/caveolin-independent endocytosis of interleukin 2 receptor (IL-2R); in the proposed model, N-WASP

boosts the ability of cortactin, a class II NPF, to uptake IL-2R (Grassart et al., 2010). Whether N-WASP is the only Arp2/3 complex activator involved in clathrin/caveolin-independent endocytosis is, however, still unclear.

1.3.4.2 WASP and protrusion generation

The types of protrusion WASP has been linked to can be broadly divided in two groups: those that drive cell motility, such as pseudopodia/lamellipodia and filopodia, and those that mediate its adhesion to and invasion/degradation of the extracellular matrix (ECM), like podosomes/invadopodia.

The terms *pseudopodia* and *lamellipodia* can both be used to refer to flat and wide, sheet-like protrusions. Evidence from different organisms suggests that WASP does not have a central role in their generation. *Dictyostelium*, for instance, extends WASP-driven pseudopodia only in the absence of SCAR/WAVE (Veltman et al., 2012), meaning that WASP is theoretically able to drive actin polymerisation at the leading edge but in practise only a substitute for the primary regulator, SCAR/WAVE. Similarly, WASP-mediated compensation for SCAR/WAVE loss has recently been observed during neuroblast migration in *C. elegans* embryo (Zhu et al., 2016). Intriguingly, WASP does not seem to compensate for non functional SCAR/WAVE in *Drosophila*, as demonstrated by the inability of cultured S2R+ cells lacking any subunit of the complex to extend lamellipodia (Kunda et al., 2003), and by the reduced number of lamellipodia extensions in hemocytes expressing a dominant negative SCAR (Evans et al., 2013). In both studies it was shown that the deletion/inactivation of WASP does not worsen the severity of the SCAR deletion/inactivation phenotype, further supporting the idea that WASP does not play a substantial role in lamellipodia extension in *Drosophila*. Remarkably, the phenotype observed in *Drosophila* cells lacking a functional SCAR/WAVE complex is recapitulated by the double deletion of SCAR/WAVE and WASP in *Dictyostelium* (Davidson et al., 2018). Even in mammalian cells, the role of N-WASP on lamellipodia extension appears trivial. For instance, fibroblasts isolated from N-WASP null mice as well as N-WASP-depleted podocytes are still able to extend normal protrusions (Schell et al., 2013; Snapper et al., 2001). Furthermore, a study on human epithelial cells demonstrated that while SCAR/WAVE is the major NPF to drive lamellipodia extension in 2D assays, while N-WASP plays a key role during 3D migration (Tang et al., 2013).

The role of WASP in the formation of long and spiky protrusions named *filopodia* is probably even less clear. When first identified, N-WASP was proposed as a filopodia inducer downstream of Cdc42, based on the observation that it stimulates the formation of filopodia when injected into mammalian cells along with dominant active Cdc42 (Miki et al., 1998a). However, the lack of N-WASP does not impair filopodia formation in mouse embryo-derived cells (Snapper et al., 2001). Defining the actual role of N-WASP in filopodia formation might be further complicated by the likely crosstalk between the Arp2/3 complex and formins, which have also been consistetly linked to filopodia formation (Schirenbeck et al., 2005). In *Dictyostelium*, a role for WASP in filopodia generation appears improbable, since a significant increase in the number of spiky protrusion is triggered by the absence of both WASP and SCAR/WAVE (Davidson et al., 2018).

WASP plays a role within adhesive/degradative structures, named *podosomes* or *invadopodia* depending on whether they refer to cancer or non-cancer cells. N-WASP has been detected within fibroblasts' podosomes, where it is recruited via a direct interaction with cortactin and activates the Arp2/3 complex (Mizutani et al., 2002). Furthermore, N-WASP-induced actin polymerisation at invadopodia has been shown in metastatic breast cancer cells (Lorenz et al., 2004). Interestingly, dynamic actin *puncta* have been observed at the base of nascent pseudopods in *Dictyostelium* cells migrating under-agarose; these structures, named *eupodia* or *knobby feet*, may exert a similar function to podosomes (Fukui et al., 1999), but whether WASP is at all involved in their formation remains to be elucidated.

1.3.4.3 WASP and vesicle trafficking

WASP-mediated Arp2/3 complex activation has been shown to propel vesicles through the cytoplasm. This has been observed, for instance, in *Xenopus* eggs (Taunton et al., 2000) and murine fibroblasts (Benesch et al., 2002). Of great interest for the purpose of this thesis is the debated role of Rho GTPases on the recruitment/activation of N-WASP at these rocketing tails. In the latter study, genetic mutations within the CRIB motif of N-WASP did not compromise its recruitment on intracellular vesicles nor even its actin nucleation activity. A role for *Dictyostelium* WASP in vesicle trafficking has also been proposed. WASP-enriched vesicles were first spotted at the front and the rear of migrating cells

(Myers et al., 2005), and subsequently characterised as Golgi-derived (Lee et al., 2009). Interestingly, Myers and colleagues hypothesised that the presence of a functional CRIB domain might not play a leading role in the recruitment of WASP on intracellular vesicles; unfortunaly they did not provide supporting evidence for this.

1.3.5 WASP regulation

Most of what we know so far about the regulation of *Dictyostelium* WASP comes from studies on mammalian N-WASP. Indeed, likely due to the remarkably similar domain composition and the comparable spectrum of functions, conclusions reached for mammalian N-WASP have been confidently extended to its orthologue in other organisms. Importantly, as will appear clear from the following sections, our current knowledge of WASP regulation is strongly based on *in vitro* evidence.

It has been estabilished that N-WASP within cells is largely inactive, kept in a folded conformation via intramolecular interactions between the VCA domain and the CRIB motif/B region. This model was proposed upon *in vitro* observation that isolated VCA domains have a higher ability to induce actin polymerisation in comparison to full length N-WASP (Rohatgi et al., 1999). Release of the autoinhibition and subsequent umasking of the Arp2/3 complex-activating region mostly depends on allosteric regulation. Rho GTPases, phospholipids, SH3 domain-containing proteins and post-translational modifications have so far been proposed to play a role in the activation of N-WASP. A schematic representation of the allosteric activation of N-WASP is shown in figure 1.7.

1.3.5.1 Rho GTPases

Cdc42 was the first Rho GTPase linked to N-WASP. This was mostly based on their direct interaction *in vitro*, and on the dramatic induction of filopodia observed in cells co-injected with dominant active Cdc42 and N-WASP (Miki et al., 1998a); in the same study no significant interaction between N-WASP and Rac was detected. Further details supporting the regulatory role of Cdc42 on N-WASP *in vitro* came shortly after from the same lab: in N-WASP-depleted *Xenopus* eggs extracts, the amount of F-actin detected by pyrene actin assay upon addition of H208D N-WASP (which fails to bind Rho GTPases) was enormously smaller than the amount detected in the presence of wild type N-

WASP (Rohatgi et al., 1999). In both papers, the authors hinted at the possibility that N-WASP is constitutively autoinhibited, and that Rho GTPases (as well as other signals) may play a role in its activation, by binding to its CRIB motif and releasing the autoinhibition. Structural details of the mutually exclusive interaction between the CRIB motif of N-WASP and its VCA domain or Cdc42 are not available, but supporting evidence can possibly be drawn from a study on hematopoietic WASP, whose CRIB motif and VCA domain are similar to N-WASP's (Kim et al., 2000). More recently, however, it has been shown that Rac1 is a much stronger activator of N-WASP than Cdc42 *in vitro*, while hematopoietic WASP appears more sensitive to Cdc42 than to Rac1 (Tomasevic et al., 2007). Rho GTPases have also been proposed as regulators of WASP in *Dictyostelium,* which does not express any Cdc42 orthologue (Rivero et al., 2001). By using a combination of yeast two hybrid and FRET microscopy, Han and colleagues concluded that RacC is the major activator of *Dictyostelium* WASP (Han et al., 2006). It is important to point out, however, that in the same study other Rac species (including the highly conserved human Rac1) were shown to interact with *Dictyostelium* WASP *in vitro*.

1.3.5.2 Phospholipids

The role of phospholipids on the activation of N-WASP is supported by a vast range of *in vitro* data; among the phospholipids present within cells, PIP2 (phosphatidylinositol 4,5-bisphosphate) has been proposed as a key player. Initial observations led to the hypothesis that PIP2 might play a role in the localisation of N-WASP to the membrane via a direct interaction with its presumed PH (Pleckstrin Homology) domain (Miki et al., 1996). Later studies, however, proposed that PIP2 does not just control N-WASP's subcelllular localisation but is instead responsible for its activation in concert with Cdc42 (Rohatgi et al., 1999). The model of co-operative regulation of N-WASP by PIP2 and Cdc42 was backed up by a later study, which also clarified that the region involved in binding to PIP2 was not a PH domain but a previously uncovered polybasic region located immediately upstream of the CRIB motif (Prehoda et al., 2000). A model whereby PIP2 provides *in vivo* instructions on when and where to trigger actin polymerisation, however, has been questioned based on at least two findings: PIP2 is evenly distributed around the cell cortex and its levels do not change significantly after stimulation, unlike those of PIP3. In this

scenario, it seems unlikely that PIP2 could account for the highly timely- and spatially-polarised induction of actin polymerisation (Insall and Weiner, 2001). A more recent study has shown that, despite to lower extent, N-WASP can also be co-operatively activated *in vitro* by Cdc42 and PIP3 (phosphatidylinositol 3,4,5-trisphosphate) (Papayannopoulos et al., 2005).

1.3.5.3 SH3 domain-containing proteins

N-WASP harbours a polyproline region, which interacts with SH3 domain containing proteins. So far, mostly Ash/Grb2 (Abundant Src homology/Growth factor receptor-bound protein 2) and Nck (non-catalytic region of tyrosine kinase adaptor protein 1) have been linked to its activation. Ash/Grb2 was initially identified as an N-WASP-interactor, and proposed to play a role in its localisation (Miki et al., 1996). However, a later work showed that Ash/Grb2 contributes to N-WASP's activation *in vitro* in concert with Cdc42 (Carlier et al., 2000).

Nck is generally considered a much more potent activator of N-WASP in comparison to Ash/Grb2. This is mostly based on early *in vitro* evidence (Rohatgi et al., 2001) later backed up by a study claiming that Nck is sufficient to fully activate N-WASP *in vitro* (Tomasevic et al., 2007). A hypothetical mechanism underlying Nck-mediated activation of N-WASP has recently been proposed: membrane-bound Nck interacts with N-WASP's polyproline stretches via its second and third SH3 domains; a short region spanning between its first and the second SH3 domains becomes engaged instead with the CRIB motif of N-WASP, leading to destabilistation of the autoinhibited conformation (Okrut et al., 2015). A model whereby SH3 domain-containing proteins activate N-WASP via interactions with its PRD is supported by the steric properties of Proline, which is frequently exposed on the surface of a polypeptide (Holt and Koffer, 2001) and might therefore establish the first contact with its regulators.

1.3.5.4 Phosphorylation

N-WASP appears to be particularly sensitive to tyrosine kinases belonging to the Src family, although modification by different members seems to lead to different outcomes. Fyn, for instance, can phosphorylate N-WASP on Tyr253, which is located between the CRIB motif and PRD. The negative charge introduced upon phosphorylation is thought to destabilise the autoinhibited conformation, triggering N-WASP activation in concert with Cdc42 and/or PIP2.

Of interest, Tyr phosphorylation of N-WASP triggers its degradation via the ubiquitin/proteasomal system (Suetsugu et al., 2002).
In addition, Lck can phosphorylate N-WASP on Tyr256, but this modification is unlikely to have a leading role in its activation, since this residue appears to be inaccessible to kinases within the autoinhibited conformation (Torres and Rosen, 2006).

1.3.6 WASP deletion throughout evolution: have we learnt the whole story?

Over the years, the WASP-encoding gene has been genetically manipulated in different model organisms and cell types. Our lab has recently succeeded in generating a *Dictyostelium* WASP knockout strain (Davidson et al., 2018), contradicting previous reports claiming that WASP is essential for *Dictyostelium* viability (Myers et al., 2005). The phenotypic consequences of WASP deletion in *Dictyostelium*, whether expected or unforeseen, will be reported in this section of the thesis and discussed within the framework of the effects of its deletion in other organisms.

1.3.6.1 *Dictyostelium* WASP is involved in clathrin-mediated endocytosis

In the absence of WASP *Dictyostelium* fails to recruit the Arp2/3 complex on clathrin-coated pits, leading to their impaired internalisation and increased lifetime (Davidson, 2014). This observation is not overly surprising given the localisation of *Dictyostelium* WASP on CCPs (Veltman et al., 2011), but also given the known effect on CME of WASP deletion/mutations in yeast (Madania et al., 1999), *Drosophila* (Kochubey et al., 2006) and murine fibroblasts (Benesch et al., 2005).
Considering the high degree of functional conservation of WASP throughout evolution, one key question that has yet to be addressed is: how can Las17/Bee1, the yeast orthologue of human N-WASP, which is devoid of a CRIB motif, be recruited on CCPs? How dependent on Rho GTPases is WASP's role in CME? This point will be further discussed in the following chapters.

1.3.6.2 *Dictyostelium* WASP does not drive pseudopodia but indirectly ensures efficient cell migration

As mentioned in section 1.3.4.2, WASP does not play a major role in the extension of pseudopodia during migration in *Drosophila* (Evans et al., 2013;

Kunda et al., 2003), *C. elegans* (Zhu et al., 2016), nor in mammals (Schell et al., 2013; Snapper et al., 2001; Tang et al., 2013). Similarly, *Dictyostelium* WASP knockout extends normal pseudopods at the expected rate (Davidson, 2014). Despite not playing a direct role in leading edge dynamics, however, WASP contributes to efficient migration, as demonstrated by the reduced speed of knockout cells (Davidson, 2014). A thorough analysis revealed that the reduced speed is due to the inability of *Dictyostelium* WASP knockout cells to retract their uropod.

Despite not being necessarily related, it is worth pointing out that in Zebrafish embryos lacking WASp (orthologue of human hematopoietic WASP) migrating neutrophils show a reduced rate of uropod retraction (Jones et al., 2013).

1.3.6.3 *Dictyostelium* WASP maintains cell polarity during migration

In the attempt to clarify the reasons behind the uropod retraction defect, a novel and unexpected role for *Dictyostelium* WASP in maintenance of cell polarity was unveiled. Normal migrating cells have a defined leading edge and uropod, with extension of the first and retraction of the latter happening synchronously to ensure a smooth forward movement. Front and rear are characterised by different molecular equipment: active Rac, for instance, is confined at the leading edge and excluded from the trailing edge. In the absence of WASP, *Dictyostelium* accumulate active Rac at the rear, leading to a sort of bipolar phenotype (Davidson, 2014). The presence of active Rac at the rear conflicts with the acto-myosin contractility, which normally allows uplifting of the trailing edge, and this in turn leads to defective uropod retraction. To the best of our knowledge, such an effect of WASP deletion on spatial restriction of active Rac has not yet been reported. However, it would be interesting to address whether the uropod retraction defect observed in Zebrafish (hematopoietic) WASp knockout neutrophils (Jones et al., 2013) is due to aberrant accumulation of Rac in its active state.

1.3.6.4 *Dictyostelium* WASP may play a role in starvation survival

Another unexpected feature of *Dictyostelium* WASP knockout is its reduced ability to grow in minimal medium, which instead supports the proliferation of wild type cells (Davidson, 2014). Their requirement for highly permissive growth conditions is likely responsible for the inability of WASP knockout cells to

efficiently aggregate into a fruiting body upon nutrient deprivation (Davidson, 2014). As for maintenance of cell polarity, the involvment of WASP in starvation survival has not been reported before.

The requirement of a CRIB motif for WASP's role in CME, the front–rear polarity defect of the WASP knockout and its reduced ability to handle nutrient deprivation are key topics of this thesis and will be discussed in depth in the following chapters.

1.3.7 Other notable WASP family members

Other members of the WASP family include the aforementioned SCAR/WAVE, WASH, WHAMM and JMY.

1.3.7.1 SCAR/WAVE

SCAR (suppressor of cAR1) was simultaneously identified in *Dictyostelium* (Bear et al., 1998) and mammals, where it is more frequently referred to as WAVE (WASP-family Verprolin-homologous) (Miki et al., 1998b). Similarly to WASP, non-metazoans and invertebrates only express one SCAR paralogue, while vertebrates express multiple paralogues. For instance, the human genome encodes three WAVE isoforms, named WAVE 1, 2 and 3 (Veltman and Insall, 2010), while yeasts do not express any (Veltman and Insall, 2010). SCAR/WAVE is stably associated with four other proteins: Sra1 (Specifically Rac binding protein1, also termed CYFIP or PIR121), Nap1 (Nck-associated protein 1, also named Hem-2), HSPC300 (hematopoietic stem/progenitor cell protein 300), and Abi-1 (Abl interactor 1) (Eden et al., 2002); the resulting complex is often referred to as WRC (WAVE regulatory complex). The crystal structure of the complex has revealed that Sra1 and Nap1 are engaged in an extensive network of interactions, providing the remaining three subunits with a large platform for their association (Chen et al., 2010). In the same work it was demonstrated that inclusion of SCAR/WAVE within the complex is required to keep it inactive, as a number of intra- and inter-molecular interactions sequester its VCA domain, preventing its actin-nucleating activity. A number of *in vitro* studies have demonstrated that SCAR/WAVE is activated in response to co-incident signals; among these, Rho GTPases (mostly prenylated GTP-bound Rac) and acidic phospholipids (predominantly PIP3) have been proposed to play a key role

(Lebensohn and Kirschner, 2009). Intriguingly enough, SCAR/WAVE does not itself harbour a Rac binding domain, but this can still exert a regulatory effect via direct interactions with other subunits of the complex. It is therefore worth asking whether the inclusion of SCAR/WAVE within the heteropentametic complex has also evolved to allow its Rac-mediated regulation. *In vivo* data regarding the role of PIP3 in SCAR/WAVE activation are less black-and-white than *in vitro* data. The absence of membrane-bound PIP3, obtained by knocking out all the known PI3 kinases, does not affect the ability of *Dictyosteliun* to protrude and move directionally, but does affect its ability to generate macropinosomes and grow at a normal rate in liquid medium (Hoeller and Kay, 2007). This finding provocatively suggests that PIP3 might not be required to activate SCAR/WAVE at the leading edge of migrating cells. It is important to point out, however, that this work was published before discovering that WASP can replace SCAR/WAVE at the leading of migrating cells (Veltman et al., 2012), and data available thus far are not sufficient to confirm that the protrusions generated in the absence of PIP3 are genuinely SCAR/WAVE-driven and not at all WASP-dependent. More recent evidence seems to further discredit a role for PIP3 in the activation of SCAR/WAVE at the leading edge: it has been shown that the presence of a PIP3 patch on the membrane strongly favours the formation of a macropinosome, with SCAR/WAVE being only recruited at the very tip, while discouraging the extension of a pseudopod (Veltman et al., 2014). Other players in the activation of SCAR/WAVE are SH3 domain-containing proteins (Eden et al., 2002), and kinases (Lebensohn and Kirschner, 2009).

As for its role within cells, the SCAR/WAVE complex is involved in the generation of pseudopodia/lamellipodia (Kunda et al., 2003) and of macropinosomes (Veltman et al., 2014).

1.3.7.2 WASH

WASH (Wiskott Aldrich Syndrome protein Homologue) is expressed in a wide range of eukaryotes, including *Dictyostelium* and humans (Linardopoulou et al., 2007). It is part of a complex (Derivery et al., 2009; Gomez and Billadeau, 2009) that also includes FAM21, SWIP, ccdc53 and Strumpellin. Structural and functional similarities between the WASH and the SCAR/WAVE complexes have been reported (Jia et al., 2010). WASH is inhibited within the complex, and ubiquitination has been proposed to play a role in its activation (Hao et al.,

2013). As for its *in vivo* functions, WASH is mostly targeted to endosomes and plays a role in maintaining their morphology (Derivery et al., 2009; Gomez and Billadeau, 2009). WASH is also involved in cargo sorting both in mammalian cells and *Dictyostelium* (Carnell et al., 2011; Derivery et al., 2009). WASH has more recently found to be involved in autophagy both in mammals and *Dictyostelium*. A study conducted on mouse embryos revealed that WASH negatively regulates autophagy by interefering with the signalling cascade that triggers the formation of omegasomes (Xia et al., 2013). In *Dictyostelium*, WASH appears to allow the maturation of autophagosomes by facilitating the sorting of degrading enzymes (King et al., 2013).

1.3.7.3 WHAMM and JMY

WHAMM (WASP homolog associated with actin, membrane and microtubules) localises at the endoplasmic reticulum (ER)/Golgi interface, where it regulates vesicle trafficking (Campellone et al., 2008). JMY (junction-mediating and regulatory protein) was initially identified as a transcription factor that boosts stress-induced p53 activity (Shikama et al., 1999), but was later described also as a NPF (Zuchero et al., 2009).

More recently, WHAMM and JMY have both been linked to autophagy. WHAMM, for instance, contributes both to the genesis of the autophagosomes and to their movement throughout the cytoplasm (Kast et al., 2015), while JMY seems to ensure efficient autophagosome formation (Coutts and La Thangue, 2015). These works demonstrate that F-actin has a role in autophagy, in agreement with what previously reported (Aguilera et al., 2012). However, they focus the attention on NPFs that are exclusively expressed in vertebrates, while autophagy is adopted by a wide range of organisms throughout evolution. It is therefore worth asking whether other, more evolutionarily ubiquitous, NPFs play a role in the formation and movement of autophagosomes in invertebrates and non-metazoans. This point will be extensively discussed in chapter 5.

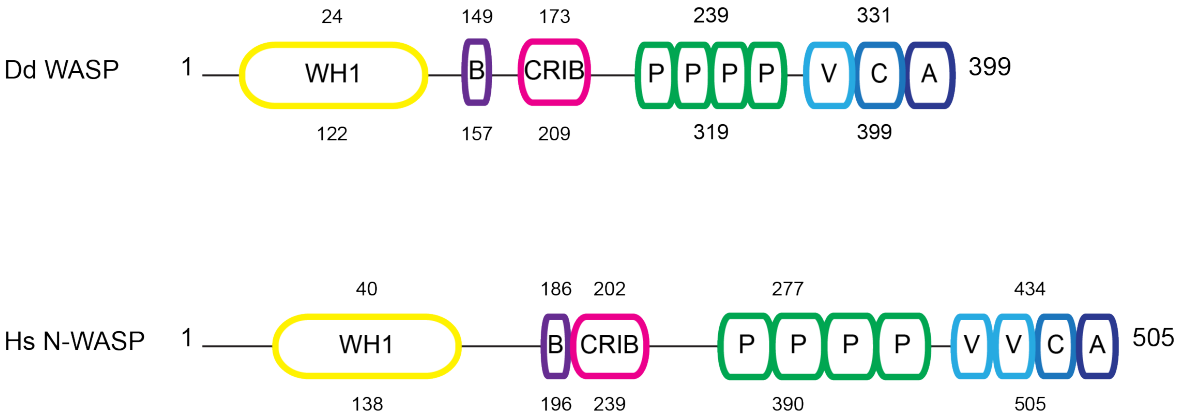

Figure 1.5 Domain composition of Dictyostelium WASP and human N-WASP.

Dictyostelium (Dd) WASP is composed of 399 amino acids, while human (Hs) N-WASP is about 100 residues longer (505 amino acids). They have a similar domain composition. From the N-terminus to the C-terminus they both harbour a WH1 domain (yellow), a basic region (purple), a CRIB motif (pink), a polyproline stretch (green), and a composite VCA domain (shades of blue). Start and end positions of each region are indicated above and below respectively. Human N-WASP harbours an additional V (also referred to as WH2) domain, which originated by duplication of the ancestral V domain during the early stages of metazoans evolution (Veltman and Insall, 2010).

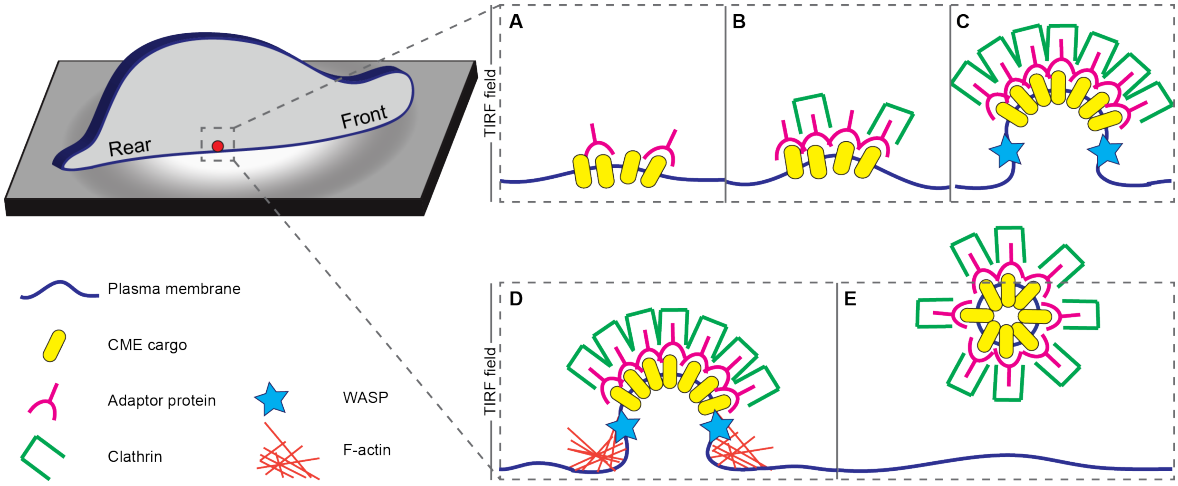

Figure 1.6 Key events during clathrin-mediated endocytosis.

Clathrin-mediated endocytosis (CME) generally occurs on the ventral membrane (in blue) at the rear half of migrating cells.

A) At the onset of CME cargo molecules (in yellow) gather on a defined region of the plasma membrane, where they are recognised by adaptor proteins (in pink).

B) Adaptor proteins act as a bridge between CME cargo and clathrin subunits (in green).

C) Multiple clathrin subunits are recruited to the site of assembly, where they generate a lattice (or triskelion). The plasma membrane enwrapped by the clathrin coat undergoes invagination to allow budding of the pit. WASP (turquoise star) localises at clathrin-coated pits (CCP).

D) WASP triggers the formation of actin filaments (in red) by recruiting and activating the Arp2/3 complex (not shown). F-actin provides the force required to narrow the CCP neck.

E) Following actin polymerisation and CCP closure, the vesicle containing transmembrane cargo and adaptor proteins is released into the cytosol.

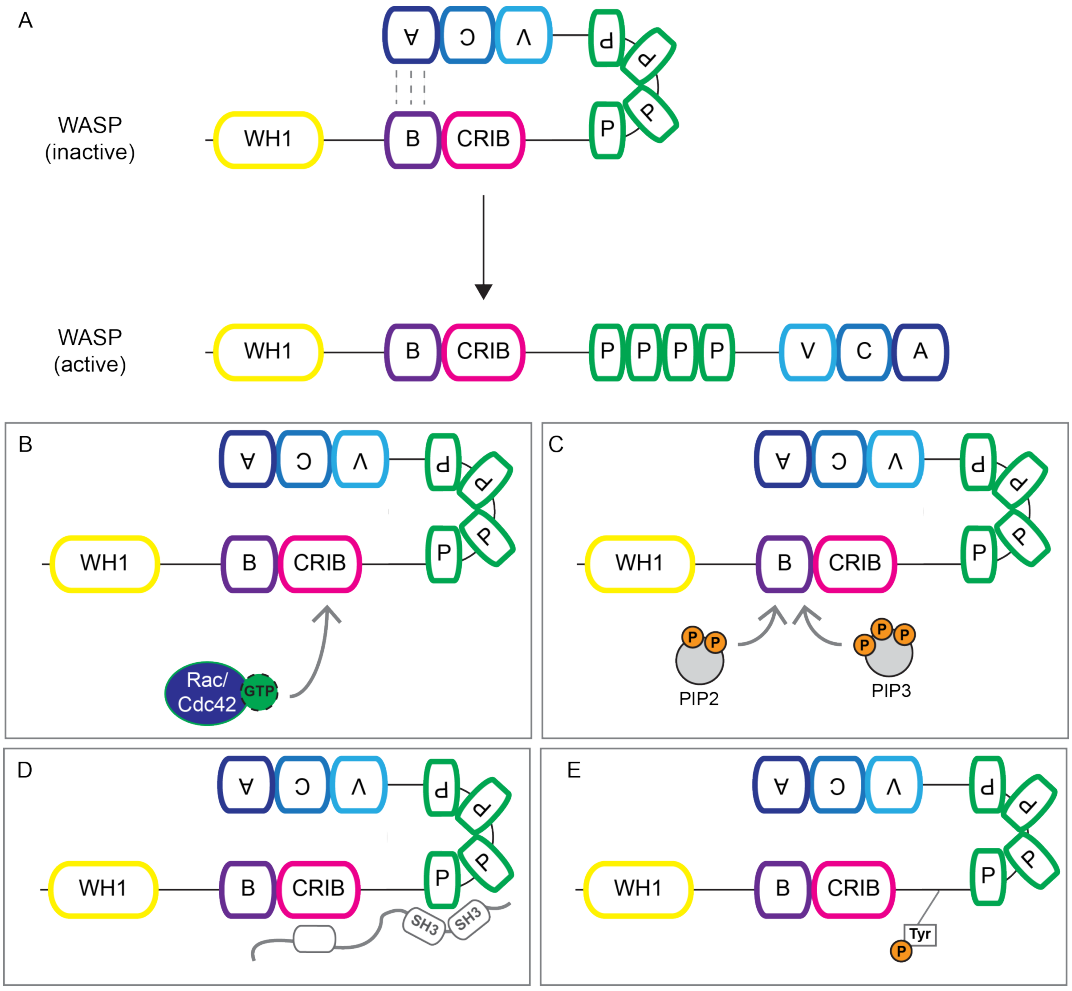

Figure 1.7 Current model of WASP activation.

A) Intramolecular interactions between the C-terminal VCA domain and the N-terminal basic region/CRIB motif (dashed grey bars, upper panel) have been proposed to keep WASP autoinhibited. Multiple activators (listed below) are thought to activate WASP by destabilising the intramolecular interactions that hold WASP in the inactive folding. Once WASP is active, its VCA domain is able to activate the Arp2/3 complex (not shown).

B) Active (GTP-bound) Rho-GTPases (Cdc42 or Rac) have been proposed to activate WASP by interacting with its CRIB motif.

C) Phospholipids, mostly PIP2 and PIP3, are thought to activate WASP by binding with its basic region.

D) SH3 domain-containing proteins (in grey) have been proposed to activate WASP by interacting with its polyproline-rich domain or, in addition, with its CRIB motif.

E) Phosphorylation is thought to contribute to WASP activation by introducing a negative charge, for instance, in proximity of the CRIB motif.

1.4 Rac and maintenance of cell polarity

1.4.1 Introduction

As mentioned in the previous section, loss of WASP compromises the ability of *Dictyostelium* to confine active Rac at the leading edge, resulting in impaired front–rear polarity. Further details on Rac, maintenance of cell polarity, and known correlations between them will be discussed here; much emphasis will be given to the strategies cells utilise to maintain appropriate locations and homeostatic levels of Rac in its active form.

1.4.2 Rac GTPase: evolutionary conservation and structure

Rac is one of the best-characterised members of the Rho family, a group of GTPases belonging to the Ras superfamily. Other notable members of the Rho family include Rho itself and Cdc42. They all are widely represented amongst eukaryotes (Madaule and Axel, 1985). Mammals express multiple Rho and Rac isoforms as well as one Cdc42 (Boureux et al., 2007); the *Dictyostelium* genome encodes several Rac isoforms but no obvious Rho nor Cdc42 (Rivero et al., 2001); yeasts possess many Rho isoforms, one Cdc42, but no discernible Rac (Boureux et al., 2007). Most eukaryotes also express a number of non-conventional Rho GTPases, whose roles and regulation are often still a mystery. All conventional Rho GTPases interact with a guanine-nucleotide, and the number of phosphate groups within the nucleotide largely determines their activation state: GTP-bound Rac, for instance, is active; GDP-bound Rac is not. Regarding its structure, Rac has a remarkably similar domain composition not only to Rho and Cdc42, but also to other members of the Ras superfamily. Accordingly, most of our current knowledge about the 3D conformation of Rac has been confidently inferred from the resolved crystal structure of Ras (Milburn et al., 1990; Pai et al., 1990). Rac harbours five *G motifs* (G1-G5), small but highly conserved stretches spanning from the N- to the C-terminus of the protein. Each G motif has a specific role (Schaefer et al., 2014). G1, also termed *P-loop*, is responsible for keeping in place magnesium and guanine-nucleotide. G2 and G3 are located within the *switch I* and *switch II* regions respectively. They are responsible for sensing the type of nucleotide bound and for promptly modifying their conformation in response to changes in the number of phosphate groups. G4 and

G5 interact with the base of the nucleotide, also contributing to maintaining it in place. Rac also harbours an *insert region*, which sits in between G4 and G5, and is absent outside the Rho family (Freeman et al., 1996). The insert region mediates the interaction between Rac and its downstream targets, such as mDia formins (Lammers et al., 2008). Lastly, the most C-terminal part of the protein is termed the *hypervariable region*, and harbours the sequence recognised by lipid transferases (Katayama et al., 1991). A schematic representation of the Rac structure is reported in figure 1.8.

1.4.3 Clear and unclear cellular roles of Rac

Over the years Rac has been linked to a wide range of cellular processes; inevitably, not all of them will be mentioned or exhaustively covered here. However, those that are more relevant for the purpose of this thesis, whether clearly demonstrated or still dubious, will be thoroughly discussed.

1.4.3.1 Membrane protrusions

The involvement of Rac in protrusion generation was one of the first to be demonstrated. Injecting fibroblasts with G12V Rac, a mutant that is much less sensitive to inactivation than wild type Rac (Diekmann et al., 1991), causes a dramatic increase in macropinocytosis and membrane ruffling (Ridley et al., 1992). We now know that Rac exerts these functions by regulating the SCAR/WAVE complex, which triggers actin polymerisation at the leading edge as well as at macropinocytic cups in different cell types and organisms, as discussed in sections 1.3.4.2 and 1.3.7.1.

1.4.3.2 Clathrin-mediated endocytosis

The involvement of Rac in CME is unclear. The first study aiming to address it reached the conclusion that active Rac negatively regulates the internalisation of clathrin-coated pits. More specifically, it was demonstrated that the expression of Q61L Rac, a mutant that like G12V Rac is less sensitive to inactivation than wild type Rac (Xu et al., 1994), dramatically impairs the ability of Hela cells to internalise labelled transferrin (Lamaze et al., 1996). Confusingly, in the same study it was shown that the expression of dominant active Rho has a comparable consequence, opening up to the possibility that

what was observed upon dominant active Rac expression may be a secondary, non specific, outcome.

A few years later another group confirmed the inhibitory effect of dominant active Rac on CME and tried to unveil the underlying mechanism (Malecz et al., 2000). In this study it was shown that active Rac interacts with synaptojanin 2, a PI 5-phosphatase, and triggers its recruitment to the membrane. Since constitutively membrane-targeted synaptojanin 2 inhibits CME (Malecz et al., 2000), and since the presence of PIP2 on the membrane had been previously linked to efficient CCPs assembly (Jost et al., 1998), Malecz and colleagues hypothesised that Rac-mediated recruitment of synaptojanin to the membrane could locally deplete PIP2 and compromise the efficiency of the endocytic machinery. However, the recruitment of adaptor proteins, clathrin, or other molecules involved in CME (like WASP, for instance), in the presence of membrane-bound synaptojanin or dominant active Rac, was never addressed.

To date it is not known whether any of the molecules involved in the internalisation of CCPs are recruited at endocytic spots in the presence of dominant active Rac, nor it is understood whether uptake inhibition is directly linked to the role of Rac in CME rather than to unrelated circumstances. An interesting hint regarding the role of Rac in CME comes from an evolution-based perspective: how do yeasts, which do not express any Rac, internalise CCPs? The importance/dispensability of active Rac for the internalisation of clathrin-coated pits will we discussed in the following chapters.

1.4.3.3 Autophagy

Rac has recently been shown to inhibit autophagy. To date, however, there is no conclusive evidence regarding either the Rac isoform involved or the underlying mechanism.

One of the studies showed that Rac1, not Rac2 nor Rac3, exerts a negative effect on autophagy. This work clearly showed that while control cells accumulate LC3- (Light Chain 3, a commonly used autophagosomal marker) positive spots upon starvation, cells expressing dominant active Rac1 fail to do so. Conversely, cells expressing lower levels of Rac1 accumulate LC3 *puncta* even when growing in nutrient medium (Aguilera et al., 2012). A previous study, however, claimed that Rac3 is the isoform that negatively regulates autophagy (Zhu et al., 2011). As the two groups performed the experiments using different

cell lines, it is possible that differences in the levels of expression of the different Rac isoforms accounts for the different outcomes.

1.4.4 Rac regulation: a little goes a long way

An excess of active Rac is a burden that cells struggle to handle: as shown early on by Ridley and colleagues, cells injected with dominant active Rac1 eventually surrender, rounding up and losing adhesion to the substrate (Ridley et al., 1992). The amount of active Rac within the cell must therefore be tightly regulated. Cells use different strategies to activate Rac, maintain its physiological levels and ensure its appropriate localisation.

1.4.4.1 Activating Rac

Rac is inactive when bound to GDP and active when bound to GTP, and the ability to cycle between the two states is of absolute importance for Rac to exert its many functions in a spatially- and temporally-regulated manner. Rac does not cycle efficiently by itself, but GEFs (guanine nucleotide exchange factors), GAPs (GTPase- activating proteins) and GDIs (guanine nucleotide dissociation inhibitors) act as training wheels to ensure a safe ride. GEFs are linked to Rac activation, GAPs negatively regulate it, GDIs seem to have a dual role. For the sake of clarity, it is important to point out that these three classes of proteins regulate the cycling process not only of Rac, but of Ras GTPases in general. Furthermore, our current understanding of their mechanism of action largely comes from pioneering studies on GTPases other than Rac.

GEFs positively regulate Rac by facilitating the exchange of GDP for GTP. This happens through a multistep process: a GEF initially interacts with inactive Rac and facilitates the release of GDP from its nucleotide-binding pocket; the resulting GEF/nucleotide-free Rac complex promptly catches a GTP, leading the way to Rac activation. The first biochemical evidence for such a mechanism came from studies on Ran (another Ras superfamily member) and Ras (Klebe et al., 1995; Lenzen et al., 1998), but the existence of a complex between Rac and its GEFs, Tiam1 (T-cell lymphoma invasion and metastasis-inducing protein 1) for instance, was also proved (Worthylake et al., 2000). Two groups of GEFs, both widely represented among eukaryotes, have so far been discovered: the more numerous Dbl family and the more recently identified DOCKs (Dedicator of cytokinesis) (Cote and Vuori, 2002). Members of the two families harbour a

different catalytic domain: a DH (Dbl-homology) domain in the former case, and DHR2 (DOCK homology region 2) in the latter. Members of both families also possess a domain responsible for membrane targeting. Whether each GEF selectively activates one Rho GTPase or has the ability to regulate multiple ones is often still unclear. For instance Tiam1, which belongs to the Dbl family, can catalise the exchange of GDP for GTP both in Rac1 and Cdc42 *in vitro*, but when expressed in cells, it induces a phenotype that strikingly recapitulates the one induced by dominant active Rac1 (Michiels et al., 1995). This suggests that Tiam1 might be preferentially employed *in vivo* to activate Rac1 despite being also able to regulate Cdc42. On the other hand, Dock180, which is a member of the DOCK family, has been linked selectively to Rac1 both *in vitro* and *in vivo* (Nolan et al., 1998).

It has been recently demonstrated that Rac1 can be SUMOylated (Castillo-Lluva et al., 2010). SUMOylation (SUMO = Small ubiquitin-like modifier) is a post-translational modification that consists of the addition of ubiquitin-like monomers but, unlike ubiquitination, it does not target proteins for degradation. Castillo-Lluva and colleagues initially asked whether the SUMO E3-ligase PIAS3 (protein inhibitor of activated STAT3) could activate Rac1. They proved this not to be the case, as a significant degree of Rac activation still occurs when levels of PIAS3 are reduced. By following the dynamic of active Rac accumulation upon growth factor stimulation, however, Castillo-Lluva and colleagues demonstrated that SUMOylation of Rac helps in maintaining a pool of active molecules.

1.4.4.2 Localising Rac

Lipidations are largely responsible for localising Rac and other GTPases to the appropriate membranous compartments. As previously mentioned, these post-translational modifications occur at their C-terminal hypervariable region, which harbours a conserved CAAX box (C=cysteine, A=any aliphatic residue, X=any residue). Targeting Rac to the right place requires two major steps. The first phase occurs in most Ras GTPases and consists of three steps collectively named the *prenylation cycle*. First, a 15/20-carbon isoprenyl group is linked to the cysteine within the CAAX box. Second, a protease cleaves the three residues that follow the modified cysteine. Third, the prenylated cysteine undergoes carboxymethylation. At this stage, the C-terminally processed GTPase can be sequestered within the cytosol. The second phase appears to confer specificity

of localisation. In the case of Rac1 a polybasic region located immediately upstream of the CAAX box has been shown to contribute to its localisation to the plasma membrane (Michaelson et al., 2001). A more recent study has further investigated the mechanisms underpinning the specificity of Rac localisation, unveiling the key role of a second lipid modification. It has been shown that palmitoylation of a cysteine residue placed near the aforementioned polybasic stretch is required for Rac localisation at the plasma membrane (Navarro-Lerida et al., 2012).

1.4.4.3 Sequestering, inactivating and degrading Rac

In order to avoid the dramatic consequences of high levels of active Rac, cells can sequester it, inactivate it, or target it for degradation.

GDIs are a very versatile tool that cells can use to stall Rac and other Rho GTPases. As revealed by the crystal structure of the Cdc42/GDI complex (Hoffman et al., 2000), GDIs harbour two major domains: a large geranygeranyl-binding region, which interacts with the lipidated C-terminus of the GTPase, and a smaller regulatory domain, which is engaged in interactions with the switch I and II regions of the GTPase. On one hand, GDIs can interact via their regulatory arm with the inactive form of Rho GTPases and hinder GDP release, therefore shielding them from the activity of GEFs (Leonard et al., 1992). On the other hand, GDIs can mediate the extraction of Rho GTPases from the membranes via a 2 step-process that requires their geranylgeranyl-binding domain (Nomanbhoy et al., 1999). As most of their functions require membrane targeting, GDI-mediated extraction presumably renders GTPases ineffective. Besides sheltering Rho GTPases from GEFs and removing them from the membrane, GDIs are also able to slow down the hydrolysis of GTP, therefore maintaining Rho GTPases in their active state (Hart et al., 1992). This apparently conflicting role of GDIs clearly testifies to the extremely tangled regulatory system of Rho GTPases.

GAPs negatively regulate Rac and other Rho GTPases by enhancing their intrinsic ability to hydrolyse the γ-phosphate of the nucleotide. They harbour a RhoGAP domain, a 150 residue-long stretch that includes a conserved *catalytic Arginine*. In the 3D structure of the GAPs, the catalytic Arginine is localised on a finger-like loop. Important details regarding their mechanism of action were unveiled when the crystal structure of the transition state of the Cdc42/Cdc42GAP complex was resolved (Nassar et al., 1998). The GAP interacts with the switch I

and switch II regions of the GTPase, causing its rotation; within the newly formed complex, the Arginine finger of the GAP faces a Glutamine residue of the GTPase backbone, which coordinates a molecule of water. It has been proposed that in the absence of GAPs the *hydrolytic water* molecule might not be stabilised enough to trigger the γ-phosphate hydrolysis; the juxtaposition of GAP's Arginine and GTPase's Glutamine might strengthen its coordination, allowing the hydrolytic reaction.

Rac is a target for different kinases, and its phosphorylation is generally linked to inactivation. Two Rac1 residues, Tyr64 and Ser71, located within or in close proximity to the switch II region, appear to be particularly sensitive to phosphorylation. Importantly, both residues are conserved in *Dictyostelium* Rac1A. Src- and Fak-mediated phosphorylation at tyrosine 64 negatively regulates Rac activity, as demonstrated by the drastically reduced amount of membrane ruffles in the presence of a phosphomimetic mutant Rac1A. From a mechanistic point of view, it has been suggested that phosphorylation of Tyr64 stabilises the interaction between Rac and its GDI, making Rac inaccessible to GEFs (Chang et al., 2011). Similarly, Akt (RAC-alpha serine/threonine-protein kinase)-mediated phosphorylation on Ser71 has been shown to inhibit Rac activity by substantially reducing its ability to bind GTP (Kwon et al., 2000).

Lastly, Rac is subjected to poly-ubiquitination, which results in its proteasome-mediated degradation. Two Rac1 Lysine residues have so far been reported as docking sites for ubiquitin chains: Lys147 and Lys166, both located between insert and hypervariable regions. Ubiquitination of Lys147 is mediated by c-IAP1 (cellular inhibitor of apoptosis 1) and XIAP (X-linked IAP) (Oberoi et al., 2012), while SCF (Skp1-Cul1-F-box) is responsible for linking a polyubiquitin chain to Lys166 (Zhao et al., 2013). Of interest, it has been shown that SCF can exert its function only on Rac1 molecules that have been previously phosphorylated by Akt on Ser71, highlighting once again the high degree of interconnection between different regulatory mechanisms. Remarkably, Lys147 and Lys166 are conserved in *Dictyostelium* Rac1A.

1.4.5 Cell polarity in motile cells

Acquiring and maintaining asymmetric morphology and uneven molecule distribution is a priority for most cells and organisms, as it underpins many fundamental events. From an evolutionary point of view, symmetry breaking is

as important for unicellular organisms as it is for multicellular ones. *S. cerevisiae*, for instance, breaks its polarity to form a bud at the onset of mitosis, or to extend a mating projection at the start of a sexual reproductive cycle. As a motile single cell, *Dictyostelium* relies on a clear distinction between a leading edge and a trailing edge to move forward smoothly. Multicellular organisms require polarisation during embryogenesis, to establish the antero-posterior and dorso-ventral axes, but also as adults, since specialised functions of different tissues are often achieved through asymmetric architecture. This thesis shall focus on front–rear polarity, a remarkably important feature not only of *Dictyostelium* but of motile cells in general. Much attention will be given to the role of Rho GTPases, lipids and mechanical properties of the cells to establish and maintain it.

1.4.5.1 Cdc42: master regulator of cell polarity, but how universal?

When it comes to linking cell polarity and Rho GTPases, Cdc42 is the best bet for most. Indeed, Cdc42 has been shown to regulate polarisation both in non-motile and motile cells. In *S. cerevisiae*, for instance, loss of Cdc42 impairs the ability of the cells to acquire the highly polarised morphology required for budding (Adams et al., 1990). Likewise, Cdc42 inhibition affects the ability of fibroblasts and neutrophil-like HL60 cells to extend a single dominant front (Nobes and Hall, 1999; Srinivasan et al., 2003). The mechanisms underlying Cdc42-mediated polarisation in motile cells are not entirely clear. As Cdc42 contributes to re-orienting the microtubule-organising centre (MTOC) toward the migratory front (Palazzo et al., 2001), and that the Golgi apparatus re-orients along with it (Kupfer et al., 1982), it has been proposed that Cdc42 might engage the microtubules to supply the leading edge with Golgi-derived vesicles enriched in factors that promote the extension of protrusions. However, this cannot be a universal mechanism, since in other cell types, such as lymphocytes, the Golgi apparatus does not face the direction of movement (Gudima et al., 1988). A universal role for Cdc42 in polarity establishment is further challenged by the fact that cells that do not express any Cdc42 isoform, like *Dictyostelium* for instance (Rivero et al., 2001), are still perfectly capable of polarisation.

1.4.5.2 PIP3: spatially restricted, but how indispensable?

PIP3 is confined at the leading edge in different types of moving cells, including *Dictyostelium* (Meili et al., 1999; Parent et al., 1998), neutrophils (Servant et al., 2000) and fibroblasts (Haugh et al., 2000). The exclusion of PIP3 from the rear depends on the phosphatase PTEN, which accumulates at the trailing edge and locally depletes it. The exclusion of PTEN from the leading edge, on the other hand, seems to rely on Cdc42, while activation of Cdc42 at the leading edge might depend on PIP3 (Li et al., 2003). Evidence provided by Li and colleagues highlights the existence of feedback loops that connect different regulatory pathways, and support a role for PIP3 in establishment of cell polarity. More recent evidence, however, conflicts with a model whereby PIP3 has a determinant role in polarisation. Indeed, in the absence of PIP3 *Dictyostelium* is still able to polarise and chemotax efficiently (Hoeller and Kay, 2007), meaning that the uneven distribution of PIP3 is not required for symmetry breaking.

1.4.5.3 Rho: watching the cell's back, but how crucial?

Rho is considered to be involved in rear retraction. Supporting evidence for such a model came from a study on monocytes, whereby Rho inhibition impaired their ability to retract their trailing edge (Worthylake et al., 2001). Confinement of Rho at the rear may be mediated by Rac, which has been shown to down-regulate its activity (Sander et al., 1999).

However, whether Rho is or not a universal factor for trailing edge retraction is debatable. Similarly to what was already asked in regards to Cdc42, how do cells that do not express any Rho orthologue, such as *Dictyostelium* (Rivero et al., 2001), retract their rear?

1.4.5.4 Rac: it all comes down to it

While, as already mentioned, dominant negative Cdc42 does not affect the ability of the cells to protrude, and PIP3 is not required to establish and maintain a defined leading edge, Rac homeostatic levels and asymmetric distribution is absolutely essential. On one hand, cells expressing dominant negative Rac cannot extend any protrusions in response to stimuli (Ridley et al., 1992), and Rac1-depleted mouse melanoblasts are drastically (although not completely) compromised in their ability to protrude (Li et al., 2011). On the

other hand, expression of constitutively active Rac causes the entire cell perimeter to ruffle, completely abolishing cell polarity (Srinivasan et al., 2003). Therefore, controlling the levels of active Rac and ensuring its spatially confined distribution are tasks that motile cells need to constantly address. The mechanisms underpinning the confinement of active Rac at the leading edge have been extensively investigated. *In vitro* evidence supports a model whereby PIP3 interacts directly with Rac1 and stimulates its GDP dissociation (Missy et al., 1998), presumably facilitating the action of other activators. However, the same work showed that Rac1 can also bind PIP2 (although to a lesser extent), and that RhoA is equally capable of interacting with both lipid species. It is therefore difficult to establish whether a direct interaction between PIP3 and Rac could account for its confinement at the leading edge. PIP3 has also been indirectly linked to Rac activation via interaction with its GEFs. P-Rex1, for instance, was initially identified as a PIP3-sensitive Rac activator in neutrophils (Welch et al., 2002). Again, in light of recent evidence pointing at the dispensability of PIP3 for protrusion formation, it is difficult to picture PIP3-mediated Rac activation or PIP3-mediated GEFs localisation as key events in the formation of protrusions and establishment and maintenance of front–rear polarity. Indeed, possible mechanisms of Rac1 activation that do not depend on PIP3 have been proposed. For instance, it has been shown that Rac and its GEF Tiam1 are recruited to early endosomes, and that trafficking of these vesicles suffices for confining its localisation at the leading edge (Palamidessi et al., 2008). More recently, an extremely fascinating new hypothesis on how active Rac is confined to the leading edge has been tested. Shifting their focus onto the mechanical properties of cells, Houk and colleagues have elegantly unveiled a major role for membrane tension in maintaining one dominant migratory front. Evidence provided led to a model whereby extension of a protrusion causes an increase in membrane tension that propagates across the entire cell, acting as a long-range inhibitor to prevent the formation of secondary leading edges (Houk et al., 2012). This work represents a great step forward both for the cell polarity and motility fields, at least for two reasons. On one hand, taking into account the mechanical features of the cells, not just their biochemical ones, it provides an original and valuable perspective to look at cells migrating within the context of a multicellular organism: how does the environment affect tension? And how are changes in tension translated into cellular responses? On the other hand, by

focusing its attention on the plasma membrane and actin cytoskeleton, common ground of all motile cells (unlike some signalling molecules), it provides a unifying model that can explain maintenance of cell polarity in potentially all motile cells, no matter their position in the evolutionary tree.

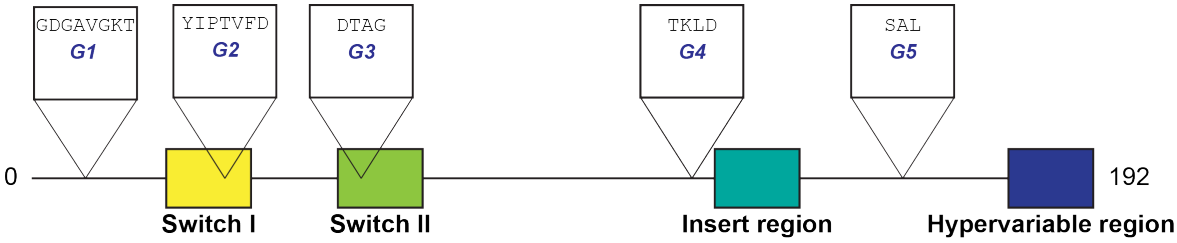

Figure 1.8 Rac domain composition.

Rac consists of four domains. The switch I (in yellow) and switch II (green) regions are located in the N-terminus and harbour the G2 and G3 motifs respectively. These domains are involved in nucleotide sensing. The insert region (in teal) mediates the interaction of Rac with its effectors. The hypervariable region (in blue) is located at the C-terminus and harbours a short stretch required for Rac to be targeted to the membrane. Outside the four major domains, Rac harbours five shorth stretches, referred to as G motifs. Beside the aforementioned G2 and G3 motif, the G1 (p-loop) interacts with magnesium and nucleotide, holding this in place. G4 and G5 also contribute to maintaining the nucleotide in place.

1.5 Aims of the thesis

1.5.1 Dissecting the role of WASP in maintenance of cell polarity

Loss of *Dictyostelium* WASP leads to defective clathrin-mediated endocytosis and impaired front–rear polarity (Davidson, 2014). While the former was not an overly surprising consequence, given the involvment of WASP orthologues in the internalisation of clathrin-coated pits in *Drosophila*, yeasts and mammals (Kochubey et al., 2006; Madania et al., 1999; Merrifield et al., 2004), the latter was unforeseen.

We aimed to understand the mechanisms underlying WASP-mediated spatial confinement of active Rac, starting by clarifying whether it is linked to its more established role in CME or represents a novel, CME-unrelated, function.

1.5.2 Clarifying the importance of Rac on WASP functionality

WASP harbours a CRIB motif, which suggests it may be a downstream effector of Rho GTPases (Burbelo et al., 1995). Accordingly, early works proposed a role for Cdc42 or Rac on WASP activation (Han et al., 2006; Miki et al., 1998a; Rohatgi et al., 1999; Tomasevic et al., 2007). These pioneering studies addressed the role of Rho GTPases on WASP activation often by using a purely biochemical approach. As a consequence, it is widely assumed but not thoroughly assessed whether in living cells WASP requires Rho GTPases indiscriminately, or whether these may be dispensable for WASP to accomplish some of its functions.

We decided to clarify the relative importance of Rac on WASP functionality during both clathrin-mediated endocytosis and protrusion generation.

1.5.3 Addressing the requirement of WASP for starvation survival

Dictyostelium WASP knockout cells have a reduced ability to proliferate in suboptimal circumstances and to handle nutrient-deprived conditions (Davidson, 2014). As with most eukaryotes, *Dictyostelium* relies on the autophagic pathway to overcome nutrient starvation. We therefore sought to understand whether WASP may be involved in autophagy.

Chapter 2 , *Materials & Methods*

2.1 Molecular Biology

Many of the experiments described in this thesis required the use of expression vectors. In some cases the DNA of interest had been previously amplified and inserted into a cloning vector, from where it could easily be cleaved and cloned into an appropriate expression plasmid (molecular subloning). In other cases a cloning vector containing the desired DNA sequence had not yet been generated in the laboratory. The fragment of interest had to be amplified from a template and introduced into a cloning plasmid, which could subsequently be utilised to generate an expression vector (molecular cloning).

2.1.1 Amplification and purification of the DNA of interest

When a cloning vector containing the desired fragment was not already available the DNA of interest was amplified by PCR (Polymerase Chain Reaction) using PrimeSTAR® Max DNA Polymerase (Clontech), which contains enzyme, buffer and dNTPs. Primers were added to the final concentration of 0.5 µM. Since most of the expression vectors used contain BglII/SpeI target sequences at the cloning site (Veltman et al., 2009a), primers were designed so that sequences recognised by BamHI (which generates compatible ends to those generated by BglII) or SpeI would flank the PCR product. Primers used to obtain some of the data presented in this thesis are listed in section 2.6. The template used for amplification was either genomic DNA/cDNA extracted from wild type *Dictyostelium* cells (AX3) or a previously purified plasmid. When possible, the number of amplification cycles used was <20. PCR products were checked via electrophoresis on agarose gel using O'GeneRuler 1 kb DNA Ladder (ThermoFisher) as a size indicator. If correct, amplified fragments were purified from the agarose gel using Zymoclean™ Gel DNA Recovery Kit (Zymo research) according the manifacture's protocol.

2.1.2 TOPO™ Cloning

The purified fragment of interest was generally inserted into a pCR™-Blunt II-TOPO™ vector using the Zero Blunt® PCR Cloning Kit. This is a quick process (30 minutes at room temperature) that does not require any ligase since the *Vaccinia* virus DNA topoisomerase I is already bound to the linearised plasmid. Furthermore, as DNA insertion disrupts the expression of a lethal *E. coli* gene, it allows reliable selection of bacteria expressing the fragment of interest.

2.1.3 Bacteria transformation

The TOPO™ vector possibly harbouring the DNA of interest (hereafter *TOPO vector*) was introduced into chemically competent DH5α *E. coli* by heat shock. A 100 µl aliquot of bacteria (stored at -80° C) was defrosted on ice and transferred into a new ice-cold tube. After addition of 1 µl of the TOPO vector the tube was kept on ice for 20 minutes and then transfered into a 42° C water bath for 1 minute and 15 seconds. 400 µl of warm SOC broth was then added to the heat-shocked bacteria and the resulting mix incubated for 1 hour at 37° C in shaking conditions (200 rpm) to allow the expression of the kanamycin resistance gene located in the TOPO vector backbone. The entire volume was later plated on a LB (Lysogeny Broth) agar plate containing 50 µg/ml of Kanamycin, which allows seletion of transformed bacteria, and incubated overnight at 37° C. Multiple individual colonies were picked after ≈ 16 hours and grown in 5 ml of LB medium plus antibiotic overnight at 37° C in shaking culture (200 rpm). Bacteria were then pelleted by centrifugation at 3000×g for 10 minutes at room temperature, the supernatant discarded, and the DNA extracted from the pellet manually using Monarch® Plasmid Miniprep Kit (New England BioLabs) or robotically using a Qiagen 8000 Bio-Robot. The isolated DNA was then verified by restriction enzyme digestion and/or by sequencing.

2.1.4 Cloning and expression vectors digestion

Cloning and expression vectors were digested with the appropriate restriction enzymes from New England BioLabs. The most commonly used enzymes were BamHI/SpeI or NgoMIV for cloning vectors and BglII/SpeI or NgoMIV for expression vectors. All digestions were carried out overnight in a 37° C water bath. Digested expression vectors were treated with 0.5 µl of CIP (Calf Intestinal Alkaline Phosphatase, New England BioLabs) for 30 minutes at room temperature; this step is required to prevent reclosure of the plasmid. Cloning and expression plasmids were then verified via electrophoresis on agarose gel, again using O'GeneRuler 1 kb DNA Ladder (ThermoFisher) as a size indicator. The desired fragments were purified from the agarose gel using Zymoclean™ Gel DNA Recovery Kit (Zymo research), and the amount of DNA measured using NanoVue (GE Healthcare Life Sciences).

2.1.4 Ligation and bacterial transformation

Purified fragment of interest and linearised expression vector were ligated using T4 DNA ligase and the accompanying 5X rapid ligation buffer (ThermoFisher). When possible, the optimal ratio insert/expression vector used was 3:1. Ligation was carried out at room temperature for 30 minutes, and a negative control devoid of insert was included. A small volume (generally 1 µl) of ligated plasmid was then introduced in chemically competent DH5α *E. coli* cells by heat shock as described in section 2.1.3. Multiple individual colonies were grown in 5 ml of LB medium in the presence of antibiotic (ampicillin or kanamycin, both used at 50 µg/ml) overnight at 37° C in shaking culture (200 rpm). A small aliquot of each tube was temporarily stored in 10% glycerol and bacteria were then pelleted for 10 minutes at room temperature. The supernatant was discarded and the DNA extracted from the pellet using a Qiagen 8000 Bio-Robot. Each miniprep was then digested for 3-4 hours at 37° C using informative restriction enzymes, and the size of the fragments obtained verified by electrophoresis on agarose gels. One correct clone was then chosen, and the stored DH5α grown at a larger scale (250 ml of LB medium plus antibiotic) for ≈ 16 hours at 37° C in shaking culture (200 rpm). Bacteria were then pelleted (3000×g at room temperature for 10 minutes), the supernatant discarded and the DNA extracted from the pellet using Invitrogen Purelink Plasmid Filter Purification Kit. The plasmid obtained was suitable for transient transfection of *Dictyostelium*. Expression plasmids utilised in this work are listed in section 2.7.

2.2 Cell Biology

2.2.1 Cell Culture

All cell lines utilised for the experiments described in this thesis are axenic strains, meaning that they are able to proliferate in the absence of living prey. As described in section 1.1.5, cells isolated from the wild were long ago subjected to a selection process aiming to render them more suitable for laboratory work. Unlike cells recovered straight from the wild, axenic strains do not need to be co-cultured with bacteria as they uptake liquid nutrients via an increased rate of macropinocytosis that is caused by mutations in a RasGAP-encoding gene (Bloomfield et al., 2015). One of the most widely used axenic strains, namely AX3, is often referred to as *wild type*. It is important to mention that despite having been extensively used to generate knockout strains, it differs from cells isolated from the wild. Strains utilised for the work presented in this thesis are listed in section 2.5. Unless otherwise stated, all strains were grown at 22° C on Petri dishes containing 10 ml of HL5 medium (Formedium) or HL5 medium including Glucose supplemented with vitamins and micro-elements (Formedium); in both cases penicillin and streptomycin (ThermoFisher) were added to a final concentration of 100 Units/ml and 100 µg/ml respectively. WASP knockout cells (AD7_1, IR204) were grown in the presence of blasticidin (10 µg/ml) as the blasticidin resistance (BsR) cassette was insert into the endogenous *wasA* locus to disrupt it (Davidson et al., 2018).

2.2.2 Cell Transfection

Dictyostelium cells were transiently transfected by electroporation. Adhering cells were resuspended in the growth medium and pelleted by centrifugation (380×g, 3 minutes at room temperature) using a tabletop centrifuge. Most of the medium was removed by aspiration and cells were spun down again using the same conditions as above. The remaining medium was completely removed and the pellet resuspended in ice-cold E-buffer (Electroporation buffer) at a concentration of ≈ 1×10^7 cells/ml. Cells were quickly transferred into chilled 2mm gap cuvettes (cell projects) along with 1-5 µg of extrachromosomal vector; electroporation was carried out at 500 V using ECM 399 Electroporation System (Harvard Apparatus U.K.). Electroporated cells were immediately returned into Petri dishes containing 10 ml of medium. Cells expressing the extrachromosomal

plasmid were selected after 24 hours by addition of either 50 µg/ml of hygromycin or 10 µg/ml of G418. Cells were maintained under selection thereafter.

2.2.3 Cell Fixation and Staining

13 mm round borosilicate glass coverlips (VWR International) were prepared prior to cell fixation as follows: treated with 80% nitric acid for 15 minutes, washed 10 times in distilled water and then twice in pure ethanol. Washed coverslips were allowed to dry under a fume hood and kept sterile thereafter. Cells were allowed to adhere for 30 minutes on washed and sterile coverslips in multiple wells of a 6well plate. Adherent cells were fixed for 15 minutes in a fixative solution containing 2% formaldehyde, 10 mM PIPES and 15% picric acid. Fixed cells were washed twice in PBS and then permeabilised with 0.2% triton X-100 diluted in PBS for 5 minutes. This was followed by a wash with 0.75% glycine diluted in PBS, a step that is required to quench the remaining formaldehyde. Coverslips were subsequently incubated for 30 minutes with blocking buffer consisting of 3% BSA (Bovine Serum Albumin) diluted in PBS. This was followed by a 1-hour incubation with the primary antibody of interest diluted as required in blocking buffer. Coverslips were then washed twice in PBS and then incubated for 1 hour with the appropriate secondary antibody (i.e. 568 goat anti-Rabbit). Coverslips were washed twice in PBS before being mounted using ProLong™ Gold Antifade Mountant with DAPI (ThermoFisher), and stored overnight at 4° C before being visualised.

2.2.4 Cell Survival in Minimal Medium

This assay was carried out to assess the ability of WASP knockout and parental cells to survive amino acid starvation. The survival rate is measured in terms of number of clear points that are generated on a bacterial lawn at regular time points following amino acid deprivation. WASP knockout and parental cells were resuspended in HL5 medium and pelleted at 380×g for 3 minutes at room temperature using a tabletop centrifuge. The pellet was then resuspended and washed three times in SIH without Arginine and without Lysine (Formedium). 5×10^5 cells/ml were subsequently transferred in flasks containing 10 ml of minimal medium and kept at 22° C in shaking conditions (100 rpm). Both strains were harvested at regular time points (every 24 hours) and seeded on SM agar

plates along with bacteria (*Klebsiella aerogenes*). Surviving amoebas will perform phagocytosis to engulf their prey, leading to local depletion of bacteria and formation of circular clear spots. To facilitate the scoring process serial dilutions (1:10 to 1:10000) of the cell cultures were made.

2.3 Microscopy

2.3.1 Phase contrast microscopy

Phase contrast microscopy was performed to monitor the speed of different cell lines moving up a chemoattractant gradient. Images were acquired using a Nikon ECLIPSE TE2000-E inverted microscope with 20x/0.45 NA or 10x/0.30 NA objectives and equipped with a QImaging Retiga EXi digital camera. Images were generally acquired every 15 seconds over a period of 1-2 hours.

2.3.2 TIRF microscopy

TIRF microscopy was mostly performed to investigate the dynamics of clathrin, WASP and Arp2/3 complex on transient *puncta* generated on the ventral surface of the cell. The system used is a modified Nikon Eclipse TE 2000-U microscope equipped with a photometrics Evolve 512 camera and a DualView DV2 emission splitter. GFP and RFP were excited using a 473 nm and 561 nm wavelength respectively. A 100x/1.40 NA TIRF objective was mostly used. Images were acquired every 1 or 2 seconds for a period of 5 or 10 minutes using the MetaMorph software.

2.3.3 Confocal microscopy

Confocal microscopy was performed to address WASP localisation and dynamics upon expression of dominant active Rac as well as to investigate the ability of WASP CRIB mutants to localise at the leading edge in the presence/absence of SCAR/WAVE. A Nikon Ti-E inverted microscope equipped with a Yokogawa CSU-X spinning disc confocal unit was used in combination with a High resolution Andor Neo sCMOS camera and a Cairn Optosplit to allow dual fluorescence imaging. A 100x/1.4 NA objective was used. GFP was excited at 488 nm, RFP at 561 nm. Images were acquired using the Andor IQ 2 software.

In addition a Olympus FV1000 was utilised, in conjunction with a 60x/1.4 NA objective. Excitation wavelengths of 488 and 561 nm were used for GFP and RFP respectively. Images were acquired using the FV10-ASW 3.0 Software, every 1 or 2 seconds for a period of 5 or 10 minutes.

2.3.4 Super-resolution microscopy

Super-resolution data were obtained using a Zeiss LSM880, a confocal microscope that allows the acquisition of high-resolution images thanks to the presence of an array of 32 individual detectors. This system was used to investigate the degree of co-localisation between WASP and components of the autophagic flux as well as to determine whether Rac could be targeted to nascent autophagosomes. A 63x/1.40 NA objective was used. GFP was excited at 488 nm, RFP at 561 nm. Images were acquired using the ZEN imaging software every 1 or 2 seconds for a period of 5 or 10 minutes. For z-stack acquisitions a distance of 0.19 µm was left between slices.

2.3.5 Microscopy-based assays

2.3.5.1 Under-agarose folate chemotaxis assay

The ability of the cells to confine Rac activity at the leading edge during migration was investigated by performing an under-agarose assay, a widely used set up whereby cells are stimulated to move up a chemoattractant gradient by crawling under a layer of agarose (Laevsky and Knecht, 2001). The conditions used to perform the experiments presented in this thesis strongly favoured pseudopod-based motility of vegetative amoebeas. In preparation for the assay a 50mm glass bottom dish (MatTek) was treated for 10 minutes with 10 mg/ml BSA, a step that aims to reduce the resistance encountered by the cells while these crawl under the agarose. Agarose (Seakem GTG) was dissolved to the final concentration of 0.4-0.6% in LoFlo (Formedium), a low fluorescence medium that has been defined to improve the quality of imaging. 5 ml of the dissolved agarose was then cast on a pre-treated glass bottom dish and allowed to set for 1 hour. Once set the agarose was cut using a scalpel so to create two wells separated by a 5 mm bridge; this was gently wriggled loose to facilitate cells' crawling. Cells of interest were resuspended in HL5 and 1 ml of cell suspension was pelleted at 380×g for 3 minutes at room temperature using a tabletop centrifuge. Most of the medium was removed by aspiration and cells were spun down again under the same conditions as above to completely remove the residual medium. The pellet was then washed in LoFlo and cells counted using CASY® Model TT Cell Counter (Innovatis). Cells were then diluted in LoFlo to a final concentration of 5×10^5 cells/ml, and 200 µl of cell suspension was seeded

on the left well created within the agarose layer. The other well was filled with 100 μM folic acid diluted in LoFlo. A square coverslip was then carefully lowered down in order to cover both wells and prevent evaporation; the glass bottom dish was thereafter incubated at 22° C. Imaging was performed 2-3 hours after setting up the assay, when a sufficient number of polarised cells could be spotted under the agarose bridge.

2.3.5.2 EHT1864 treatments

Cells expressing a red-tagged active Rac marker (pakB CRIB-mRFPmars2) or a GFP-tagged WASP were resuspended in HL5 and measured using CASY® Model TT Cell Counter (Innovatis). Cells were pelleted at 380×g for 3 minutes at room temperature using a tabletop centrifuge and the medium removed by aspiration. Cells were spun down again using the same conditions as above and the residual medium completely removed. The pellet was resuspended in LoFlo to a concentration of 10^7 cells/ml and a low volume (10 μl) of cell suspension seeded on a borosilicate glass 8well chamber (ThermoFisher) containing 190 μl of LoFlo; cells were allowed to adhere for 1 hour. In the meantime the Rac inhibitor EHT1864 (Onesto et al., 2008) was diluted in LoFlo at 2X the final concentrations (50 μM to 100 nM). Imaging was performed prior to addition of the inhibitor (to monitor the dynamics of the probe in the presence of active Rac), during addition of the drug (to visualise its most acute effects) and for 15-20 minutes after treatment (to verify whether cells could recover).

2.3.5.3 Induction of G12V Rac1 expression

Cells expressing G12V Rac1A under a doxycycline-inducible promoter along with GFP-WASP or RFP-tagged active Rac marker were resuspended in HL5 and 1 ml of cell suspension was pelleted at 380×g for 3 minutes at room temperature using a tabletop centrifuge. Most of the medium was removed by aspiration and cells were spun down again to allow complete removal of remaining HL5. Cells were resuspended in LoFlo or SIH, counted using a CASY® Model TT Cell Counter (Innovatis) and seeded in 2 ml of LoFlo or SIH to a final concentration of 5×10^5 cells/ml on a borosilicate glass 8well chamber (ThermoFisher) or on a 35 mm glass bottom dish (MatTek). After 1 hour all cells were adherent and doxycycline was added to a final concentration of 10 μg/ml to yield G12V Rac1A expression

(Veltman et al., 2009b). Timelapse acquisition (generally 5 seconds interval for 2-3 hours) was started shortly after.

2.3.6 Image processing

Images acquired using phase contrast, TIRF or confocal microscopes were exported as .TIFF files while those acquired using the super-resolution confocal were exported as .CZI files. Images were all imported into Fiji software (Schindelin et al., 2012) and processed as required, including cropping and linear brightness/contrast adjustment. TIRF images were processed using the Windowed-Sinc Filter (Kunito Yoshida, Department of Biological Sciences, Imperial College London), which is often adopted during signal processing. Clathrin, WASP and Arp2/3 complex *puncta* lifetime was quantified using the MTrackJ plugin (Meijering et al., 2012). The same plugin was utilised along with a Chemotaxis Tool plugin (Gerhard Trapp and Elias Horn, ibidi GmbH) to measure speed and directionality of migrating cells. Kymographs were obtained using the reslice tool available in Fiji, which allows visualisation of the fluorescence intensity of a probe of interest across a straight line over time. Images acquired using the super-resolution confocal microscope were subjected to Airyscan processing, which allows to obtained a more resolved image by reassigning information generated by individual detectors within the composite array.

2.4 Biochemistry

2.4.1 GST-Rac1A/GST-RacC Pulldown assay

Pulldown assays typically required 5 days.

Day 1.

E. coli BL21were transformed with purified pGexRac1A or pGEXRacC as described in section 2.1.3. Heat-shocked cells were then plated overnight on ampicillin-containing SM plates.

Day 2.

One BL21 colony was picked, transferred to a round bottom Polystyrene tube containing 5 ml of LB medium and ampicillin and grown at 37° C in shaking conditions (200 rpm). After ≈ 7.5 hours (average time needed) the bacterial suspension to reach the OD_{600} of 2, and a small volume (250 µl) was transferred to a flask containing 2.5 L of LB and ampicillin. This was kept at room temperature overnight in shaking conditions (100 rpm). A small aliquot of bacterial suspension was stored at -80° C in the presence of 10% glycerol for later experiments.

Day 3.

The OD_{600} of the bacterial culture was checked at regular intervals using a BioPhotometer® (Eppendorf) until it reached the value of 0.4; the average time required was 21 hours. When the desired value was reached cells were induced to express the GST-Rac fragment by addition of 500 µM IPTG (Isopropyl ß-D-1-thiogalactopyranoside). The flask was then kept overnight at room temperature in shaking conditions (100 rpm).

Day 4.

The bacterial suspension was transferred to 1 l plastic tubes kept on ice and spun down at 4° C 3000 rpm for 20 minutes. The supernatant was removed and the pellet lysed in 10 ml of ice-cold bacteria lysis buffer. The final volume (≈ 25 ml) was then transferred into a 50 ml falcon tube kept on ice and sonicated 10 times at the maximum power with 10 seconds interval in between cycles using a Soniprep 150 (MSE). The lysate was then centrifuged at 4° C for 10 minutes at 12096×g using an Avanti J-25 centrifuge (Beckman Coulter); after this step the supernatant (≈ 15 ml) was recovered and the pellet discarded. Meanwhile beads (Glutathione High Capacity Magnetic Agarose Beads, from Sigma-Aldrich) were prepared as follows: 1 ml of beads was washed with 400 µl of Rac buffer,

recovered using a magnet, washed and recovered again and resuspended in Rac buffer to the final volume of 1 ml. Beads and supernatant from bacterial lysate were then incubated for 2 hours on a rotating mixer at 4° C. After 2 hours the beads were washed once with 10 ml of Rac buffer, collected using a magnet and resuspended in Rac buffer to a final volume of 2 ml. At this stage the unbound fraction was stored in 10% glycerol for later experiments. To verify that GST-Rac1A (or GST-RacC) was effectively bound to the beads a small volume of resuspended beads was run on a gel and stained with InstantBlue Protein Stain (Expedeon) after incubation at 100 ° C for 5 minutes in 2x NuPAGE™ LDS Sample Buffer (ThermoFisher). The resuspended beads were then split in two 1.5 ml tubes and incubated with either GDP (Guanosine 5′-diphosphate sodium salt, Sigma-Aldrich) or GTPγs (Guanosine 5′-[β,γ-imido]triphosphate trisodium salt hydrate, Sigma-Aldrich). EDTA and CIP phosphatase were also added to a final concentration of 15 mM and 100 Units respectively. The two tubes were incubated overnight on a rotating mixer at 4° C.

Day 5.

In order to facilitate closure of Rac's nucleotide-binding pocket, magnesium chloride was added to the two tubes to a final concentration of 60 mM; this was followed by 30 minutes incubation on a rotating mixer at 4° C. After this time the beads were captured using a magnet and resuspended in Rac buffer to a final volume of 1 ml; tubes were kept on ice at all times. At this point *Dictyostelium* cells were resuspended in HL5 and pelleted at 600×g for 6 minutes at 4° C; the supernatant was aspirated and cells spun down again using the same conditions as above to allow complete removalof the medium. Generally two confluent plates were used for each cell line. The pellet was resuspended in 1 ml of *Dictyostelium* lysis buffer, left on ice for a few minutes and then spun down at 16000×g for 10 minutes at 4° C. The supernatant was then collected and transferred in a new ice-cold 1.5 ml tube. A variable volume of beads (50-100 µl) was added to the *Dictyostelium* lysate and incubated for 1 hour on a rotating mixer at 4° C. A small aliquot of lysate was kept aside as the input the pulldown will be normalised against after performing a Western blot. After 1 hour the tubes were placed on a magnet and the unbound fraction (often referred to as flow-through) collected and stored in 10% glycerol. The beads were then washed twice with 1 ml of washing buffer. After complete removal of the remaining liquid the beads were resuspended in 60 µl of 2x NuPAGE™ LDS Sample Buffer

(ThermoFisher), incubated at 100 ° C for 5 minutes and ultimately collected using a magnet. The same step was performed with the Dictyostelium lysate previously kept aside. A Western blot was then performed as described in section 2.4.3.

2.4.2 Treatment with NH_4Cl

This assay was performed as described previously (Calvo-Garrido et al., 2011) on either untransfected or transiently expressing GFP-Tkt-1 wild type cells. In both cases cells were resuspended in HL5 and pelleted at 380×g for 3 minutes at room temperature using a tabletop centrifuge. The medium was removed by aspiration and the cells spun down again using the same conditions as above in order to completely remove the medium. The pellet was resuspended in HL5 and cells seeded in 4 wells of a 6well plate. These were allowed to adhere to the bottom of the dish for 1 hour, when ammonium chloride was added to three wells at different final concentrations: 50, 100 and 150 mM; cells in one of the wells were left untreated as a control. The medium was removed after two hours and replenished by fresh HL5 containing ammonium to the same concentration as before. After two hours the medium was removed and cells were resuspended in RIPA buffer and kept on ice for a few minutes. The lysate was then pelleted at high speed (16000×g for 10 minutes at 4° C) and the supernatant transferred in a new ice-cold 1.5 ml tube. A small aliquot of the cell lysate was diluted in the presence of 4x NuPAGE™ LDS Sample Buffer (ThermoFisher) and DTT in preparation of Western blot analysis so that 6 µg of total protein was loaded in each lane.

2.4.3 Western blot

Cells were generally lysed using RIPA buffer, as described in the previous section, or by adding resuspended cells to a boiling mix containing 2x NuPAGE™ LDS Sample Buffer, Halt™ Protease Inhibitor Cocktail and DTT as a reducing agent. In the former case the lysate was kept on ice for a few minutes, pelleted at 16000×g for 10 minutes at 4° C and the supernatant transferred to a new ice-cold 1.5 ml tube. A small aliquot of the lysate (generally 10 µl) was diluted in Precision Red Advanced Protein Assay (Cytoskeleton, Inc.) and the total amount of protein estimated by measuring the OD_{600} using a BioPhotometer® (Eppendorf). The amount of protein loaded on a gel for immunoblotting was

decided based on the efficiency of the primary antibody used. In the latter case cells were boiled for 5 minutes and then spun down at 16000×g for 10 minutes at 4° C. The supernatant was then transferred to a new ice-cold 1.5 ml tube and loaded on a gel. A small volume of prepared samples (10-20 µl) was loaded on NuPAGE™ 4-12% Bis-Tris protein gels (ThermoFisher) and subjected to electrophoresis at 80-150 V for 1-2 hours using NuPAGE™ MOPS SDS Running Buffer (ThermoFisher). PageRuler™ Plus Prestained Protein Ladder (ThermoFisher) was loaded alongside the samples of interest as a molecular weight marker. After 1-2 hours the gel was gently moved to a box containing NuPAGE™ Transfer Buffer (ThermoFisher) and kept for a few minutes on a rocking shaker at 30 rev/min; the same procedure was applied to a pre-cut nitrocellulose membrane (0.45 µm pore size, Amersham™ Protran®, Merck). Proteins were transferred from gel to membrane at 80-100 V for 1 hour. The membrane was then blocked for 1-hour in the presence of 5% semi-skimmed milk (or 5% BSA) diluted in TBS (Tris-buffered saline). The blocked membrane was then incubated overnight at 4° C (or alternatively for 1-2 hours at room temperature) with the primary antibody of interest. The membrane was then washed three times with TBST (Tris-buffered saline, 0.1% Tween 20) and incubated with the appropriated secondary antibody diluted in 5% BSA in TBST; typically this step required 1 hour and occurred at room temperature. A list of primary and secondary antibodies used to perform the experiments presented in this thesis is reported in section 2.8. The membrane was then washed three times with TBST, scanned using Odyssey CLx (LI-COR) and analysed using Image Studio software (LI-COR). When normalisation to the total amount of cellular proteins was required the membrane was incubated for 1 hour a room temperature with Alexa-680 conjugated streptavidin (ThermoFisher), which recognised one major band from *Dictyostelium* cell lysates corresponding to biotinylated MCCC1 (mitochondrial 3-methylcrotonyl-CoA carboxylase α) (Davidson et al., 2013).

2.5 List of strains

AD7_1	Ax3, *wasA*::bsr^{R}
AD7_6	AX3, *wasA*::bsr^{R} parent
DBS0235601	NC4A2, *clc*:: bsr^{R}
AD12_21	JH8, *scrA*:pyr5-6, $^{tet\text{-}on}$*scrA*; G418^{R}, *wasA*::bsr^{R}

The clathrin light chain knockout strain was kindly provided by the Dicty Stock Center (http://www.dictybase.org).

2.6 List of primers

oCA46	ggatccATGCAAGCAATTAAATG
oCA47	actagtTTATAAAATGTTGCAACCACCTGAA
oSB5	CATTCTCTGGATCCCATTCCAAATCTTTCTCTTCCGATGAA
oSB6	AGAGAAAGATTTGGAATGGGATCCAGAGAATGGTTTTGATA
oSB15	TGCGTTGGTTGGAGCTGATGCTTCCAAATCTTTCTCTTCCGAT
oSB16	GCATCAGCTCCAACCAACGCAAAACATGAAAGTCATATTGGTTGG

All primers are written 5' to 3' from left to right; the sequence in lower case in oCA46 and oCA47 correspond to the BamHI and SpeI restriction sites respectively.

2.7 List of plasmids

pCA37	Co-expression vector containing GFP- WASP and pakB CRIB-mRFPmars2
pCA44	Co-expression vector containing GFP-ΔCRIB WASP and pakB CRIB-mRFPmars2
pCA46	Co-expression vector containing GFP-**CRIB WASP and pakB CRIB-mRFPmars2
pCA64	Co-expression vector containing GFP-WASP and mRFPmars-Atg18
pCA74	Co-expression vector containing GFP-**CRIB WASP and Lifeact-mRFPmars2
pCA75	Co-expression vector containing GFP-WASP and Lifeact-mRFPmars2
pCA76	Expression vector containing GFP-Rac1A

pCA86	Expression vector containing GFP-Rac1A and CLC-mRFPmars
pCA88	Expression vector containing GFP-Rac1A and mRFPmars-Atg18
pCA90	Inducible expression vector containing GFP-G12V Rac1A
pDM656	Co-expression vector containing GFP-WASP and CLC-mRFPmars
pDM859	Expression vector containing pakB CRIB-mRFPmars2
pDM934	Expression vector containing GFP-WASP CRIB
pDM945	Co-expression vector containing HSPC300-GFP and pakB CRIB-mRFPmars2
pDM987	Inducible expression vector containing untagged G12V Rac1A
pSBZ9	Expression vector containing GFP-ΔCRIB WASP
pSBZ13	Expression vector containing GFP-**CRIB WASP
pSBZ14	Expression vector containing GFP-WASP
pSBZ16	Co-expression vector containing GFP-ΔCRIB WASP and mRFPmars2-ArpC4
pSBZ18	Co-expression vector containing GFP-**CRIB WASP and mRFPmars2-ArpC4
pSBZ19	Co-expression vector containing GFP-WASP and mRFPmars2 ArpC4
pSBZ21	Co-expression vector containing GFP-ΔCRIB WASP and CLC-mRFPmars
pSBZ23	Co-expression vector containing GFP-**CRIB WASP and CLC-mRFPmars
p803	Expression vector containing GFP-Tkt-1
pGEXRac1A	Bacterial expression vector encoding GST-tagged *Dictyostelium* Rac1A
pGEX RacC	Bacterial expression vector encoding GST-tagged *Dictyostelium* RacC

pCA expression vectors listed here are some of those generated as a result of my own PhD work. pDM plasmids were acquired from Douwe Veltman, pSBZ plasmids from Stephen Barratt; pGEX vectors were a gift of Dr. Arjan Kortholt (University of Groningen), p803 was previously described (Calvo-Garrido et al., 2011) and kindly provided by the Dicty Stock Center (http://www.dictybase.org).

2.8 List of antibodies

Primary Antibodies			
Target	**Host**	**Dilution**	**Source**
RFP	Rat	1:2000	Chromotek
GFP	Rat	1:1000	Chromotek
WASP	Rabbit	1:10000	Soldati Lab
Atg8	Rabbit	1:10000	Biogenes
GST	Mouse	1:1000	Abcam

Secondary Antibodies				
Target	**Host**	**Fluorophore**	**Dilution**	**Source**
Rat	Goat	Alexa Fluor 680	1:10000	ThermoFisher
Rabbit	Goat	DyLight 800	1:10000	ThermoFisher
Mouse	Donkey	Alexa Fluor 680	1:10000	ThermoFisher
Mouse	Goat	DyLight 800	1:10000	ThermoFisher
Rabbit	Goat	Alexa Fluor 568	1:500	ThermoFisher

2.9 Buffers recipes

DNA gel loading buffer (6x)

Sucrose	40%
Bromophenol blue	0.25%
Xylene cyanol	0.25%

LB medium

Bacto-tryptone (Difco)	1%
Bacto-yeast extract (Difco)	0. 5%
NaCl	17 mM
Adjusted to pH 7	

SOC broth (Formedium)

Tryptone	20 g/l
Yeast extract	5 g/l
NaCl	0.5 g/l
$MgSO_4$	2.44 g/l
Glucose	3.6 g/l
Adjusted to pH 7	

HL5 medium including Glucose (Formedium)

Peptone	14 g/l
Yeast Extract	7 g/l
Glucose	13.5 g/l
KH2PO4	0.5 g/l
Na2HPO4	0.5 g/l

HL5 medium including Glucose supplemented with vitamins and micro-elements (Formedium)

Peptone	5 g/l
Yeast Extract	5 g/l
Tryptone	5 g/l
KH2PO4	1.2 g/l
Na2HPO4	0.35 g/l

Glucose	10 g/l
FM Vitamins and Micro-elements*	0.01 g/l (* as present in SIH defined minimal medium)

SIH defined minimal medium (Formedium)

Amino Acids	
Arg	700 mg/l
Asp	300 mg/l
Asp A	150 mg/l
Cys	300 mg/l
GluA	545 mg/l
Gly	900 mg/l
His	300 mg/l
Ile	600 mg/l
Leu	900 mg/l
Lys	1250 mg/l
Met	350 mg/l
Phe	550 mg/l
Pro	800 mg/l
Thr	500 mg/l
Trp	350 mg/l
Val	700 mg/l
Vitamins	
Biotin	0.02 mg/l
Cyanocobalamin	0.01 mg/l
Folic Acid	0.2 mg/l
Lipoic Acid	0.4 mg/l
Riboflavin	0.5 mg/l
Thiamine	0.6 mg/l
Micro Elements	
Na2EDTA.2H2O	4.84 mg/l
ZnSO4	2.3 mg/l
H3BO3	1.11 mg/l
MnCl2.4H2O	0.51 mg/l
CoCl2.6H2O	0.17 mg/l

CuSO4.5H2O	0.15 mg/l
(NH4)6Mo7O24.4H2O	0.1 mg/l
Minerals	
NH4Cl	53.5 mg/l
CaCl2.2H2O	2.94 mg/l
FeCl3	16.2 mg/l
MgCl2.6H2O	81.32 mg/l
KH2PO4	870 mg/l
Carbon Source	
Glucose	10000 mg/l

LoFlo medium (Formedium)

Glucose	11 g/l
KH_2PO_4	0.68 g/l
Casein Peptone	5 g/l
NH_4Cl	26.8 g/l
$MgCl_2$	37.1 g/l
$CaCl_2$	1.1 g/l
$FeCl_3$	8.11 g/l
Na_2-EDTA	4.84 g/l
$ZnSO_4$	2.30 g/l
H_3BO_3	1.11 g/l
$MnCl_2.4H_2O$	0.51 g/l
$CoCl_2$	0.17 g/l
$CuSO_5.5H_2O$	0.15 g/l
$(NH_4)_6Mo_7O_{24}.4H_2O$	0.1 g/l
Adjusted to pH 6.5	

E-buffer

Sör buffer (KH_2PO_4 + Na_2HPO_4)	10 mM
Sucrose	50 mM

Fixative solution

Formaldehyde	2%
Picric acid	15%, saturated

PIPES	1 mM
Adjusted to pH 6.5	

Bacteria lysis buffer

Triton X-100	1%
Halt™ Protease Inhibitor Cocktail	1X
DTT	1 mM

Rac buffer

Tris HCl pH 7.5	50 mM
NaCl	100 mM
Halt™ Protease Inhibitor Cocktail	1X
DTT	1 mM

***Dictyostelium* lysis buffer**

Tris HCl pH 8	50 mM
NaCl	100 mM
$MgCl_2$	30 mM
Triton X-100	0.1%
Halt™ Protease Inhibitor Cocktail	1X
DTT	1mM

Washing buffer

Tris HCl pH 8	50 mM
NaCl	100 mM
$MgCl_2$	30 mM
Halt™ Protease Inhibitor Cocktail	1X
DTT	1 mM

RIPA buffer

NaCl	150 mM
Tris HCl pH 7.5	10 mM
EDTA	1 mM
Triton X-100	1%
SDS	0.1%

Halt™ Protease Inhibitor Cocktail	1X
DTT	1 mM

Chapter 3 , *Results – part I*

WASP maintains cell polarity and contributes to active Rac homeostasis via a CRIB-mediated interaction

3.1 Preface

WASP is an actin nucleation-promoting factor (NPF) mostly known as a key player during clathrin-mediated endocytosis (CME). This role has been kept unchanged in a billion years, as suggested by the fact that organisms as far apart in the evolutionary tree as yeasts and mammals utilise a remarkably conserved WASP orthologue to drive the internalisation of clathrin-coated pits (CCPs) (Madania et al., 1999; Merrifield et al., 2004). *Dictyostelium* WASP has also been observed on CCPs (Veltman et al., 2011), where transient bursts of F-actin had been previously detected (Brady et al., 2010). It did not therefore come as a surprise that in *Dictyostelium* WASP knockout cells the formation of actin filaments on CCPs is strongly reduced, leading to their impaired internalisation (Davidson, 2014). Under normal circumstances CCPs are observed at the rear half of migrating cells. This is due to the fact that the time required for CCPs to be endocytosed is longer than the time required for pseudopodia to be extended, implying that CCPs in the process of being internalised are swept at the back of the cell while this moves forward. In WASP knockout cells uninternalised CCPs accumulate within the uropod, where they originate a cluster of discrete long-lived *puncta* (Davidson, 2014).

One of the most unexpected features of *Dictyostelium* WASP knockout cells was their inability to maintain front–rear polarity. Indeed, while migrating wild type cells confine the CRIB motif of Pak, used as a reporter for active Rac (Itoh et al., 2002), at the leading edge, WASP knockout amoebas also aberrantly accumulate it at the trailing edge (Davidson, 2014).

The effect of WASP deletion on cell polarity is fascinating. How does WASP control the spatial distribution of active Rac? Is its role in maintenance of cell polarity linked to its role in CME, or is it a distinct and novel function?

It was initially reasoned that in a scenario whereby active Rac or Rac activators (i.e. Rac GEFs) are recycled via CME, the impaired CCPs internalisation caused by WASP deletion may account for the aberrant localisation of the active Rac marker at the trailing edge in knockout cells.

However, live-cell imaging experiments revealed that the active Rac marker is normally not present on dynamic clathrin-coated pits, and that the only instance where the two probes co-localise is at the rear of WASP null cells (Davidson, 2014). It was therefore difficult to establish whether under normal

circumstances Rac in its active form is embedded within clathrin-coated pits and recycled via CME.

As for the hypothesis that Rac activators may be CME cargo, the co-localisation between clathrin and the Rac GEF gxcJJ was investigated. This choice was dictated by the fact that a previous study conducted in our lab concluded that gxcJJ (and inconsistently gxcG and roco5) is the only *Dictyostelium* Rac GEFs enriched on ventral *puncta* (Douwe Veltman, unpublished data). However, co-localisation analysis revealed that gxcJJ spots do not coincide with clathrin *puncta* (Andrew J. Davidson, Peter A. Thomason, unpublished data), weakening the possibility that the Rac GEF may be recycled via CME.

The following section describes further experiments that have been carried out in the attempt to characterise the molecular details of WASP-mediated maintenance of cell polarity.

3.2 Rac1 does not appear to be recycled via clathrin-mediated endocytosis

As already mentioned, neither the active Rac marker (Davidson, 2014) nor Rac activators (Andrew J. Davidson, Peter A. Thomason, unpublished data) are discretely enriched on clathrin-coated pits under normal circumstances. We decided to explore the possibility that Rac itself, independently of its activation state, may be incorporated within clathrin-coated pits and recycled via CME. To test this hypothesis, we performed live-cell imaging on cells co-expressing Rac and clathrin light chain (CLC).

It was mandatory, however, to first decide which of the Rac species was the most appropriate to look at. Indeed, the CRIB motif of pakB specifically indicates the presence of Rac in its active state but does not discriminate between different Rac species. *Dictyostelium* expresses multiple Rho family isoforms (Eichinger et al., 2005). Seven of these belong to the Rac subfamily: Rac1A, Rac1B, Rac1C, RacF1, RacF2, RacB and RacA (Rivero et al., 2001). Among them, Rac1A shows a very high degree of similarity (85% identity, 92% similarity) to human Rac1 (figure 3.1), which is the most ubiquitously expressed among the mammalian Rac isoforms (Didsbury et al., 1989; Haataja et al., 1997), and has been linked to pseudopodia extension. Rac1 has been first associated with protrusions in fibroblasts, since the expression of dominant negative Rac1 rendered the cells unable to protrude in response to different stimuli (Ridley et al., 1992); similarly, depletion of Rac1 but not of Rac3 affects lamellipodia formation in glioblastoma cells (Chan et al., 2005). However, more recent evidence suggests that both Rac2 and Rac3 can compensate for the lack of Rac1 (Steffen et al., 2013), hinting at the possibility that all three Rac species could drive the extension of lamellipodia and that their relative abundance in different cell types may dictate which of them is the major driver of protrusions. Since Rac1A is also the most highly expressed isoform in *Dictyostelium* (data from http://dictyexpress.biolab.si/), we decided to focus our attention on it.

We cloned Rac1A under an actin promoter, which generally leads to the overexpression of the downstream gene, and added an N-terminal GFP tag. Previous reports suggested that the overexpression of wild type Rac1A causes *Dictyostelium* to form an exaggerated number of spiky, filopodia-like,

protrusions (Dumontier et al., 2000). We therefore first addressed whether wild type cells could tolerate the expression of the newly generated GFP-Rac1A-encoding vector. As shown in figure 3.2 and in movie 1, GFP-Rac1A is abundantly cytosolic but also clearly enriched at the leading edge of migrating cells at all time points (blue lines). GFP-Rac1A does not tend to localise at the uropod during migration (red lines), although it can occasionally be observed at the rear. Representative values of GFP-Rac1A intensity are reported in the fluorescence plot at the bottom. No obvious sign of aberrant filopodia formation was detected, meaning that wild type cells tolerate the newly generated GFP-Rac1A-expression vector.

We then went on testing whether Rac could be incorporated within clathrin-coated pits. Clathrin-mediated endocytosis mostly occurs on the ventral surface of the cell and its dynamics are best-monitored when the first ≈ 100 nm at the bottom of the cell are selectively illuminated (Merrifield et al., 2002). TIRF (Total Internal Reflection Fluorescence) microscopy is generally considered as an appropriate tool. Clathrin appears in *puncta* that sit on the basal membrane for few tens of seconds; disappearance from the TIRF field is considered as a *bona fide* sign of their internalisation (Merrifield et al., 2002). As reported in figure 3.3 and in movie 2, GFP-Rac1A does not appear to be discretely enriched on clathrin-coated pits. Kymograph and fluorescence plot, which report the dynamics of either clathrin or Rac over time, also suggest that no obvious recruitment of Rac occurs on clathrin *puncta*. As a comparison, GFP-Dajumin, which has been identified as a cargo during CME in *Dictyostelium*, extensively co-localises with clathrin (Macro et al., 2012).

This result suggests that Rac1 itself is not embedded within CCPs and therefore not recycled via CME. This evidence, in addition to the lack of active Rac enrichment on CCPs (Davidson, 2014), and to the lack of co-localisation between clathrin and Rac activators (Andrew J. Davidson, Peter A. Thomason, unpublished data) may be interpreted as meaning that WASP controls Rac activity via a CME-unrelated mechanism. However, we strongly believe that a decisive approach to rule out a role for CME in maintenance of cell polarity is to analyse the spatial distribution of the active Rac marker in cells lacking clathrin. Clathrin light (*clc*-) and heavy chain (*chc*-) knockout strains have been previously

generated (Niswonger and O'Halloran, 1997; Wang et al., 2003), meaning that clathrin is not required for *Dictyostelium* viability. However, loss of clathrin significantly affects cells' wellbeing, making them poorly suitable for manipulation and rendering unsuccessful our repeated efforts to transfect them. We are currently considering the generation of an inducible *chc* knockout in order to switch off the expression of clathrin only when needed.

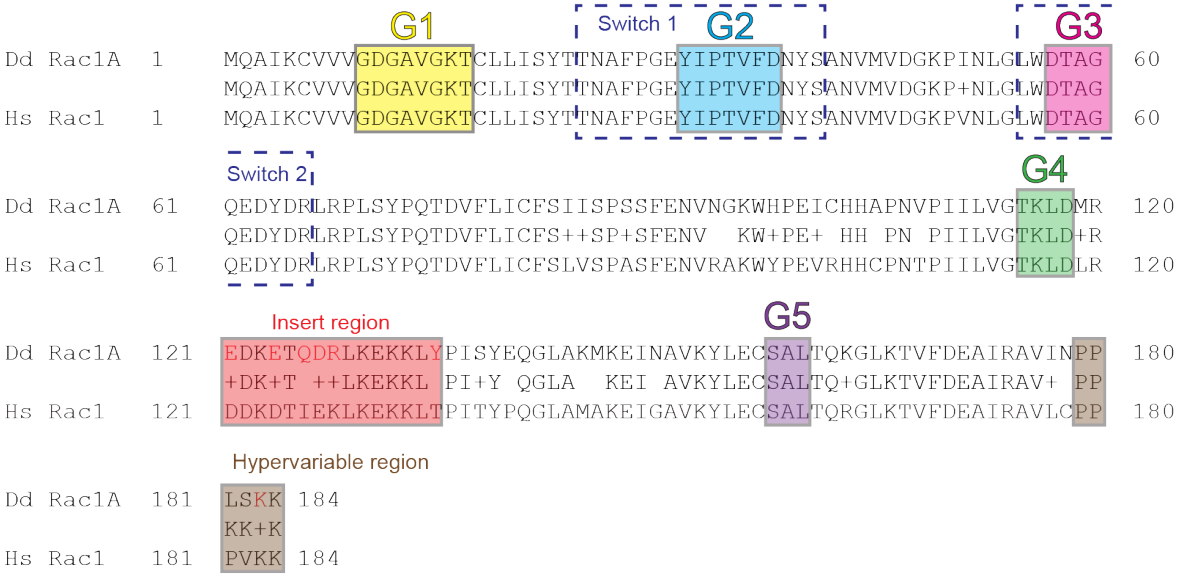

Figure 3.1 *Dictyostelium* Rac1A and Human Rac1 show high degree of similarity.

Dd refers to *Dictyostelium* Rac1A, Hs to human Rac1. Overall, the two proteins are 85% identical and 92% similar. No difference at all can be detected between their G1 motif (yellow box), switch1 (first dashed blue square) and switch2 (second dashed blue square) regions, G4 (green box) and G5 motifs (purple box). Some differences can be found within the insert region (red box), responsible for the interaction with downstream effectors, and the hypervariable region (brown box). Of interest, C178, which has been proposed to play a major role in the localisation of Rac1 to cholesterol-rich subdomains of the plasma membrane (Navarro-Lerida et al., 2012), is not present in *Dictyostelium* Rac1A.

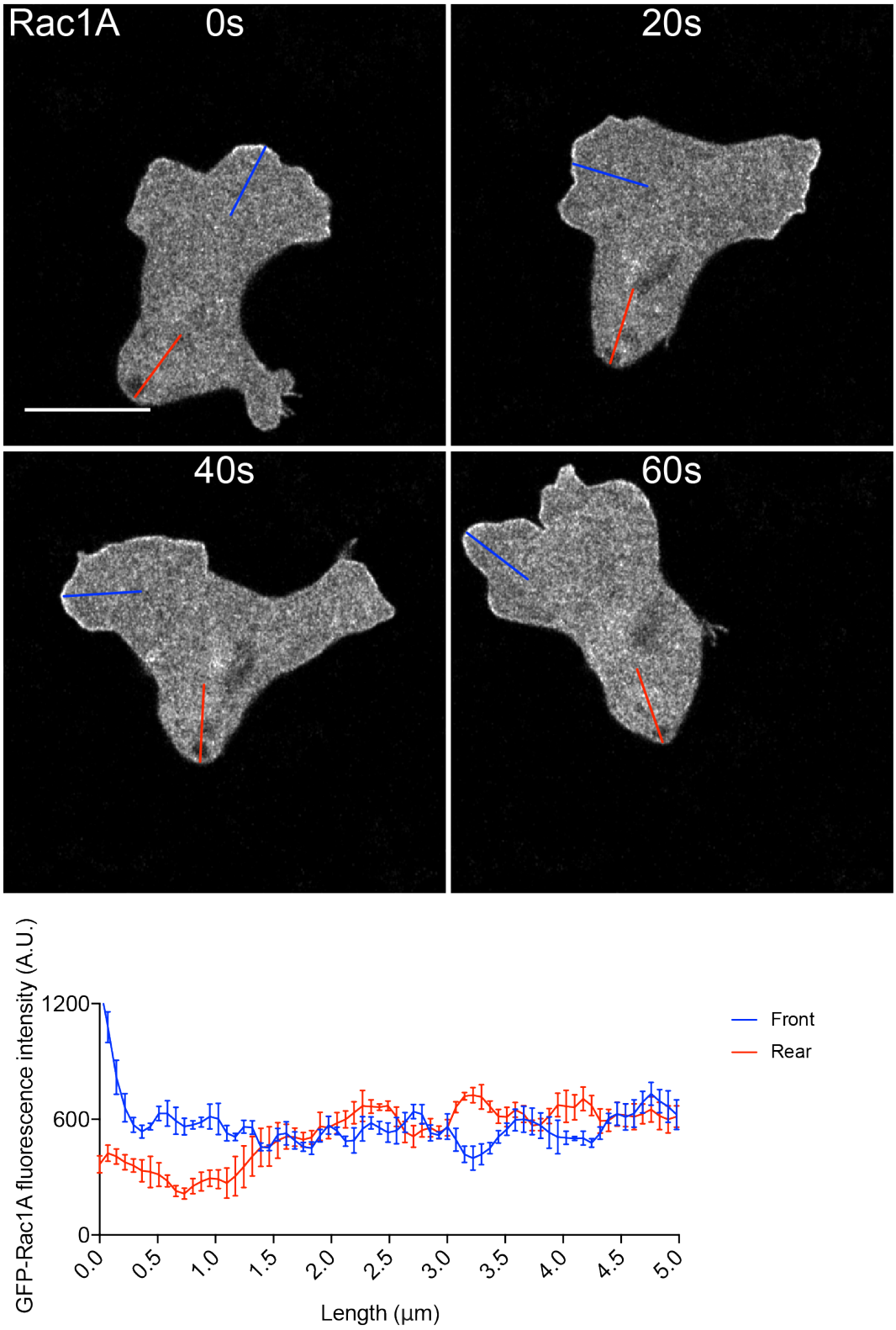

Figure 3.2 Wild type cells tolerate overexpression of Rac1A.

It was previously shown that overexpression of wild type caused the formation of aberrant filopodia (Dumontier et al., 2000). We generated a new extrachromosomal vector to express GFP-tagged Rac1A under an actin promoter, and verified whether cells could tolerate it by super-resolution live-cell imaging. As shown in the montage at the top, GFP-Rac1A is abundantly cytosolic but is

also clearly recruited to the plasma membrane, presumably when active. No increase in the number of spiky protrusions upon overexpression of Rac1A was recorded, meaning that wild type cells can handle high levels of Rac1A. GFP-Rac1A is highly enriched at the leading edge during migration (blue line), while is generally excluded from the rear (red line), as reported in the fluorescence plot at the bottom. For both lines, the origin of the graph corresponds to their intersection with the plasma membrane. the Scale bar represents 10 μm.

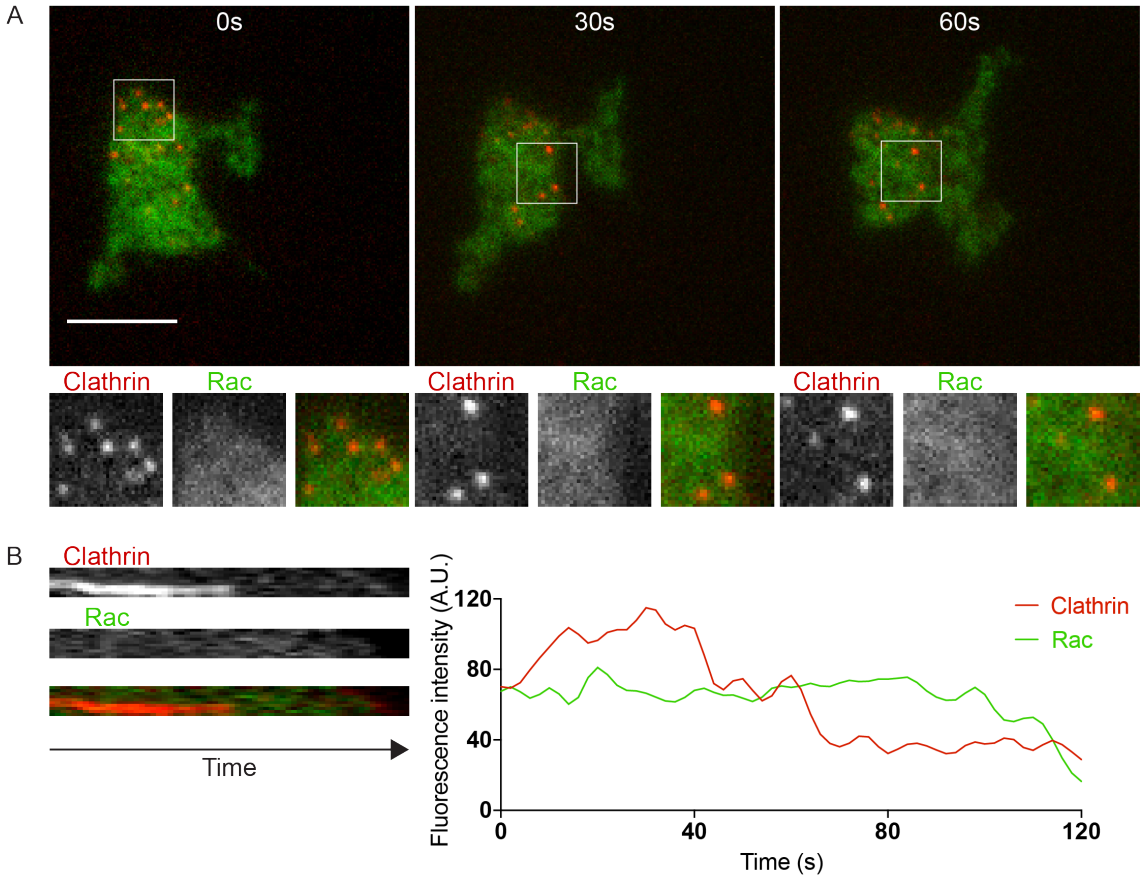

Figure 3.3 Rac does not appear to be recycled via clathrin-mediated endocytosis.

CME mostly occurs on the ventral surface of migrating cells and is therefore generally monitored using TIRF microscopy. Clathrin light chain, a commonly used marker for CME, generates *puncta* that sit on the ventral surface of the cell for few tens of seconds, up to the point when actin polymerisation occurs and the CCP is pinched off and internalised. We asked whether membrane-bound Rac could be recycled via CME.

A) CLC shows a dynamic punctate localisation, with most of the spots being generated at the rear; Rac, instead, shows a diffuse signal. No sign of Rac enrichment on CCPs can be spotted at any time. Scale bar represents 10 µm.

B) and C) Kymograph and fluorescence plots show no discernible recruitment of Rac on CCPs, further supporting the idea that Rac is not recycled within clathrin-coated pits.

3.3 WASP requires a functional CRIB motif to exclude active Rac from the trailing edge

As introduced at the end of the previous section, we have found that neither Rac (regardless of its activation state) nor its activators appear to be recycled via CME. These results may suggest that WASP controls Rac activity via a CME-unrelated mechanism. However, since it has not yet been possible to assess the ability of clathrin-deficient cells to restrict Rac activity, the role of WASP in maintenance of cell polarily cannot at this stage be teased apart from its role in CME.

We sought to uncover the molecular requirements for WASP to spatially restrict Rac activity. In particular, we aimed to understand whether WASP relies on a direct interaction with active Rac to confine it at the leading edge during migration. As shown in figure 3.4, *Dictyostelium* WASP harbours a conserved CRIB motif (Cdc42 and Rac interacting/binding motif) (Burbelo et al., 1995) and is therefore able to interact with active Rac.

Proteins harbouring a CRIB motif are generally considered downstream effectors of Rho GTPases. Accordingly, as will be extensively discussed in the next chapter of this dissertation, active Rho GTPases have been proposed to activate both mammalian N-WASP (Miki et al., 1998a; Rohatgi et al., 1999; Tomasevic et al., 2007) and *Dictyostelium* WASP (Han et al., 2006) by interacting with the NPFs' CRIB motif. The possibility that a CRIB-mediated interaction is also required for WASPs to control the GTPases, however, has never been explored. Given that *Dictyostelium* does not seem to express any Cdc42 orthologue (Rivero et al., 2001), we asked whether a direct, CRIB-mediated, interaction between WASP and active Rac is required for the former to control the latter.

To test this model, we genetically manipulated the GTPase binding motif of WASP. Two mutants were generated: ΔCRIB WASP and **CRIB WASP, collectively referred to as *WASP CRIB mutants*. The first consists of a deletion of 14 residues (Δ173-186) located within the core of the CRIB motif (Burbelo et al., 1995). This mutation has been previously introduced in Wsp, the WASP orthologue in *Drosophila* (Tal et al., 2002). The second WASP CRIB mutant harbours a two-amino acid substitution: two conserved residues, Isoleucine in position 173 (Ile173) and Phenylalanine in position 179 (Phe179), were mutated in alanine. These two residues were chosen in collaboration with Dr. Shehab Ismail (CRUK

Beatson Institute) for at least two reasons. First, they are conserved between Human WASP and N-WASP, *Dictyostelium* WASP and *Drosophila* Wsp, which suggests that they may be crucial for the interaction between WASP and Rho GTPases. Second, their position within the 3D structure of the protein suggests that they have a key role in establishing an interaction with different hydrophobic regions of the GTPase (Abdul-Manan et al., 1999). A schematic representation of the two WASP CRIB mutants is reported in figure 3.5. The effect of these mutations on WASP functionality will be extensively discussed in the next chapter of this thesis; for the time being it is important to point out that both mutations affect the N-terminus of the CRIB motif. This choice is dictated by the fact that a structural study on hematopoietic WASP (which harbours a CRIB motif that is similar to the one found in ubiquitous WASPs) has revealed that the C-terminal region of the CRIB, not its N-terminus, interacts with the VCA domain and is therefore required to keep WASP folded into an auto-inhibited conformation (Kim et al., 2000). Based on this evidence, mutating the N-terminal region of the CRIB motif should not interfere with the activation/inactivation of WASP.

We first assessed whether the CRIB mutations genuinely abrogate the ability of WASP to interact with active Rac. To do so we performed GST-pulldown assays using bacterially purified GST-Rac1A loaded with either GDP (to reproduce the inactive state) or GTPγs, a non-hydrolysable analogue of GTP that maintains the Rho GTPase in its active state. We also performed pulldown assays using GST-RacC, since this unconventional Rac species has been proposed to regulate *Dictyostelium* WASP (Han et al., 2006). As shown in figure 3.6, both CRIB mutations impair the interaction between WASP and active Rac1 as well as between WASP and RacC. None of them hampers its subcellular localisation or its ability to induce actin polymerisation on clathrin-coated pits, as will be discussed in the next chapter.

We therefore went on addressing whether a functional CRIB motif is required for WASP to confine Rac activity at the leading edge during migration. To do so, we transiently transfected WASP knockout cells with red-tagged active Rac marker and GFP-tagged WASP, either full-length wild type or CRIB mutant. Transfected cells were there analysed during directed migration in an under-agarose chemotaxis assays, a commonly used set up that allows cells to acquire a

polarised morphology (Laevsky and Knecht, 2001). As shown in figure 3.7 and movie 3, WASP knockout cells transiently expressing GFP-WASP (rescue) confine the active Rac marker at the front at almost all time points; the active Rac reporter can occasionally be observed at the trailing edge, but the accumulation is transient and generally coincides with a pseudopod that has been swept at the back of the cell. On the contrary, WASP knockout cells expressing either WASP CRIB mutants aberrantly accumulate active Rac at the trailing edge at almost all time points.

Overall, the evidence presented here strongly suggests that WASP requires a functional CRIB motif to interact with active Rac and exclude it from the trailing edge during migration.

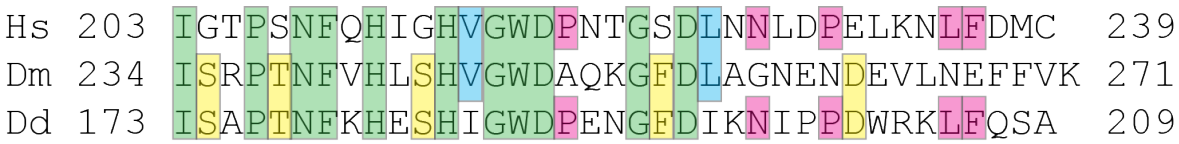

Figure 3.4 The CRIB motif of WASP is conserved throughout evolution.

The Cdc42 and Rac interacting/binding motif of WASP is a stretch of 36 residues, some of which have been maintained during evolution. A comparison between *Dictyostelium* (Dd) WASP, Drosophila (Dm) Wsp, and human (Hs) N-WASP shows that 11 out of 36 amino acids are completely unchanged (green rectangles) across evolution, 5 out of 36 residues are conserved between amoebas and Drosophila (yellow rectangles), 2 out of 36 amino acids are identical between *Drosophila* and humans, while 5 out of 36, curiously located in the C-terminal region of the motif, are conserved between *Dictyostelium* and humans (pink rectangles). Overall, the N-terminal region, referred to as the core of of the CRIB motif (Burbelo et al., 1995), shows the highest degree of similarity between different organisms.

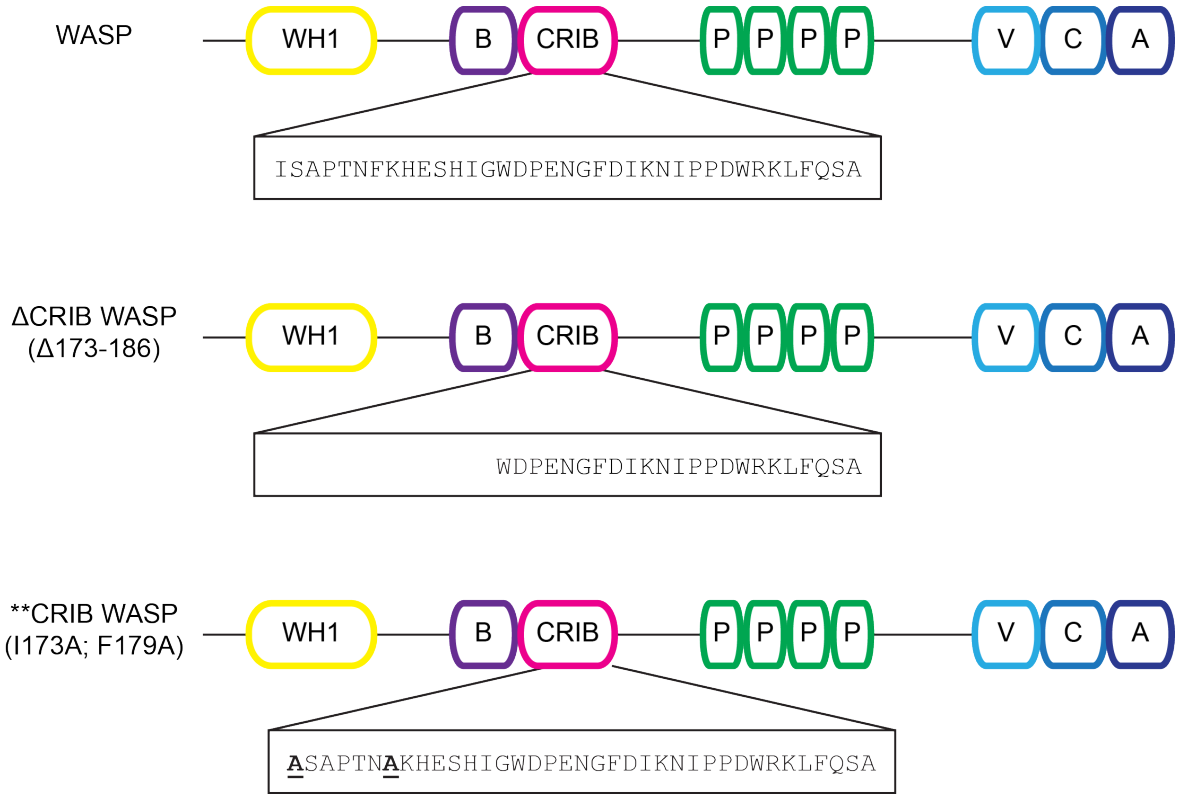

Figure 3.5 Genetic manipulation of the CRIB motif of WASP.

The wild type sequence of the WASP CRIB motif is shown in the top panel. In order to investigate the role of WASP in confining active Rac at the front of migrating cells, two types of mutation have been introduced. The first consists in the deletion of 14 residues (ΔCRIB WASP, middle panel), which has already been described for *Drosophila* Wsp (Tal et al., 2002). The second (**CRIB WASP, bottom panel) consists in the combination of two point mutations: I173A and F179A. Importantly, these residues are conserved in both *Drosophila* Wsp and human N-WASP.

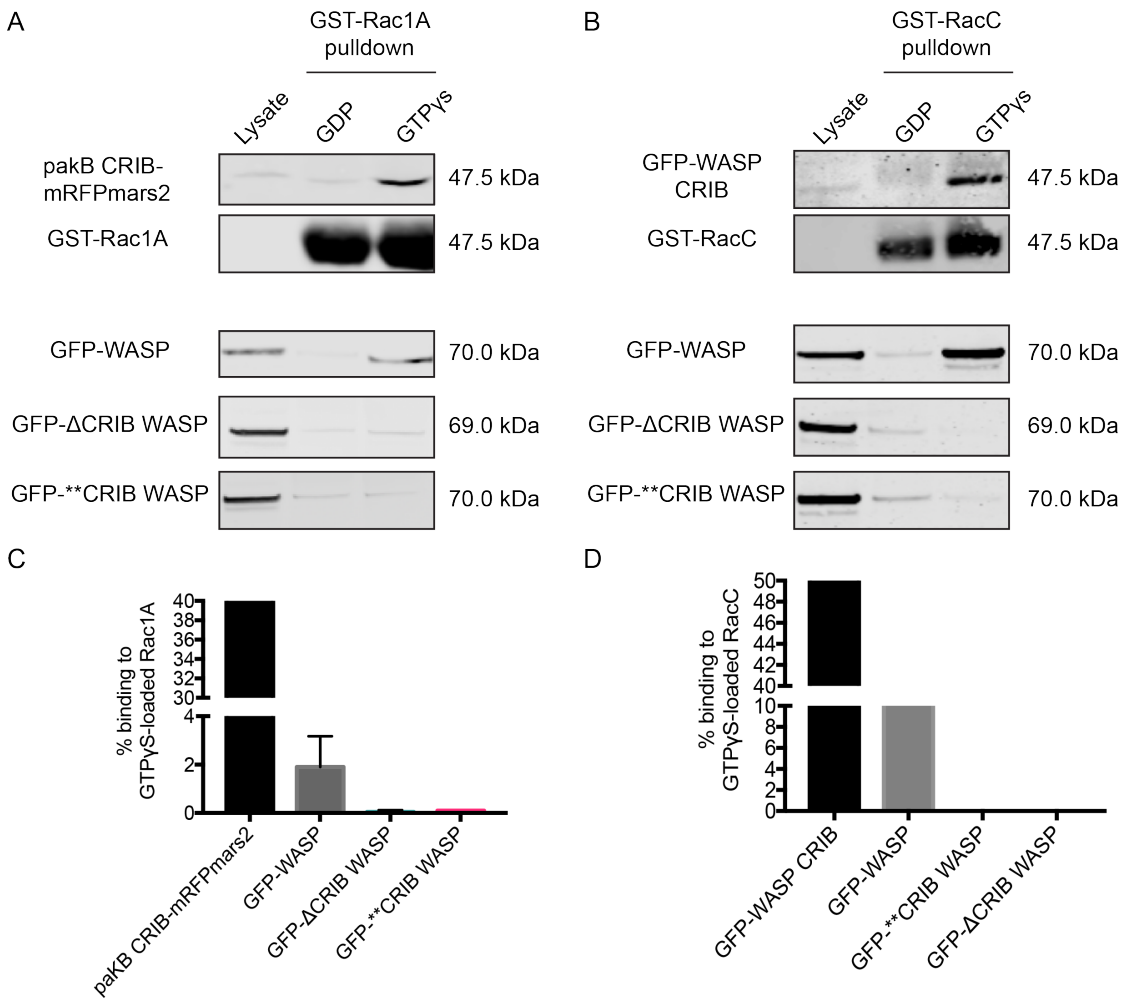

Figure 3.6 Mutations in the WASP CRIB motif affect its binding to active Rac1A and RacC.

GST pulldown assays were performed to assess the ability of GFP-ΔCRIB WASP and GFP-**CRIB WASP to interact with Rac1A (A, left-hand side, n=3) and RacC (B, right-hand side, n=1). Bacterially purified Rac was loaded on beads, and its nucleotide-binding pocket filled with either GDP or GTPγs. Positive controls (pakB CRIB-mRFPmars2 or GFP-WASP CRIB) were used to ensure the feasibility and reproducibility of our approach. As shown on the top rectangles in both A and B, positive controls specifically bind to the active form of Rac. As shown in the second line from the top in both A and B, a relatively small proportion of GFP-WASP present in the lysate binds to active Rac. Moving down to the third line, GFP-ΔCRIB WASP fails to bind to either active Rac1A and RacC, likewise GFP-**CRIB WASP (bottom line in both A and B). Binding to Rac1A and RacC of all species analysed, including the positive control, has been normalised for the amount of protein in the lysate, as reported in C and D respectively. WB: Anti-GFP for GFP-WASP CRIB, GFP-WASP, GFP-ΔCRIB WASP, GFP-**CRIB WASP; Anti-RFP for pakB CRIB-mRFPmars2; Anti-GST for GST-Rac1A and GST-RacC.

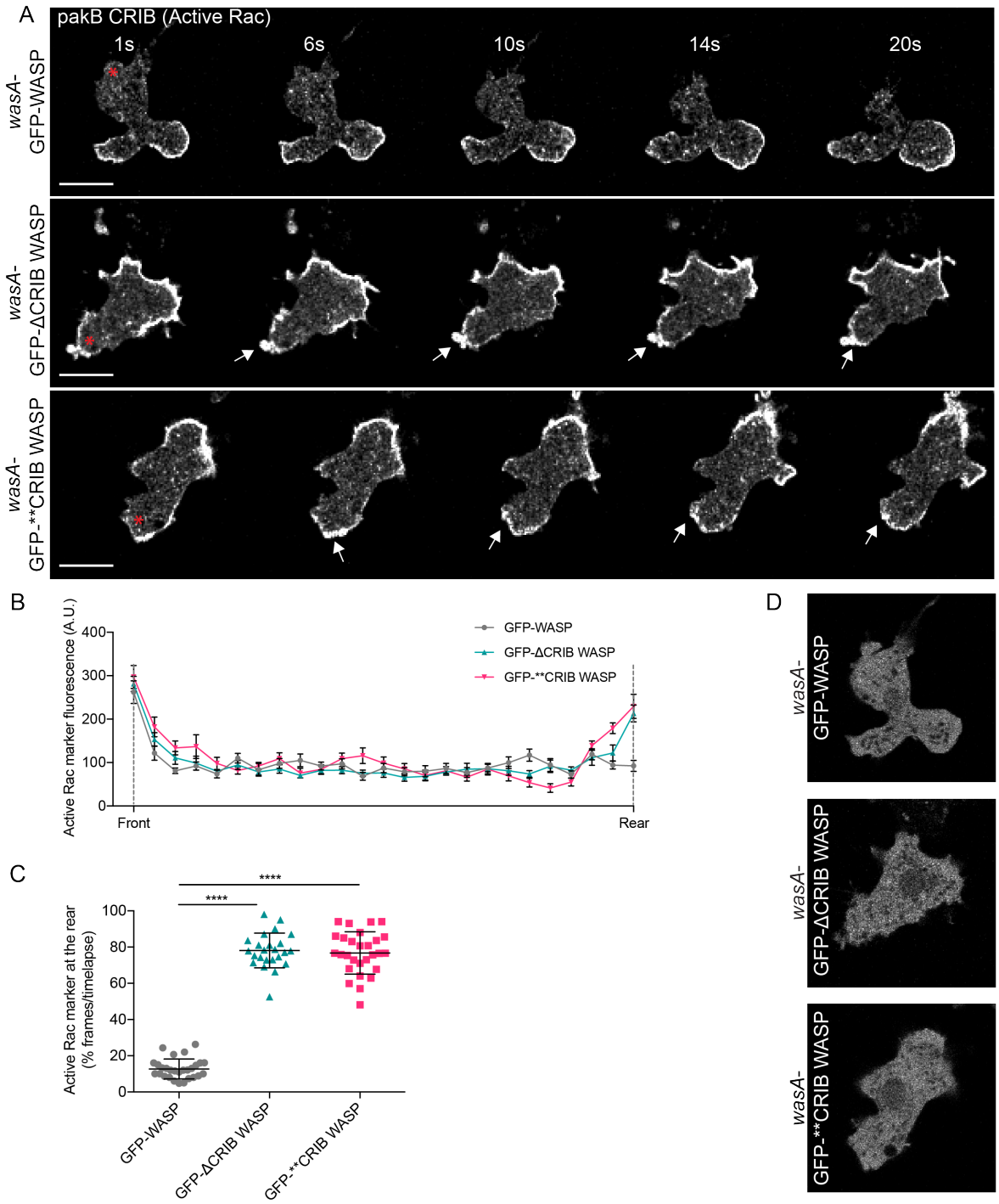

Figure 3.7 A functional CRIB motif is required for WASP to exclude active Rac from the trailing edge.

A) Montage obtained by super-resolution live-cell imaging showing WASP knockout (*wasA*-) cells expressing pakB CRIB (active Rac marker) along with GFP-WASP (rescue, top panel), or GFP-ΔCRIB WASP (middle panel) or GFP-**CRIB WASP (bottom panel). In the presence of a functional WASP CRIB motif (top panel), the active Rac marker is confined at the leading edge and excluded from the rear (red asterisk); in the presence of a non functional WASP CRIB motif

(middle and bottom panels), the active Rac marker is accumulated at the rear (red asterisk) at all time points (white arrows). Representative frames showing the expression of GFP-WASP, GFP-ΔCRIB WASP or GFP-**CRIB WASP are shown in panel D. Scale bars represent 10 μm.

B) Fluorescence plot showing the pakB CRIB (active Rac marker) fluorescence intensity across a straight line connecting the front to the rear of one representative cell/condition over 10 time points. Cells expressing GFP-tagged full-length wild type WASP (grey line) show the expected peak of active Rac marker at the front, but not at the rear. Cells expressing GFP-ΔCRIB WASP (teal line) or GFP-**CRIB WASP (pink line) show the predicted peak of active Rac marker at the leading edge, but also a peak at the trailing edge.

C) Frequency of pakB CRIB (active Rac marker) enrichment at the rear of migrating cells expressing GFP-WASP (grey plot), GFP-ΔCRIB WASP (teal plot) or GFP-**CRIB WASP (pink plot). While in the presence of a functional CRIB motif active Rac is accumulated at the trailing edge in 13% of the frames (mean= 12.71% ± 1.04; error represents S.E.M.), cells expressing GFP-ΔCRIB WASP accumulate active Rac at the trailing edge more frequently (mean= 76.74% ± 2.21; error represents S.E.M.). Similarly, cells expressing GFP-**CRIB WASP show pakB CRIB accumulation at their rear in 78.11% of the frames (S.E.M.= 1.96). Shapiro-Wilk test showed that all samples are normally distributed: p GFP-WASP= 0.07, p GFP-ΔCRIB WASP= 0.46, p GFP-**CRIB WASP= 0.55. Data analysis (unpaired t-test) confirmed that there is a significant difference in the frequency of active Rac marker accumulation at the rear between cells expressing GFP-WASP and GFP-WASP CRIB mutants (GFP-WASP vs GFP-ΔCRIB WASP: $p<0.0001$; GFP-WASP vs GFP-**CRIB WASP: $p<0.0001$ GFP-WASP: n= 2924 frames, 28 cells over 3 independent experiments. GFP-ΔCRIB WASP: n= 2735 frames, 24 cells over 3 independent experiments. GFP-**CRIB WASP: n=2891 frames, 28 cells over 3 independent experiments.

D) Representative frames of WASP knockout (*wasA*-) cells transiently expressing pakB CRIB (shown in panel A) along with GFP-WASP (rescue, top panel), GFP-ΔCRIB WASP (middle panel) or GFP-**CRIB WASP (bottom panel). No discrete *puncta* can be detected due to the fact that the focal plane chosen is not in proximity of the cell-substrate adhesion, where CME occurs.

3.4 WASP requires a functional CRIB motif to maintain functional levels of membrane-bound Rac

Cells expressing WASP CRIB mutants accumulate active Rac at the rear as well as at the front. We aimed to understand whether the aberrant localisation of active Rac was accompanied by an increase in its overall levels. In other words, we asked whether a functional WASP CRIB motif is required to maintain homeostatic levels of active Rac, or just to spatially confine it at the leading edge. We first tried to biochemically assess the amount of active Rac in cells expressing either GFP-WASP or GFP-WASP CRIB mutants. We reasoned that a GST-pulldown assay using pakB CRIB, which binds to the active Rac present in cell lysates, as bait could have answered our question. This approach, however, was hampered by the lack of a reliable antibody that could recognise *Dictyostelium* Rac1A. Despite extensive tests on numerous commercially available antibodies, one that could detect *Dictyostelium* Rac1 under the conditions used for the GST-pulldown was not found. An estimation of the levels of active Rac in cells expressing GFP-WASP or GFP-WASP CRIB mutants could therefore not be achieved using a biochemical approach.

We decided to use an indirect, microscopy-based, approach to compare the levels of active Rac in cells expressing full-length wild type WASP or either WASP CRIB mutant. This method, which has not been used before, takes advantage of the pakB CRIB dynamics. As previously mentioned, the CRIB motif of pakB can be used as a reporter for active Rac (Itoh et al., 2002) since it binds with high affinity to different Rac species (including *Dictyostelium* Rac1A) *in vitro* (de la Roche et al., 2005). It is well established that Rac is mostly membrane-bound when in its active state, and that exchange of GTP for GDP is the major route to trigger its dissociation (Moissoglu et al., 2006). Given that active Rac is largely bound to the membrane, and that the CRIB motif of pakB faithfully reflects its localisation, we asked whether the amount of plasma membrane labelled by the active Rac marker could provide insights on the cellular levels of GTP-bound Rac.

To determine whether a positive correlation between levels of active Rac and membrane-targeted pakB CRIB exists, we analysed the localisation of red-tagged active Rac marker in wild type cells also expressing untagged dominant active (G12V) (Diekmann et al., 1991) Rac1A under a doxycycline-inducible promoter. As shown in figure 3.8, prior to doxycycline treatment, and therefore of G12V

Rac1A expression (top panel), the active Rac marker is localised on a relatively small percentage of the cell membrane (i.e., at sites of macropinosome formation). Conversely, upon doxycycline treatment and increased levels of dominant active Rac1A (bottom panel), cells accumulate the pakB CRIB all around the cell perimeter. As a consequence, they lose polarity and acquire a *pancake*- or *fried egg-like* shape.
These data suggest that there is a correlation between the amount of active Rac within cells and the fraction of plasma membrane labelled by the active Rac marker. Furthermore, high levels of active Rac clearly lead to reduced cell polarity and increased roundness.

We then assessed whether cells expressing GFP-WASP CRIB mutants have increased levels of membrane-targeted active Rac marker. We transiently transfected WASP knockout cells with a co-expression vector encoding red-tagged pakB CRIB and GFP-tagged full-length wild type WASP or either WASP CRIB mutants. We then imaged transfected cells and quantified the proportion of plasma membrane labelled by the active Rac marker as well as cell roundness. As shown in figure 3.9, the active Rac marker labels only a small percentage (≈ 26%) of the cell perimeter in the presence of GFP-tagged full-length wild type WASP; this generally corresponds to sites of macropinosomes or pseudopodia generation. A significantly higher proportion of the cell outline is marked by the active Rac marker in the presence of GFP-ΔCRIB WASP and GFP-**CRIB WASP (≈ 47% and ≈ 49% respectively); this is accompanied by a marked increase in cell roundness. It is extremely important to point out at this stage that unlike in figure 3.8, where high levels of active Rac were induced by the presence of G12V Rac1A under a doxycycline-inducible promoter, in this case (figure 3.9) the cortical localisation of pakB CRIB exclusively reflects the endogenous levels of active Rac.

The evidence presented here shows that in the absence of a functional WASP CRIB motif a larger proportion of the cell membrane is labelled by pakB CRIB, reasonably reflecting higher levels of active Rac. This result may be interpreted as meaning that WASP does not simply control the localisation of GTP-bound Rac but rather preside over its overall levels, ensuring the maintenance of its physiological amount.

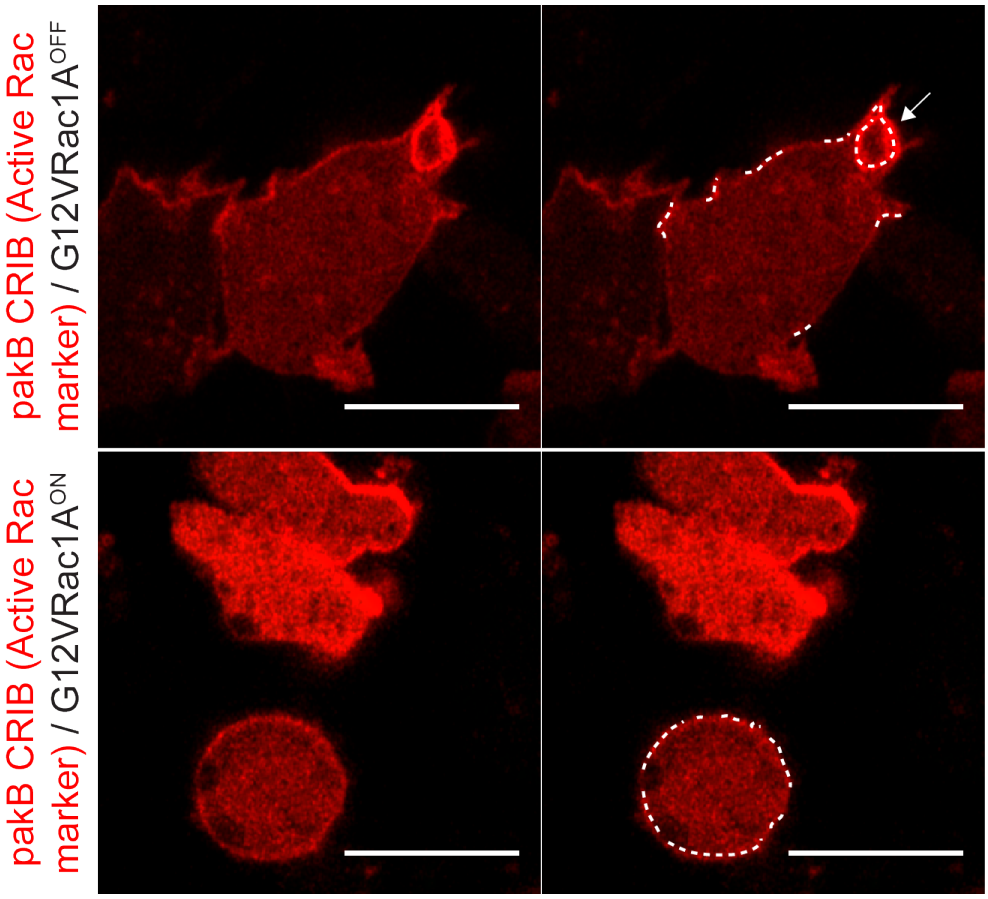

Figure 3.8 Positive correlation between levels of active Rac and proportion of plasma membrane labelled by the active Rac marker.

WASP knockout cells were transfected with two extrachromosomal plasmids: 1) a co-expression vector encoding GFP-WASP (rescue, GFP channel not shown) and pakB CRIB-mRFPmars2; 2) an inducible vector harbouring untagged G12V Rac1A under a doxycycline-inducible (dox-on) promoter. In the absence of doxycycline (top panel) cells appear normally polarised, with the active Rac marker confined on a rather small proportion of the cell perimeter (highlighted by the white dashed line on the right-hand side), which includes a macropinosome (white arrow). Upon doxycycline treatment (bottom panel) a dramatic increase of membrane-bound active Rac marker occurs, as highlighted by the white dashed line on the right-hand side. In the presence of high levels of active Rac cells are completely unable to polarise. Scale bars represent 10 μm.

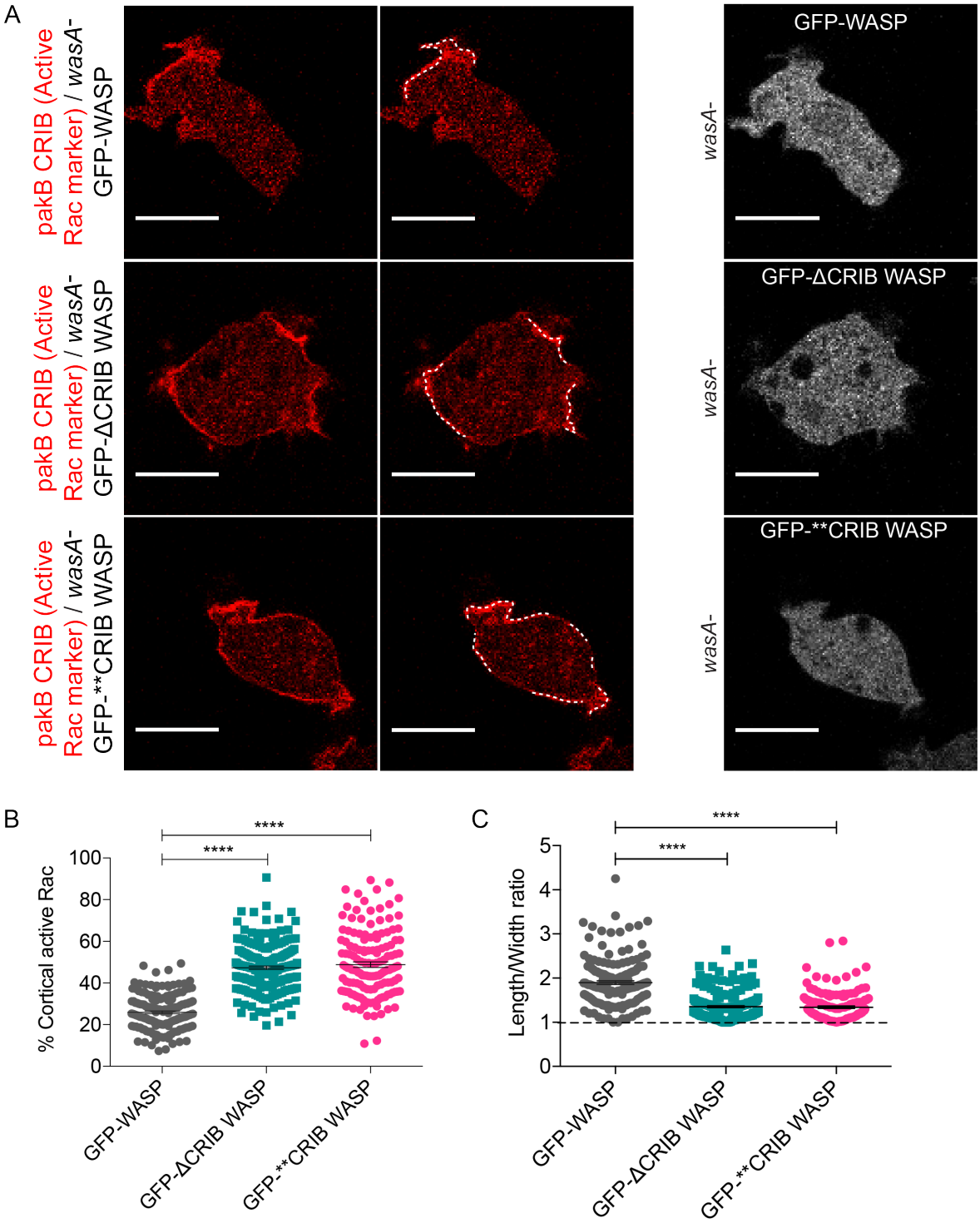

Figure 3.9 A functional WASP CRIB motif is required to maintain physiological levels of membrane-bound active Rac.

A) WASP knockout cells expressing GFP-WASP (rescue, top panel, GFP channel shown on the right-hand side) accumulate pakB CRIB (active Rac marker) on a relatively small proportion of the cell cortex. On the contrary, WASP knockout cells expressing GFP-ΔCRIB WASP (GFP channel shown on the right-hand side, middle panel) or GFP-**CRIB WASP (GFP channel shown on the right-hand side, bottom panel) accumulate active Rac marker on a larger proportion of the cell

membrane. The white dashed line on the right-hand side of each panel outlines PakB CRIB-positive segments of the cell perimeter. No discrete *puncta* of GFP-WASP, GFP-ΔCRIB WASP or GFP-**CRIB WASP can be detected; this is due to the fact that the focal plane chosen is not in proximity of the cell-substrate adhesion, where CME occurs. Scale bars represent 10 μm.

B) Quantitative analysis of the percentage of cell membrane labelled by the active Rac marker in cells expressing GFP-WASP (grey plot), GFP-ΔCRIB WASP (teal plot) and GFP-**CRIB WASP (pink plot) gave the following result. GFP-WASP: mean= 25.9% ± 0.65; error represents S.E.M.; n=168 cells over 3 independent experiments. GFP-ΔCRIB WASP: mean= 47.3% ± 0.79; error represents S.E.M.; n=204 cells over 3 independent experiments. GFP-**CRIB WASP: mean=48.8% ± 1.31; error represents S.E.M; n= 145 cells over 3 independent experiments. Shapiro-Wilk test revealed that only two samples are normally distributed: p GFP-WASP= 0.24, p GFP-ΔCRIB WASP= 0.13, p GFP-**CRIB WASP= 0.02. Therefore a Mann-Whitney test was performed to assess the difference between samples. Data analysis reveals what follows: GFP-WASP vs GFP-ΔCRIB WASP: $p<0.0001$; GFP-WASP vs GFP-**CRIB WASP: $p<0.0001$.

C) Measurement of the length/width ratio of cells expressing GFP-WASP (grey plot), GFP-ΔCRIB WASP (teal plot) and GFP-**CRIB WASP (pink plot) reveals that in the absence of a functional WASP CRIB motif cells appear rounder with reduced axes ratio. GFP-WASP: mean= 1.90 ± 0.04; error represents S.E.M.; n=168 cells over 3 independent experiments. GFP-ΔCRIB WASP: mean= 1.35 ± 0.02; error represents S.E.M.; n=204 cells over 3 independent experiments. GFP-**CRIB WASP: mean=1.34 ± 0.03; error represents S.E.M; n= 145 cells over 3 independent experiments. Shapiro-Wilk test revealed that samples are not normally distributed ($p< 0.05$). Therefore a Mann-Whitney test was performed, revealing that GFP-WASP vs GFP-ΔCRIB WASP: $p<0.0001$; GFP-WASP vs GFP-**CRIB WASP: $p<0.0001$.

3.5 WASP helps cells handle an excess of active Rac

It appears clear that WASP requires a functional CRIB motif to spatially restrict active Rac and likely to regulate its overall levels. We sought to identify other approaches to further test this model. We reasoned that precious information could be gathered by evaluating how cells lacking WASP or expressing WASP CRIB mutants handle dominant active Rac.

Virtually all cells struggle in the presence of a mutant Rac that lingers in its active state for longer than its wild type counterpart. Mammalian fibroblasts expressing G12V Rac1, for instance, progressively round up and detach from the substrate (Ridley et al., 1992). Similarly, in the presence of dominant active Q61L Rac (Xu et al., 1994) HeLa cells acquire a flat and round morphology and have a block in CME (Lamaze et al., 1996). A concoction of direct (i.e. block in macropinocytosis) and secondary effects (i.e. harmfully increased membrane tension) eventually pushes cells expressing dominant active Rac towards a state whereby recovery is no longer a possibility.

We hypothesised that if cells lacking WASP or expressing a non-functional WASP CRIB motif have higher basal levels of active Rac in comparison to wild type cells, overloading them with a burden of G12V Rac1A should push them much faster (or much more dramatically) towards this point of no return. To test this conjecture we cloned GFP-G12V Rac1A under a doxycycline-inducible promoter, transiently introduced it in WASP knockout or wild type cells, and performed live-cell imaging after induction. As shown in figure 3.10, even in the absence of doxyxycline both wild type (*wasA*+, top panels) and WASP knockout cells (*wasA*-, bottom panels) show some green fluorescence, meaning that the doxycycline-inducible vector generated has a certain degree of leakiness. Nevertheless, the GFP- signal in uninduced cells is dim and mostly cytosolic. Western blot analysis revealed that induction of GFP-G12V Rac1A expression, at least during the first two hours of induction, seems to reach higher levels in wild type than in WASP knockout cells. Though intriguing, this observation might simply reflect the heterogeneity of the population: being a transient transfection, it is likely that not all cells have been transfected with the same efficiency or contain the same number of copies of the plasmid. We are therefore planning to stably introduce the construct in the genome of wild type and WASP knockout cells in order to minimise the variability in expression.

Despite an increase in the levels of GFP-G12V Rac1A can be detected by Western blot within two hours of induction, the dramatic morphological change that typically accompanies high levels of dominant active Rac cannot be observed within this timeframe. This suggests that a longer induction is required for the cells to express sufficient levels of GFP-G12V Rac1A. We therefore supplied wild type and WASP knockout cells transfected with the dox-on GFP-G12V Rac1A vector with doxycycline, and analysed them by live-cell imaging for up to 10 hours post-induction. Figure 3.11 shows representative images of wild type and WASP knockout cells dealing with high levels of dominant active Rac after 8 hours from doxycycline treatment; a short timelapse is shown in movie 4. The differences are obvious. Wild type cells accumulate active Rac around most of the cell perimeter, assuming a scarcely polarised morphology. Nevertheless, they have smooth edges and occasionally extend a new pseudopod-like protrusion. As expected (Ridley et al., 1992), they tend to lose adhesion to the substrate, wobbling in place until a new contact with the bottom of the dish has been established. Similarly, WASP knockout cells accumulate dominant active Rac all around the plasma membrane, but acquire a completely different shape. Indeed, these cells become dramatically spiky, extending long filopodia in basically every direction; they appear to be more adherent that wild type cells, as they do not lose contact with the substrate as often.

It is difficult at this stage to reach a fully justified conclusion about the molecular basis of such a noticeable difference, but some speculations can be propounded. A compelling possibility arises from a recent work from our lab, showing that in the absence of both SCAR/WAVE and WASP *Dictyostelium* generates numerous spiky protrusions, mostly driven by formin dDia2 (Davidson et al., 2018). We demonstrated that this is due to a competition between WASP family members and formins: under normal conditions SCAR/WAVE (and in its absence WASP) override formins, favouring the formation of flat protrusions rather than spiky ones; in the absence of WASP family members, however, formins are unlocked and free to induce the formation of filopodia. What WASP family members and formins are competing over is presumably a pool of monomeric G-actin or shared activators. Of great relevance, SCAR/WAVE (and in its absence WASP) and formins are both regulated by Rac1 (Lebensohn and Kirschner, 2009; Li and Higgs, 2003; Schirenbeck et al., 2005; Veltman et al.,

2012). Is it therefore reasonable to hypothesise that the balance between pseudopodia and filopodia is influenced by the levels of GTP-bound Rac? In other words, can the amount of active Rac within cells determine whether these will generate flat protrusions or spiky ones?

Based on evidence presented in this chapter we hypothesise that WASP contributes to maintenance of homeostatic levels of active Rac, which are just sufficient to activate SCAR/WAVE and trigger the formation of pseudopodia. Overloading wild type cells with dominant active Rac causes a sort of widespread SCAR/WAVE-driven protrusion, leading to increased cell roundness. Conversely, WASP knockout cells have higher basal levels of active Rac, and overloading them with G12V Rac1A could quickly interfere with the pseudopodia/filopodia competition, allowing the formation of spiky protrusions. It will therefore be interesting to investigate whether dDia2 localises at the tip of filopodia reported in figure 3.11, and whether cells expressing GFP-WASP CRIB mutants show the same phenotype upon overexpression of dominant active Rac. The model proposed here is summarised in figure 3.12.

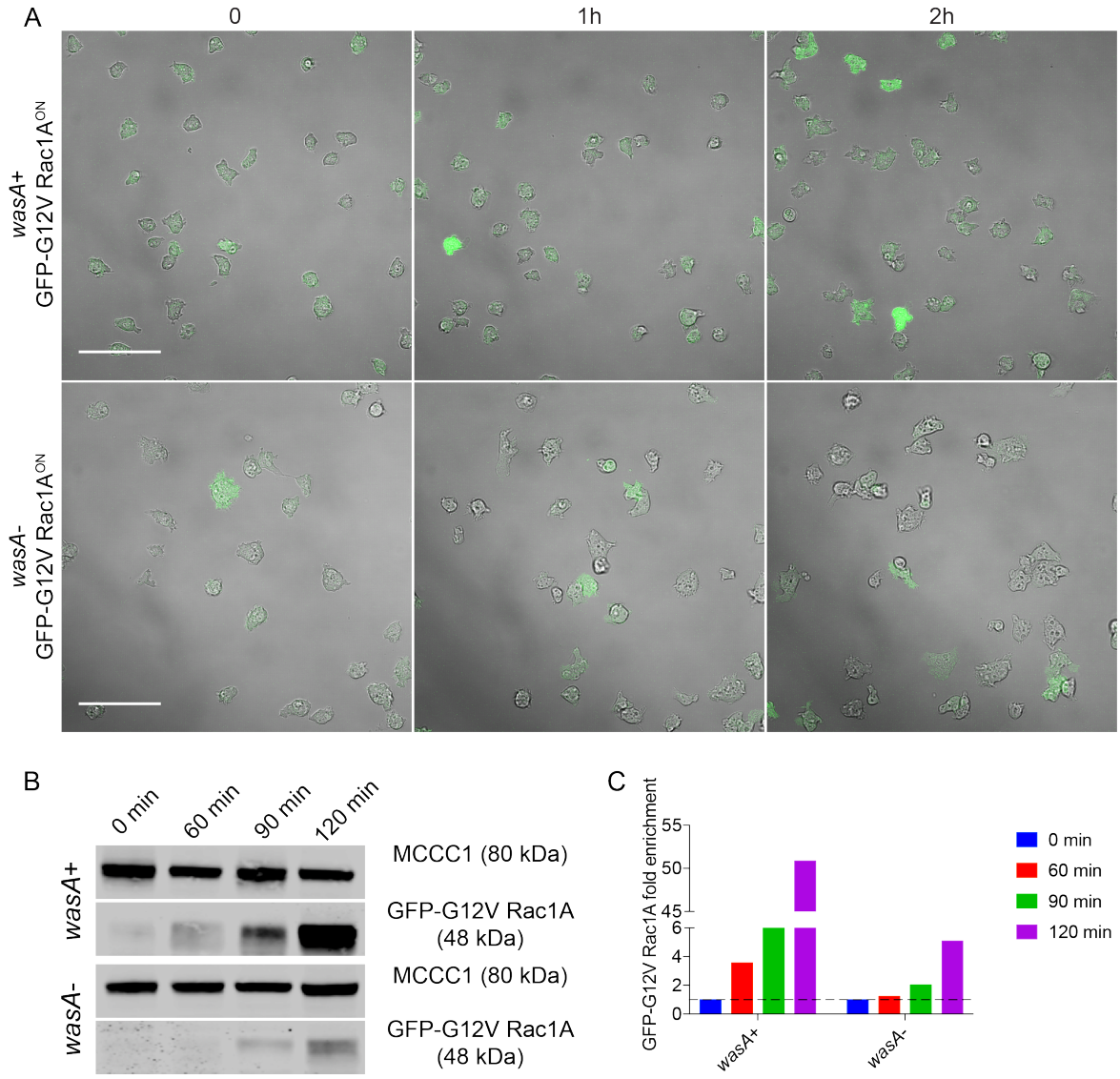

Figure 3.10 Validation of the doxycycline-inducible GFP-G12V Rac1A expression vector.

A) Wild type (top panel) and WASP knockout cells (bottom panel) were transiently transfected with an expression vector containing the G12V Rac1A-encoding sequence under a dox-on promoter. The green signal visualised in the absence of doxycycline by confocal microscopy points out a degree of leakiness. Scale bars represent 50 µm.

B) GFP Western blot on wild type (top two panels) and WASP knockout cells (bottom two panels) transfected with the inducible expression vector and harvested prior to doxycycline treatment (0 min), or 60, 90 and 120 min after induction. MCCC1 was used as loading control as previously described (Davidson et al., 2013).

C) Quantification of the GFP-G12V Rac1A levels normalised for MCCC1 upon doxycycline treatment (n=1).

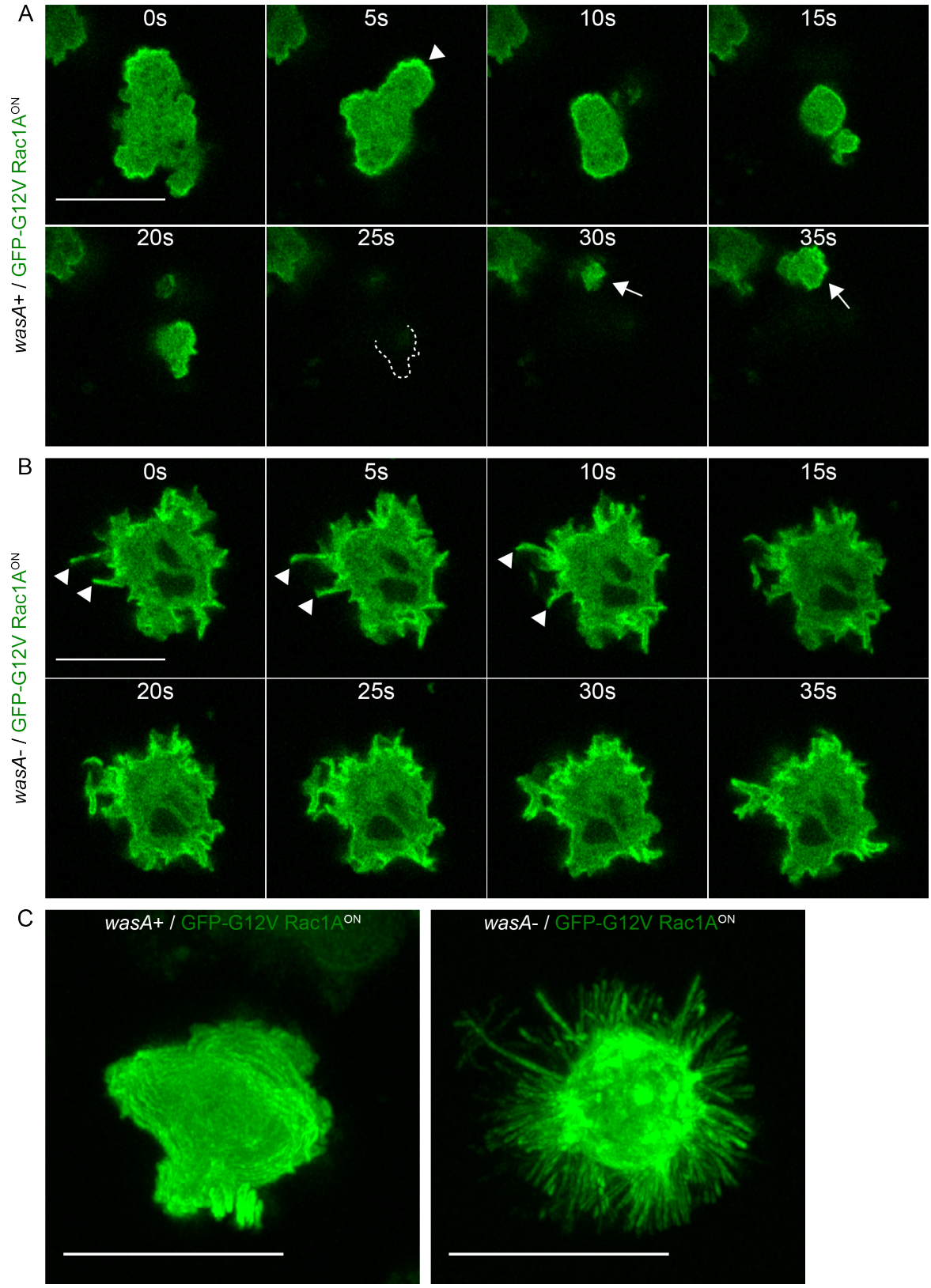

Figure 3.11 Wild type and WASP knockout cells handle dominant active Rac differently.

A) Super-resolution live-cell imaging revealed that wild type (*wasA*+) cells transfected with doxycycline-inducible GFP-G12V Rac1A accumulate it in a large proportion of the plasma membrane after 8 hours from induction. They have

smooth edges, are poorly polarised but manage to sporadically extend flat protrusions (white arrowhead at 5s). They frequently lose contact with the substrate but promptly try to adhere again; white dashed line at 25s outlines a detached cell, white arrows at 30 and 35 seconds point at the same cell trying to re-establish contacts with the substrate. Scale bar represents 10 μm.

B) WASP knockout (*wasA*-) cells transfected with doxycycline-inducible GFP-G12V Rac1A accumulate it all around the cell perimeter within long, spiky and fairly stable protrusions; representative filopodia are highlighted by white arrowheads in some of the time points. These cells are overall more adhesive in comparison to those in A). Scale bar represents 10 μm.

C) 3D reconstruction of *wasA*+ cells expressing GFP-G12V Rac1A (left-hand side) and *wasA*- cells expressing GFP-G12V Rac1A (right-hand side) 8 hours post-induction. Due to their loss of adhesion wild type cells are fairly unsettled, making it difficult to generate a clean z-stack. On the contrary, WASP knockout cells are quite still, and the z-stack obtained beautifully shows the incredibly high number of filopodia triggered by the presence of dominant active Rac. Scale bars represent 10 μm.

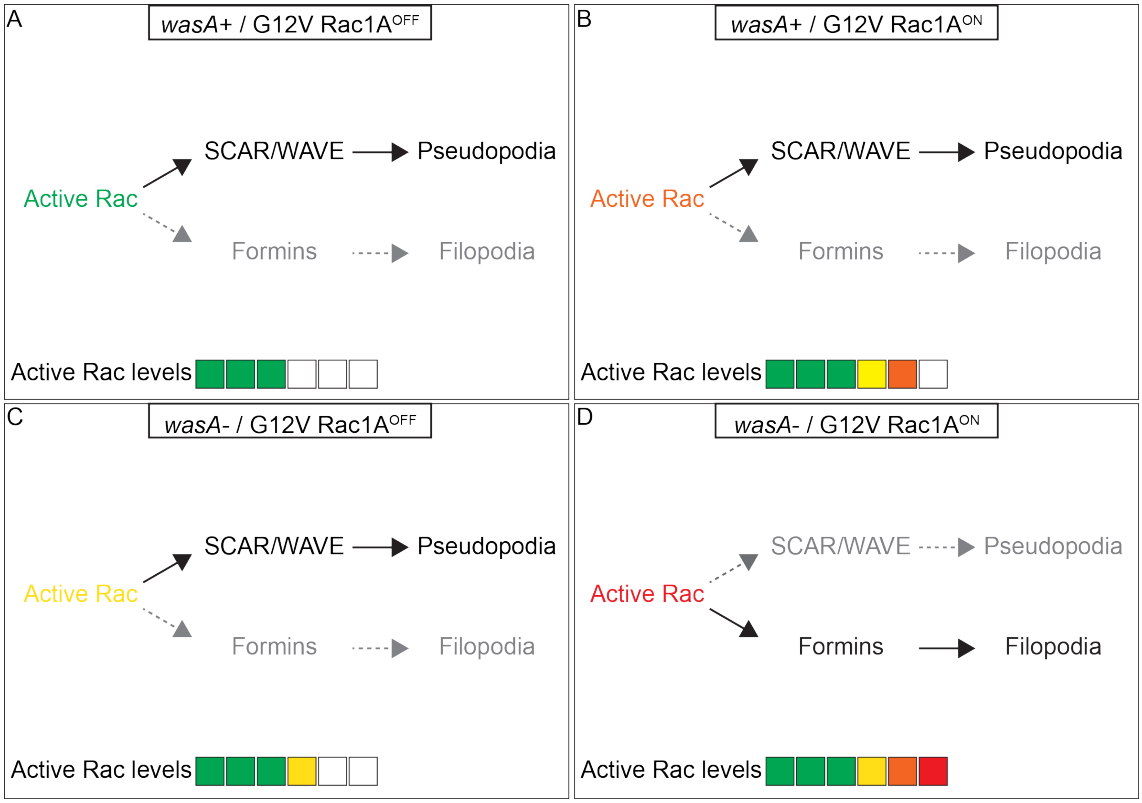

Figure 3.12 Possible model to explain the different G12V Rac1A handling dynamics of wild type and WASP knockout cells.

Our lab recently demonstrated that competition between WASP family members, mostly SCAR/WAVE, and formins occurs within cells and dictates the type of motility adopted. In more details, formation of pseudopodia/lamellipodia is largely favoured, while generation of filopodia by formins is strongly boosted in the absence of both SCAR/WAVE and WASP (Davidson et al., 2018). Formins (i.e. dDia2) and SCAR/WAVE (and in its absence WASP) (Veltman et al., 2012) are both regulated by Rac1 (Lebensohn and Kirschner, 2009; Schirenbeck et al., 2005), and is therefore plausible that the two actin nucleators compete for the cellular pool of active Rac, with SCAR/WAVE clearly showing stronger avidity than formins. We propose that in wild type cells (A) WASP contributes to maintenance of homeostatic levels of active Rac (green squares), and that the amount of active Rac available is sufficient to activate SCAR/WAVE but not formins, resulting in the formation of pseudopodia. When wild type cells express GFP-G12V Rac1A (B) the levels of active Rac are increased (orange square) up to the point to compromise adhesion and cell polarity, but not high enough to activate formins, at least not within the timeframe considered for this experiment. In the absence of WASP (C) the basal levels of Rac in its active state are likely higher (figure 3.9 and yellow square) and able to compromise cell

polarity, but are again not high enough to activate formins. When cells lacking WASP express dominant active Rac (D), the amount of active Rac available reaches quickly the threshold required to activate formins (red square), allowing the formation of an incredibly high number of filopodia.

3.6 WASP requires a functional CRIB motif to exclude active Rac from the cleavage furrow during cytokinesis

Cytokinesis is a fascinatingly complex process that requires the action of several molecules and their highly orchestrated regulation. A successful cell division underpins conservation of genetic information, ultimately ensuring perpetuation of the species. It does not therefore come as a surprise that *Dictyostelium* has evolved multiple types of cytokinesis to achieve the highest success rate possible. Myosin II contraction around the cleavage furrow to trigger the separation of the two daughter cells was the first mechanism of cell division uncovered in *Dictyostelium*. This model was supported by an early study showing that myosin II localises at the bridge connecting the two newly formed cells (Yumura and Fukui, 1985). Accordingly, a following study showed that genetic manipulation of *mhc* (myosin heavy chain) disrupts cytokinesis (De Lozanne and Spudich, 1987). It became clear later, however, that myosin is indispensable only for cells growing in the absence of a substratum to perform cytokinesis, while is unnecessary when cells divide in adhering conditions (Zang et al., 1997). Thus, at least two types of cell division exist: cytokinesis A, which is myosin-dependent, and cytokinesis B, which requires adhesion but not myosin. Both types of division are cell-cycle dependent, meaning that they occur at the end of telophase, when replicated chromosomes have already been equally sorted between the two daughter cells. *Dictyostelium* can perform a third type of cell division, named cytokinesis C (or *traction-mediated cytofission*), which is not connected to cell cycle progression (Nagasaki et al., 2002). During cytokinesis C, a portion of cytoplasm containing one or more nuclei is pinched off from a multinucleated cell.

We realised early on that some of the WASP knockout cells expressing GFP-WASP CRIB mutants were obviously larger than WASP knockout cells expressing GFP-WASP (rescue) when growing in adhering conditions. As a comparison, WASP knockout cells struggle to divide only when growing in the absence of a substratum, but appeared to be able to perform cytokinesis when kept in adhering conditions (Davidson, 2014). We hypothesised that WASP knockout cells expressing GFP-WASP CRIB mutants may have a cytokinesis defect. To test it, we allowed them to attach to coverslips, fixed them and stained them with DAPI (4',6-diamidino-2-phenylindole, which binds tightly to DNA). As shown in figure 3.13 A and quantified in B, the vast majority (≈ 91%) of cells expressing full-

length wild type WASP only have one nucleus, while this percentage is reduced in cells expressing GFP-ΔCRIB WASP or GFP-**CRIB WASP (67% and 69% respectively). Conversely, a significant increase in the number of cells having more than 2 nuclei can be observed: from just 1.6% in cells expressing full-length wild type WASP to 20% and 17% in cells expressing GFP- ΔCRIB WASP and GFP-**CRIB WASP respectively. As reported in figure 3.13 C, some of the cells expressing GFP-WASP CRIB mutants have more than 20 nuclei, with the highest number of nuclei per cell recorded of 70 (D).

Why would the absence of a functional WASP CRIB motif impair cytokinesis? In light of the complexity of the process and the existence of multiple options to execute it, different theories appear conceivable. The fact that cells expressing GFP-WASP CRIB mutants struggle to divide when growing in adhering condition, however, suggests that cytokinesis failure is not strictly due to altered myosin function. We sought to understand whether the inability of cells expressing a WASP CRIB mutant to complete cytokinesis when growing on a dish maybe due to their high levels of active Rac, which we have described throughout this chapter.

It has long been established that Rac is not required for cytokinesis: Rac-depleted *C. elegans* embryos, for instance, do not undergo any aberrant cell division (Jantsch-Plunger et al., 2000). On the contrary, evidence suggests that Rac must be kept at bay during cytokinesis. For instance, the centralspindlin complex, which orchestrates cytokinesis in a wide range of organisms, contains a RacGAP named CYK4. Its deletion leads to the formation of a rough eye phenotype in *Drosophila*, which can be reverted by knocking down the three Rac isoforms present in *Drosophila* (D'Avino et al., 2004). Similarly, knocking down Rac rescues the phenotype caused by inactivating mutations within the GAP domain of CYK4 in *C. elegans* (Canman et al., 2008). The reason behind the need to control Rac levels at the onset of cytokinesis has been recently unveiled. In wild type cells Rac activity is confined at the daughter cells' poles, where it presumably contributes to push them in opposite directions. In the presence of CYK4-GAP mutations, active Rac become aberrantly accumulated at the cleavage furrow; this is followed by an increase in the strength of the adhesions, which hampers the ability of the two newly originated cells to be pulled apart.

Therefore maintaining homeostatic levels of Rac is mandatory to ensure the formation of a ductile cleavage furrow (Bastos et al., 2012).
With this in mind, and aware that cells expressing WASP CRIB mutants appear to have higher levels of active Rac, we hypothesised that their defect in cytokinesis was due to the presence of a firm and active Rac-enriched cleavage furrow.
To test our hypothesis we transiently transfected WASP knockout cells with a co-expression vector harbouring a GFP-tagged WASP (either full-length wild type, ΔCRIB mutant or **CRIB mutant) and a red-tagged pakB CRIB. We then performed live-cell imaging on cells performing cytokinesis. As shown in figure 3.14, in the presence of full-length wild type WASP active Rac is accumulated at the poles of the daughter cells, not at all within the cleavage furrow. These cells divide smoothly and quickly. On the contrary, cells expressing WASP CRIB mutants struggle to become separated, pull themselves further away from the cleavage furrow, which appears to aberrantly retain active Rac.

This evidence suggests that a direct interaction with active Rac may be required for WASP to exclude active Rac from the cleavage furrow and ensure maintenance of polarity during cytokinesis.

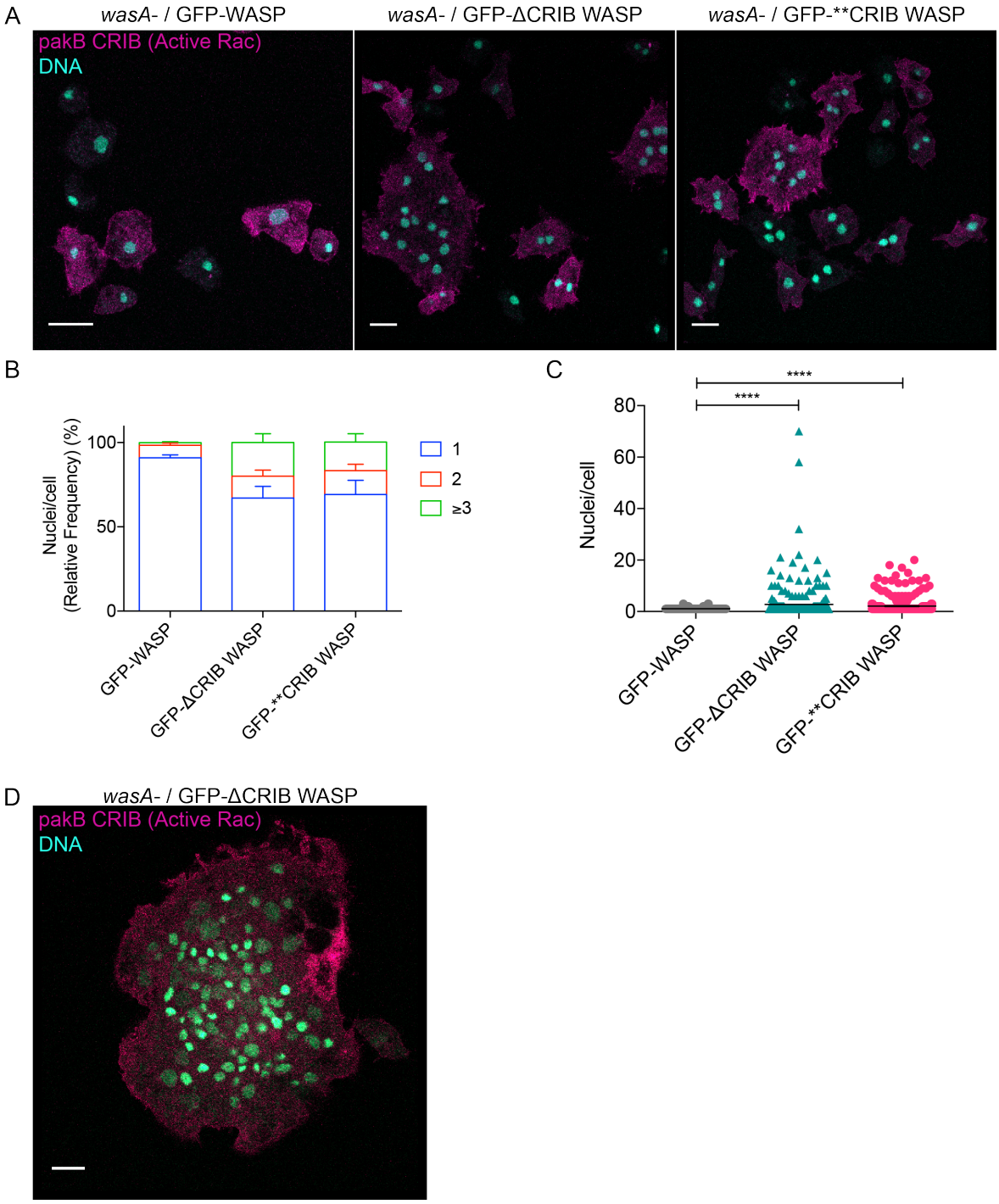

Figure 3.13 A functional WASP CRIB motif is required to ensure completion of cytokinesis in adhering conditions.

A) WASP knockout cells were transiently transfected with a co-expression vector encoding GFP-WASP and pakB CRIB-mRFPmars2 (GFP channel not shown, rescue, left panel), or with GFP-ΔCRIB WASP and pakB CRIB-mRFPmars2 (GFP channel not shown, central panel), or with GFP-**CRIB WASP and pakB CRIB-mRFPmars2 (GFP channel not shown, right panel). Transfected cells were grown in the presence of a substrate and then fixed and stained with DAPI. While cells expressing full-length wild type WASP are mostly mononucleated, a proportion

of those expressing either WASP CRIB mutants have more than one nucleus, suggesting a defect in cytokinesis. Scale bars represent 10 µm.

B) Quantification of the proportion on mono- and multinucleated cells in the presence of WASP CRIB mutants. In the presence of a functional CRIB motif most cells show only one nucleus: $mean_{1\ nucleus}$= 90.97% ± 1.75; error represents S.E.M.; $mean_{2\ nuclei}$= 7.43% ± 1.26; error represents S.E.M.; $mean_{>3nuclei}$= 1.57% ± 0.55; error represents S.E.M.; n= 376 cells over 3 independent experiments. Cells expressing a non-functional WASP CRIB motif are generally multinucleated. In the case of cells expressing GFP-ΔCRIB WASP, for instance: $mean_{1\ nucleus}$= 67.07% ± 6.95; error represents S.E.M.; $mean_{2\ nuclei}$= 12.97% ± 3.62; error represents S.E.M.; $mean_{>3nuclei}$= 20.00% ± 5.27; error represents S.E.M.; n= 332 cells over 3 independent experiments. In the case of cells expressing GFP-**CRIB WASP: $mean_{1\ nucleus}$= 69.17% ± 8.4; error represents S.E.M.; $mean_{2\ nuclei}$= 14.20% ± 3.73; error represents S.E.M.; $mean_{>3nuclei}$= 16.97% ± 4.93; error represents S.E.M.; n= 370 cells over 3 independent experiments. Data analysis (two-way ANOVA, multiple comparison) confirmed that a significant difference exists between the proportion of mononucleated cells expressing full-length wild type or either WASP CRIB mutants (GFP-WASP vs GFP-ΔCRIB WASP: p=0.0003; GFP-WASP vs GFP-**CRIB WASP: p=0.0006; GFP-ΔCRIB WASP vs GFP-**CRIB WASP: p=0.87). No difference exists between the number of binucleated cells expressing full-length wild type or either WASP CRIB mutants (GFP-WASP vs GFP-ΔCRIB WASP: p=0.41; GFP-WASP vs GFP-**CRIB WASP: p=0.27; GFP-ΔCRIB WASP vs GFP-**CRIB WASP: p=0.95). A significant difference can be measured between the proportion of cells expressing full-length wild type or either WASP CRIB mutants that have more than 3 nuclei (GFP-WASP vs GFP-ΔCRIB WASP: p=0.0022; GFP-WASP vs GFP-**CRIB WASP: p=0.0079; GFP-ΔCRIB WASP vs GFP-**CRIB WASP: p=0.75).

C) Number of nuclei per cell in the presence/absence of a functional WASP CRIB motif. $mean_{GFP\text{-}WASP}$= 1.10 ± 0.02; error represents S.E.M.; $mean_{GFP\text{-}\Delta CRIB\ WASP}$= 2.77 ± 0.33; $mean_{GFP\text{-}**CRIB\ WASP}$= 2.12 ± 0.14 error represents S.E.M.. Shapiro-Wilk test revealed that samples are not normally distributed ($p<0.05$). A Mann-Whitney test was therefore utilised. It revealed that a significant difference in the number of nuclei/cell exists between cells expressing GFP-WASP and GFP-ΔCRIB WASP ($p<0.0001$) as well as between cells expressing GFP-WASP and GFP-**CRIB WASP ($p<0.0001$).

D) Some of the cells expressing GFP-WASP CRIB mutants have more than 20 nuclei. Scale bar represents 10 μm.

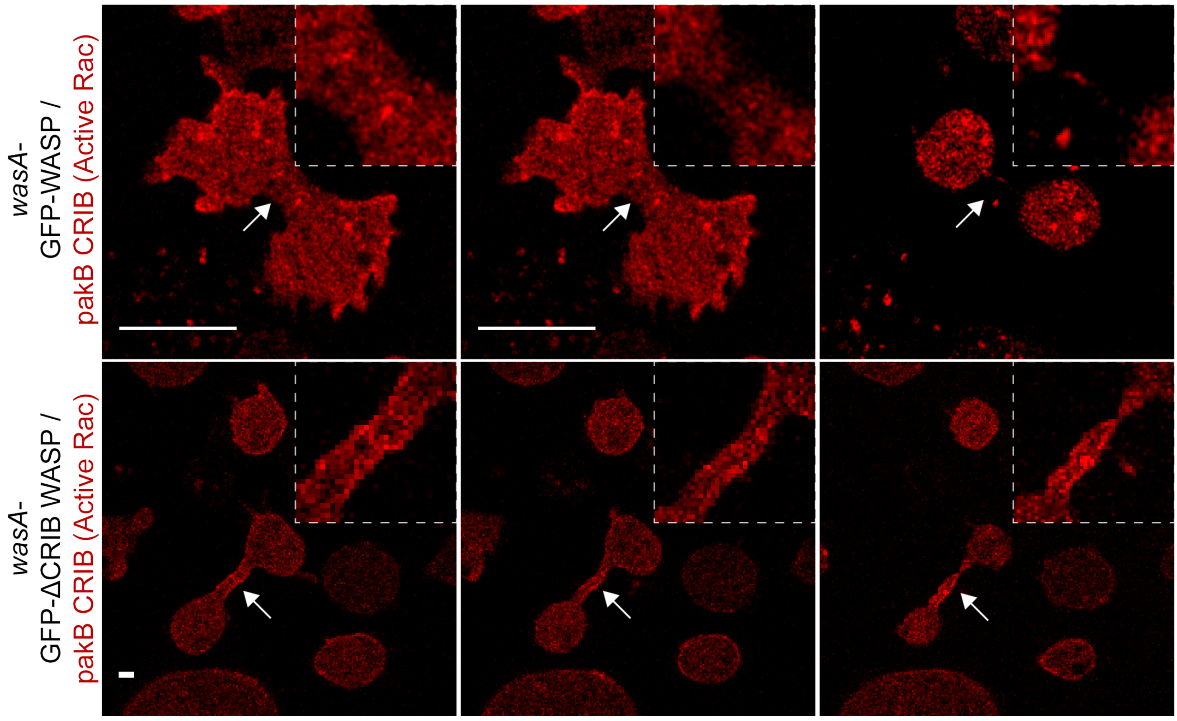

Figure 3.14 A functional WASP CRIB motif is required to exclude active Rac from the cleavage furrow during cytokinesis.

Cytokinesis was monitored by super-resolution live-cell imaging in WASP knockout cells transiently transfected with a co-expression vector encoding GFP-WASP and pakB CRIB-mRFPmars2 (GFP channel not shown, rescue, top panel), or with GFP-ΔCRIB WASP and pakB CRIB-mRFPmars2 (GFP channel not shown, bottom panel). As shown in the montage at the top, active Rac is not normally accumulated at the cleavage furrow but rather at the cell cortex of the daughter cells. These are quickly separated as abscission of the bridge occurs. The white arrows point at the cleavage furrow, which is shown in greater details in the zoomed images within the dashed squares. Cells expressing a CRIB-mutated WASP, instead, pull themselves further away from one another in the attempt to overcome a defect in cleavage furrow constriction. Active Rac is aberrantly accumulated at the bridge connecting the two daughter cells, presumably hampering its detachment and its subsequent severing. As above, white arrows indicate the cleavage furrow, which is showed in greater details in the zoomed images within the dashed squares. Scale bars represent 10 μm.

3.7 Chapter 3 summary

In this chapter we have explored the molecular mechanisms underlying WASP-mediated maintenance of cell polarity.

We started by asking whether WASP relies on clathrin-mediated endocytosis to confine active Rac at the leading edge of migrating cells. Early evidence from our lab demonstrated that active Rac is not enriched on clathrin-coated pits under normal circumstances (Davidson, 2014), and that Rac activators (such as Rac GEFs) are likely not recycled via clathrin-mediated endocytosis (Andrew J. Davidson, Peter A. Thomason, unpublished data). To gather more direct evidence regarding the importance of CME for the spatial restriction of Rac, we investigated the degree of co-localisation between clathrin and Rac itself. Live-cell imaging experiments showed that Rac does not appear to be enriched on clathrin-coated pits. Altogether, these results may be interpreted as meaning that WASP confines Rac activity and maintains cell polarity via a CME-unrelated mechanism. However, only addressing the ability of clathrin-deficient cells to spatially confine active Rac will allow us to clarify whether or not WASP's role in maintenance of cell polarity is distinct from its role in CME.

As for the molecular requirements for WASP to maintain cell polarity, we decided to explore the idea that WASP utilises its CRIB motif to interact directly with active Rac and control its spatial distribution. We have shown here that a functional CRIB motif is required to prevent aberrant accumulation of GTP-bound Rac at the rear. Indeed, cells lacking endogenous WASP but expressing a WASP CRIB mutant have compromised front–rear polarity.

Moreover, we have provided evidence suggesting that the presence of a functional CRIB motif is required for WASP to maintain homeostatic cellular levels of active Rac. Taking into account that Rac is tightly coupled to the cell membrane when in its active state (Moissoglu et al., 2006), and that tagged Pak CRIB faithfully reports the localisation of active Rho GTPases (Itoh et al., 2002), we have shown that in cells expressing a CRIB-mutated WASP a larger proportion of the plasma membrane is enriched in active Rac marker. This hints at the possibility that WASP may contribute via its CRIB motif to maintain physiological levels of active, membrane-bound, Rac.

We have also shown that WASP, presumably via its CRIB motif, helps cells to handle high levels of dominant active Rac. When presented with excessive G12V Rac wild type cells react by generating a large ruffle, which leads to increased

roundness and decreased cell adhesion. Strikingly different, cells lacking WASP extend long and stable filopodia when overloaded with dominant active Rac. We speculate that the higher basal levels of active Rac caused by the lack of WASP (and, presumably, by the lack of a functional WASP CRIB motif) may trigger such a dramatic difference. Based on the competition between SCAR/WAVE and formins that our lab has recently uncovered (Davidson et al., 2018), and on the fact that SCAR/WAVE and formins are both regulated by Rac1, we hypothesised that in the absence of WASP and in the presence of high levels of G12V Rac, the amount of active Rac available within the cells may be high enough to interfere with the aforementioned competition, leading to the formation of aberrant filopodia.

Lastly, we have shown that the presence of a functional WASP CRIB motif is required for cells to complete cytokinesis in adhering condition. When kept in the presence of a substrate, cells expressing a WASP CRIB mutant often fail to divide and become severely multinucleated. We sought to understand whether high basal levels of active Rac may account for such a dramatic phenotype. Indeed, it has been demonstrated that active Rac must be removed from the cleavage furrow, and that dominant active Rac aberrantly accumulates at the connecting bridge hampering the separation of the two daughter cells (Bastos et al., 2012). We showed here that the presence of a functional WASP CRIB motif is required for the cells to exclude active Rac from the cleavage furrow and ensure efficient cytokinesis.

Overall, we have gathered evidence in support of a model whereby the CRIB-mediated interaction between WASP and active Rac is required for safeguarding cell polarity during migration and cytokinesis, and likely to ensure maintenance of homeostatic levels of active Rac.

Chapter 4 , *Results – part II*

WASP does not require a direct interaction with active Rac to induce actin polymerisation on clathrin-coated pits

4.1 Preface

As mentioned in section 1.3.5, most of what we currently know about the role of Rho GTPases on the regulation of ubiquitous WASPs throughout evolution comes from pioneering studies on mammalian N-WASP.

Early work from the Takenawa lab demonstrated that N-WASP requires an intact CRIB motif to interact with dominant active Cdc42 *in vitro*, and that their interaction is required for N-WASP to stimulate the formation of filopodia (Miki et al., 1998a). Miki and colleagues proposed a model whereby active Cdc42 binds to the CRIB motif of N-WASP and facilitates its activation by unmasking its otherwise hidden C-terminal region, which mediates actin dynamics (Miki et al., 1998a). The same group provided shortly after further evidence strengthening the idea of active Cdc42 as an allosteric activator of N-WASP. In more details, it was shown that the isolated C-terminal VCA domain of N-WASP triggers actin polymerisation with higher efficiency when compared to full-length N-WASP *in vitro*, and that addition of active Cdc42 (along with PIP2) strongly boosts the ability of full-length N-WASP to trigger actin polymerisation *in vitro* (Rohatgi et al., 1999). More recently, Tomasevic and colleagues have provided *in vitro* evidence pointing out that N-WASP stimulates actin polymerisation at a significantly higher rate in the presence of active Rac rather than of Cdc42, while hematopoietic WASP appears to be more responsive to Cdc42 (Tomasevic et al., 2007). Largely based on *in vitro* evidence, these works contributed to the establishment of a dogma whereby active Rho GTPases (Cdc42 or Rac), in addition to other signals (such as SH3 domain-containing proteins and phospholipids), activate N-WASP by releasing the auto-inhibition. This model has not been formally questioned throughout the years despite conflicting evidence exists. For instance Las17, the WASP orthologue in yeasts, drives the internalisation of clathrin-coated pits in a remarkably similar way to *Dictyostelium* WASP or mammalian N-WASP despite lacking a CRIB motif, hinting at the possibility that a direct interaction between active Rho GTPases and WASP may be dispensable for the latter to drive endocytosis. Furthermore, it has been shown that N-WASP does not require a functional CRIB motif to be recruited to and induce actin polymerisation on rocketing tails in murine fibroblasts (Benesch et al., 2002). Moreover, it has been suggested that *Dictyostelium* WASP localises on intracellular vesicles independently of its CRIB motif (Myers et al., 2005), although supporting evidence has not been published.

Notably, a *Drosophila* Wsp mutant lacking 14 amino acids from the N-terminal region of its CRIB motif (analogous to the ΔCRIB WASP mutant presented in section 3.3), and therefore unable to interact with active Rho GTPases, rescues the Wsp bristle-loss phenotype (Tal et al., 2002), again suggesting that WASP may not require active Rho GTPases to exert at least some of its functions.

Given the genetic tractability of *Dictyostelium* and the high degree of conservation of WASP and Rac across evolution, we realised that we could incisively address the importance/dispensability of active Rho GTPases for WASP functionality. Given that *Dictyostelium* does not appear to express any Cdc42 orthologue (Rivero et al., 2001), we specifically aimed to assess the role of active Rac for WASP's activation.

4.2 WASP and active Rac do not show overlapping punctate localisation

We started our investigation using a visual approach: we reasoned that if active Rac has a role in the activation of WASP the two molecules should co-localise within the same cellular area or structure. It is important to mention at this stage that while reporters exist that specifically indicate Rac in its active state (i.e. pakB CRIB), no marker that could discriminate between inactive and active WASP is available. However, taking into account that WASP is able to trigger actin polymerisation when localised at discrete areas of the cell (i.e. a *punctum* on the ventral membrane) rather than when evenly distributed throughout the cytosol, WASP localisation is considered as a *bona fide* sign of its activation. To address whether WASP and active Rac co-localise we co-expressed GFP-WASP and red-tagged active Rac marker (pakB CRIB-mRFPmars2) in WASP knockout cells, and analysed their subcellular localisation by live-cell imaging. As shown in figure 4.1, GFP-WASP is found on transient ventral *puncta*, allegedly all endocytic spots, which are rarely formed at the front of migrating cells. WASP can also be occasionally found at the leading edge of migrating *Dictyostelium* cells, but its role in pseudopodia extension is likely negligible under normal circumstances, since WASP knockout cells generate normal SCAR/WAVE-driven protrusions (Davidson, 2014). As previously mentioned, pakB CRIB is enriched at the leading edge, since active Rac at this site triggers actin polymerisation to power motility. Active Rac is not enriched on WASP-positive spots.

How informative is the lack of co-localisation? Is it crucial for regulators and downstream effectors to be in the same place? As a comparison, we decided to investigate the degree of co-localisation between active Rac and SCAR/WAVE, for which GTP-bound Rac has also been proposed as a main activator based on *in vitro* evidence (Lebensohn and Kirschner, 2009). As shown in figure 4.2, active Rac and SCAR/WAVE co-localise at the leading edge of migrating cells. The two molecules often exhibit a different pattern, with SCAR/WAVE occupying only the tip of pseudopodia and active Rac marker being distributed over a thicker area.

On one hand our data show that SCAR/WAVE and active Rac can be detected within the same region of the cell, in support of a model whereby SCAR/WAVE requires an interaction with prenylated GTP-bound Rac to be localised/activated. On the other hand we point out that WASP and active Rac

do not show overlapping distribution, at least not within ventral spots. This observation led to at least two hypotheses: 1) WASP does not require active Rac to be activated/recruited on *puncta*, or 2) Rac-mediated activation of WASP occurs deeper into the cytosol prior to WASP recruitment on ventral spots, and is therefore not visible when focusing on the basal membrane.

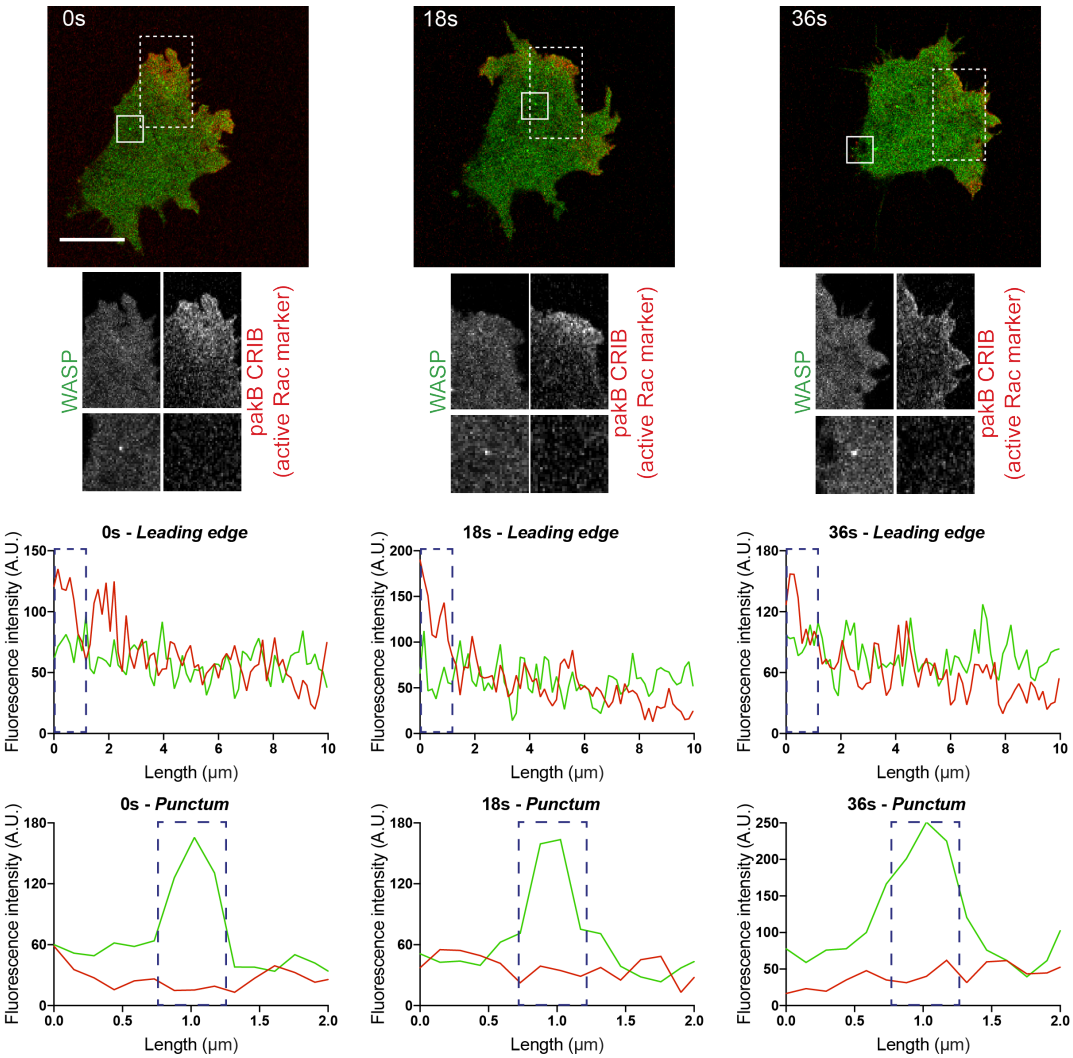

Figure 4.1 WASP and active Rac marker do not show overlapping subcellular localisation.

WASP knockout cells were transfected with a co-expression vector encoding GFP-WASP (rescue) and pakB CRIB-mRFPmars2 (active Rac marker). Transfected cells were analysed by super-resolution live-cell imaging during directed migration. Active Rac marker consistently localises at the leading edge (zoomed within a dashed rectangle at all time points), while GFP-WASP is found at dynamic spots (each of which is referred to as a *punctum*) that mostly occur at the rear half of the cell and never appear to be enriched in active Rac marker. Individual spots, which are thought to be events of clathrin-mediated endocytosis, are depicted in greater detail within the solid squares at all time points. Scale bar represents 10 μm. Fluorescence plots below report the fluorescence intensity of GFP-WASP (in green) and pakB CRIB-mRFPmars2 (in red) across a 10 μm straight line connecting leading edge to cytosol (named *leading edge*, top fluorescence plots) or across a 2 μm straight line that includes

a WASP spot (named *punctum*, bottom fluorescence plots). Fluorescence plots confirmed that WASP and active Rac tend to localise to distinct areas of the cell (dashed blue rectangles).

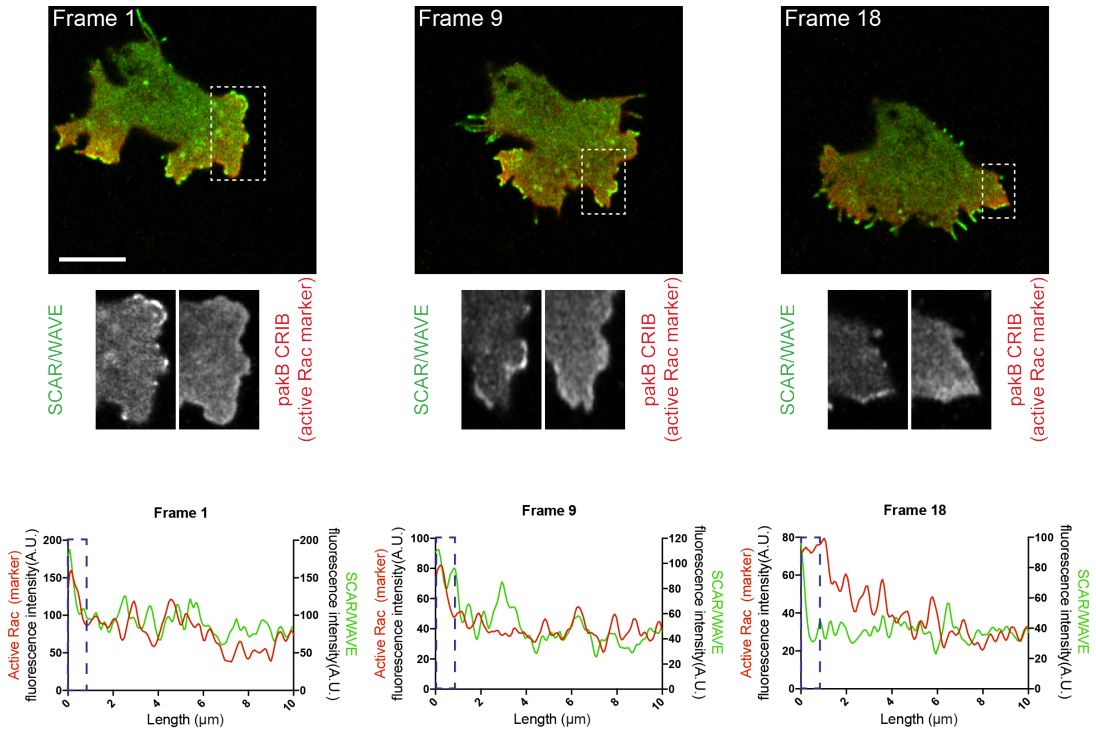

Figure 4.2 SCAR/WAVE and active Rac marker co-localise at the leading edge during migration.

In the attempt to understand whether active Rac regulates WASP despite no sign of co-localisation between the two molecules, we asked whether SCAR/WAVE (which has also been linked to Rac-mediated regulation) could instead be observed in the same region of the cell as the active Rac marker. To do so we transfected wild type cells with a co-expression vector encoding GFP-HSPC300 (one of the subunits of the SCAR/WAVE complex) and pakB CRIB-mRFPmars2. We then investigated the localisation of both probes by super-resolution live-cell imaging. SCAR/WAVE and active Rac marker are both found at the front of the cells during migration, as well as on occasionally generated lateral protrusions. Scale bar represents 10 μm. Fluorescence plots at the bottom report the intensity of HSPC300 (in green) and active Rac marker (in red) across a 10 μm straight line that includes the leading edge at three time points. These confirm that a peak of both molecules can be detected at the front of migrating cells (dashed blue rectangles).

4.3 Rac inhibition does not affect WASP localisation

To tease apart the two hypotheses we decided to deplete all active Rac available within cells by treating them with high doses of a Rac inhibitor. At least two Rac inhibitors have been optimised for use in mammalian cells and are commercially available, but none of them has been used on *Dictyostelium* before.
We tested two compounds: NSC23766 (Gao et al., 2004) and EHT1864 (Onesto et al., 2008), which have different mechanisms of action. NSC23766 prevents GEF-mediated activation of Rac by binding to a Rac region otherwise recognised by activators like Tiam1. EHT1864, instead, avidly interacts with Rac and hampers nucleotide binding, rendering it substantially inert. To monitor Rac localisation and dynamics upon treatment with the inhibitors we transfected wild type cells with a red-tagged reporter for active Rac (pakB CRIB- mRFPmars2) and performed super-resolution live-cell imaging. NSC23766 failed to cause any effect on *Dictyostelium*, even when used at significantly higher concentrations than suggested (data not shown). As reported in figure 4.3 EHT1864 instead triggers a rapid and dramatic effect when used at concentrations of at least 3 μM: cells round up quickly and the active Rac marker loses its membrane localisation.

Having proved that EHT1864 effectively inhibits Rac in *Dictyostelium*, we went on addressing whether WASP activation and dynamics are at all affected by Rac inhibition. To answer our question we transfected WASP knockout cells with GFP-WASP (rescue) and red-tagged active Rac marker (pakB CRIB-mRFPmars2) and analysed WASP localisation and dynamics upon treatment with EHT1864. As we aimed to kill Rac completely we decided to utilise a concentration of 50 μM, which has been extensively employed by for *in vitro* and *in vivo* studies (Onesto et al., 2008) and, as predicted by data shown in figure 4.3, quickly exerts the desired effect. Cells treated with such a high concentration of Rac inhibitor can be informative for about 15 minutes: after this time they massively de-adhere from the substrate and float away. As shown in figure 4.4 and in movie 5, GFP-WASP can be detected on discrete bright *puncta* that stand out from the otherwise evenly cytosolic signal prior to inhibitor addition. As expected, EHT1864 causes a dramatic alteration of cell morphology, resulting in cells rounding up within one minute from the treatment. In sharp disagreement with

the current model of Rac-mediated activation of WASP, however, dynamic GFP-WASP-positive spots are generated at least up to 15 minutes after the treatment. No statistical difference could be measured in the lifespan of WASP *puncta* generated prior to/upon addition of Rac inhibitor, although long-lived ones seem more prevalent in the presence of the drug. Similarly, the rate of WASP spot formation appears to be unaffected by the treatment.

These data show that WASP does not lose its ability to generate dynamic *puncta* when active Rac is no longer available within the cell.

Intriguingly, GFP-WASP occasionally localises at the edges of C-shaped vesicles, which appear to be formed in just a few seconds (yellow arrows at 2s and 6s); speculations on what these structures are and what their role is will be provided in chapter 5.

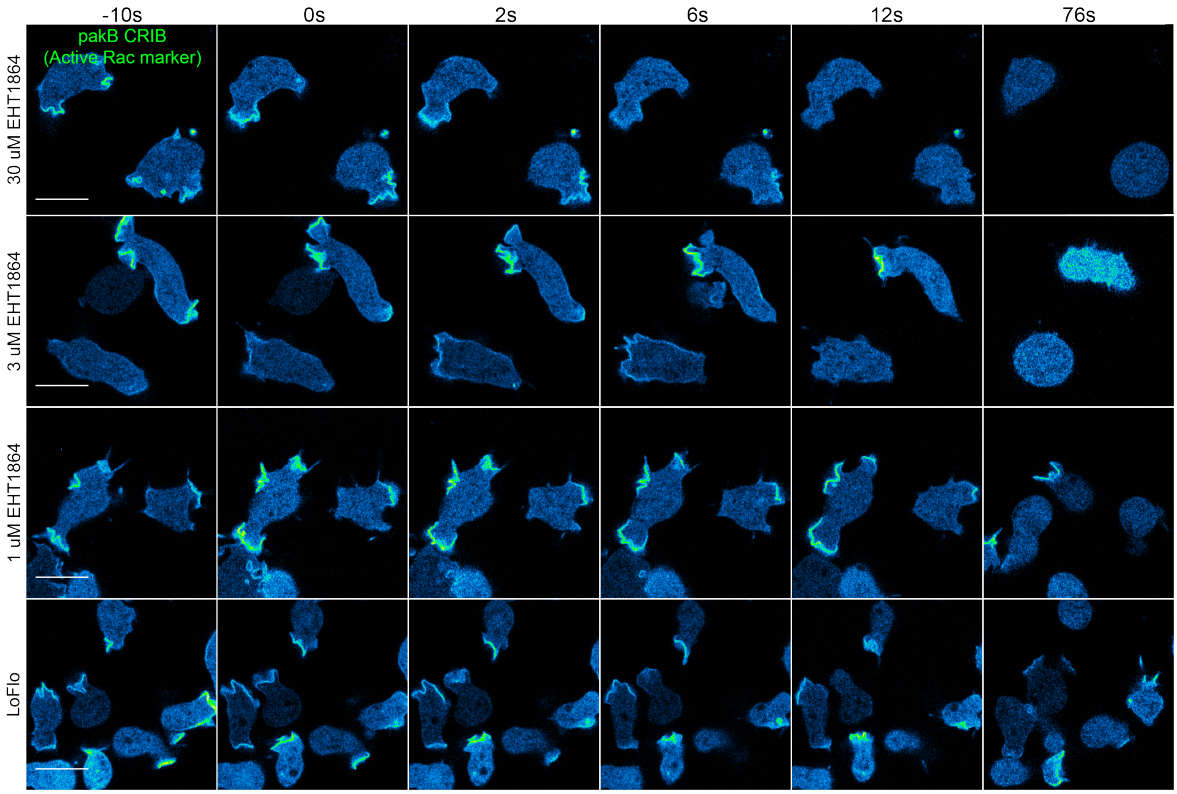

Figure 4.3 EHT1864 effciently inhibits *Dictyostelium* Rac.

In order to assess the ability of EHT1864 to inhibit Rac in *Dictyostelium* wild type cells were transfected with a red-tagged reporter for active Rac (pakB CRIB-mRFPmars2, shown here in Green Fire Blue LUT), treated with different concentrations of the compound, and analysed by super-resolution live-cell imaging. As a control, cells were trated with LoFlo, a low florescence medium where the drug had been diluted (bottom panel). In all conditions the active Rac marker localises at the cell membrane prior to inhibitor treatment (-10s), often at sites of macropinosome formation. Upon addition of 30 µM EHT1864 (top panel line, 0s) cells react quickly, rounding up completely within 12 seconds; after this time no active Rac marker can be spotted on the cell membrane. 3 µM (second panel line) is in our hand the minimum effective EHT1864 concentration, capable of entirely inhibiting Rac within less than two minutes. Lastly, 1 µM EHT1864 (third panel line) does not suffice to inhibit Rac in *Dictyostelium*: despite a reduction in membrane-targeted pakB CRIB can be detected between 12s and 76s, cells eventually recover from the treatment, restarting to form macropinosomes (data not shown). Other concentrations tested but not reported here include: 100 nM, 300 nM and 10 uM. Scale bars represent 10 µm.

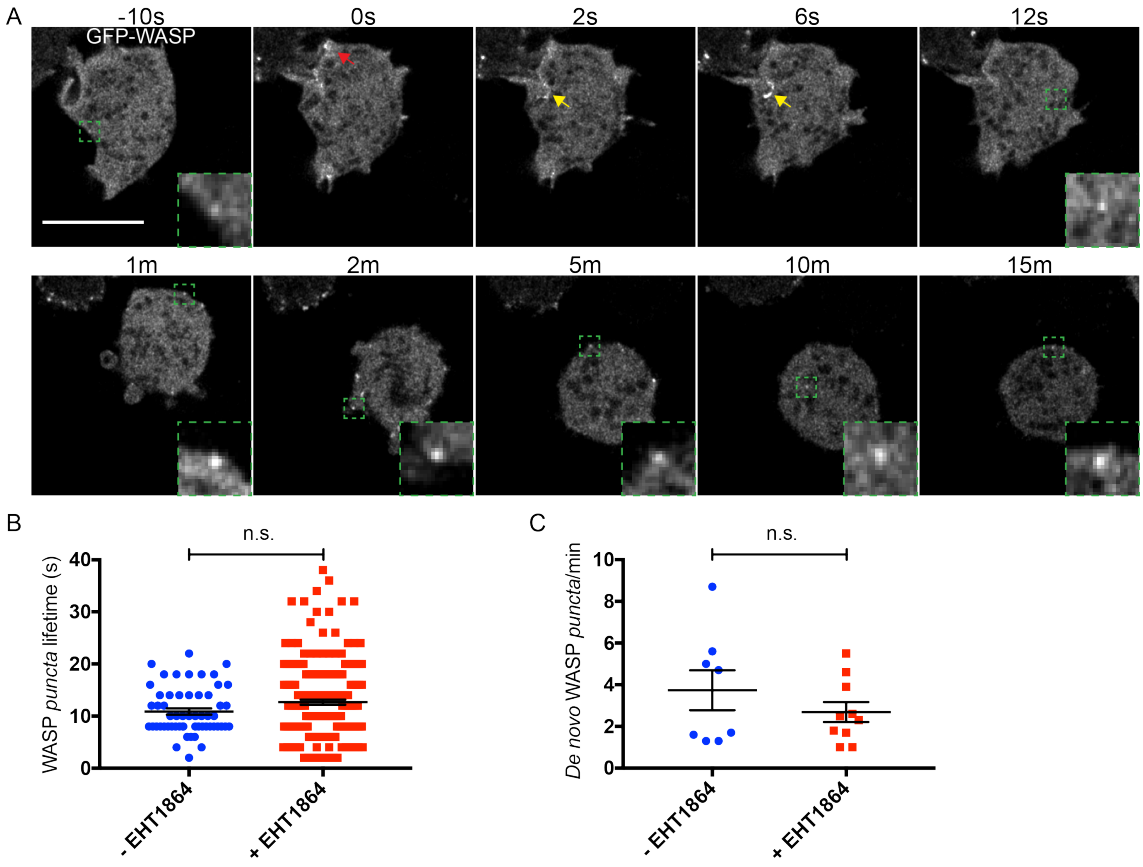

Figure 4.4 Rac inhibition does not affect WASP localisation.

To clarify whether Rac inhibition suppressed WASP localisation/dynamics we performed super-resolution live-cell imaging on WASP knockout cells co-expressing GFP-WASP (rescue) and active Rac marker (pakB CRIB-mRFPmars2, channel not shown) treated with high concentration of EHT1864 (50 μM).

A) Before addition of the drug (-10s) GFP-WASP can be spotted on a *punctum* formed near the plasma membrane. The cell reported here does not contain any WASP-positive spot at the time the inhibitor is added (0s), but GFP-WASP localises on a patch highlighted by the red arrow, which may be a macropinosome. No WASP *puncta* are observed at 2s and 6s from the treatment, but GFP-WASP is curiously spotted on the edge of a C-shaped vesicle (yellow arrows). As shown at all later time points (1m, 2m, 5m, 10m, 15m) WASP is able to generate dynamic spots even when Rac is completely inhibited, as can be inferred from the dramatic rounding up the cells have undergone. Enlarged and brightened individual WASP spots are shown within dashed green squares. Scale bar represents 10 μm.

B) The lifetime of individual WASP *puncta* has been measured before and after EHT1864 treatment. Shapiro-Wilk test revealed that the two samples are not

normally distributed ($p < 0.05$), and data analysis was therefore performed using a Mann-Whitney test. It revealed that no statistical difference exists in the lifetime of WASP puncta prior to and upon addition of Rac inhibitor ($p = 0.2023$). Untreated cells (-EHT1864): mean= 10.88 sec ± 0.59, error represents S.E.M.; n= 57 *puncta* over 3 independent experiments. Treated cells (+EHT1864): mean= 12.67 sec ± 0.49, error represents S.E.M.; n= 213 *puncta* over 3 independent experiments.

C) The rate of WASP *puncta* generation prior to and upon addition of the drug was quantified. Shapiro-Wilk test showed that the two samples are normally distributed (p -EHT1864= 0.10; p +EHT1864= 0.30), and statistical analysis was performed using unpaired t-test. It showed that the number of WASP spots generated per minute in the presence of the inhibitor is not different from the number of WASP spots generated within the same timeframe in untreated cells ($p=0.3130$). Untreated cells (-EHT1864): mean= 3.74 *puncta*/min ± 0.96, error represents S.E.M.; n= 8 cells over 3 independent experiments. Treated cells (+EHT1864): mean= 2.69 *puncta*/min ± 0.48, error represents S.E.M.; n= 10 cells over 3 independent experiments.

4.4 Mutations in the CRIB motif impair WASP's ability to bind active Rac without affecting its punctate localisation or preventing its recruitment on CCPs

The lack of co-localisation between WASP and active Rac along with the ability of WASP to generate dynamic spots in the presence of the Rac inhibitor EHT1864 suggest that Rac-independent mechanisms of WASP activation must occur in living cells. To gather further evidence in support of this hypothesis we addressed the functionality of WASP CRIB mutants, which have lost their ability to interact with GTP-bound Rac, as described in section 3.3.
We started by asking whether these mutants could form dynamic *puncta*. Based on the accepted model of Rac-mediated activation of WASP (Han et al., 2006), and on the assumption that WASP is active when present on ventral spots, we should expect no sign of localisation of the WASP CRIB mutants. To clarify it, we transfected WASP knockout cells with an extrachromosomal vector encoding GFP-WASP (rescue) or GFP-tagged ΔCRIB WASP or **CRIB WASP. Transfected cells were then analysed by confocal live-cell imaging during directed migration. As shown in figure 4.5, GFP-tagged full-length wild type WASP localises to discrete spots that are generally, but not universally, found at the trailing edge. Occasionally, GFP-WASP can also be spotted at the leading edge but, as described previously, its role in pseudopodia extension is trivial. In agreement with the Rac inhibitor data, but in sharp contrast with the model of Rac-mediated activation of WASP, we found that GFP-tagged WASP CRIB mutants are able to generate discrete *puncta,* which are indistinguishable from those generated by GFP-WASP. Therefore our data strongly suggest that WASP does not rely on the availability of active Rac or on a direct interaction with active Rac to generate dynamic spots.
Of great interest, we noticed that GFP-tagged ΔCRIB WASP and **CRIB WASP were also occasionally localised at the leading edge. This curious observation, which has been only briefly followed up, will be described in section 4.7.

To further address the functionality of the WASP CRIB mutants we verified whether these retained the ability to be recruited to clathrin-coated pits. To do this we transfected WASP knockout cells with a co-expression vector encoding GFP-tagged WASP, either full-length wild type, ΔCRIB or **CRIB, and RFP-tagged clathrin light chain. We gently compressed the cells before TIRF imaging in order

to reduce motility and facilitate timelapse acquisition. As shown in figure 4.6 and in movie 6, under normal circumstances the number of clathrin spots exceeds that of WASP spots. This tends to be true at all time points due to the fact that clathrin sits on the ventral surface of the cell for few tens of seconds, while WASP appears on a pre-existing clatrin *punctum* as a brief burst lasting 5-10 seconds. Shortly after its recruitment WASP abandons the TIRF field along with clathrin, and this is considered as a *bona fide* sign of a CCP internalisation (Merrifield et al., 2002). A representative example of clathrin disappearing following WASP recruitment is reported in A, highlighted by the dashed blue rectangles in the kymograph and the fluorescence plot.
Most of the clathrin-coated pits (≈ 65%, referred to as *subpopulation A*) recruit GFP-WASP within the duration of the timelapse (shown in A). Some CCPs (referred to as *subpopulation B*), however, fail to do so and remain within the TIRF field for the entire acquisition (shown in B). Therefore, our data show that under normal circumstances two groups of clathrin-coated pits can be distinguished: those that recruit WASP for just a few seconds and are then internalised (A), and those that fail to recruit WASP within the duration of the timelapse and have therefore a longer lifespan (B).

GFP-ΔCRIB WASP and GFP-**CRIB WASP can also be recruited on clathrin-coated pits, as shown in figure 4.7 and figure 4.8 respectively. In both cases a subset of CCPs (referred to as *subpopulation A*) shows a normal-like dynamics, whereby a brief burst of either GFP-tagged WASP CRIB mutants is detected on a pre-existing clathrin *punctum*. In these cases, as previously reported for GFP-WASP, a peak of GFP-ΔCRIB WASP or GFP-**CRIB WASP is followed by a drop in clathrin fluorescence, suggesting that the clathrin-coated pit has been taken up. This is highlighted by the dashed blue squares in panel A of both figures.
Similarly to what is reported for GFP-WASP, a subpopulation of CCPs (referred to as *subpopulation B*) fails to recruit either GFP-tagged WASP CRIB mutants within the duration of the timelapse, as shown in panel B of both figures. The number of clathrin spots that do not appear to recruit GFP-ΔCRIB WASP or GFP-**CRIB WASP within the duration of the timelapse is higher than in cells expressing GFP-WASP, as reported in figure 4.9 A.
A third group of clathrin *puncta* exists in cells expressing either GFP-tagged WASP CRIB mutants *(*referred to as *subpopulation C*): those that recruit the

CRIB-mutated nucleation-promoting factor but occasionally fail to be internalised, as indicated by the incomplete drop of clathrin fluorescence following a peak of either GFP-tagged WASP CRIB mutants. Representative examples are shown in figure 4.7 C (and in movie 7) and figure 4.8 C. Of interest, we noticed that under these circumstances both GFP-ΔCRIB WASP and GFP-**CRIB WASP do not appear as brief bursts, but rather sit on the clathrin spot for an extended period of time (up to 276 seconds, as will be reported in figure 4.9 B) without necessarily causing its clear internalisation. It cannot be established at this stage whether there is an overlap between subpopulations B and C, that is whether some of the CCPs that do not appear to recruit WASP CRIB mutants within the duration of the timelapse are in truth CCPs that have previously recruited the mutated NPF without however being endocytosed.

We have not yet succeeded in obtaining definitive numbers regarding the lifetime of clathrin-coated pits in cells expressing GFP-WASP CRIB mutants. This is due to the fact that the duration of timelapse acquisition that we have chosen (5 minutes) has been proved to be insufficient for a significant proportion of clathrin-coated pits to be internalised. We are therefore planning to image the cells for a longer timeframe and to extend the acquisition interval, in order to keep the cells not continuously exposed to the laser for a prolonged period of time.

As for the reason behind the lack of CCPs internalisation despite recruitment of either GFP-tagged WASP CRIB mutants, we first hypothesised that it could be due to the occasionally reduced ability of GFP-ΔCRIB WASP and GFP-**CRIB WASP to trigger actin polymerisation via the Arp2/3 complex once recruited on clathrin *puncta*.

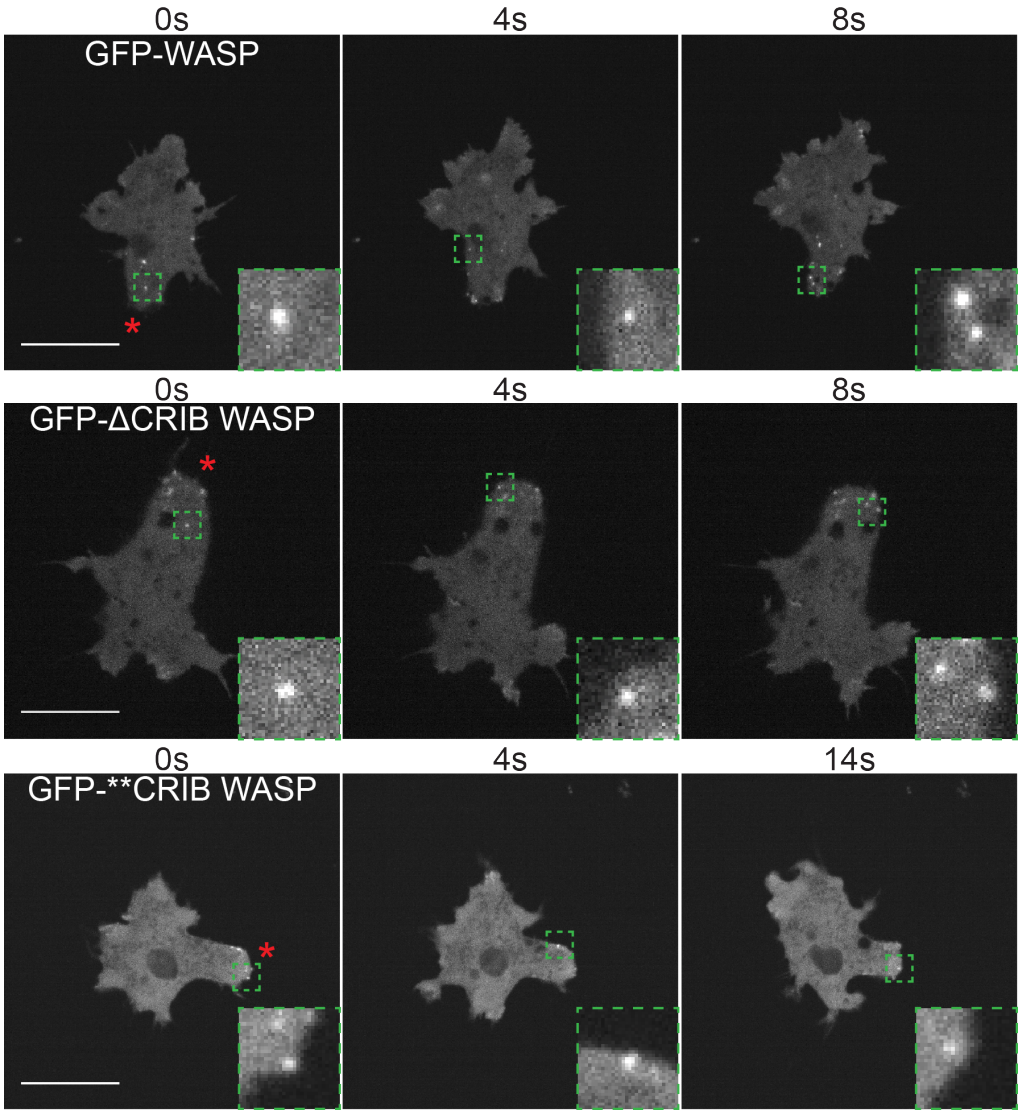

Figure 4.5 WASP does not require a direct interaction with active Rac to generate dynamic *puncta*.

In order to address the need of a direct interaction with active Rac for WASP to localise on dynamic spots, we transiently transfected WASP knockout cells with an expression vector encoding either GFP-WASP (rescue), GFP-ΔCRIB WASP or GFP-**CRIB WASP, and analysed their behaviour during directed migration using confocal live-cell imaging. As expected, GFP-WASP (top panel) localises on discrete short-lived *puncta*, which are generally present at all time points and formed at the rear of the cells (red asterisk). In disagreement with the currently accepted model of WASP activation/localisation by Rho GTPases, the presence of a functional CRIB motif (and therefore of a direct interaction with active Rac) is not required for WASP to generate dynamic spots. Indeed, both GFP-ΔCRIB WASP (middle panel) and GFP-**CRIB WASP (bottom panel) transiently localise on bright spots, which also tends to accumulate to the rear half (red asterisks).

Enlarged and brightened individual *puncta* are depicted within green dashed squares at the bottom right corner of each time point. Scale bars represent 10 µm.

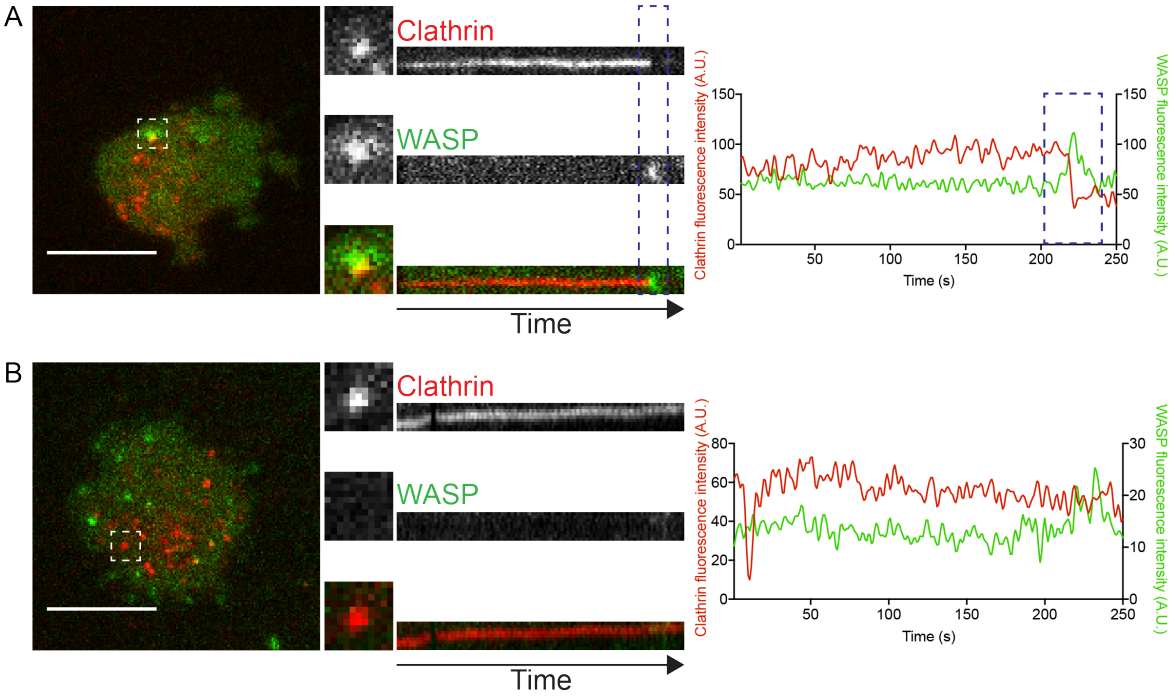

Figure 4.6 Wild type WASP is generally recruited on clathrin-coated pits and facilitates their internalisation.

WASP knockout cells transiently expressing full-length wild type GFP-tagged WASP and red-tagged clathrin (CLCA-mRFPmars2) were compressed under agarose and analysed by TIRF live-cell imaging. As shown in the still image taken from a timelapse on the top left corner, clathrin spots (in red) are normally more numerous that WASP spots (in green); this is due to the fact that clathrin *puncta* have a long lifespan, as they sit on the basal membrane for more than one hundred seconds on average, while WASP tends to appear in short burst that precede internalisation of the coated pit.

A) Most clathrin-spots eventually recruit WASP. As reported by the kymograph (left-hand side) and the fluorescence plot (right-hand side) the two molecules briefly overlap and disappear synchronously from the TIRF field, which suggests the clathrin-coated pit has been internalised. Scale bar represents 10 μm.

B) Some clathrin-enriched *puncta* fail to recruit WASP within the frame of the timelapses, which is generally of 5 minutes; as a result, the clathrin spots sit on the ventral surface of the cells for a longer time than those reported in A). Scale bar represents 10 μm.

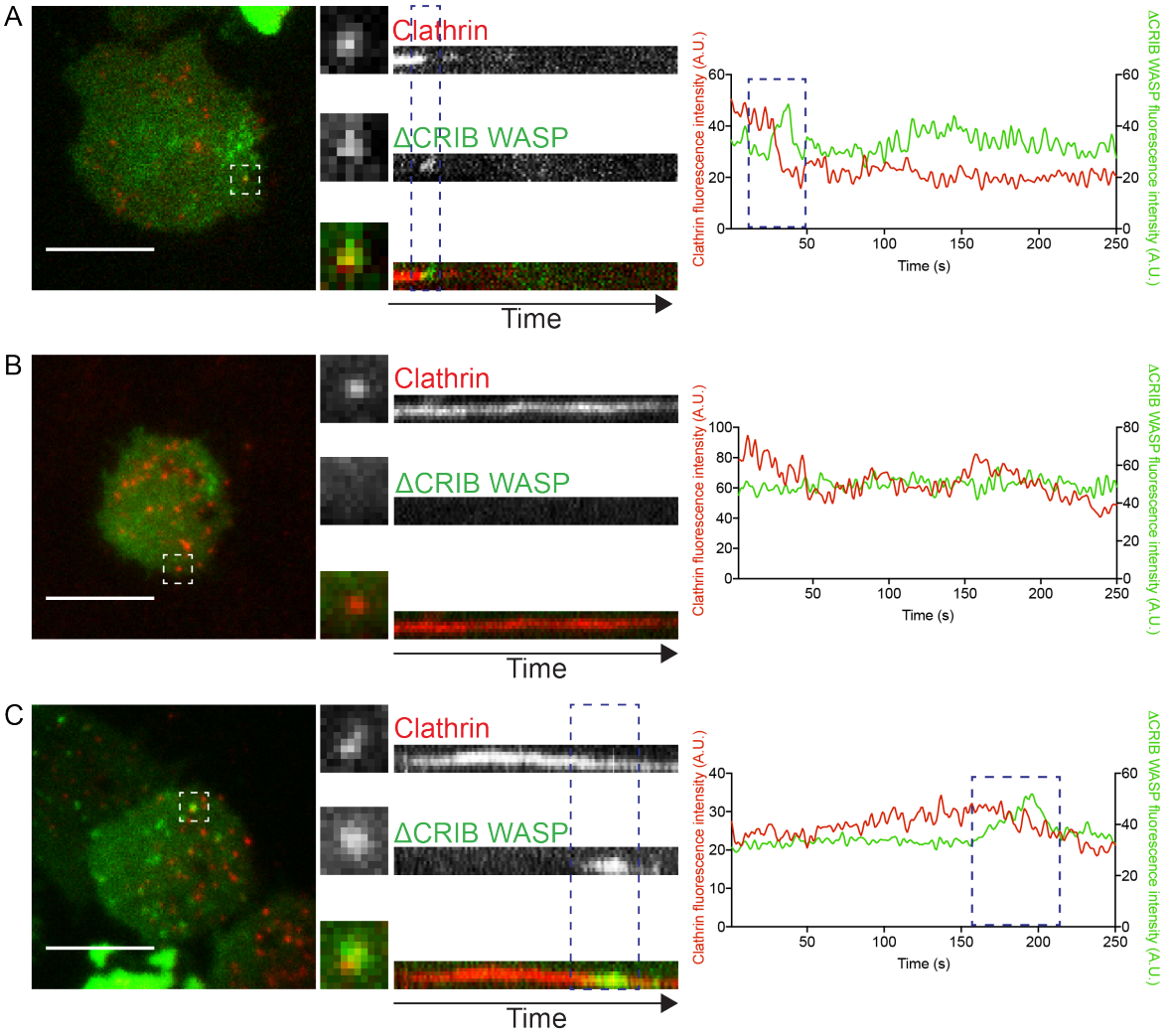

Figure 4.7 ΔCRIB WASP can be recruited on clathrin-coated pits despite occasionally failing to trigger their internalisation.

A) GFP-ΔCRIB WASP has the ability to drive internalisation of CCPs with a normal-like dynamics: it appears as a brief burst on a pre-existing clathrin spot and causes a sharp drop in clathrin intensity, as highlighted by the dashed blue rectangle in the kymograph and the fluorescence plot. Scale bar represents 10 μm.

B) A subpopulation of clathrin *puncta* does not appear to recruit GFP-ΔCRIB WASP within 5 minutes, which is the average duration of the timelapses. Likely as a consequence of the lack of WASP-driven actin polymerisation, clathrin remains trapped in the TIRF field for the entire acquisition. Scale bar represents 10 μm.

C) Some of the CCPs recruit GFP-ΔCRIB WASP for an extended period of time but fail to be internalised, as demonstrated by the lack of clathrin fluorescence drop following a peak of GFP-ΔCRIB WASP. A representative example is highlighted by

the blue dashed rectangle in the kymograph and the fluorescence plot. In this case the GFP-tagged WASP CRIB mutant sits on a pre-existing clathrin *puncta* for a much longer time than what observed in A). It eventually disappears from the TIRF field but leaves clathrin behind. It is plausible that the group of CCPs described in B) at least partially overlaps with this population of CCPs. Scale bar represents 10 μm.

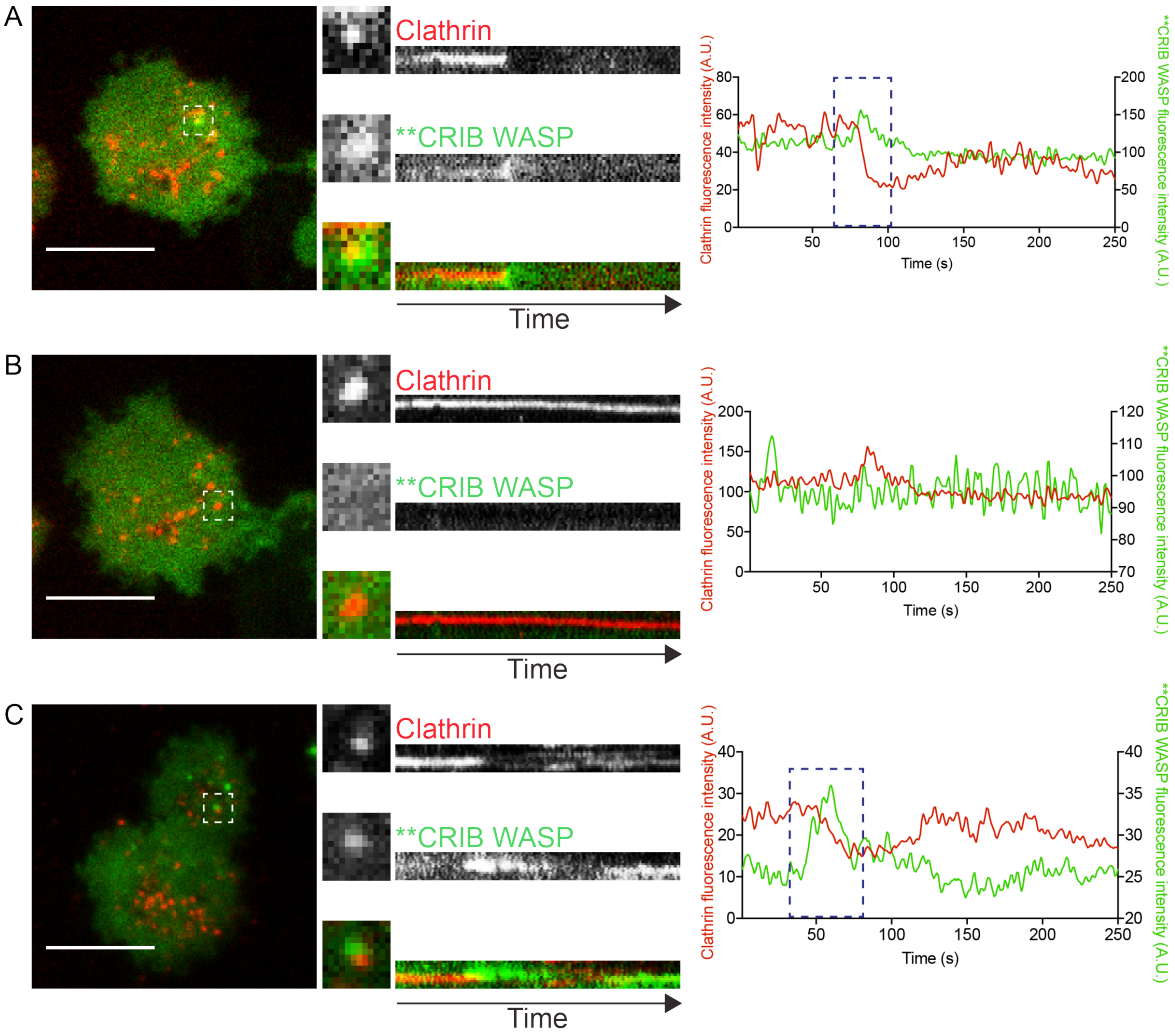

Figure 4.8 **CRIB WASP can be recruited on clathrin-coated pits despite occasionally failing to trigger their internalisation.

A) Part of the *puncta* generated by GFP-**CRIB WASP occurs on pre-existing clathrin spots. Once recruited, GFP-**CRIB WASP quickly drives the internalisation of the CCP and therefore disappears along with clathrin from the TIRF field. The brief overlap between clathrin and **CRIB WASP is highlighted by the dashed blue rectangles in the fluorescence plot and the kymograph. Scale bar represents 10 µm.

B) Part of the clathrin spots generated in cells expressing GFP-**CRIB WASP do not seem to recruit it within the length of the timelapses, which is approximately of 5 minutes. The lack of actin polymerisation on this subgroup of CCPs leads to their increased lifetime and likely to a failure in their internalisation. Scale bar represents 10 µm.

C) Unlike in cells expressing GFP-tagged full-length wild type WASP, where WASP either sits briefly on a CCP and takes it up or does not get recruited at all, cells

expressing GFP-**CRIB WASP (or GFP-ΔCRIB WASP) show a third subpopulation of clathrin-coated pits: those that recruit the CRIB-mutated NPF for an extended period of time but do not necessarily become internalised. A longer-lived GFP-**CRIB WASP *puncta* is highlighted by the dashed blue rectangle in both kymograph and fluorescence plot. Scale bar represents 10 μm.

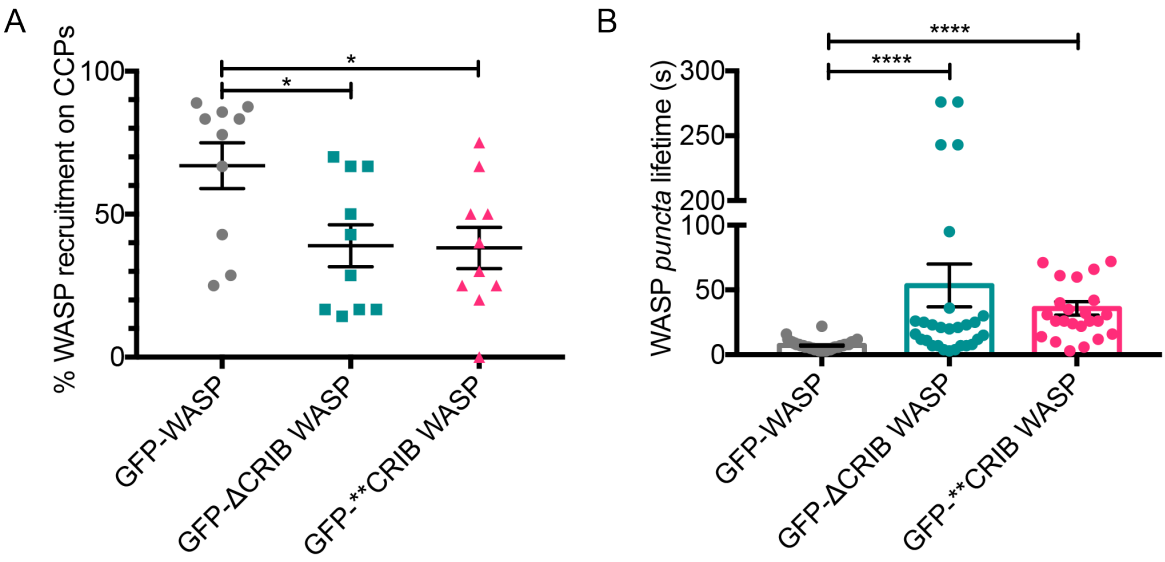

Figure 4.9 The absence of a functional CRIB motif affects WASP dynamics on clathrin-coated pits.

A) Quantitative analysis of the CCPs dynamics revealed that GFP-tagged WASP CRIB mutants are recruited to a smaller percentage of clathrin *puncta* within the duration of the timelapse in comparison to GFP-tagged full-length wild type WASP. While GFP-WASP (grey plot) localises on ≈ 67% of the CCP (mean= 66.97 ± 7.97; n= 77 clathrin *puncta* in 10 cells over 4 independent experiments), GFP-ΔCRIB WASP (teal plot) localises on ≈ 39% of the CCP (mean= 38.93 ± 7.34; n= 74 clathrin *puncta* in 10 cells over 6 independent experiments) and GFP-**CRIB WASP (pink plot) gets recruited on ≈ 38% (mean= 38.17 ± 7.19; n=65 clathrin *puncta* in 10 cells over 4 independent experiments). Shapiro-Wilk test revelaed that samples two of the samples are not normally distributed (p GFP-WASP= 0.01, p GFP-ΔCRIB WASP= 0.04, p GFP-**CRIB WASP= 0.90). A Mann-Whitney test was therefore performed. It revealed that a significant difference between the frequency of WASP recruitment on CCPs in the presence/absence of a functional CRIB motif. GFP-WASP vs. GFP-ΔCRIB WASP: p= 0.01; GFP-WASP vs. GFP-**CRIB WASP: p= 0.02.

B) Quantitative analysis of the WASP spots dynamics in the presence/absence of a functional CRIB motif demonstrated that while the vast majority of the *puncta* generated by GFP-tagged full-length wild type WASP only last for few seconds (grey plot; mean= 7.15 seconds ± 0.48; n= 52 WASP spots in 10 cells over 4 independent experiments), spots generated by GFP-tagged WASP CRIB mutants are often longer-lived. GFP- ΔCRIB WASP (teal plot) for instance lasts ≈ 53 seconds on average (mean= 53.43 ± 16.56; n= 28 spots in 10 cells over 6

independent experiments). Similarly, GFP-**CRIB WASP (pink plot) has an average lifespan of ≈ 36 seconds (mean= 35.75 ± 5.13; n= 24 spots in 10 cells over 4 independent experiments). Shapiro-Wilk test revelaed that samples two of the samples are not normally distributed ($p< 0.05$). A Mann-Whitney test was therefore performed. It revealed a significant difference in the lifetime of WASP spots in the presence/absence of a functional CRIB motif. GFP-WASP vs. GFP-ΔCRIB WASP: $p<0.0001$; GFP-WASP vs. GFP-**CRIB WASP: $p<0.0001$.

4.5 Mutations in the WASP CRIB motif do not affect its ability to trigger actin polymerisation via the Arp2/3 complex

The analysis of clathrin-coated pit dynamics presented in the previous section shows that a direct interaction with active Rac is not required for WASP to be recruited on clathrin *puncta*. It also points out, however, that the absence of a functional CRIB motif affects their internalisation process to some extent. Indeed, while some CCPs are promptly internalised following recruitment of either WASP CRIB mutants, other clathrin-coated pits fail to be endocytosed despite prolonged recruitment of the CRIB mutated NPF (figures 4.7 C and 4.8 C).

Why would the recruitment of GFP-tagged WASP CRIB mutants on CCPs not be sufficient to trigger their internalisation? We asked whether the defective uptake of CCPs in the presence of GFP-ΔCRIB WASP or GFP-**CRIB WASP could be a consequence of their reduced ability of to stimulate actin polymerisation via the Arp2/3 complex. On one hand we reasoned that this was a plausible hypothesis given that branched actin filaments facilitate the inward expansion of the pit by providing the force to overcome membrane tension (Aghamohammadzadeh and Ayscough, 2009; Boulant et al., 2011), and a reduced amount of F-actin could explain the impaired/delayed endocytosis. On the other hand, however, lack of Arp2/3 complex recruitment on discretely localised WASP has never been observed. Although any sort of disengagement between a discretely localised nucleation-promoting factor and its target actin nucleator appeared improbable, it was important to keep in mind that localisation of mutated WASH without discernible Arp2/3 complex recruitment was previously reported (Hao et al., 2013).

We therefore went on testing whether a functional CRIB motif is required for WASP to trigger actin polymerisation via the Arp2/3 complex once recruited on ventral pits. To do this we firstly co-expressed GFP-tagged WASP, either full-length wild type, ΔCRIB or **CRIB, and a red tagged subunit of the Arp2/3 complex. We gently squashed transfected cells under agarose prior to live-cell TIRF imaging in order to keep them still and obtain more informative data. As shown in figure 4.10, whether or not equipped with a functional CRIB motif WASP co-localises with ArpC4 on *puncta* generated at the basal membrane of the cells. This suggests that a direct interaction with active Rac is not necessary for WASP to recruit the Arp2/3 complex on ventral spots.

Similarly to what was described in the previous section regarding the existence of different subpopulations of clathrin/WASP spots, WASP/ArpC4 *puncta* tend to show a bimodal distribution. We found that WASP and Arp2/3 complex appear into the TIRF field and leave it in a rigorously synchronous fashion, independently of the presence of a functional CRIB motif. However, while all spots generated by wild type WASP are short-lived (panel A), only a subset of *puncta* generated by ΔCRIB WASP and **CRIB WASP appears as a brief burst (panels B and C respectively). A subgroup of ΔCRIB WASP and **CRIB WASP *puncta* sits along with ArpC4 on the ventral surface of the cells for a significantly longer time than expected, as shown in the representative example reported in panel D.

To further confirm that actin has been polymerised on *puncta* generated by WASP CRIB mutants, we co-expressed either GFP-WASP or GFP-**CRIB WASP along with red-tagged Lifeact, a short pepdite that binds to F-actin without affecting its dynamics (Riedl et al., 2008). We then verified whether the two probes co-localised on ventral *puncta* by super-resolution live-cell imaging during directed cell migration. As shown in figure 4.11 and in movie 8, both wild type WASP and **CRIB WASP are clearly enriched on ventral spots. It is easy to notice that while *puncta* generated by GFP-WASP are sparse and discrete at all time points, those generated by **CRIB WASP are more numerous and often clustered at the trailing edge. This is likely due to the fact that spots that do not become internalised or take a significantly longer time to do so are swept at the back of the cell while this moves forward. Remarkably, F-actin can be clearly detected on spots generated by both WASP and **CRIB WASP, further proving that a direct interaction with active Rac is not required for WASP to induce actin polymerisation on ventral spots.

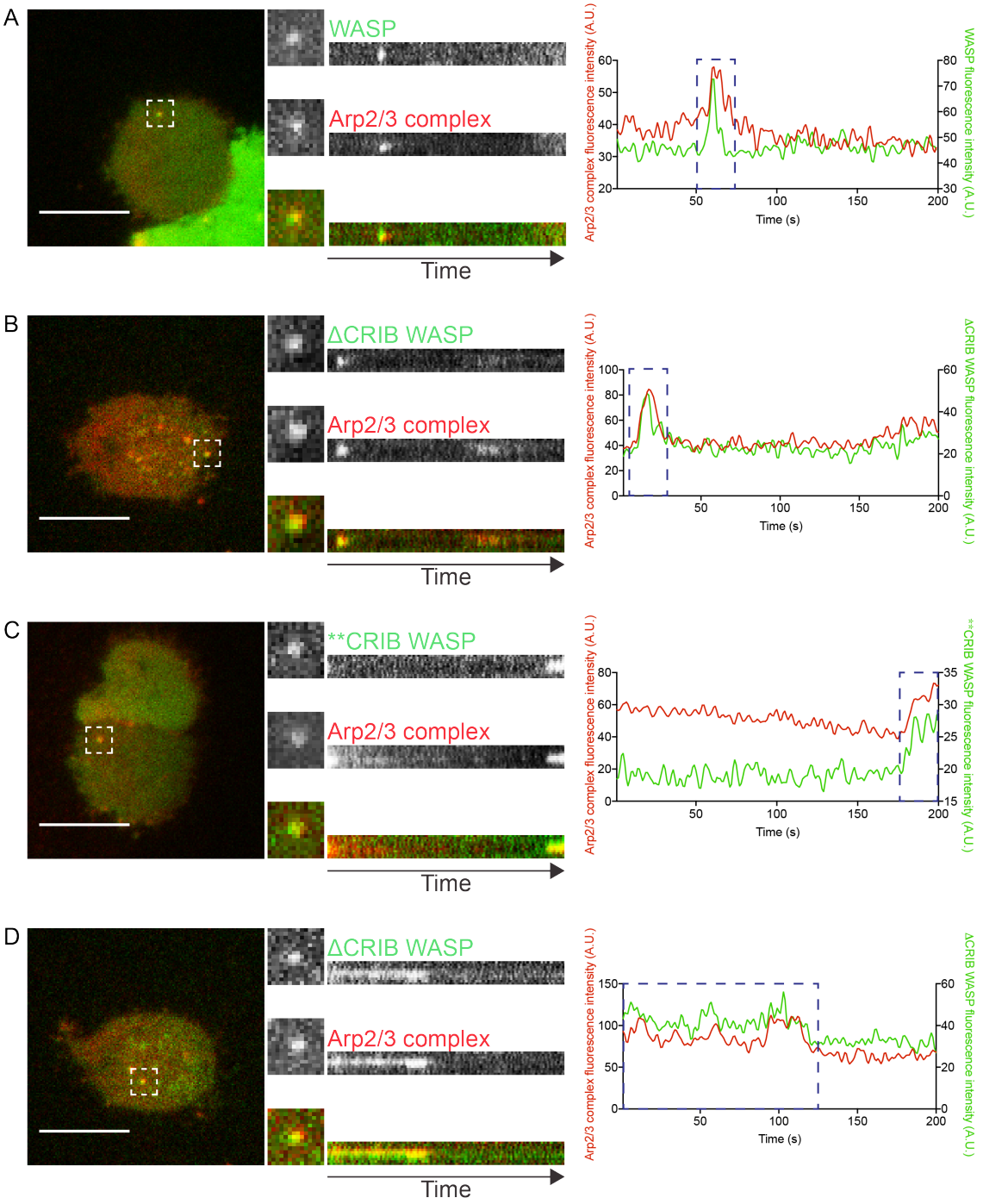

Figure 4.10 A direct interaction with active Rac is not required for WASP to recruit the Arp2/3 complex on ventral *puncta*.

A) WASP knockout cells were transiently transfected with a co-expression vector encoding GFP-WASP (rescue) and a red-tagged subunit of the Arp2/3 complex (mRFPmars2-ArpC4). Expressing cells were gently squashed under agarose to reduce motility and analysed by live-cell TIRF imaging. WASP and ArpC4 consistently appear into the TIRF field at the same time; they briefly overlap, as highlighted by the kymograph and the dashed blue square in the fluorescence

plot, and quickly abandon the TIRF field in a synchronous way. Scale bar represents 10 μm.

B) WASP knockout cells transiently expressing GFP-ΔCRIB WASP and mRFPmars2-ArpC4 were compressed under a slab of agarose and the dynamics of their ventral *puncta* analysed by live-cell TIRF microscopy. GFP-ΔCRIB WASP *puncta* in the ventral membrane tend to be more numerous than GFP-WASP spots, in agreement with the existence of a subpopulation of GFP-ΔCRIB WASP spots that has an increased lifetime, as discussed in section 4.4. Remarkably, however, a set of *puncta* generated by GFP-ΔCRIB WASP appears into the TIRF field alongside red-tagged ArpC4 and abandons it with a dyamics that is indistinguishable from that of GFP-WASP spots. The two only briefly overlap, as shown by the kymograph and highlighted by the dashed blue rectangle in the fluorescence plot. Scale bar represents 10 μm.

C) WASP knockout cells were transiently transfected with a co-expression vector encoding GFP-**CRIB WASP and mRFPmars2-ArpC4. Transfected cells were then analysed by live-cell TIRF microscopy after being gently compressed under agarose. The example of *punctum* highlighted by the white dashed square clearly shows that **CRIB WASP and Arp2/3 complex co-localise. The peak of **CRIB WASP and ArpC4 fluorescence is highlighted by the dashed blue rectangle in the fluorescence plot. Scale bar represents 10 μm.

D) A subpopulation of spots generated by GFP-ΔCRIB WASP has an increased lifetime, in agreement with the clathrin/ΔCRIB WASP data reported in figure 4.7. As emphasised by the kymograph and the fluorescence plot, the GFP-tagged WASP CRIB mutant occasionally becomes stuck in the ventral membrane of the cell for a longer time than normally required despite recruiting the Arp2/3 complex. The two probes eventually disappear from the TIRF field, but it cannot be established whether the clathrin-coated pit that presumably sits underneath the ΔCRIB WASP/Arp spot has been internalised or not. Scale bar represents 10 μm.

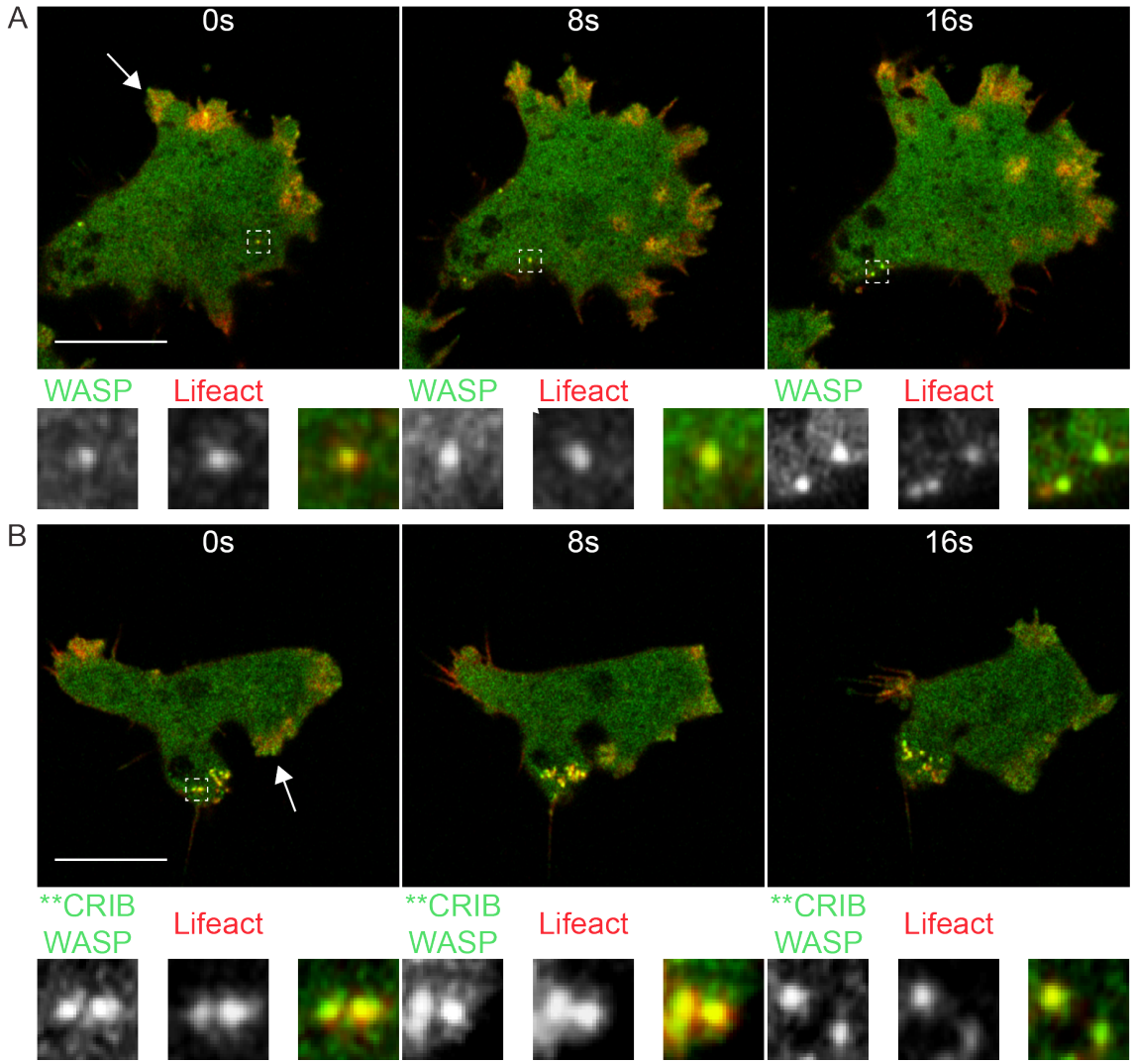

Figure 4.11 A direct interaction with active Rac is not required for WASP to trigger the formation of actin filaments on ventral *puncta*.

A) WASP knockout cells were transiently transfected with a co-expression vector encoding GFP-WASP (rescue) and a red-tagged reporter for F-actin (Lifeact-mRFPmars2). The cells were then analysed by super-resolution live-cell imaging during directed migration. As expected, F-actin is enriched at the leading edge (white arrow), where it decorates pseudopodia and, to a lesser extent, macropinocytic cups. Furthermore, Lifeact is clearly detected on WASP spots, which are again mostly generated at the rear half of migrating cells. A representative *punctum* indicated by the dashed white square is enlarged and brightened at the bottom of each timepoint. Scale bar represents 10 µm.

B) WASP knockout cells transiently expressing GFP-**CRIB WASP and Lifeact-mRFPmars2 were visualised during directed migration. As expected, Lifeact can be detected at the leading edge, as indicated by the white arrow, where it drives the extension of pseudopodia and of macropinosomes. Importantly, actin

is being polymerised on GFP-**CRIB WASP spots, as demonstrated by the co-localisation between the GFP-tagged WASP CRIB mutant and red-tagged F-actin reporter. A representative example is highlighted by the dashed white square and emphasised at the bottom of each time points. Spots generated by GFP-**CRIB WASP tend to last longer than those generated by GFP-WASP and, presumably as a consequence of their increased lifespan, are often accumulated at the rear of a moving cell. Scale bar represents 10 μm.

4.6 The extended lifetime of the WASP CRIB mutants *puncta* may be due to high cellular levels of active Rac

Data described so far suggest that WASP CRIB mutants have the ability to activate the Arp2/3 complex on clathrin-coated pits. In light of this finding it can be inferred that the extended lifetime of *puncta* generated by WASP CRIB mutants is not due to the lack of actin filament formation, and that the cause of their altered dynamics ought to be looked for elsewere. We sought to understand whether their extended lifetime may be a secondary effect of the increased levels of active Rac, which in turn are caused by the lack of a functional WASP CRIB motif, as described in the previous chapter of this thesis.
As mentioned in section 1.4.3.2, high levels of active Rac have been shown to severely compromise the ability of the cells to perform clathrin-mediated endocytosis (Lamaze et al., 1996). The reasons behind such a dramatic observation were later chased by another group, which hinted at the possibility that high levels of active Rac might affect the recruitment/assembly of the endocytic machinery at sites of CME by locally depleting PIP2 (Malecz et al., 2000). Importantly, the actual ability of molecules involved in endocytosis, like WASP for instance, to localise at sites of CCPs assembly in the presence of high levels of active Rac has never been tested.
We felt it was important to first address whether WASP can be recruited on ventral spots in the presence of high levels of active Rac, and secondly whether an excess of active Rac could be responsible for the increased lifetime of WASP *puncta*. To address our questions we transfected WASP knockout cells with two extrachromosomal vectors, the first encoding GFP-WASP (rescue) and the second containing untagged G12V Rac1A under a dox-on promoter. We then performed live-cell imaging to investigate WASP localisation and dynamics before and upon induction of dominant active Rac. As shown in figure 4.12, cells are fairly polarised until up to 60 minutes from doxycycline treatment; this is likely due to the fact that the levels of G12V Rac1A are not yet sufficient to trigger a dramatic morphological change. Within this timeframe GFP-WASP is rarely enriched at the cortex but highly localised on ventral spots. Within a short time cells start to ruffle and lose their polarity, as previously described in mammalian cells upon injection of dominant active Rac (Ridley et al., 1992). GFP-WASP strikingly re-localises to membrane ruffles, as it appears more clearly from the image taken 70 minutes post-induction (yellow arrowhead). Importantly, *de novo*

WASP *puncta* are generated even after 2 hours from induction, when cells are irremediably rounded up, meaning that WASP recruitment on basal pits is not affected by the presence of high levels of dominant active Rac.
In agreement with our hypothesis, the lifespan of WASP *puncta* increases progressively over the 120 minutes elapsed from induction. As reported in the kymograph in figure 4.13 A and quantified in B, prior to doxycycline treatment GFP-WASP generates dynamic spots that appear as brief burst lasting 9 seconds on average. After 45 minutes and up to 1 hour from induction the lifespan of WASP spots is slightly but not significantly increased (16 and 13 seconds on average respectively). At 70 minutes post-induction, in conjunction with the change in cell shape, the lifetime of WASP *puncta* is dramatically increased to 38 seconds on average. The lifespan of WASP spots appears even more strikingly extended after 80 and 120 minutes from G12V Rac1A induction, reaching the average values of 172 and 242 seconds respectively.

Data presented here suggest that WASP recruitment on ventral spots is not affected by the presence of G12V Rac1, at least in part discouraging a model whereby the inhibitory effect of high levels of active Rac on CME is linked to a defective recruitment/assembly of the endocytic machinery. Evidence provided demonstrates, however, that excessive active Rac negatively regulates WASP dynamics on basal spots, possibly explaining the increased lifetime of clathrin, WASP and Arp2/3 complex *puncta* observed in cells lacking a functional WASP CRIB motif.

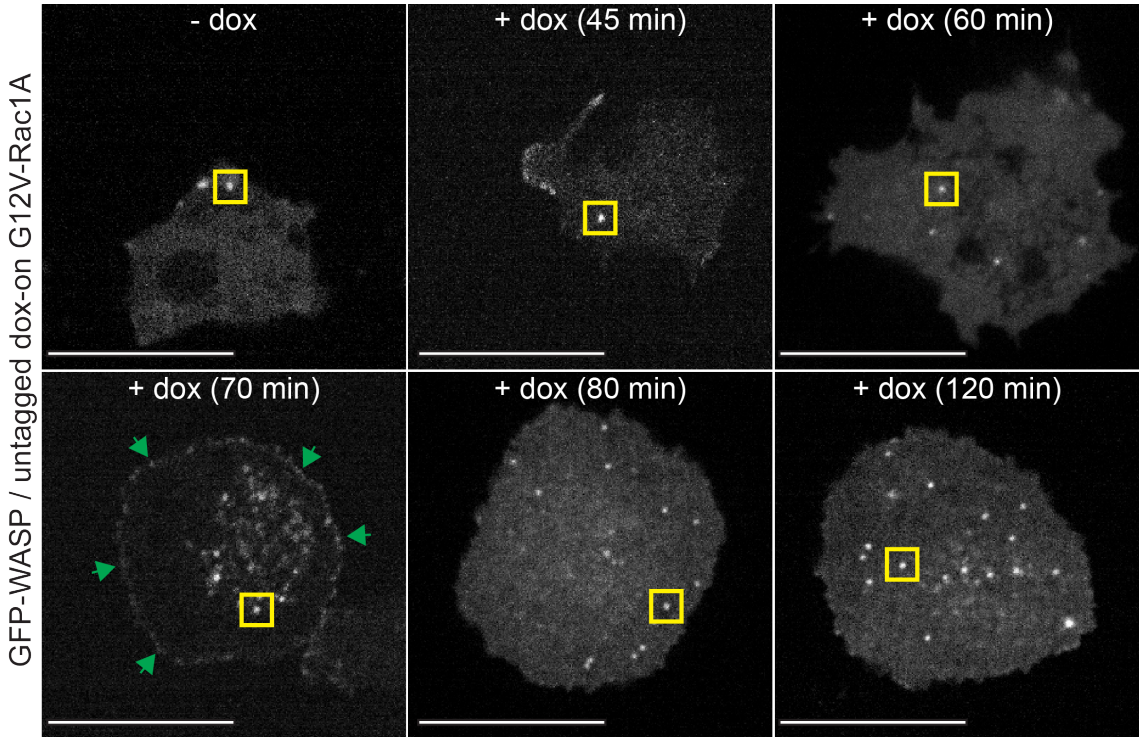

Figure 4.12 Dominant active Rac does not impair WASP recruitment on ventral *puncta*.

WASP knockout cells expressing GFP-WASP (rescue) and a doxycycline-inducible untagged G12V Rac1A were analysed by confocal live-cell imaging. Cells appear polarised prior to and up to 1 hour from doxycycline treatment (top panels) but undergo a dramatic conformational change from 70 minutes after induction (bottom panels). GFP-WASP is only occasionally detected at the cell cortex at the early time points; an example of cortical GFP-WASP signal is reported at 45 minutes (second panel), presumably depicting a macropinosome. After 70 minutes from doxycycline addition, GFP-WASP massively localises to membrane ruffles. This is particularly clear in the representative image at the bottom left corner, pointed out by the green arrowheads. The localisation of GFP-WASP at ventral spots is not affected by the expression of dominant active Rac, since *puncta* are generated even after 2 hours from induction. The increased number of GFP-WASP positive spots visible at later timepoints (bottom panels) is not due to an increase in the number of *de novo* GFP-WASP spots but rather to their altered dynamics. Kymographs derived from WASP *puncta* indicated by solid yellow squares/rectangles at different time points are reported in figure 4.13. Scale bars represent 10 μm.

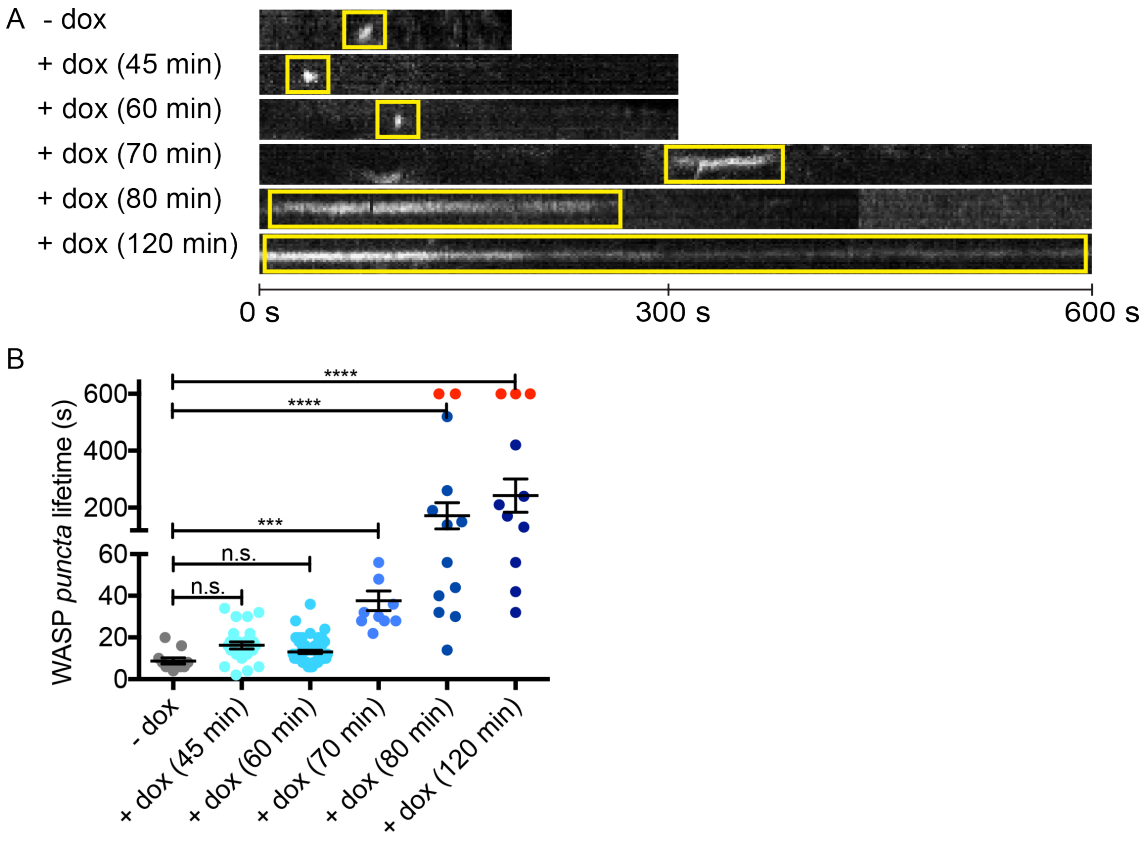

Figure 4.13 The lifetime of WASP *puncta* directly correlates with the cellular levels of active Rac.

WASP knockout cells were transiently transfected with a GFP-WASP- encoding plasmid (rescue) and a vector containing a doxycycline-inducible untagged G12V Rac1A. The dynamics of GFP-WASP spots generated in the presence/absence of G12V Rac1A was investigated by confocal live-cell imaging.

A) Representative kymographs of GFP-WASP *puncta* generated prior to G12V Rac1A induction (-Dox) or 45, 60, 70, 80 and 120 minutes post doxycycline treatment. Individual *puncta* are highlighted by solid yellow squares/rectangles at all time points. In the absence of any G12V Rac1A expression and up to 1 hour from its induction GFP-WASP generates brief burst, which appear and disappear within few seconds. On the contrary, from 70 minutes on GFP-WASP generate spots that sit on the ventral surface of the cell for an increasingly longer time. After 120 minutes a subpopulation of GFP-WASP *puncta* remains visible for the entire duration of the timelapse.

B) Quantitative analysis of the WASP *puncta* lifetime prior to/upon induction of G12V Rac1A expression. GFP-WASP spots generated before addition of doxycycline last ≈ 9 seconds ($mean_{-dox}$= 8.7 ± 1.5 seconds; error represents S.E.M.; n= 11 *puncta*, 1 experiment). GFP-WASP spots generated 45 and 60

minutes after G12V Rac1A induction last slightly longer ($mean_{45\ min}$= 16.2 ± 1.7 seconds; error represents S.E.M.; n= 25 *puncta*, 1 experiment. $mean_{60\ min}$= 13.1 ± 0.8 seconds; error represents S.E.M.; n= 54 *puncta*, 1 experiment). The effect of dominant active Rac on GFP-WASP *puncta* lifetime increases significantly after 70 minutes from induction: $mean_{70\ min}$= 37.6 ± 4.7 seconds; error represents S.E.M.; n= 10 *puncta*, 1 experiment. It is however after 80 and 120 minutes that the effect of G12V Rac1A on GFP-WASP spots lifetime appear more dramatic: $mean_{80\ min}$= 171.6 ± 46.1 seconds; error represents S.E.M.; n= 18 *puncta*, 1 experiment. $mean_{120\ min}$= 242.1 ± 58.3 seconds; error represents S.E.M.; n= 14 *puncta*, 1 experiment. Shapiro-Wilk test revealed that only two samples are normally distributed: p_{-dox} = 0.0032; $p_{45\ min}$= 1332; $p_{60\ min}$< 0.0001; $p_{70\ min}$= 0520; $p_{80\ min}$ = 0.0001; $p_{120\ min}$= 0.0056. Therefore a Kruskal-Wallis test was performed. It revealed that no significant difference exists in the lifetime of GFP-WASP *puncta* prior to G12V Rac1A induction and up to 60 minutes from doxycycline addition ($p_{45\ min}$= 0.0724; $p_{60\ min}$= 0.4154). GFP-WASP spots generated at 70, 80 and 120 minutes are instead significantly longer-lived than those generated before induction (p= 0.0002, p<0.0001 and p<0.0001 respectively). Red dots are those that fail to disappear within the duration of the timelapse.

4.7 WASP does not require a direct interaction with active Rac to localise at the leading edge but does require it to extend pseudopodia in the absence of SCAR/WAVE

Evidence described in this chapter demonstrates that WASP does not require a direct interaction with active Rac to induce actin polymerisation on clathrin-coated pits, in agreement with the lack of active Rac localisation on ventral *puncta*.

CME is so far the best-characterised role of WASP, but a previous work from our lab suggested that it can also trigger actin polymerisation at the leading edge, a role that becomes more prominent in the absence of SCAR/WAVE. Under these circumstances WASP still generates dynamic spots at the trailing edge but is also relocalised at the front (Veltman et al., 2012). What recruits WASP at the leading edge in the absence of SCAR/WAVE is supposedly GTP-bound Rac (Veltman et al., 2012), as this consistently localises at the front along with SCAR/WAVE in wild type cells (see figure 4.2). Based on this hypothesis it was unexpected to observe WASP CRIB mutants being occasionally recruited at the leading edge of migrating wild type cells, as briefly mentioned in section 4.4 and shown in figure 4.14 (white arrowheads).

The recruitment of WASP molecules that are unable to interact with active Rac at the leading edge is curious. On one hand it shows that the CRIB motif is not responsible for targeting WASP to the front of migrating cells, on the other hand it raises an important question: can WASP drive the extension of pseudopodia if unable to interact with active Rac? We reasoned this was an unlikely possibility, but nevertheless we decided to address it.

We therefore specifically asked whether a direct interaction with active Rac, which we have proved to be dispensable for WASP to trigger actin polymerisation on CCPs, is also not required for WASP to drive the extension of actin-rich protrusions. To answer this question we ulitised an inducible SCAR/WAVE and WASP double knockout (henceforth referred to as *inducible double knockout*). In this strain, which has been recently generated in the lab (Davidson, 2014), the expression of WASP has been completely abolished while that of SCAR/WAVE occurs as long as the cells are kept in the presence of doxycycline. We transiently transfected these cells with an extrachromosomal vector encoding GFP-tagged WASP CRIB mutants. Transfected cells deprived of doxycycline for 48

hours were then tested for their ability to migrate toward a source of chemoattractant. As shown in figure 4.15, cells expressing either GFP-tagged WASP CRIB mutants manage to move up a gradient of folate as long as the expression of SCAR/WAVE is kept on. In more details, GFP-ΔCRIB WASP- and GFP-**CRIB WASP-expressing cells grown in the presence of doxycycline migrate at the speed of ≈ 6 and 5.5 μm/min respectively. These values are both slightly lower than the average speed of wild type cells in this assay, which is of ≈ 10 μm/min; this may be due to the inability of cells expressing either GFP-tagged WASP CRIB mutants to smoothly retract their uropod, as described in section 3.3 of this dissertation. Once the expression of SCAR/WAVE is turned off by doxycycline deprivation, the cell speed drops significantly to ≈ 2 and 2.5 μm/min in cells expressing GFP-ΔCRIB WASP and GFP-**CRIB WASP respectively.

We hypothesised that such a dramatic reduction in motility may be caused by the impaired ability of cells expressing either GFP-tagged WASP CRIB mutant to extend actin-filled protrusions in the absence of SCAR/WAVE. To test our theory we performed live-cell imaging on inducible double knockout cell expressing GFP-ΔCRIB WASP and GFP-**CRIB WASP that have been kept in the presence/absence of doxycycline. As shown in figure 4.16, cells expressing either GFP-tagged WASP CRIB mutants can protrude normally as long as SCAR/WAVE is expressed. Whether or not WASP CRIB mutants occasionally localised at the front in the presence of SCAR/WAVE actively contribute to the activation of the Arp2/3 complex, or are instead quiet spectators, is not clear. In the absence of SCAR/WAVE, however, cells do not generate any pseudopodia.

These results, despite the need for further confirmation, raise at least two important considerations. First, the localisation of WASP at the leading edge (as well as at ventral *puncta*) does not depend on its CRIB motif, meaning that other domains control WASP's subcellular localisation. This finding, despite seemingly unimportant, clearly underscores the incompleteness of our knowledge about WASP dynamics. Second, WASP is an incredibly versatile nucleation-promoting factor, able to fulfil multiple roles within the cells, and undeniably able to respond to different upstream signals under different circumstances: it does not require an interaction with active Rac to trigger actin polymerisation at CCPs

but does require it to stimulate the formation of actin filaments at the front of migrating cells in the absence of SCAR/WAVE.

Importantly, the existence of distinct WASP subpopulations within cells leads us to question the absoluteness of early *in vitro* data on WASP regulation: how well do they represent the heterogeneity of WASP molecules in living cells?

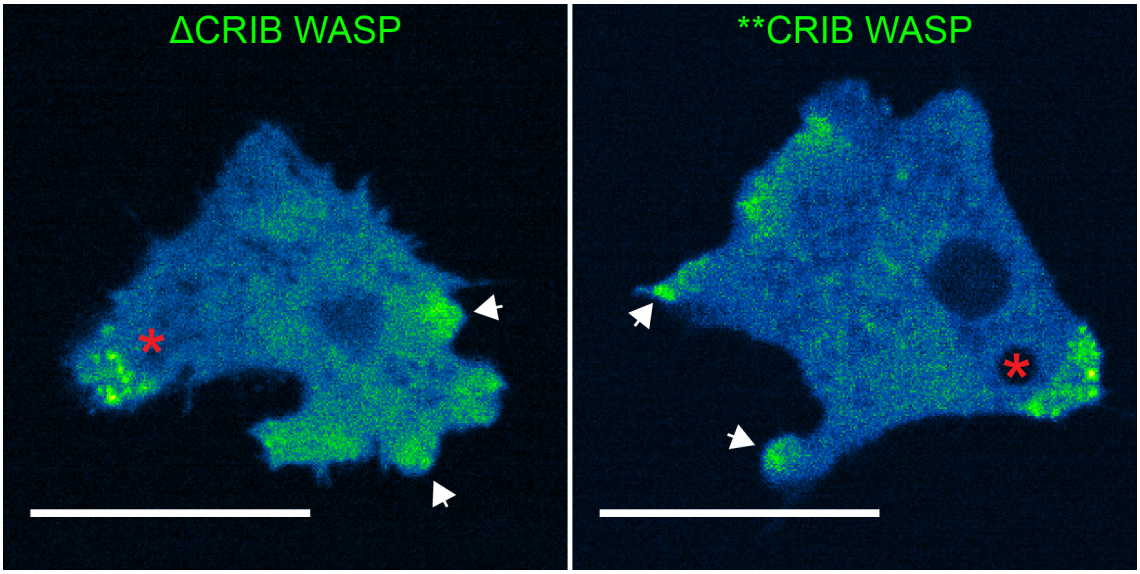

Figure 4.14 A functional CRIB motif is not required for WASP to occasionally localise at the leading edge.

GFP-WASP does not generally localise at the leading edge in wild type cells, since SCAR/WAVE is the major driver of pseudopodia extension. Its localisation at the front is enhanced in the absence of SCAR/WAVE, as cells rewire to fulfil the need of generating a leading edge; it has been hypothesised that WASP may be targeted to the front via a direct interaction with active Rac (Veltman et al., 2012). GFP-tagged WASP CRIB mutants expressed in WASP knockout cells are, however, occasionally recruited at the leading edge during migration (white arrowhead), and more often at the expected *puncta* that cluster at the trailing edge (indicated by the red asterisk), suggesting that the CRIB motif is not responsible for the recruitment of WASP at the front of polarised cells. Scale bars represent 10 μm.

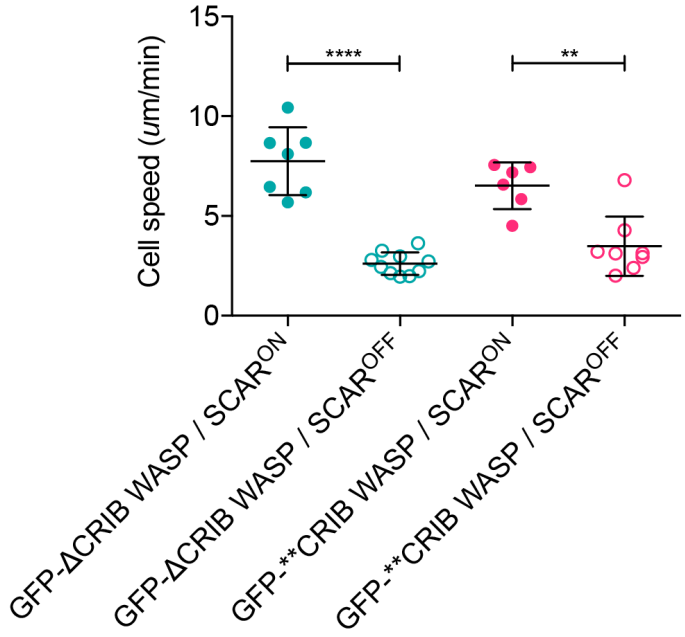

Figure 4.15 A direct interaction with active Rac is required for WASP to support cell motility in the absence of SCAR/WAVE.

Inducible double knockout cells were utilised to assess the ability of GFP-tagged WASP CRIB mutants to drive forward movement in the absence of SCAR/WAVE. This strain has been genetically modified so that the expression of endogenous WASP is completely abolished while the expression of SCAR/WAVE is strongly reduced following 48 hours of doxycycline deprivation. Inducible double knockout cells were transfected with either GFP-tagged WASP CRIB mutants; selected cells were kept in the presence or absence of doxycycline and their speed quantified during directed migration. Cells expressing GFP-ΔCRIB WASP migrate at 7.7 *u*m/min (± 0.6; error represents S.E.M; n= 7 cells, 1 experiment) in the presence of SCAR/WAVE and at 2.6 *u*m/min (± 0.2; error represents S.E.M; n= 10 cells, 1 experiment) when the expression of SCAR/WAVE is turned off. Statistical analysis (unpaired t test) reveals a significant difference ($p<0.0001$). Cells expressing GFP-**CRIB WASP migrate at 6.5 *u*m/min (± 0.5; error represents S.E.M; n= 6 cells, 1 experiment) as long as the expression of SCAR/WAVE is still on, and at the reduced value of 3.5 *u*m/min (± 0.5; error represents S.E.M; n= 8 cells, 1 experiment) when SCAR/WAVE is no longer expressed. Shapiro-Wilk test was performed to assess the normal distribution of the samples, which was not confirmed for only one of them: p GFP-ΔCRIB WASP $SCAR^{ON}$= 0.56, p GFP-ΔCRIB WASP $SCAR^{OFF}$= 0.55, p GFP-**CRIB WASP $SCAR^{ON}$= 0.28, p GFP-**CRIB WASP $SCAR^{OFF}$= 0.03). Unpaired t-test revealed that a significant difference exists in the speed of GFP-ΔCRIB WASP $SCAR^{ON}$ vs GFP-ΔCRIB WASP $SCAR^{OFF}$ ($p<0.0001$).

Mann-Whitney test revealed a significant difference in the speed of GFP-**CRIB WASP $SCAR^{ON}$ vs GFP-**CRIB WASP $SCAR^{OFF}$ (p= 0.0047). The average speed of cells expressing SCAR/WAVE and GFP-ΔCRIB WASP or GFP-**CRIB WASP is slightly lower that that of wild type cells under the same conditions (≈ 10 um/min). This is likely caused by the reduced ability of cells expressing GFP-tagged WASP CRIB mutants to normally retract their uropod (see figure 3.7).

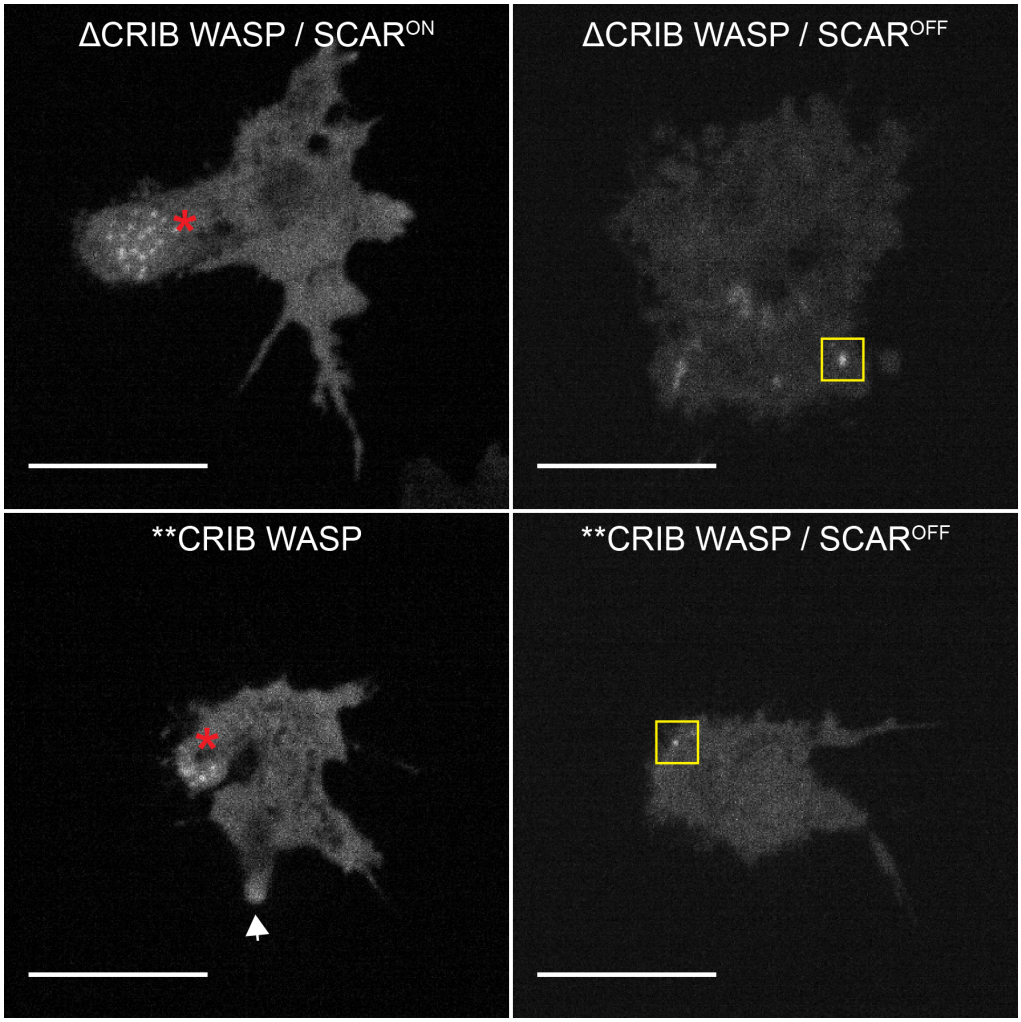

Figure 4.16 A functional CRIB motif is required for WASP to extend a leading edge in the absence of SCAR/WAVE.

We asked whether the reduced speed of cells expressing GFP-ΔCRIB WASP or GFP-**CRIB WASP but no SCAR/WAVE was caused by their inability to extend protrusions. To test it, we performed confocal live-cell imaging on inducible double knockout cells expressing either GFP-tagged WASP CRIB mutants. As shown in the left-hand side panels, GFP-ΔCRIB WASP (top) and GFP-**CRIB WASP (bottom) clearly localise on *puncta* that tend to cluster at the trailing edge (indicated by the red asterisk) and occasionally at the extending pseudopodia (white arrowhead). Cells appear polarised, with defined front and rear. When the expression of SCAR/WAVE is turned off (right-hand side panels) cells expressing GFP-ΔCRIB WASP (top) and GFP-**CRIB WASP (bottom) lose their ability to generate flat protrusions, resulting in a round morphology. Of interest, either GFP-tagged WASP CRIB mutants generate ventral spots in the absence of SCAR/WAVE, as highlighted by the yellow solid squares. Scale bars represent 10 μm..

4.8 Chapter 4 summary

In this chapter we have clarified the role of active Rac in the activation/localisation of WASP in living cells.

We first pointed out that WASP and active Rac do not co-localise on ventral *puncta*, an observation that has not been made before and that inevitably led us to question the importance of active Rac for WASP functionality. As a comparison, we have shown that SCAR/WAVE and active Rac are instead both enriched at the leading edge of migrating cells, in support of a model whereby the Rho GTPase in its active state plays a role in activating the SCAR/WAVE complex at the front during migration.

To further address the importance of GTP-bound Rac for WASP functionality we have optimised the conditions to chemically inhibit the Rho GTPase, and analysed WASP dynamics upon treatment with high doses of the Rac inhibitor EHT1864. Our data show that the ability of WASP to generate dynamic spots is not controlled by the availability of Rac in its active state.

Remarkably comparable results were obtained when the effect of mutations in the CRIB motif of WASP on its ability to generate dynamic *puncta* was assessed. Indeed, preventing a direct interaction between WASP and active Rac does not affect the ability of the CRIB-mutated nucleation-promoting factor to localise on ventral spots.

We went on assessing whether the internalisation of clathrin-coated pits, which is the best characterised role for WASP so far, was at all affected by the absence of a functional CRIB motif. Evidence gathered shows that while some of the CCPs are taken up with the expected dynamics upon recruitment of the CRIB-mutated NPF, some fail to be endocytosed despite prolonged recruitment of either WASP CRIB mutants.

We aimed to clarify whether the defective internalisation of a subset of CCPs observed in cells lacking a functional WASP CRIB motif was caused by a reduced rate of actin polymerisation. In other words we asked whether the CRIB-mutated WASPs were less able to activate the Arp2/3 complex and stimulate the formation of branched actin filaments on CCPs. Live-cell imaging has revealed that actin polymerisation occurs normally on such *puncta*, as demonstrated by the co-localisation between either GFP-tagged WASP CRIB mutants and red-tagged ArpC4 or Lifeact.

We therefore hypothesised that the impaired rate of endocytosis may be a secondary effect of the higher levels of active Rac in cells expressing WASP CRIB mutants, as was discussed in chapter 3. Indeed, it was previously shown that high levels of active Rac hamper clathrin-mediated endocytosis (Lamaze et al., 1996), supposedly by preventing the assembly of the endocytic machinery (Malecz et al., 2000). Our results show that the presence of high levels of active Rac does not impede the recruitment of WASP on ventral *puncta* but does affect their dynamics by rendering the spots substantially longer-lived. We suggest that the increased lifetime of clathrin, WASP and Arp2/3 complex *puncta* observed in cells expressing GFP-tagged WASP CRIB mutant is secondarily linked to the higher levels of active Rac, which are in turn caused by the lack of a functional WASP CRIB motif.

Lastly, we only briefly assessed the importance of a direct interaction between active Rac and WASP for the latter to drive forward movement in the absence of SCAR/WAVE, which is the major pseudopodia maker under normal conditions. We demonstrate that while a direct interaction with active Rac is not required for WASP to trigger actin polymerisation via the Arp2/3 complex on CCPs, it is indispensable for WASP to drive the formation of actin-filled protrusions that drive migration. This result clearly shows that WASP can be employed by the cells to fulfil different roles, some of which imply a regulatory role for active Rac while others do not.

Chapter 5 , *Results – part III*

WASP plays a role in autophagy

5.1 Preface

This chapter describes a series of experiments that have been carried out in the attempt to achieve two main goals. The first was to extend early observations suggesting that WASP is required for *Dictyostelium* to proliferate in minimal medium (Davidson, 2014) and to investigate the underlying mechanisms. The second was to explore possible CME-unrelated mechanisms by which WASP could contribute to maintain cellular homeostasis of active Rac, a role that has been discussed in the previous chapters of this thesis.

Most of the results reported here represent the first step towards a clearer understanding of WASP functions; some of them will require further confirmation and clarification but for the time being they all point out that much is yet to know about WASP roles within cells.

5.2 WASP is involved in autophagy

As mentioned throughout this dissertation, WASP is mostly known as a key player during clathrin-mediated endocytosis, a role that appears to be conserved in oganisms as far apart in the evolutionary tree as *Dictyostelium* (Davidson, 2014), yeasts (Madania et al., 1999), *Drosophila* (Kochubey et al., 2006) and mammals (Merrifield et al., 2004). Whether or not WASP has a central role in other cellular functions is surprisingly still unclear.

An intriguing suggestion came from experiments aiming to assess the ability of *Dictyostelium* WASP knockout cells to grow in SIH, a defined minimal medium obtained from the most widely used HL5 and SM media by adjusting the amount of different amino acids in order to reflect their actual usage in wild type cells (Han et al., 2004). SIH contains, for instance, a reduced amount of Arginine in comparison to HL5. Unexpectedly, these experiments showed that cells lacking WASP struggled to proliferate at a normal rate in minimal medium while perfectly capable to grow at the expected rate in HL5 (Davidson, 2014). This suggested that WASP is required for cells to proliferate normally in less nutrient conditions. Further evidence hinting at the possibility that WASP may contribute to the wellbeing of cells in suboptimal circumstances came from experiments addressing the ability of knockout cells to aggregate into fruiting bodies upon nutrient deprivation. Repeated tests proved that loss of WASP strongly impairs the capability of starving amoebas to develop into a multicellular organism (Davidson, 2014). Since facing the lack of nutrients, especially of amino acids, and satisfying the energetic demand of fruiting body formation requires a smooth autophagic flux (Onodera and Ohsumi, 2005; Otto et al., 2004),we hypothesised that WASP may be involved in autophagy.

One established approach to unveil a defect in autophagy in *Dictyostelium* is to measure survival upon amino acids deprivation (King et al., 2011). In more detail, strain of interest and appropriate controls are seeded in SIH lacking Arginine and Lysine; since both amino acids are essential for growth, under these circumstances cells can survive only if able to digest their own components via autophagy. Cells are harvested at regular time points and plated on a bacteria lawn; surviving cells will locally deplete bacteria by performing phagocytosis, leading to the formation of clear spots. The number of colonies formed, generally large enough to be scored within a few days, is representative of the number of cells that have survived amino acid deprivation. As shown in

figure 5.1, and as expected based on early data from full SIH (Davidson, 2014), while wild type cells (*wasA*+, in blue) overcome the lack of Arginine and Lysine, cells lacking WASP (*wasA*-, in red) struggle to withstand the same conditions, resulting in a more than 10 fold drop in survival after just 24 hours. As a comparison, *Dictyostelium* strains lacking components of the autophagic flux are almost entirely non viable after 48 hours under the same conditions (King et al., 2011). These data confirm that WASP supports cell survival under amino acid-depleted conditions, and encouraged us to clarify its role in autophagy.

Autophagy, however, is a complex process and not easy to dissect. It involves multiple cellular compartments and several molecular players, many of which are probably yet to be characterised. It is significantly boosted by lack of nutrients (Takeshige et al., 1992) and mechanical stress (King et al., 2011) but occurs at basal levels under non-harmful circumstances (Hara et al., 2006; Komatsu et al., 2005). It can lead to degradation of random portions of cell content, and therefore being non-selective (Kopitz et al., 1990), or drive the clearance of specific organelles, like mitochondria (Kanki et al., 2009; Okamoto et al., 2009), or specific proteins (Shintani and Klionsky, 2004).

Autophagosome assembly is triggered by a signalling cascade that results in the accumulation of PI3P (Phosphatidylinositol 3-phosphate) on a discrete portion of the endoplasmic reticulum (ER) (Axe et al., 2008). The PI3P-rich site expands sideways originating the *omegasome*, which accomodates the isolation membrane (Axe et al., 2008). This keeps growing until it becomes a fully closed autophagosome thanks to the addition of membranous portions, which could be provided by ER (Yla-Anttila et al., 2009), Golgi apparatus (Mari et al., 2010; Yamamoto et al., 2012), plasma membrane (Ravikumar et al., 2010), or mitochondria (Hailey et al., 2010). This is later detached from the original docking site and ultimately fused to lysosomes.

Different Arp2/3 complex activators have so far been shown to play a role in autophagy. WHAMM, for instance, appears at the PI3P-rich ER regions as well as on detached autophagosomes, suggesting that it may have a role during both earlier and later steps of autophagy (Kast et al., 2015). JMY, on the other hand, appears to mediate the formation of autophagosomes (Coutts and La Thangue, 2015) but not their movement within the cytosol. WASH, a more ubiquitous NPF across evolution, has been shown to regulate autophagy in mammals (Xia et al., 2013) and *Dictyostelium* (King et al., 2013), for instance by facilitating PI3P

enrichment on the ER membranes or by mediating autophagosome maturation. Of interest, the SCAR/WAVE complex has also been recently demonstrated to contribute to the formation of autophagosomes upon mechanical stress in plants (Wang et al., 2016). No evidence linking WASP to autophagy has been published to date, giving us the unique opportunity to explore it.

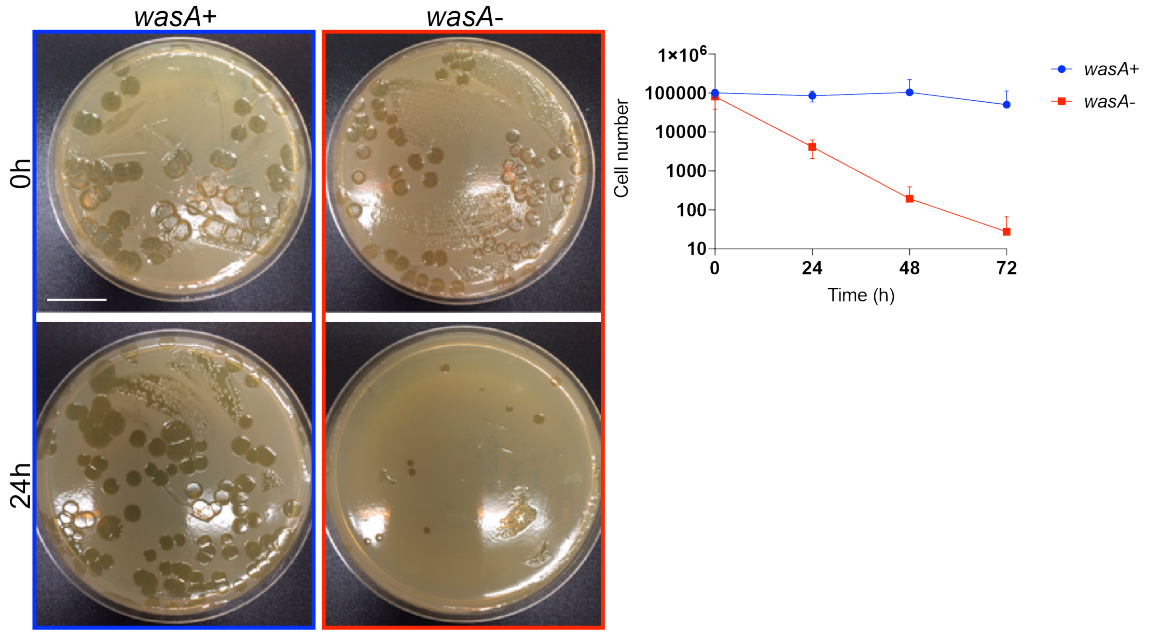

Figure 5.1 WASP supports cell survival upon Lysine and Arginine starvation.

Wild type parental strain (*wasA*+, blue rectangle) and WASP knockout cells (*wasA*-, red rectangle) were kept for 72 hours in minimal SIH medium lacking Arginine and Lysine. Both strains were harvested at regular time points (every 24 hours) and plated on agar plates alongside edible bacteria. In the presence of plentiful prey surviving cells will switch to phagocytosis to support their own growth. Local depletion of bacteria results in the formation of clear spots, which grow rounder and become large enough to be scored within a few days. The number of spots positively correlates with the number of cells that have survived amino acid deprivation.

Wild type cells rely on autophagy to survive the lack of two essential amino acids and the number of colonies formed at 24-48 and 72 hours post Arginine/Lysine starvation is therefore not affected (blue line on the right-hand side graph). WASP knockout cells, on the contrary, struggle to survive in the absence of the two amino acids; this results in the formation of a reduced number of smaller colonies after just 24 hours. As indicated by the red line on the righ-hand side graph, very few WASP knockout cells are viable after 72 hours in the absence of Lysine and Arginine (n=2). Scale bar represents 2 cm.

5.3 WASP *puncta*: more than just clathrin-coated pits!

We started our investigation by asking at which step of the autophagic flux WASP may intervene. Does it contribute to the formation of autophagosomes, or to their movement throughout the cytosol, or to something else?
We decided to initially assess the involvement of WASP in the genesis of autophagosomes. The reason behind this choice is that before developing into fully closed vesicles, newly formed autophagosomes appear as discrete *puncta* that are enriched in autophagosomal markers like Atg8 and Atg18 (*Dictyostelium* orthologues of mammalian LC3 and WIPI respectively) (King et al., 2011). Spots generated by GFP-labelled Atg8 or Atg18, for instance, are remarkably similar to those generated by GFP-WASP.
We therefore asked whether any of the WASP *puncta* detected on the basal membrane of the cells could be an autophagosome. This hypothesis strongly disagrees with the assumption that WASP-positive dynamic *puncta* are clathrin-coated pits that become internalised (Davidson, 2014; Kim et al., 2000; Kochubey et al., 2006; Merrifield et al., 2004).
We decided to question this assumption by using two different approaches. First, by testing the ability of WASP to generate *puncta* in the absence of clathrin; second, by carefully monitoring WASP dynamics in wild type cells in order to spot any clathrin-negative WASP-positive *puncta*.
Our first question, whether or not WASP can generate dynamic *puncta* in a clathrin null background, has so far been only partially addressed largely due to technical challenges. Indeed, while *Dictyostelium* clathrin light chain (CLC) (Wang et al., 2003) knockout cells are relatively healthy, easy to expand in culture and to transfect, those lacking the gene encoding clathrin heavy chain (CHC) (Niswonger and O'Halloran, 1997) are significantly less suitable for manipulation. The phenotypic details of the two strains will not be discussed in depth here, but a major difference between them needs to be highlighted, as it influences the interpretation of our results. While the absence of clathrin heavy chain impairs the internalisation of GFP-tagged Dajumin, so far the only known cargo for CME in *Dictyostelium*, loss of clathrin light chain does not seem to markedly affect it (Macro et al., 2012). From a mechanistic point of view this may be due to the fact that in the absence of light chains the heavy chains can still assemble into a triskelion (Wang et al., 2003), although the resulting lattice has been shown to have a reduced capability to associate with the membrane

(Wang et al., 2003). Despite several attempts, we have not yet succeeded in transfecting clathrin heavy chain knockout cells in order to visualise WASP localisation and dynamics. However, we have been able to transiently transfect clathrin light chain knockout cells with an extrachromosomal plasmid harbouring sequences encoding GFP-tagged WASP and RFP-tagged ArpC4. As reported in figure 5.2, WASP and the Arp2/3 complex co-localise on dynamic *puncta* in the absence of clathrin light chain. This could either suggest that WASP can trigger actin polymerisation in a completely clathrin-independent fashion, or that under these circumstances WASP can be recruited on a triskelion that is solely made by heavy chain subunits. It will therefore be useful to clarify whether or not heavy chain lattices lay underneath WASP *puncta* observed in a *clc* null background.
Our second question, whether any of the WASP *puncta* generated in cells expressing both clathrin heavy and light chains are formed independently of a lattice, has given an encouraging although still partial answer. To address it, we transiently transfected clathrin light chain knockout cells with an extrachromosomal vector encoding red-tagged clathrin light chain (CLC-mRFPmars, rescue) and GFP-tagged WASP. Transfected cells were gently squashed under agarose to facilitate live-TIRF imaging. It is important to emphasise that this experiment has been carried out based on the assumption that under these circumstances, given the availability of tagged CLC, no triskelion exclusively composed by heavy chains will be generated; CLC dynamics should therefore reflect the dynamics of virtually every lattice. Figure 5.3 and movie 10 show an example of WASP spot being generated on a pre-existing clathrin *punctum* (panel A), and an example of WASP short burst not occurring on a long-lasting clathrin spot (panel B). What proportion of WASP *puncta* appears independently of clathrin is currently under investigation.

Our data demonstrate for the first time the existence of a subpopulation of WASP molecules that may be able to dynamically associate with the membrane in a clathrin-independent fashion. As already mentioned, we cannot currently rule out the possibility that triskelions exclusively made out of clathrin heavy chains, which were not tagged in our experiment, lay underneath CLC-negative WASP *puncta*. Despite the need for further clarification, our evidence suggests that WASP may execute some clathrin-independent roles within cells, one of them being autophagy.

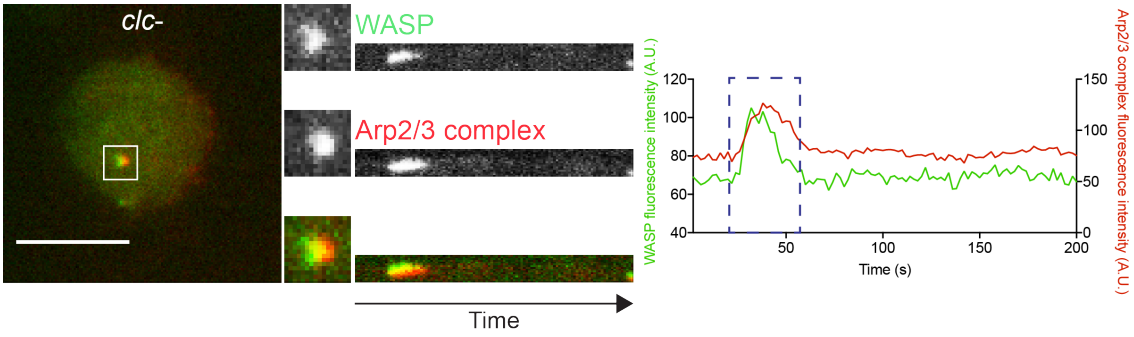

Figure 5.2 WASP generates dynamic *puncta* in the absence of clathrin light chain.

Clathrin light chain knockout cells (*clc*-) were transfected with a co-expression vector encoding GFP-WASP and mRFPmars2-ArpC4. Selected cells were gently squashed under agarose to facilitate live-cell TIRF imaging. As shown on the left-hand side, the absence of clathrin light chain does not affect the abilty of GFP-WASP to form ventral *puncta* and to recruit the Arp2/3 complex. Kymograph and fluorescence plot on the right hand side provide further insights into the temporal dynamics of GFP-WASP and mRFPmars2-ArpC4. A synchronous peak of the two molecules is highlighted by the dashed blue rectangle. Scale bar represents 10 µm.

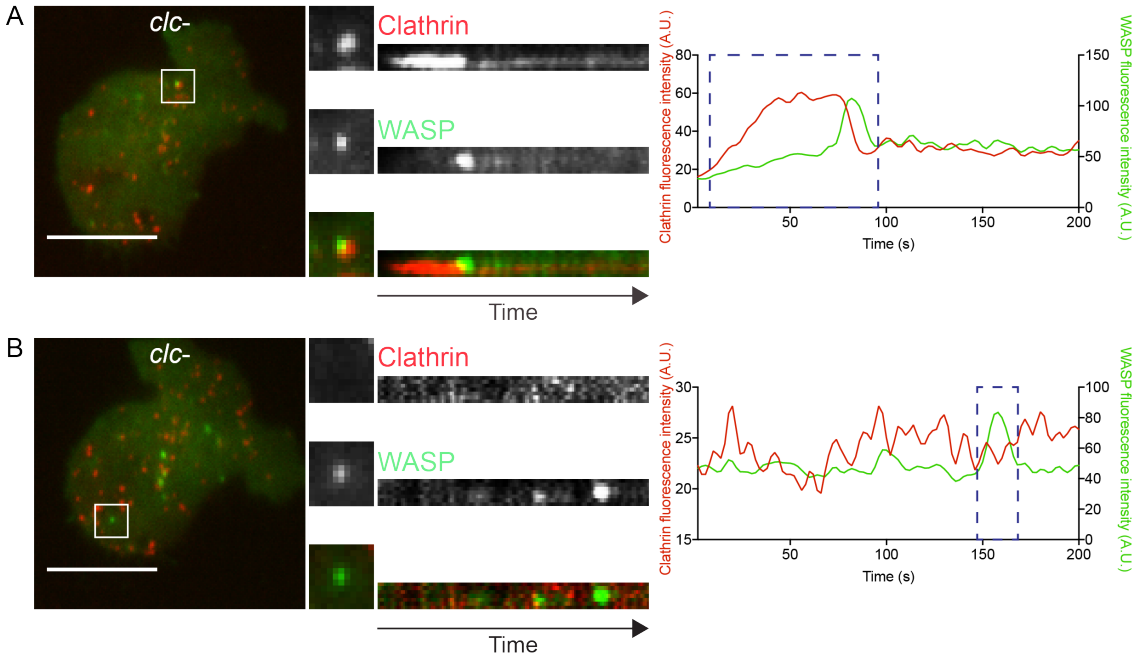

Figure 5.3 WASP generates CLC-negative *puncta* in the presence of both clathrin heavy and light chains.

Clathrin light chain knockout cells (*clc*-) were transiently transfected with a co-expression vector encoding GFP-WASP and CLC-mRFPmars (rescue). Transfected cells were gently squashed under agarose to facilitate live-cell TIRF imaging.

A) A subset of WASP *puncta* is formed on a pre-existing clathrin spot, in agreement with the established role for WASP during clathrin-mediated endocytosis. As demonstrated by kymograph and fluorescence plot, GFP-WASP is recruited on a longer-lived clathrin *punctum*; the two molecules briefly overlap (dashed blue rectangles) and the drop in fluorescence that follows is considered as a *bona fide* sign of CCP internalisation. Scale bar represents 10 µm.

B) WASP can be detected on dynamic spots that do not appear to overlap with clathrin light chain, used here as a marker for CME. This is clearly shown by kymograph and fluorescence plot (dashed blue rectangle). Scale bar represents 10 µm.

5.4 WASP decorates autophagosomes

Having raised the possibility that some of the WASP *puncta* do not coincide with clathrin encouraged us to hypothesise that some of them may be autophagosomes. We initially aimed to assess the co-localisation between endogenous WASP and endogenous autophagosomal markers by immunofluorescence. This technical choice was dictated by the fact that extra caution is needed when drawing any conclusion from experiments that utilise the overexpression of tagged Atg8 (LC3), as this has been shown to generate autophagy-independent aggregates in transiently transfected mouse embryonic fibroblasts (Kuma et al., 2007). It is important to mention at this stage that GFP-Atg8 is well optimised for use in *Dictyostelium*, and that its localisation and dynamics prior to and upon induction of autophagy have been explored: GFP-Atg8 is mostly cytosolic with only few visible *puncta* under normal circumstances, while it is detected on a significantly larger number of spots following mechanical stress or nutrient deprivation (King et al., 2011). However, while the anti-Atg8 antibody at our disposal was suitable for immunofluorescence and specifically labelled individual *puncta*, the anti-WASP antibody failed to detect discrete structures, even when pre-absorbed on fixed WASP knockout cells (data not shown). Given the impossibility to utilise our antibody to detect endogenous WASP, we decided to perform immunofluorescence on WASP knockout cells expressing GFP-WASP (rescue) fixed and stained with the anti-Atg8 antibody. As shown in figure 5.4, endogenous Atg8 is evenly distributed throughout the cytosol in non-starved and non-heavily compressed cells, with only one spot clearly detectable. Exogenous GFP-WASP has a similar localisation pattern, although two *puncta* stand out from the homogenous cytosolic signal. Of the two WASP spots shown in this representative example, one perfectly overlaps with Atg8 (dashed square) while the other does not (solid square).
This evidence reinforces the hypothesis that WASP may be involved in autophagy in addition to its most established role in clathrin-mediated endocytosis.

In order to gain insights into the dynamics of WASP during autophagy we decided to perform live-cell imaging. Two autophagosomal markers have so far been particularly useful to monitor the autophagic flux in *Dictyostelium*: Atg8 and Atg18, again *Dictyostelium* orthologues of mammalian LC3 and WIPI respectively.

From a temporal perspective the two molecules only partially overlap, as they play different roles during autophagy. Atg18 is known to be recruited to PI3P-rich ER regions and appears to act upstream of Atg8, specifically by facilitating its lipidation (Polson et al., 2010). Labelled Atg18 allows us to follow exclusively the earlier stages of the autophagic flux, as it appears to be removed from autophagosomes once these are fully closed. Atg8 is also recruited to expanding autophagosomes but remains bound to the inner and outer membranes of mature autophagosomes (Kabeya et al., 2000) until these fuse to lysosomes. Therefore labelled Atg8 allows us to monitor a significantly longer portion of the autophagic flux.

As we aimed to follow WASP dynamics over the longest timeframe possible we started our investigation by performing live-cell imaging on WASP knockout cells transiently co-expressing GFP-WASP (rescue) and red-tagged Atg8. It appeared immediately clear, however, that this approach would have not answered our questions. Indeed, while the addition of a GFP tag does not affect the localisation of Atg8, an mRFP-tag had a significant impact on it, making our co-expression vector substantially unusable for the purpose of our experiments. A GFP-Atg8, on the other hand, could not be used to perform the experiments we intended to, since a comparable effect of a red tag has been observed for WASP, and this can only be used when coupled to GFP.

Having realised that assessing the co-localisation of WASP and Atg8 in living cells would have not been achievable in the short term, we decided to focus our attention on Atg18. We transiently transfected WASP knockout cells with a co-expression vector encoding GFP-WASP (rescue) and mRFPmars-Atg18. Transformed cells were heavily squashed under agarose prior to live imaging in order to induce autophagy (King et al., 2011). As shown in figure 5.5, GFP-WASP and mRFPmars-Atg18 occasionally co-localise. This occurs within a distinctive structure that appears to expand progressively while simultaneously organise itself into a multilobate vesicle. Data so far suggest that each cell shows one multilobe structure, and that while mRFPmars-Atg18 strongly accumulates within the lobes, GFP-WASP also tends to decorate its entire outline.

What these structures are and which of the autophagy steps they may represent is unclear and in need of thorough analysis. For the time being it is however important to linger on the possible reasons for which they have not been

previously observed. We speculate that this may caused by at least two facts. First, GFP-WASP is largely cytosolic: its homogeneous distribution makes it difficult to spot unknown features. Second, as already mentioned throughout this dissertation, our knowledge regarding WASP localisation and functionality above the TIRF field is poor.

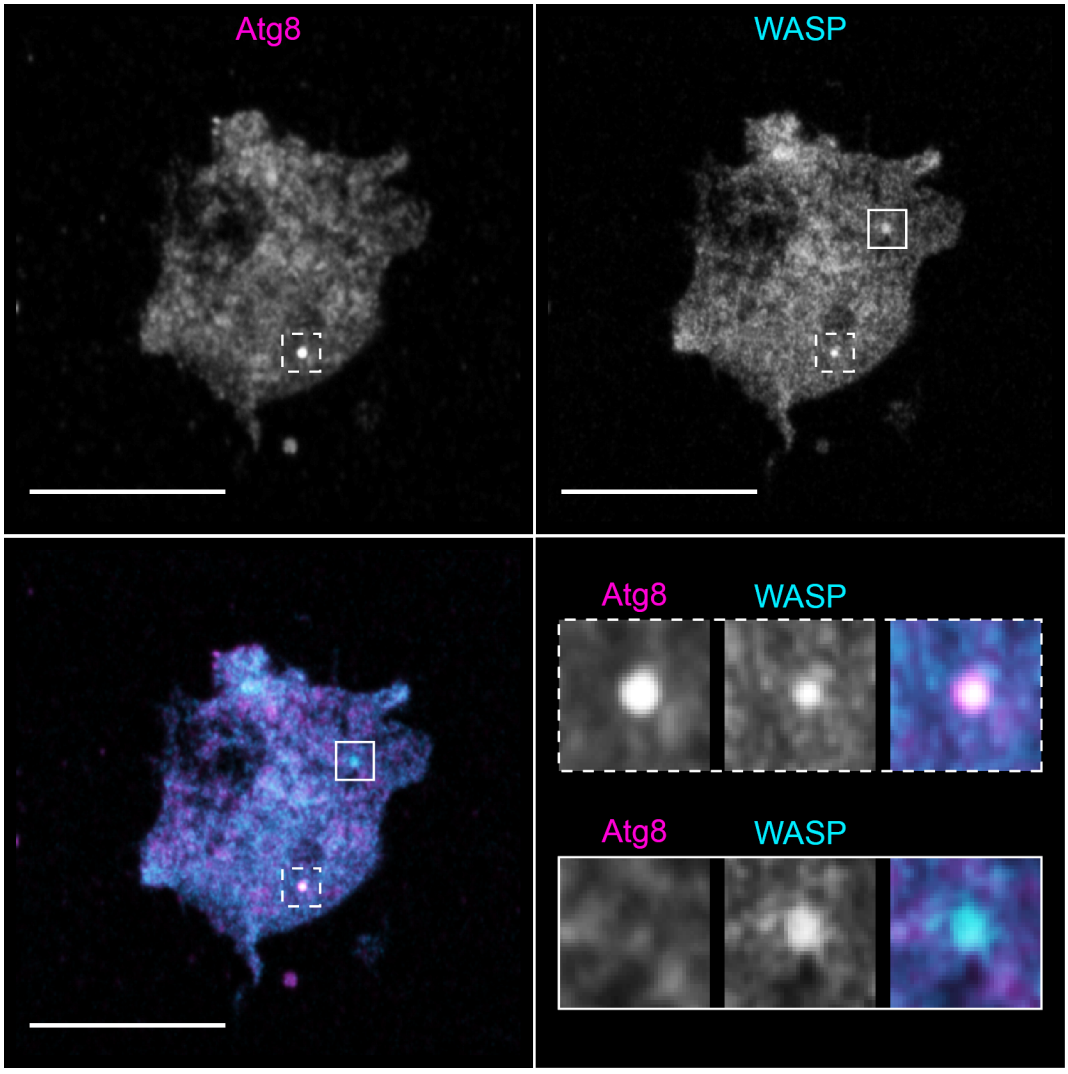

Figure 5.4 WASP and endogenous Atg8 show a partially overlapping punctate localisation.

WASP knockout cells were transfected with an extrachromosomal vector encoding GFP-WASP (rescue). Transfected cells were grown in rich medium, fixed and stained using an anti-Atg8 antibody. Super-resolution microscopy revealed that, as expected given the lack of autophagy-inducing conditions, Atg8 is largely cytosolic with only one detectable *punctum*. GFP-WASP also gives a diffuse signal, although two *puncta* can clearly be identified. In support of the hypothesis of WASP involvement in autophagy, one of the GFP-WASP spots co-localises with endogenous Atg8 (dashed square). Another GFP-WASP *puncta*, likely representing an event of CME, does not co-localise with Atg8 (solid square). Scale bars represent 10 μm.

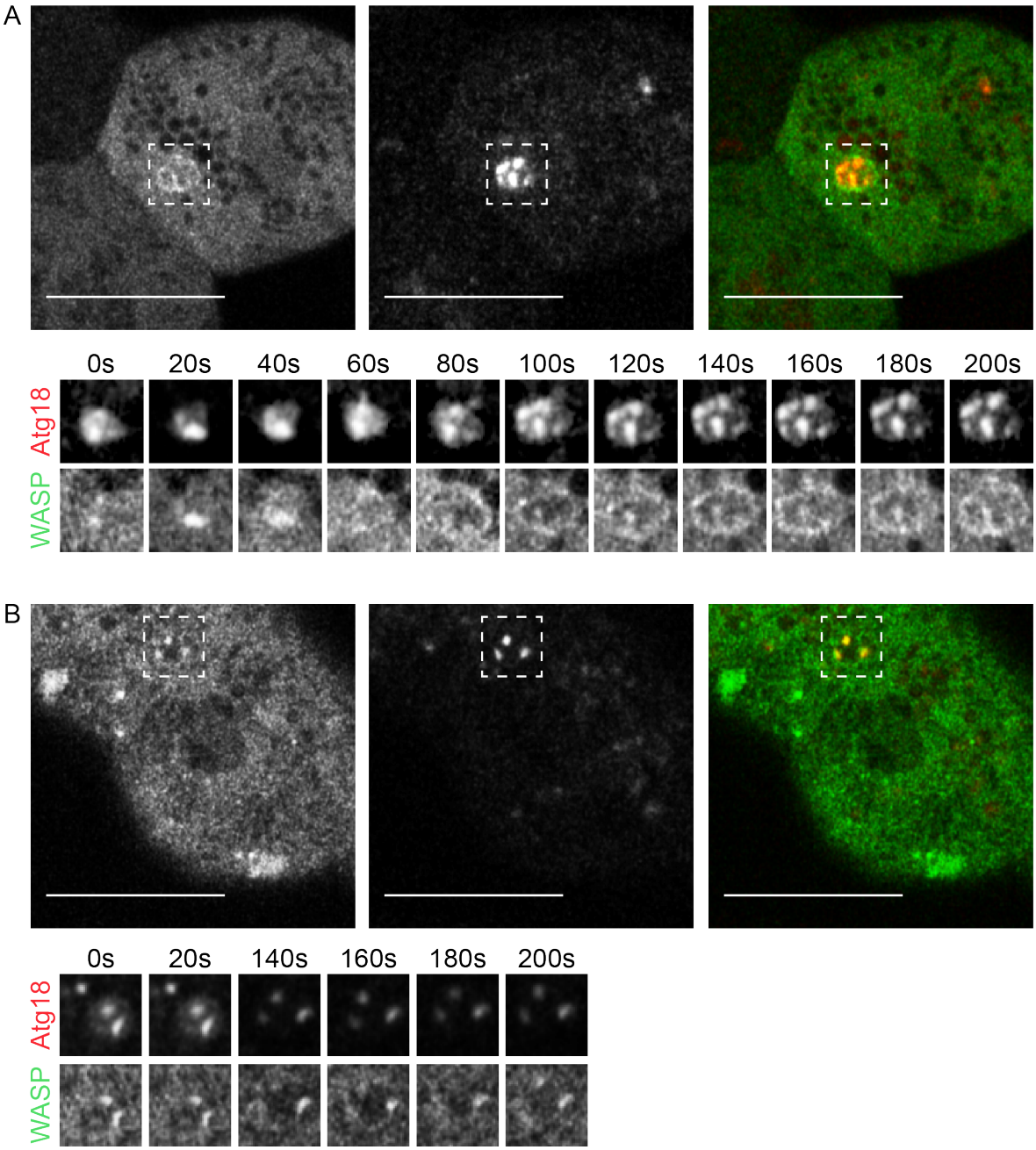

Figure 5.5 WASP and the early autophagosomal marker Atg18 co-localise on dynamic lobate structures.

A) and B) WASP knockout cells were transfected with an extrachromosomal vector encoding GFP-WASP (rescue) and mRFPmars-Atg18, which is believed to localise on nascent autophagosomes. Selected cells were heavily squashed under agarose in order to induce autophagy and analysed by super-resolution live-cell imaging. Under these conditions the two probes are tatgeted to a lobate structure, which is highlighted by a dashed square in both examples. Evidence gathered so far suggests that this is highly dynamic and tends to unfold progressively until it becomes a large multilobate vesicle. GFP-WASP appears to define its outline and occasionally localise on individual clusters, while

mRFPmars-Atg18 seems to be mostly confined on individual lobes. GFP-WASP and mRFPmars-Atg18 are also occasionally found within individual *puncta*. Scale bars represent 10 μm.

5.5 Levels of endogenous WASP are affected by autophagy inhibition

It has been established that some of the molecules regulating autophagy are also potential substrates of the degradative flux. This is for instance the case of p62/SQSTM1 (hereafter p62), which binds to poly-ubiquitinated proteins facilitating their incorporation within autophagosomes (Bjorkoy et al., 2005). On one hand p62 depletion hampers the formation of autophagosomes, pointing at its key role during the early steps of autophagy; on the other hand a block in the autophagic flux leads to increased levels of p62, suggesting that its availability is controlled via autophagy (Bjorkoy et al., 2005). Intrigued by the dual, regulator/substrate, role of components of the autophagic flux, and wishing to further address the involvement of WASP in autophagy, we asked whether a block in the autophagic flux would affect the levels of WASP.

In order to arrest the degradative pathway we treated cells with ammonium chloride (NH_4Cl) (Calvo-Garrido et al., 2011), a lysosomotropic agent able to penetrate the lysosomal membrane and induce a net increase in the organelles' luminal pH. Since an acidic pH is essential for complete degradation of cargo proteins, ammonium chloride irremediably compromises the ability of the lysosomes to clear their content. The assay described by Calvo-Garrido and colleague is based on detection of free GFP fragments deriving from proteolitic cleavage of GFP-Tkt-1, a GFP-tagged cytosolic protein. Such fragments do not accumulate under normal circumstances, as they are quickly cleaved within acidic lysosomes. Following a four-hour treatment with 150 mM NH_4Cl, however, the GFP fragments remain trapped within neutralised lysosomes; as their degradation cannot proceed further they become detectable by Western blot. An example of free GFP accumulation upon lysosome neutralisation is shown in figure 5.6 A. In agreement with what previously observed by Calvo-Garrido and colleagues, free GFP fragments (27 kDa, green rectangle) are poorly detectable in untreated cells (0 mM) or in those that have been subjected to low (50 mM) doses of ammonium chloride. On the contrary, a clearly distinguishable GFP band appears upon treatment with 100 mM NH_4Cl, although the maximal block in the autophagic flux is obtained when cells are kept in the presence of 150 mM ammonium chloride. The enrichment in free GFP normalised against GFP-Tkt-1 is reported in panel B.

Having been able to visualise a block in the autophagic flux, we went on addressing whether this could affect the levels of endogenous WASP. To do this

we repeated the described experiment on untransfected wild type cells. After four hours in medium containing different concentrations of ammonium chloride cells were lysed and levels of WASP measured by Western blot. As shown in figure 5.6 C, levels of endogenous WASP are affected by a block in the autophagic flux. A detectable increase in the total amount of WASP can be appreciated when cells experience a minimum concentration of 100 mM ammonium chloride; again, the maximal increase is obtained at the concentration of 150 mM. Data from two independent experiments, reported in panel D, reveal that under these circumstances the increase in WASP protein spans from 1.8 to 7.8 fold.

This result is important for at least two reasons. On one hand, by providing information about endogenous WASP and not its exogenously expressed GFP-tagged version, it strengthens the hypothesis of WASP's involvement in autophagy. On the other hand it reveals a previously undescribed mechanism by which cells regulate their levels of WASP.

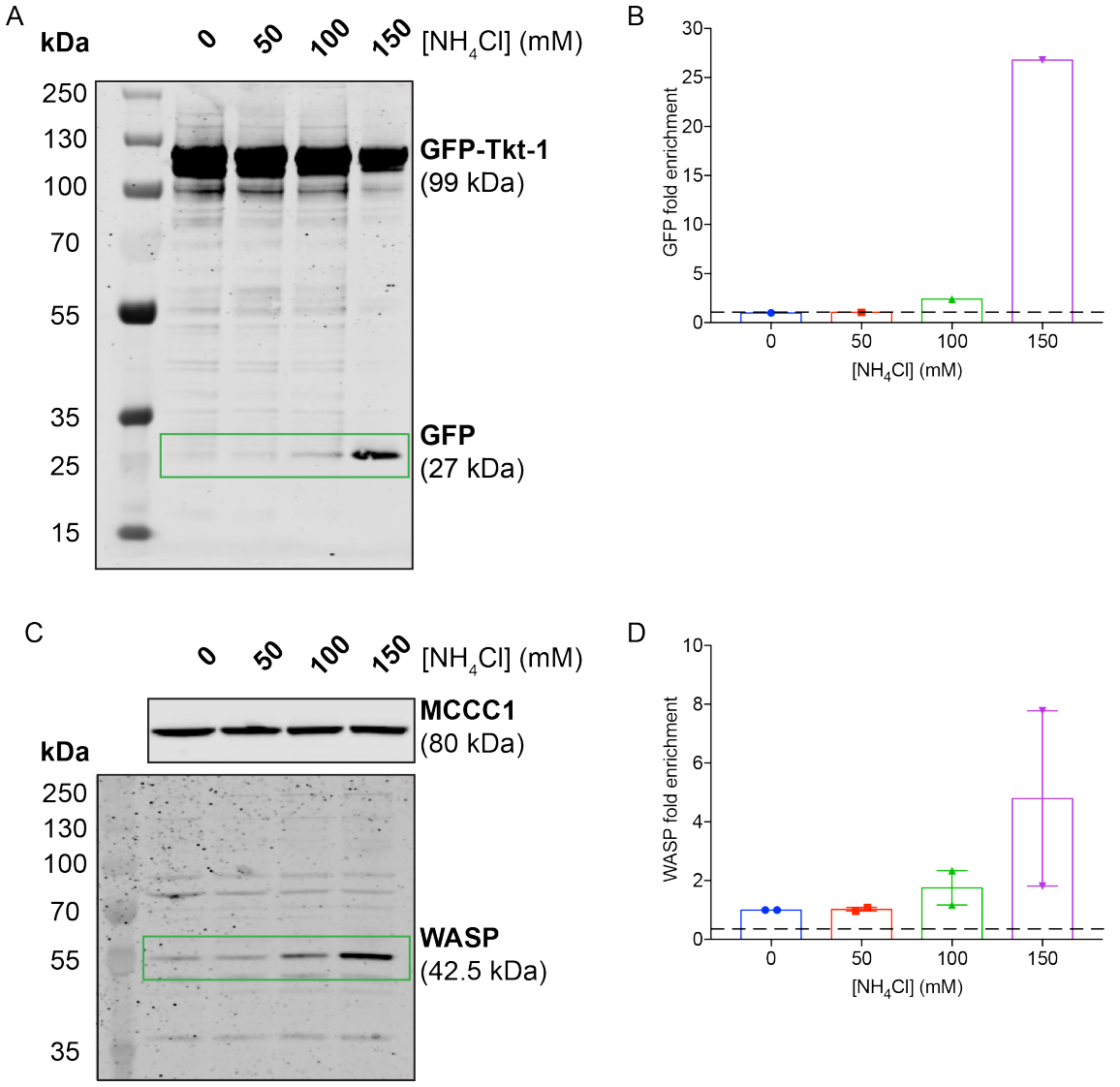

Figure 5.6 Autophagy controls the levels of endogenous WASP.

A) and B) Wild type cells were transfected with an extrachromosomal vector encoding GFP-Tkt-1, a 99kDa enzyme whose levels are regulated via autophagy. Transfected cells were treated for four hours with increasing concentrations (50-100-150 mM) of ammonium chloride (NH_4Cl), a lysosomotropic agent able to neutralise lysosomes and arrest cargo degradation. Untreated cells (0 mM) were used as a control. As highlighted by the green rectangle in panel A, free GFP fragments are accumulated upon a block of the autophagic flux, which is optimally induced at the concentration of 150 mM. As quantified in panel B at the highest concentration a >25 fold enrichment in free GFP can be measured (n=1).

C) and D) To address whether levels of endogenous WASP are controlled via autophagy the experiment described above was performed on untransfected wild type cells. As shown in C, the amount of WASP detected by western blot is

remarkably increased following a four-hour period in 150 mM NH_4Cl. As quantified in D, the increase in WASP levels under these circumstances spans from 1.8 to 7.8 fold (n=2). MCCC1 has been used as a loading control as previously described (Davidson et al., 2013).

5.6 WASP harbours a putative LIR (LC3-interacting region)

We next aimed to clarify which of its domains could mediate WASP recruitment on autophagosomes.

As described in section 1.3.1, WASP has a defined domain composition, which includes a WH1 domain, a basic region, a CRIB motif, a polyproline stretch and a composite VCA C-terminal segment. We initially speculated that one of the known domains of WASP may be responsible for targeting it to autophagosomes (i.e. its basic region may interact directly with acidic phospholipids on the isolation membrane or on the phagophore). It has however been demonstrated that some of the proteins involved in autophagy harbour a defined motif that connects them to core components of the autophagic flux. This motif has been termed LIR (LC3-interacting region) (Pankiv et al., 2007) or alternatively AIM (Atg8- family interacting motif) (Noda et al., 2010). Examples of LIR-containing proteins include the aforementioned p62 (Pankiv et al., 2007) and NBR1 (neighbor of BRCA1 gene 1) (Kirkin et al., 2009; Pankiv et al., 2007). The minimal LIR was initially proposed to be a stretch of 11 residues grouped into two key regions: an acidic triplet, often composed by three Aspartatic acid residues, and a hydrophobic cluster, generally consisting of a conserved Tryptophan and a Leucine two positions downstream (Ichimura et al., 2008). Following the identification of more LIR-bearing proteins, the minimum number of residues necessary and sufficient to interact with components of the autophagy machinery has been reduced to 8 (Johansen and Lamark, 2011). The consensus sequence can be written as $X_{-3}\,X_{-2}\,X_{-1}\,W_0\,X_{+1}\,X_{+2}\,L_{+3}\,X_{+4}$, whereby acidic residues are common in positions -3, -2 and -1, a Tryptophan (or alternatively a Phenylalanine or a Tyrosine) sits in position 0, and a Leucine (or alternatively a Isoleucine or a Valine) occupies the +3 position. An LC3-interacting region has been recently identified within the sequence of JMY (Coutts and La Thangue, 2015), while it does not seem to be present in WHAMM, despite this being also involved in autophagy (Kast et al., 2015). We therefore wondered whether there could be a LIR in *Dictyostelium* WASP. As shown in figure 5.7, *Dictyostelium* WASP harbours a putative LIR motif, located in the N-terminal region and partially overlapping with the CRIB motif. It shows the key Tryptophan in position 0, an acidic residue (Aspartic acid) in position -1, a conserved Leucine in position +3, and is remarkably similar to the LC3-interacting region identified in other proteins, including human p62 (Pankiv et al., 2007), human NBR1 (Kirkin et

al., 2009) and human JMY (Coutts and La Thangue, 2015). To the best of our knowledge WASP is the first identified *Dictyostelium* protein to harbour a presumed LC3-interacting region.

We are currently aiming to test the biochemical interaction between WASP and LC3 by performing pulldown assays using GFP-WASP or GFP-Atg8 as a bait.

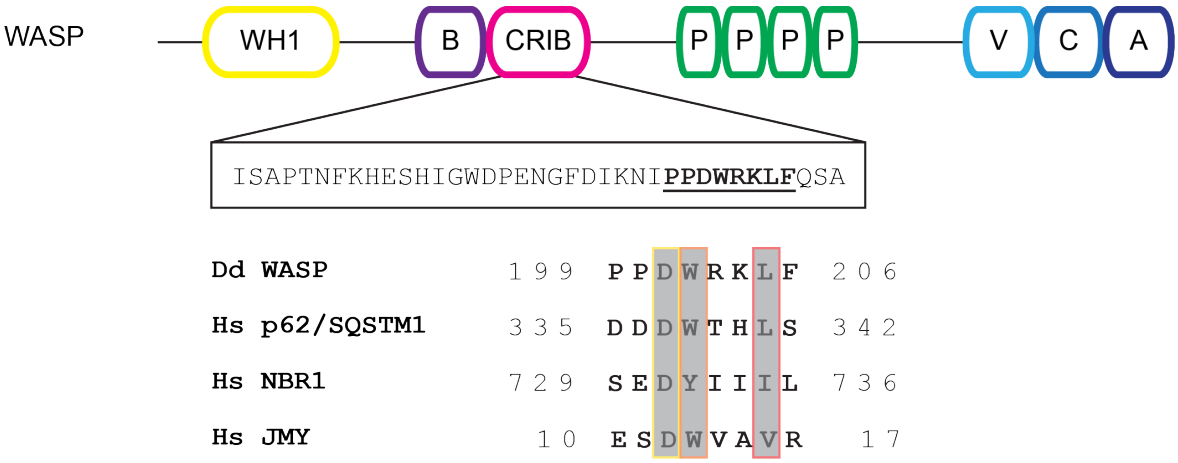

Figure 5.7 WASP harbours a putative LC3-interacting region.

The presence of a LIR (LC3 interacting region) is a feature of many but not all autophagy players. This is composed of eight residues and includes a key Tryptophan (indicated as W_0), which is only occasionally replaced by a phenylalanine (F) or a tyrosine (Y), a highly conserved leucine in position +3, and a variable number of acidic residues (often Aspartic, D, or Glutammic, E, acid) in positions -1, -2 and -3. A LIR has been identified in human (Hs) p62, NBR1 and JMY. We aimed to clarify whether such motif is also present in *Dictyostelium* (Dd) WASP. This appears to be a possibility: buried within its CRIB motif, WASP harbours a putative LIR, which contains the conserved Tryptophan preceded by a Aspartic acid and followed by a Leucine three residues downstream.

5.7 Could autophagy control the levels of active Rac?

Evidence provided in chapter 3 suggest that WASP restricts Rac activity and it may also contribute to maintain homeostatic levels of active Rac. Data reported so far in chapter 5 point out that a novel role for WASP in autophagy. We decided to explore the possibility that autophagy may represent the mechanism by which WASP contributes to active Rac homeostasis.

A role for autophagy in the maintenance of appropriate levels of RhoA, a GTPase that belongs to the same family as Rac, has been recently reported (Belaid et al., 2013). In more details, it was found that p62 mediates the recruitment of active RhoA within autophagosomes, where the GTPase is normally degraded. Inhibiting autophagosome formation leads to aberrant accumulation of active RhoA at the cleavage furrow, where it hampers cytokinesis leading to the formation of multinucleated cells (Belaid et al., 2013). It is important to mention that Belaid and colleagues addressed whether a smooth autophagic flux may also regulate other GTPases (including Rac) or their regulatory molecules. The localisation of Rac upon autophagy inhibition was not tested, but pulldown assays appeared to discourage a role for this degradative pathway in the maintenance of homeostatic levels of active Rac, at least in renal murine cells.

To test whether autophagy may represent a means of Rac regulation in our system we investigated the degree of co-localisation between GFP-tagged Rac1A and mRFPmars-Atg18 by super-resolution live-cell imaging prior to and upon induction of autophagy by mechanical stress. As shown in figure 5.8 and movie 10, in the absence of compression (panel A) mRFPmars-Atg18 is intriguingly accumulated at the trailing edge (marked by a red asterisk) but can also be found on a small number of *puncta*. One of them, highlighted in the yellow dashed square, appears to co-localise with GFP-Rac1A. The fluorescence plot reported below provides further insights into the arrangement of the two molecules within the discrete spot: it appears that GFP-Rac1A decorates the outline of the *punctum*, while mRFPmars-Atg18 occupies its central area. Upon induction of autophagy by mechanical stress (panel B and movie 11) cells lose their front-rear polarity and appear rounder than their unsquashed counterparts; mRFPmars-Atg18 is now spotted at the edges of doughnut-shaped vesicles (solid blue square) as well as on smaller *puncta* (dashed blue square). Remarkably, GFP-Rac1A clearly localises on both structures. Fluorescence plots revelaed that

the two molecules have an almost perfectly overlapping distribution within both structures.

These data suggest that autophagy may represent an additional, previously undescribed, mechanism by which cells control the levels of Rac1A. Whether or not WASP is also present on these structures is currently under investigation.

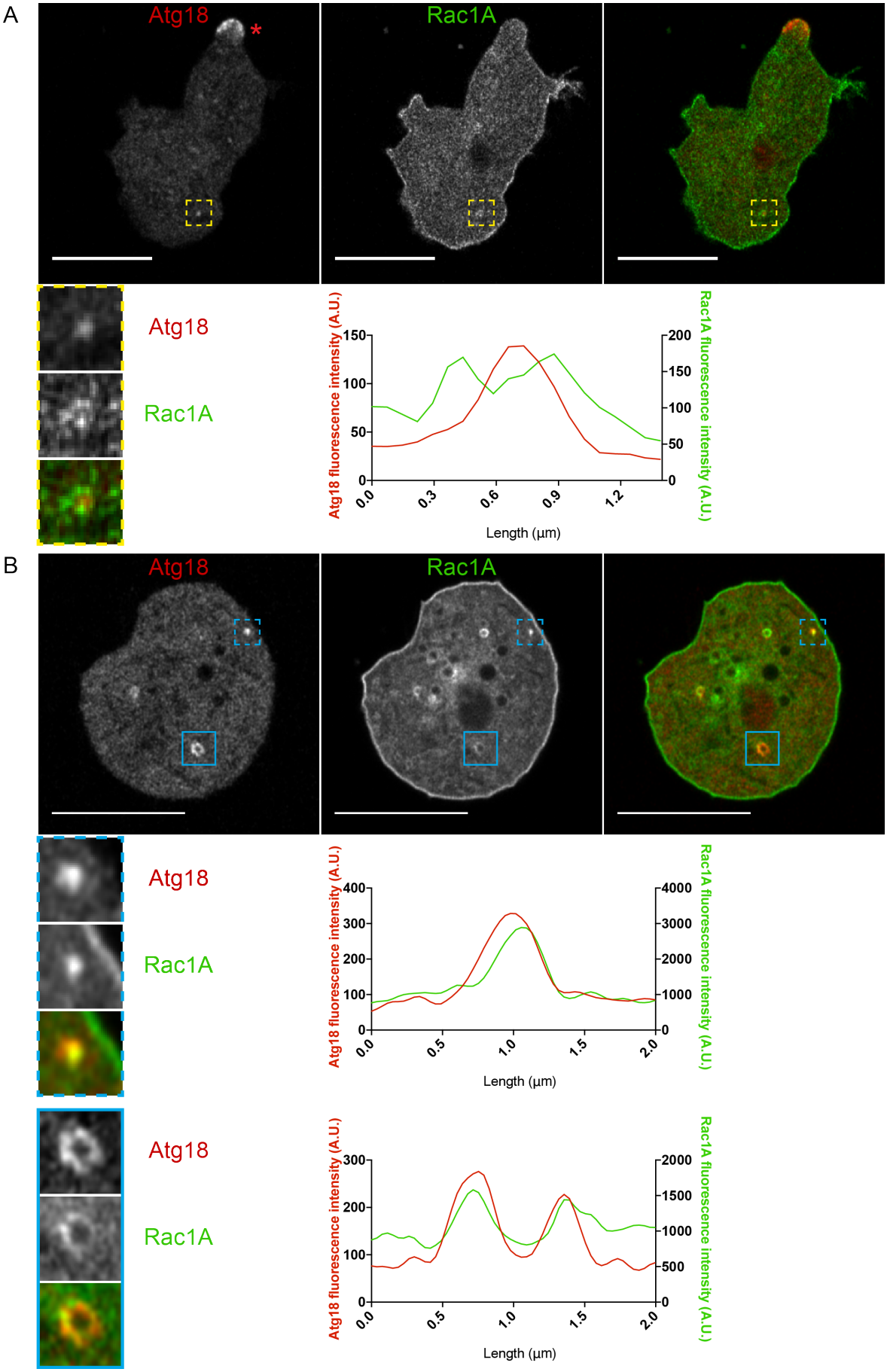
A
Atg18
Rac1A
Atg18
Rac1A
Atg18 fluorescence intensity (A.U.)
Rac1A fluorescence intensity (A.U.)
Length (µm)
B
Atg18
Rac1A
Atg18
Rac1A
Atg18
Rac1A
Atg18 fluorescence intensity (A.U.)
Rac1A fluorescence intensity (A.U.)
Length (µm)
Atg18 fluorescence intensity (A.U.)
Rac1A fluorescence intensity (A.U.)
Length (µm)

Figure 5.8 Rac1A co-localises with the early autophagosomal marker Atg18.

A) Wild type cells were transfected with an extrachromosomal vector encoding GFP-Rac1A and mRFPmars-Atg18. Selected cells were analysed by super-resolution live-cell imaging during directed migration. Under these circumstances cells are only gently compressed, and therefore autophagy occurs at basal levels; accordingly, only few mRFPmars-Atg18-positive *puncta* can be detected. Intriguingly, mRFPmars-Atg18 seems to localise at the trailing edge of migrating cells, which is labelled by a red asterisk. GFP-Rac1A is instead highly enriched around the cell perimeter, although excluded from the rear. Of great interest, GFP-Rac1A can be also spotted at the edges of a small ring-shaped vesicle, which appears to surround an mRFPmars-Atg18 spot (dashed yellow square). This is shown in greater details in the three enlarged squares reported below. The fluorescence plot shown on the right-hand side also suggests that GFP-Rac1A may envelop an mRFPmars-Atg18 *punctum*. Scale bars represent 10 μm.

B) Wild type cells expressing GFP-Rac1A and mRFPmars-Atg18 were heavily compressed under agarose in order to induce autophagy. The localisation of the two molecules was then investigated by super-resolution live-cell imaging. As expected, cells have lost their front-rear polarity and appear significantly rounder than those shown in A). mRFPmars-Atg18 can be found on more numerous discrete structures, including small *puncta* (dashed blue square) and ring-shaped vesicles (solid blue square). Remarkably, GFP-Rac1A can be spotted within both individual *puncta* and doughnut-shaped vesicles. In comparison to the distribution of the two molecules described in A), in heavily compressed cells mRFPmars-Atg18 and GFP-Rac1A appear to overlap perfectly, as further suggested by the fluorescence plots reported on the right-hand side. In addition to its localisation on mRFPmars-Atg18-positive structures, GFP-Rac1A is also detected all around the cell perimeter. Scale bars represent 10 μm.

5.8 Chapter 5 summary

In this chapter, we have demonstrated a novel role for WASP in autophagy, and started to elucidate the molecular details of its involvement in this conserved degradative pathway. Furthermore, we began to explore the possibility that autophagy may control cellular homeostasis of active Rac.

Two sets of evidence from our lab suggested that WASP is required for cells to survive in unfavourable conditions (Davidson, 2014). First, *Dictyostelium* WASP knockout cells do not proliferate when kept in SIH, a minimal medium that instead supports rapid growth of their parental strain. Second, *Dictyostelium* WASP knockout cells fail to develop into a multicellular organism in response to nutrient deprivation. Since the ability of cells to handle suboptimal circumstances greatly relies on autophagy (Calvo-Garrido et al., 2011; Onodera and Ohsumi, 2005; Otto et al., 2004), we hypothesised that WASP may be essential for this degradative pathway to be efficiently executed. By comparing the survival rate of knockout and wild type cells in the absence of Lysine and Arginine, two essential amino acids, we were able to confirm that *Dictyostelium* WASP is involved in autophagy.

In order to clarify at which step of the autophagic flux WASP may be required, we analysed the degree of co-localisation between GFP-WASP and two different autophagosomal markers, Atg8 (*Dictyostelium* orthologue of mammalian LC3) and Atg18 (*Dictyostelium* orthologue of mammalian WIPI). Pilot immunofluorescence experiments demonstrate a partially overlapping punctate distribution of GFP-WASP and endogenous Atg8, hinting at the possibility that some of the spots generated by GFP-WASP may in truth be autophagosomes. This evidence conflicts with the assumption that WASP generates *puncta* with the unique goal to facilitate the internalisation of clathrin-coated pits. As a relevant digression, it is important to mention that data reported in section 5.3, despite not yet conclusive, suggest that WASP may indeed have clathrin-independent subcellular localisation(s) and function(s).

A further evidence strengthening the novel concept of WASP playing a role in autophagy came from live-cell imaging experiments, whereby the dynamic localisation of GFP-WASP and red-tagged Atg18 was analysed. Upon autophagy induction by mechanical stress the two molecules were spotted within the same structure, an expanding multilobate vesicle that will require further experiments to be fully characterised.

At least two more pieces of evidence contributed to confirm the involvement of WASP in autophagy.

We have demonstrated that levels of endogenous WASP are significantly increased following a block in the autophagic flux, which suggests that WASP may at the same time be regulator and substrate of the autophagic pathway. Such a dual role has been previously demonstrated for other autophagy players, including p62 (Bjorkoy et al., 2005).

Moreover, we have identified a putative LC3-interacting region (LIR) at the N-terminus of WASP. This short stretch, which has been recognised in other key autophagy players such as p62 (Pankiv et al., 2007), NBR1 (Kirkin et al., 2009) and JMY (Coutts and La Thangue, 2015), mediates their direct interaction with core components of the autophagic machinery. We are currently assessing whether the presence of a putative LIR is reflected in a biochemical interaction between WASP and Atg8.

Lastly, we have recently started to explore the possibility that autophagy could control Rac levels. Our ultimate goal is to understand whether WASP may exploit the autophagic machinery in order to maintain active Rac homeostasis, a novel role that has been discussed in chapter 3 of this dissertation. Evidence so far indicates that GFP-Rac1A and mRFPmars-Atg18 co-localise within small *puncta* and enlarged C-shaped vesicles. These appear to be rare under non-harmful circumstances but becomes more numerous once autophagy has been induced, for instance by mechanical stress.

Despite the need for further clarification, evidence provided here tempt us to speculate, for instance, that WASP may interact with active Rac and target it to nascent autophagosomes in order to maintain its appropriate levels and safeguard cell polarity during migration and cytokinesis.

Chapter 6 , *Final discussion and open questions*

6.1 Results summary

Three main results have been presented in this thesis:
1) WASP safeguards cell polarity during migration and cytokinesis by interacting with Rac and confining its activity.
2) WASP does not require a direct interaction with active Rac to trigger actin polymerisation on clathrin-coated pits.
3) WASP plays a role in autophagy.

These points will be summarised and discussed in this chapter, aiming to emphasise their contribution to a deeper understanding of several, often intertwined, aspects of cell behaviour.

6.2 WASP safeguards cell polarity during migration and cytokinesis by interacting with Rac and confining its activity

6.2.1 WASP-mediated maintenance of cell polarity may be CME-independent

WASP is a nucleation-promoting factor (NPF) mostly known as as key player during clathrin-mediated endocytosis (CME). This function is evolutionarily conserved, as it is maintained in yeasts (Madania et al., 1999), *Dictyostelium* (Davidson, 2014), *Drosophila* (Kochubey et al., 2006) and mammals (Merrifield et al., 2004). Our lab has recently demonstrated that, in addition to a severe block in CME, loss of WASP causes *Dictyostelium* to accumulate active Rac at the trailing edge, resulting in impaired front–rear polarity (Davidson, 2014). Here we aimed to characterise the molecular mechanisms underlying WASP-mediated control of Rac activity.

Our first goal was to determine whether or not the role of WASP in maintenance of cell polarity coincides with its role in CME. In other words, we sought to clarify whether the aberrant accumulation of active Rac was caused by the inability of clathrin-coated pits (CCPs) to be internalised in the absence of WASP. We reasoned that in a scenario whereby Rac or its activators (i.e. GEFs) are recycled within CCPs, loss of WASP and subsequent block in CME may account for the accumulation of active Rac at the trailing edge.

However, early data from our lab discouraged the hypothesis that Rac GEFs are CME cargo. Indeed, it was shown that gxcJJ, the only *Dictyostelium* Rac GEF consistently detected on ventral *puncta* (Douwe Veltman, unpublished data) does not co-localise with clathrin (Andrew J. Davidson, Peter A. Thomason, unpublished data). We report here that Rac itself is not enriched on clathrin *puncta*, which suggests that the GTPase (like its GEFs) may not be recycled via CME.

The fact that neither Rac nor its activators are detected within CCPs can be interpreted as meaning that WASP contributes to the spatial confinement of active Rac via a CME-unrelated mechanism. However, we strongly believe that a crucial experiment to clarify whether the endocytic apparatus has a role in Rac activation and localisation is to assess the ability of cells lacking clathrin to spatially confine active Rac. Clathrin light chain and clathrin heavy chain are both dispensable for *Dictyostelium* viability, as demonstrated by the fact that the two encoding genes (*clc* and *chc* respectively) have been succesfully deleted

(Niswonger and O'Halloran, 1997; Wang et al., 2003). Although viable, cells lacking clathrin (especially those not expressing heavy chain subunits) are poorly suitable for manipulation. Despite repeated attempts to transfect them, we have not yet succeeded in assessing their ability to spatially confine active Rac. We are currently considering generating an inducible *chc* knockout strain in order to switch off the expression of clathrin only when needed.

It is important to mention that the role of CME in Rac activation and spatial confinement has been previously explored in other systems (Palamidessi et al., 2008), although the evidence provided is not conclusive. Regarding the role of the endocytic machinery on Rac activation, Palamidessi and colleagues provided biochemical evidence that cells lacking clathrin heavy chain (CHC) failed to produce detectable levels of GTP-bound Rac. Confusingly, however, it was also shown that an acute approach to block CME (keeping the cells at 16° C) did not affect cells' ability to activate Rac. As for the role of the endocytic machinery on spatial confinement of active Rac, this work showed that photoactivatable Rac can translocate from endosomes to the plasma membrane, and postulates that endosomes bearing active Rac may be rerouted to sites of protrusions. However, the ability of cells lacking clathrin to confne active Rac at the migratory front was not assessed.

Therefore, whether CME contributes to Rac activation and/or to spatial confinement is still an open question.

6.2.2 WASP requires a direct interaction with active Rac to maintain cell polarity

In the attempt to uncover the molecular requirements for WASP to maintain cell polarity, we asked whether the NPF (Nucleation Promoting Factor) requires a direct interaction with active Rac to spatially confine it.

Dictyostelium WASP harbours a CRIB (Cdc42 and Rac interacting/binding) (Burbelo et al., 1995) motif, likewise its human orthologue N-WASP (Miki et al., 1996). Proteins containing this conserved stretch are widely expressed throughout evolution (Pirone et al., 2001) and, despite being often functionally unrelated, share a common feature: all are believed to be downstream effectors of Rac and/or Cdc42. Accordingly, the role of Rho GTPases on WASP activation has been extensively investigated, and a CRIB-mediated interaction is thought to be required for active Rac to regulate both *Dictyostelium* WASP and human N-

WASP (Han et al., 2006; Tomasevic et al., 2007). The possibility that a CRIB-mediated interaction is required for WASP to regulate Rac, instead, has never been explored.

To test this hypothesis we genetically manipulated the CRIB motif of WASP by deleting 14 core amino acids (Burbelo et al., 1995) or mutating two conserved residues. Both mutations render WASP unable to interact with active Rac. Cells expressing a CRIB-mutated WASP fail to exclude active Rac from the trailing edge during migration and from the cleavage furrow during cytokinesis.

On one hand, this result suggests that WASP-mediated maintenance of cell polarity requires a direct interaction with active Rac. On the other hand, it points out that the CRIB motif may not simply act as a recognition tag for upstream regulators.

6.2.3 WASP may contribute to maintain homeostatic levels of active Rac

The presence of active Rac both at the front and the rear of cells expressing WASP CRIB mutants led us to ask whether a functional CRIB motif is required for WASP to maintain homeostatic levels of active Rac, not just to spatially restrict it.

Due to the lack of a reliable anti-Rac antibody, we have not yet been able to compare the amount of active Rac in cells lacking a functional WASP CRIB motif and in wild type cells. However, we have utilised a microscopy-based approach to gather insights into the effect of a non-functional CRIB motif on the levels of membrane-bound Rac. We have demonstrated that cells expressing WASP CRIB mutants accumulate active Rac marker on a higher proportion of their plasma membrane in comparison to wild type cells. A comparable effect on the percentage of plasma membrane labelled by the active Rac marker can be observed when the expression of dominant active (G12V) Rac is induced in wild type cells. Furthermore, cells expressing WASP CRIB mutants tend to be rounder than wild type cells, a feature that has been previously linked to increased levels of active Rac (Ridley et al., 1992). Although indirect, this evidence suggests that lack of a functional WASP CRIB motif may interfere with active Rac homeostasis.

Of interest, despite not necessarily related, it has been recently shown that deletion of hematopoietic WASP in murine dendritic cells leads to increased

levels of active Rac2, and it has been proposed that high levels of active Rac2 may be responsible for the skin conditions developed by Wiskott-Aldrich Syndrome patients (Baptista et al., 2016). The molecular mechanisms by which WASP could control Rac2 activity under normal circumstances, however, were not clarified.

6.3 WASP does not require a direct interaction with active Rac to trigger actin polymerisation on clathrin-coated pits

6.3.1 What determines WASP's subcellular localisation and activity?

Active WASP is able to stimulate the formation of actin filaments; inactive WASP is not. Early evidence demonstrated that WASP is by default inactive, folded in an auto-inhibited conformation that masks its actin-polymerising domain (Rohatgi et al., 1999). Upon activation, WASP acquires the ability to localise at discrete cellular structures or areas, where it triggers actin polymerisation. For instance, WASP stimulates brief burst of F-actin on CCPs, and also the formation of actin filaments at the leading edge, although this tends to occur only in the absence of SCAR/WAVE (Veltman et al., 2012). What targets WASP to CCPs or to the front of migrating cells is surprisingly unclear, nor is it understood which of its domains is primarily involved. In light of the fact that WASP triggers actin polymerisation only when discretely localised, it seems likely that the signals that activate WASP are also responsible for its localisation. What activates WASP in living cells, however, is itself an unsolved conundrum, as will be discussed in more detail in the next section.

An interesting hint on what may determine WASP's subcellular localisation comes from an evolutionary point of view. Yeast Las17, *Dictyostelium* WASP, *Drosophila* Wsp and mammalian N-WASP trigger actin polymerisation on CCPs in a remarkably similar manner, despite being separated by a billion years of evolution (Davidson, 2014; Kochubey et al., 2006; Madania et al., 1999; Merrifield et al., 2004). It seems therefore reasonable to hypothesise that the domain(s) responsible for targeting WASP to clathrin *puncta* is/are present in all four proteins. Figure 6.1 reports the domain composition of WASP proteins that have so far been shown to localise on clathrin-coated pits. The only two regions that are shared by all WASP orthologues are the VCA domain and the polyproline stretch. Basic region and CRIB motif have been lost in yeasts' Las17, the WH1 domain is not present in *Dictyostelium* WASP B. As mentioned in section 1.3.2, WASP B is an unconventional and poorly expressed isoform (data from http://dictyexpress.biolab.si/) that can localise on CCPs (Veltman and Insall, 2010); however, a more recent study has raised the possibility that WASP isoforms devoid of a WH1 domain may in truth form a separate group of WASP-

related proteins, which has been termed WAWH (WASP without WH1 domain) (Kollmar et al., 2012).

By comparing the domain composition of different WASP orthologues (including the debated WASP B) it can therefore be hypothesised that molecules interacting with the Proline-rich domain (i.e. SH3 domain-containing proteins) or with the C-terminal VCA domain (i.e. actin) may be essential for WASP to be recruited on clathrin-coated pits and trigger their internalisation. While a role for SH3 domain-containing proteins in WASP activation has been proposed (Carlier et al., 2000; Miki et al., 1996; Okrut et al., 2015; Rohatgi et al., 2001; Tomasevic et al., 2007), the hypothesis that actin may regulate WASP has never been explored.

6.3.2 WASP does not require a direct interaction with active Rac to be activated on clathrin-coated pits

As mentioned in the previous section, what determines WASP's activation and subcellular localisation is unclear. Several studies have shown that release of WASP autoinhibition requires the joint effort of different activators, including Rho GTPases (Cdc42 or Rac), phospholipids and SH3 domain-containing proteins (Han et al., 2006; Miki et al., 1998a; Papayannopoulos et al., 2005; Rohatgi et al., 1999; Tomasevic et al., 2007). To these pioneering works goes the credit of having highlighted the complexity of WASP regulation. Nevertheless, it is important to acknowledge that they mostly utilised *in vitro* approaches, and that some of the evidence provided have not been entirely confirmed by functional studies in living cells.

The importance of Rho GTPases for WASP activation and localisation is particularly controversial. For instance, in sharp disagreement with the aforementioned *in vitro* data, it has been shown that a mutated CRIB motif does not affect the ability of murine N-WASP to localise on tails that propel vescicles throughout the cytosol (Benesch et al., 2002). Similarly, a CRIB-mutated Wsp is able to rescue the Wsp null phenotype in *Drosophila* (Tal et al., 2002). Furthermore, we have reported here that treating cells with a potent Rac inhibitor or mutating the CRIB motif of WASP do not affect the ability of the NPF to localise on clathrin-coated pits in *Dictyostelium*. We have also shown that once recruited on CCPs the CRIB-mutated WASP is able to trigger actin

polymerisation, meaning that a direct interaction with active Rac is also not required for WASP to activate its downstream effectors.

However, we have shown that some of the CCPs that recruit a CRIB-mutated WASP remain trapped on the basal membrane despite Arp2/3 complex activation. Given that actin polymerisation occurs as expected on these CCPs, we reason that their defective uptake is not simply caused by a dysfunctional endocytic machinery. Instead, we speculate that impaired endocytosis under these circumstances is a secondary effect of increased levels of active Rac, in agreement with what previously observed (Lamaze et al., 1996). We propose that cells expressing WASP CRIB mutants have higher levels of active Rac in comparison to wild type cells, and that this leads to increase membrane tension, ultimately affecting the ability of the cells to deform their plasma membrane in order to allow internalisation of CCPs (Aghamohammadzadeh and Ayscough, 2009; Boulant et al., 2011; Diz-Munoz et al., 2013). To test our hypothesis, we intend to assess the ability of longer-lived CCPs to be effectively internalised when cells expressing a CRIB-mutated WASP are kept under conditions that reduce plasma membrane tension. For instance, we are planning to treat cells with a low dose of a Rac inhibitor and/or to modify the tonicity of the medium.

6.3.4 WASP requires a direct interaction with active Rac to be activated at the leading edge in the absence of SCAR/WAVE

Previous work from our lab demonstrated that, in addition to its role in CME, WASP is able to trigger actin polymerisation at the leading edge of migrating cells to compensate for the loss of SCAR/WAVE (Veltman et al., 2012). The versatility of WASP is fascinating and not completely understood. For instance, one interesting and still unanswered question is: does WASP respond to distinct upstream regulators when localising at clathrin-coated pits or at the leading edge?

In light of the fact that active Rac directly regulates SCAR/WAVE (Lebensohn and Kirschner, 2009) and localises at the front of migrating wild type cells cells, it was proposed that active Rac may mediate the recruitment of WASP at the leading edge in the absence of SCAR/WAVE (Veltman et al., 2012). Evidence described in this thesis, however, demonstrates that active Rac is not required for WASP to localise to and trigger actin polymerisation on clathrin-coated pits.

We therefore sought to understand whether a direct interaction with active Rac was similarly not required for WASP to trigger the formation of actin filaments at the migratory front.

Taking advantage of a SCAR/WAVE and WASP inducible double knockout strain (Davidson, 2014), we made two major observations. First, we showed that WASP CRIB mutants are able to occasionally localise (at least partially) at the leading edge in the presence of SCAR/WAVE. This suggests that signals other than Rac are responsible for WASP recruitment at the migratory front. Second, we demonstrated that WASP CRIB mutants are unable to drive the extension of pseudopodia when the expression of SCAR/WAVE is suppressed. This suggests that when the interaction with active Rac is prevented, WASP cannot initiate actin polymerisation to extend a pseudopod.

In summary, our data demonstrate that WASP is able to respond to different upstream signals in order to fulfil different roles: it does not require a direct interaction with active Rac to trigger actin polymerisation on clathrin-coated pits, but does require it to stimulate the formation of branched actin filaments at the leading edge.

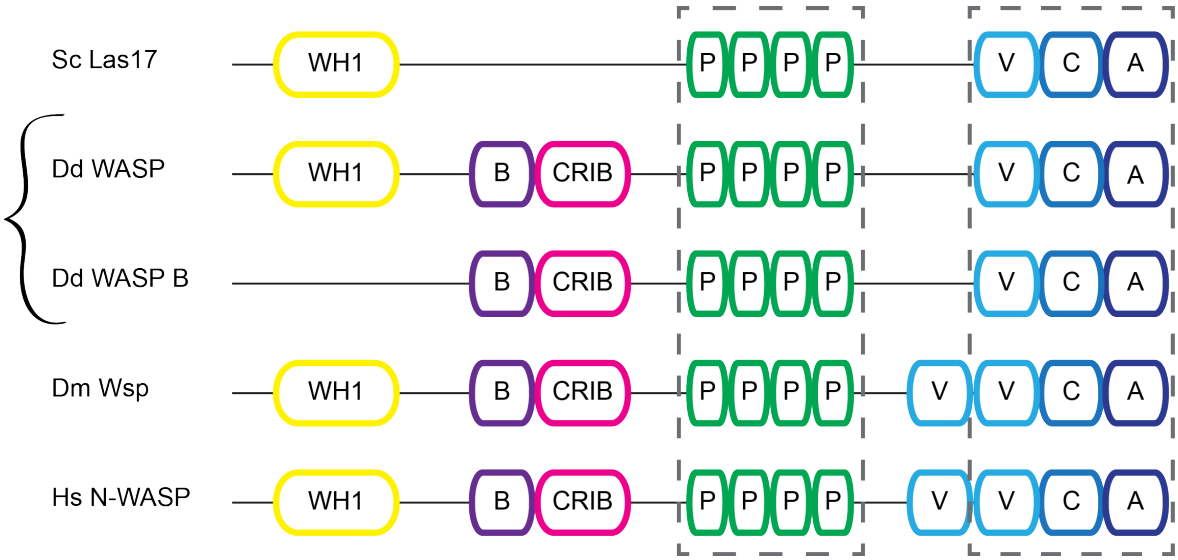

Figure 6.1 Domain composition of the WASP protein across evolution

Analysis of the domain composition (not to scale) of WASP orthologues that are able to localise on clathrin-coated pits revealed that only two regions have been kept unchanged throughout evolution: the polyproline stretch and the VCA domain, both highlighted by a dashed grey rectangle. Yeasts (Sc) Las17 lacks basic region (B) and CRIB motif. *Dictyostelium* (Dd) WASP B lacks the WH1 domain. Human (Hs) N-WASP, *Drosophila* (Dm) Wsp and *Dictyostelium* (Dd) WASP all harbour a WH1 domain, a basic region, a CRIB motif, a polyproline stretch and a VCA domain. Dm Wsp and Hs N-WASP harbour an additional V domain, which results from duplication of the ancestral V domain (Veltman and Insall, 2010)

6.4 WASP plays a role in autophagy

6.4.1 WASP is required for *Dictyostelium* to overcome the lack of essential amino acids

Our lab has recently observed that WASP knockout cells struggle to proliferate in minimal medium, and fail to aggregate into a fruiting body upon nutrient deprivation (Davidson, 2014). This observation is curious. Why would loss of WASP affect the capability of *Dictyostelium* to handle less permissive conditions? We asked whether this phenotype could be linked to the inability of WASP knockout cells to perform CME. Evidence in the literature, however, appears to discourage this hypothesis: both clathrin heavy and light chains mutants are indeed able to generate fruiting bodies, although the later stages of the process are delayed (Niswonger and O'Halloran, 1997; Wang et al., 2003). It is therefore plausible that WASP supports *Dictyostelium* growth in suboptimal conditions via a CME-unrelated mechanism. Here we have shown that WASP is required for *Dictyostelium* to survive in the absence of two essential amino acids. Since survival in amino acid-depleted conditions relies on autophagy (Onodera and Ohsumi, 2005), and *Dictyostelium* strains lacking some components of the autophagic flux show aberrant development (Otto et al., 2004), we hypothesised that WASP may be involved in autophagy. Here we have described multiple observations in support of this conjecture, although a deeper understanding of WASP's role in autophagy will require further experiments.

6.4.2 WASP on autophagosomes: why have we never observed it before?

In the attempt to clarify the role of WASP within autophagic flux we have explored its subcellular localisation under conditions that stimulate autophagy. We have shown here that upon mechanical stress WASP can be detected within large multilobate structures that are also labelled by Atg18, an early autophagosomal marker (orthologue of mammalian WIPI). It is not yet clear what these structures are and what their function is, but the presence of a protein that contributes to the early steps of autophagy tempts us to speculate that they may contribute to the genesis of autophagosomes, for instance by acting as a source of membranous segments.

Having observed WASP on such a distinct cellular feature encourages us to pursue the characterisation of its role in autophagy, but at the same time imposes a reflection: why have these large multilobate vesicles never been observed before? We believe that one of the underlying reasons is that our knowledge about WASP dynamics is mostly focussed on the TIRF field. On one hand, concentrating our analysis on the first ≈100 nm at the bottom of the cell has yelded conspicuous insights on WASP function during clathrin-mediated endocytosis. On the other hand, however, it has limited our familiarity with WASP dynamics elsewhere in the cell. Furthermore, the highly cytosolic distribution of WASP, especially of its GFP fusion, has hampered the identification of unknown features, which may become apparent only in the presence of other markers as reference.

6.4.3 WASP harbours a putative LIR: could it be an adaptor protein?

We have pointed out here that WASP harbours a putative LIR (LC3 internacting region), which mediates the interaction with core components of the autophagy machinery. Several proteins harbouring a LIR have been described to date, including human p62, NBR1 and JMY (Coutts and La Thangue, 2015; Kirkin et al., 2009; Pankiv et al., 2007). To the best of our knowledge, WASP is the first protein harbouring a putative LIR to be identified in *Dictyostelium*. Whether or not WASP interacts with Atg8 (LC3 orthologue in *Dictyostelium*), and whether their interaction is mediated by the putative LIR motif of WASP is currently under investigation. If confirmed, the interaction between WASP and Atg8 would provide useful insights into the role of the NPF during autophagy. Particularly intriguing is the possibility that WASP may be linked to selective autophagy, an emerging type of autophagy whereby molecular adaptors act as a bridge bringing cargo proteins in close proximity of key components of the autophagic machinery. This is, for instance, the case of p62, which interacts with ubiquitinated proteins and facilitates their engulfment within autophagosomes (Pankiv et al., 2007). Interestingly, it has been shown that Las17 (WASP orthologue in yeasts) plays a role in Cytoplasm-to-Vacuole Targeting (Cvt) pathway, an example of selective autophagy in yeasts, and that this requires a functional C-terminal domain (Monastyrska et al., 2008).

6.4.4 Does WASP control Rac by targeting it to autophagosomes?

The involvement of WASP in autophagy is an interesting discovery *per se*. However, it could also provide a potential mechanism to explain why cells lacking WASP or expressing a CRIB-mutated WASP fail to restrict Rac activity. Here we have reported preliminary evidence suggesting that Rac can be detected on autophagosomes both prior to and upon induction of mechanical stress, suggesting that autophagy may regulate Rac even under normal circumstances. The importance of the autophagic machinery for cells to maintain Rho GTPase homeostasis has been previously reported (Belaid et al., 2013). In this work it was shown that the adaptor protein p62 facilitates the sequestration of active RhoA within autophagosomes, ultimately ensuring completion of cytokinesis. It is therefore tempting to speculate that WASP may facilitate the incorporation of active Rac within autophagosomes by utilisig its CRIB motif and putative LIR. However, whether or not WASP is responsible for targeting Rac to autophagosomes, and which mechanisms are involved, remains to be addressed.

6.5 Our Working Model

Evidence presented in this thesis, in addition to previous work (Davidson, 2014; Lamaze et al., 1996; Lebensohn and Kirschner, 2009; Veltman et al., 2012), leads us to propose the following model.

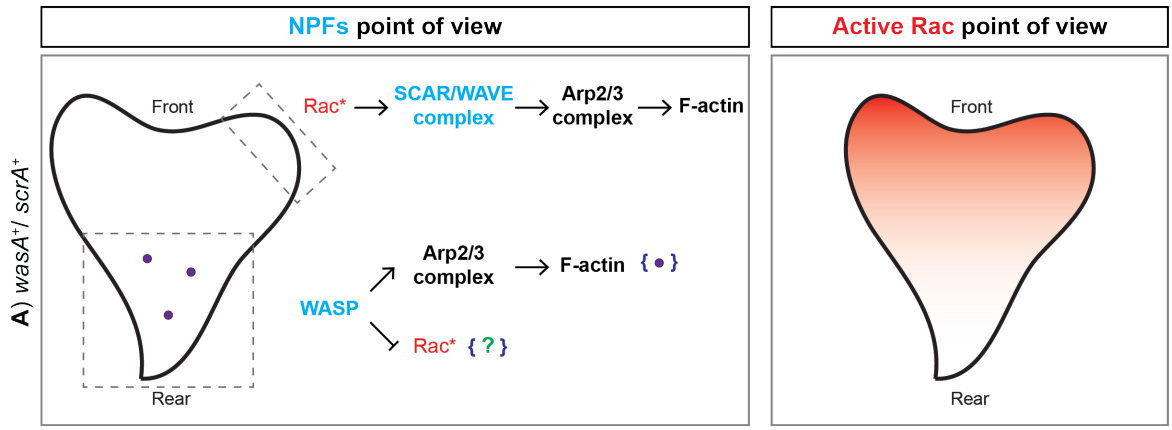

Figure 6.2 Working Model (A)

A) In the presence of both WASP (encoded by *wasA*) and SCAR/WAVE (encoded by *scrA*), *Dictyostelium* has a defined front and rear. At the leading edge SCAR/WAVE stimulates the formation of branched actin filaments within pseudopodia, driving the cell forward. SCAR/WAVE activation is dependent on active Rac (Rac*) and other signals (Lebensohn and Kirschner, 2009). At the rear WASP stimulates actin polymerisation on clathrin-coated pits (CCPs, purple dots) to drive their internalisation (Davidson, 2014). Evidence presented in this thesis suggest this to be Rac*-independent. Data reported in this thesis also suggest that WASP interacts directly with Rac* and restricts its activity. The underlying mechanisms are yet to be clarified (green question mark).

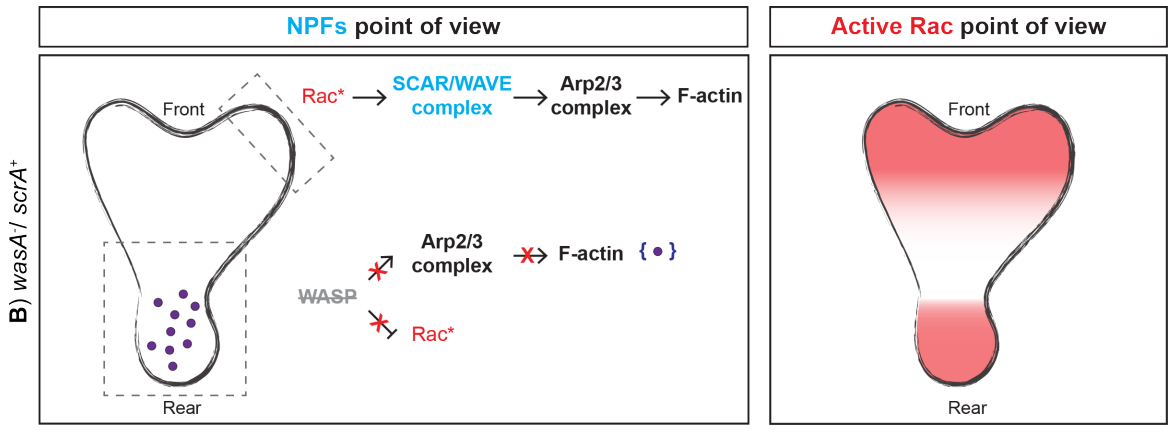

Figure 6.2 Working Model (B)

B) In the absence of WASP (*wasA*-) the front-rear polarity of migrating *Dictyostelium* is compromised (Davidson, 2014). The localisation of SCAR/WAVE at the leading edge is not affected (Davidson, 2014), meaning that cells can still generate pseudopodia and move forward. At the rear, loss of WASP causes CCPs (purple dots) to remain uninternalised due to the lack of Arp2/3 complex recruitment (Davidson, 2014) and leads to aberrant accumulation of active Rac (Davidson, 2014). Evidence presented in this thesis suggests that the two effects may not be linked, and demonstrates that WASP requires a functional CRIB motif to confine Rac activity.

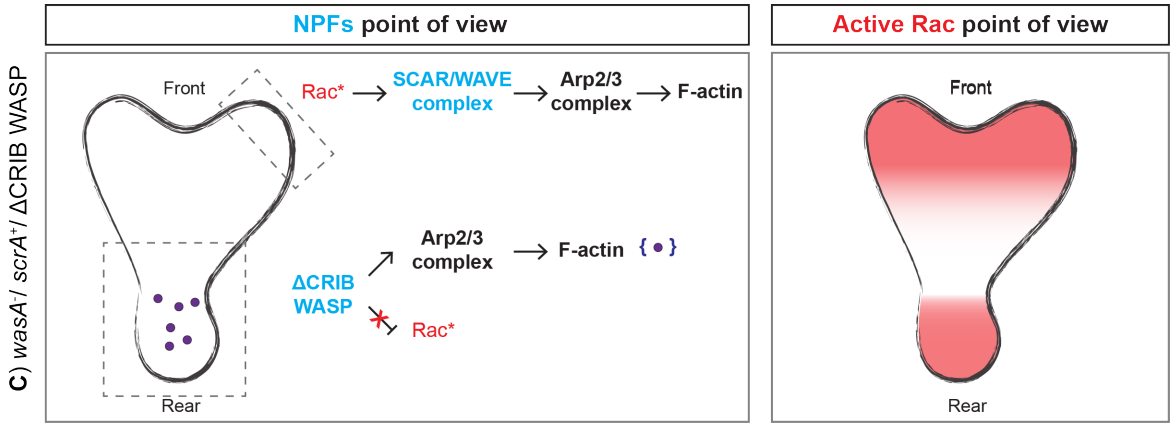

Figure 6.2 Working Model (C)

C) In the presence of SCAR/WAVE and WASP CRIB mutants (i.e., ΔCRIB WASP), and in the absence of WASP (*wasA*-), the front-rear polarity of *Dictyostelium* is still compromised. At the rear, WASP is able to trigger actin polymerisation on CCPs (purple dots) but not to restrict Rac activity. The extended lifetime of some CCPs recruiting WASP CRIB mutants may result from the presence of aberrant active Rac, which has been shown to inhibit CME (Lamaze et al., 1996).

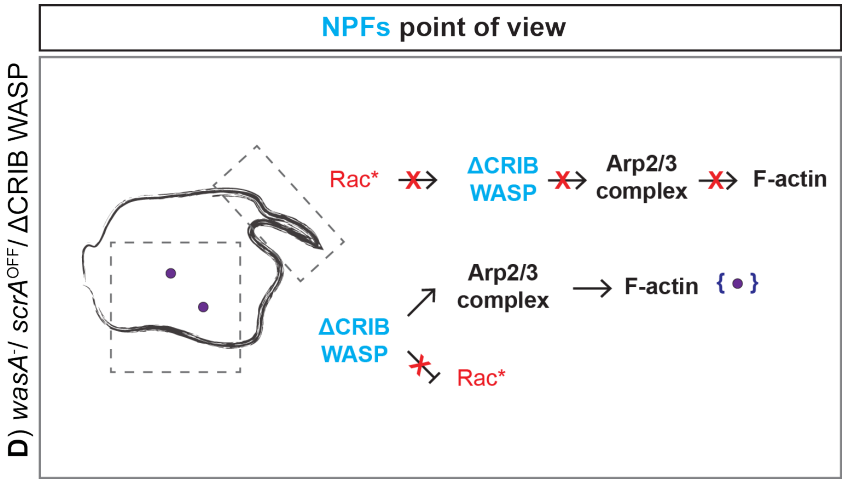

Figure 6.2 Working Model (D)

D) In the absence of both SCAR/WAVE (*scrA*^{OFF}) and WASP (*wasA*-), and in the presence of WASP CRIB mutants (i.e., ΔCRIB WASP) cells fail to extend a leading edge. WASP CRIB mutants can still localise on ventral *puncta* (purple dots), but cannot initiate actin polymerisation to extend pseudopodia. Since full length WASP is able to trigger actin polymerisation at the leading edge in the absence of SCAR/WAVE (Veltman et al., 2012), we conclude that WASP requires a direct interaction with active Rac to activate the Arp2/3 complex at sites of protrusions.

6.6 Concluding remarks

Here the role of WASP in maintenance of cell polarity and autophagy was explored, and the importance of Rho GTPases on WASP activation investigated.

We have provided a set of evidence suggesting that WASP contributes to the spatial confinement of active Rac during directed migration and cytokinesis, and hinted at the possibility that WASP's role in maintenance of cell polarity may be distinct from its role in clathrin-mediated endocytosis. Data described in this thesis demonstrate that spatial restriction of Rac activity requires a direct interaction between WASP and the GTPase, which occurs via the NPF's CRIB motif. Furthermore, our results encourage a model whereby WASP does not simply control spatial distribution of active Rac, but also its overall cellular levels. The mechanism(s) underpinning WASP-mediated maintenance of cell polarity are yet to be clarified.

We have also started to uncover the molecular details of WASP's involvement in autophagy. We have demonstrated that WASP is required for cells to survive amino acid deprivation, and that upon autophagy induction WASP localises on large multilobate vesicles alongside components of the autophagic flux. We have also reported that WASP harbours a putative LIR motif, a conserved stretch shared by proteins involved in selective autophagy, raising the possibility that WASP could act as an adaptor protein and facilitate the incorporation of cargo molecules within autophagosomes.

As for its regulation, we have shown here that WASP is able to respond to different upstream regulators: it does not require a direct interaction with active Rac to be activated on clathrin-coated pits, but does require it to trigger actin polymerisation at the leading edge in the absence of SCAR/WAVE. This result emphasises the complexity of WASP regulation in living cells and underscores the incompleteness of our knowledge, currently based on early *in vitro* works that may not reflect the apparent versatility of WASP in living cells.

Different questions are still unanswered. Some of them arise from findings described throughout this thesis; others have been waiting for an answer for a longer time. We believe that clarifying the mechanism by which WASP restricts active Rac and/or controls its levels deserves immediate attention. Efforts will be made to determine whether this is a novel function of WASP, or is instead linked to its role in clathrin-mediated endocytosis. Also, dissecting the role of WASP in autophagy will provide incredibly helpful insights to better understand

the role of the actin cytoskeleton is this evolutionarily conserved pathway. Lastly, we strongly feel that fundamental features of WASP dynamics, such as what determines its localisation and activation in living cells, should be soon unveiled.

Bibliography

Abdul-Manan, N., B. Aghazadeh, G.A. Liu, A. Majumdar, O. Ouerfelli, K.A. Siminovitch, and M.K. Rosen. 1999. Structure of Cdc42 in complex with the GTPase-binding domain of the 'Wiskott-Aldrich syndrome' protein. *Nature*. 399:379-383.

Abercrombie, M., J.E. Heaysman, and S.M. Pegrum. 1971. The locomotion of fibroblasts in culture. IV. Electron microscopy of the leading lamella. *Exp Cell Res*. 67:359-367.

Adams, A.E., D.I. Johnson, R.M. Longnecker, B.F. Sloat, and J.R. Pringle. 1990. CDC42 and CDC43, two additional genes involved in budding and the establishment of cell polarity in the yeast Saccharomyces cerevisiae. *J Cell Biol*. 111:131-142.

Aghamohammadzadeh, S., and K.R. Ayscough. 2009. Differential requirements for actin during yeast and mammalian endocytosis. *Nat Cell Biol*. 11:1039-1042.

Aguilera, M.O., W. Beron, and M.I. Colombo. 2012. The actin cytoskeleton participates in the early events of autophagosome formation upon starvation induced autophagy. *Autophagy*. 8:1590-1603.

Axe, E.L., S.A. Walker, M. Manifava, P. Chandra, H.L. Roderick, A. Habermann, G. Griffiths, and N.T. Ktistakis. 2008. Autophagosome formation from membrane compartments enriched in phosphatidylinositol 3-phosphate and dynamically connected to the endoplasmic reticulum. *J Cell Biol*. 182:685-701.

Baarlink, C., H. Wang, and R. Grosse. 2013. Nuclear actin network assembly by formins regulates the SRF coactivator MAL. *Science*. 340:864-867.

Baptista, M.A., M. Keszei, M. Oliveira, K.K. Sunahara, J. Andersson, C.I. Dahlberg, A.J. Worth, A. Lieden, I.C. Kuo, R.P. Wallin, S.B. Snapper, L. Eidsmo, A. Scheynius, M.C. Karlsson, G. Bouma, S.O. Burns, M.N. Forsell, A.J. Thrasher, S. Nylen, and L.S. Westerberg. 2016. Deletion of Wiskott-Aldrich syndrome protein triggers Rac2 activity and increased cross-presentation by dendritic cells. *Nat Commun*. 7:12175.

Bastos, R.N., X. Penate, M. Bates, D. Hammond, and F.A. Barr. 2012. CYK4 inhibits Rac1-dependent PAK1 and ARHGEF7 effector pathways during cytokinesis. *J Cell Biol*. 198:865-880.

Bear, J.E., J.F. Rawls, and C.L. Saxe, 3rd. 1998. SCAR, a WASP-related protein, isolated as a suppressor of receptor defects in late Dictyostelium development. *J Cell Biol*. 142:1325-1335.

Begg, D.A., R. Rodewald, and L.I. Rebhun. 1978. The visualization of actin filament polarity in thin sections. Evidence for the uniform polarity of membrane-associated filaments. *J Cell Biol*. 79:846-852.

Belaid, A., M. Cerezo, A. Chargui, E. Corcelle-Termeau, F. Pedeutour, S. Giuliano, M. Ilie, I. Rubera, M. Tauc, S. Barale, C. Bertolotto, P. Brest, V. Vouret-Craviari, D.J. Klionsky, G.F. Carle, P. Hofman, and B. Mograbi. 2013. Autophagy plays a critical role in the degradation of active RHOA, the control of cell cytokinesis, and genomic stability. *Cancer Res*. 73:4311-4322.

Beltzner, C.C., and T.D. Pollard. 2004. Identification of functionally important residues of Arp2/3 complex by analysis of homology models from diverse species. *J Mol Biol*. 336:551-565.

Benesch, S., S. Lommel, A. Steffen, T.E. Stradal, N. Scaplehorn, M. Way, J. Wehland, and K. Rottner. 2002. Phosphatidylinositol 4,5-biphosphate (PIP2)-induced vesicle movement depends on N-WASP and involves Nck, WIP, and Grb2. *J Biol Chem*. 277:37771-37776.

Benesch, S., S. Polo, F.P. Lai, K.I. Anderson, T.E. Stradal, J. Wehland, and K. Rottner. 2005. N-WASP deficiency impairs EGF internalization and actin assembly at clathrin-coated pits. *J Cell Sci*. 118:3103-3115.

Bjorkoy, G., T. Lamark, A. Brech, H. Outzen, M. Perander, A. Overvatn, H. Stenmark, and T. Johansen. 2005. p62/SQSTM1 forms protein aggregates degraded by autophagy and has a protective effect on huntingtin-induced cell death. *J Cell Biol*. 171:603-614.

Bloomfield, G., D. Traynor, S.P. Sander, D.M. Veltman, J.A. Pachebat, and R.R. Kay. 2015. Neurofibromin controls macropinocytosis and phagocytosis in Dictyostelium. *Elife*. 4.

Bonner, J.T., D.S. Barkley, E.M. Hall, T.M. Konijn, J.W. Mason, G. O'Keefe, 3rd, and P.B. Wolfe. 1969. Acrasin, Acrasinase, and the sensitivity to acrasin in Dictyostelium discoideum. *Dev Biol*. 20:72-87.

Bork, P., C. Sander, and A. Valencia. 1992. An ATPase domain common to prokaryotic cell cycle proteins, sugar kinases, actin, and hsp70 heat shock proteins. *Proc Natl Acad Sci U S A*. 89:7290-7294.

Boulant, S., C. Kural, J.C. Zeeh, F. Ubelmann, and T. Kirchhausen. 2011. Actin dynamics counteract membrane tension during clathrin-mediated endocytosis. *Nat Cell Biol*. 13:1124-1131.

Boureux, A., E. Vignal, S. Faure, and P. Fort. 2007. Evolution of the Rho family of ras-like GTPases in eukaryotes. *Mol Biol Evol*. 24:203-216.

Brady, R.J., C.K. Damer, J.E. Heuser, and T.J. O'Halloran. 2010. Regulation of Hip1r by epsin controls the temporal and spatial coupling of actin filaments to clathrin-coated pits. *J Cell Sci*. 123:3652-3661.

Brefeld, J.O. 1869. Dictyostelium mucoroides, ein neuer Organismus aus der Verwandtschaft der Myxomyceten. *Abhandlungen der Senckenbergischen Naturforschenden Gesellschaft*. 7:85-107.

Brock, D.A., T.E. Douglas, D.C. Queller, and J.E. Strassmann. 2011. Primitive agriculture in a social amoeba. *Nature*. 469:393-396.

Burbelo, P.D., D. Drechsel, and A. Hall. 1995. A conserved binding motif defines numerous candidate target proteins for both Cdc42 and Rac GTPases. *J Biol Chem*. 270:29071-29074.

Calvo-Garrido, J., S. Carilla-Latorre, A. Mesquita, and R. Escalante. 2011. A proteolytic cleavage assay to monitor autophagy in Dictyostelium discoideum. *Autophagy*. 7:1063-1068.

Campellone, K.G., N.J. Webb, E.A. Znameroski, and M.D. Welch. 2008. WHAMM is an Arp2/3 complex activator that binds microtubules and functions in ER to Golgi transport. *Cell*. 134:148-161.

Canman, J.C., L. Lewellyn, K. Laband, S.J. Smerdon, A. Desai, B. Bowerman, and K. Oegema. 2008. Inhibition of Rac by the GAP activity of centralspindlin is essential for cytokinesis. *Science*. 322:1543-1546.

Cao, L.G., D.J. Fishkind, and Y.L. Wang. 1993. Localization and dynamics of nonfilamentous actin in cultured cells. *J Cell Biol*. 123:173-181.

Carlier, M.F., P. Nioche, I. Broutin-L'Hermite, R. Boujemaa, C. Le Clainche, C. Egile, C. Garbay, A. Ducruix, P. Sansonetti, and D. Pantaloni. 2000. GRB2 links signaling to actin assembly by enhancing interaction of neural Wiskott-Aldrich syndrome protein (N-WASp) with actin-related protein (ARP2/3) complex. *J Biol Chem*. 275:21946-21952.

Carlier, M.F., D. Pantaloni, J.A. Evans, P.K. Lambooy, E.D. Korn, and M.R. Webb. 1988. The hydrolysis of ATP that accompanies actin polymerization is essentially irreversible. *FEBS Lett*. 235:211-214.

Carnell, M., T. Zech, S.D. Calaminus, S. Ura, M. Hagedorn, S.A. Johnston, R.C. May, T. Soldati, L.M. Machesky, and R.H. Insall. 2011. Actin polymerization driven by WASH causes V-ATPase retrieval and vesicle neutralization before exocytosis. *J Cell Biol*. 193:831-839.

Castillo-Lluva, S., M.H. Tatham, R.C. Jones, E.G. Jaffray, R.D. Edmondson, R.T. Hay, and A. Malliri. 2010. SUMOylation of the GTPase Rac1 is required for optimal cell migration. *Nat Cell Biol*. 12:1078-1085.

Castrillon, D.H., and S.A. Wasserman. 1994. Diaphanous is required for cytokinesis in Drosophila and shares domains of similarity with the products of the limb deformity gene. *Development*. 120:3367-3377.

Chan, A.Y., S.J. Coniglio, Y.Y. Chuang, D. Michaelson, U.G. Knaus, M.R. Philips, and M. Symons. 2005. Roles of the Rac1 and Rac3 GTPases in human tumor cell invasion. *Oncogene*. 24:7821-7829.

Chang, F., C. Lemmon, D. Lietha, M. Eck, and L. Romer. 2011. Tyrosine phosphorylation of Rac1: a role in regulation of cell spreading. *PLoS One*. 6:e28587.

Chen, W.T. 1989. Proteolytic activity of specialized surface protrusions formed at rosette contact sites of transformed cells. *J Exp Zool*. 251:167-185.

Chen, Z., D. Borek, S.B. Padrick, T.S. Gomez, Z. Metlagel, A.M. Ismail, J. Umetani, D.D. Billadeau, Z. Otwinowski, and M.K. Rosen. 2010. Structure and control of the actin regulatory WAVE complex. *Nature*. 468:533-538.

Commisso, C., S.M. Davidson, R.G. Soydaner-Azeloglu, S.J. Parker, J.J. Kamphorst, S. Hackett, E. Grabocka, M. Nofal, J.A. Drebin, C.B. Thompson, J.D. Rabinowitz, C.M. Metallo, M.G. Vander Heiden, and D. Bar-Sagi. 2013. Macropinocytosis of protein is an amino acid supply route in Ras-transformed cells. *Nature*. 497:633-637.

Cosson, P., and T. Soldati. 2008. Eat, kill or die: when amoeba meets bacteria. *Curr Opin Microbiol*. 11:271-276.

Cote, J.F., and K. Vuori. 2002. Identification of an evolutionarily conserved superfamily of DOCK180-related proteins with guanine nucleotide exchange activity. *J Cell Sci*. 115:4901-4913.

Coutts, A.S., and N.B. La Thangue. 2015. Actin nucleation by WH2 domains at the autophagosome. *Nat Commun*. 6:7888.

Cox, E.C., C.D. Vocke, S. Walter, K.Y. Gregg, and E.S. Bain. 1990. Electrophoretic karyotype for Dictyostelium discoideum. *Proc Natl Acad Sci U S A*. 87:8247-8251.

D'Avino, P.P., M.S. Savoian, and D.M. Glover. 2004. Mutations in sticky lead to defective organization of the contractile ring during cytokinesis and are enhanced by Rho and suppressed by Rac. *J Cell Biol*. 166:61-71.

Davidson, A.J. 2014. The role of WASP family members in Dictyostelium discoideum cell migration. University of Glasgow.

Davidson, A.J., C. Amato, P.A. Thomason, and R.H. Insall. 2018. WASP family proteins and formins compete in pseudopod- and bleb-based migration. *J Cell Biol*. 217:701-714.

Davidson, A.J., J.S. King, and R.H. Insall. 2013. The use of streptavidin conjugates as immunoblot loading controls and mitochondrial markers for use with Dictyostelium discoideum. *Biotechniques*. 55:39-41.

de la Roche, M., A. Mahasneh, S.F. Lee, F. Rivero, and G.P. Cote. 2005. Cellular distribution and functions of wild-type and constitutively activated Dictyostelium PakB. *Mol Biol Cell*. 16:238-247.

De Lozanne, A., and J.A. Spudich. 1987. Disruption of the Dictyostelium myosin heavy chain gene by homologous recombination. *Science*. 236:1086-1091.

Derivery, E., C. Sousa, J.J. Gautier, B. Lombard, D. Loew, and A. Gautreau. 2009. The Arp2/3 activator WASH controls the fission of endosomes through a large multiprotein complex. *Dev Cell*. 17:712-723.

Derry, J.M., H.D. Ochs, and U. Francke. 1994. Isolation of a novel gene mutated in Wiskott-Aldrich syndrome. *Cell*. 79:following 922.

Didsbury, J., R.F. Weber, G.M. Bokoch, T. Evans, and R. Snyderman. 1989. rac, a novel ras-related family of proteins that are botulinum toxin substrates. *J Biol Chem*. 264:16378-16382.

Diekmann, D., S. Brill, M.D. Garrett, N. Totty, J. Hsuan, C. Monfries, C. Hall, L. Lim, and A. Hall. 1991. Bcr encodes a GTPase-activating protein for p21rac. *Nature*. 351:400-402.

Diz-Munoz, A., D.A. Fletcher, and O.D. Weiner. 2013. Use the force: membrane tension as an organizer of cell shape and motility. *Trends Cell Biol*. 23:47-53.

Doi, M., M. Wachi, F. Ishino, S. Tomioka, M. Ito, Y. Sakagami, A. Suzuki, and M. Matsuhashi. 1988. Determinations of the DNA sequence of the mreB gene and of the gene products of the mre region that function in formation of the rod shape of Escherichia coli cells. *J Bacteriol*. 170:4619-4624.

Dominguez, R. 2004. Actin-binding proteins--a unifying hypothesis. *Trends Biochem Sci*. 29:572-578.

Dumontier, M., P. Hocht, U. Mintert, and J. Faix. 2000. Rac1 GTPases control filopodia formation, cell motility, endocytosis, cytokinesis and development in Dictyostelium. *J Cell Sci*. 113 (Pt 12):2253-2265.

Eden, S., R. Rohatgi, A.V. Podtelejnikov, M. Mann, and M.W. Kirschner. 2002. Mechanism of regulation of WAVE1-induced actin nucleation by Rac1 and Nck. *Nature*. 418:790-793.

Egile, C., I. Rouiller, X.P. Xu, N. Volkmann, R. Li, and D. Hanein. 2005. Mechanism of filament nucleation and branch stability revealed by the structure of the Arp2/3 complex at actin branch junctions. *PLoS Biol*. 3:e383.

Eichinger, L., J.A. Pachebat, G. Glockner, M.A. Rajandream, R. Sucgang, M. Berriman, J. Song, R. Olsen, K. Szafranski, Q. Xu, B. Tunggal, S. Kummerfeld, M. Madera, B.A. Konfortov, F. Rivero, A.T. Bankier, R. Lehmann, N. Hamlin, R. Davies, P. Gaudet, P. Fey, K. Pilcher, G. Chen, D. Saunders, E. Sodergren, P. Davis, A. Kerhornou, X. Nie, N. Hall, C. Anjard, L. Hemphill, N. Bason, P. Farbrother, B. Desany, E. Just, T. Morio, R. Rost, C. Churcher, J. Cooper, S. Haydock, N. van Driessche, A. Cronin, I. Goodhead, D. Muzny, T. Mourier, A. Pain, M. Lu, D. Harper, R. Lindsay, H. Hauser, K. James, M. Quiles, M. Madan Babu, T. Saito, C. Buchrieser, A. Wardroper, M. Felder, M. Thangavelu, D. Johnson, A. Knights, H. Loulseged, K. Mungall, K. Oliver, C. Price, M.A. Quail, H. Urushihara, J. Hernandez, E. Rabbinowitsch, D. Steffen, M. Sanders, J. Ma, Y. Kohara, S. Sharp, M. Simmonds, S. Spiegler, A. Tivey, S. Sugano, B. White, D. Walker, J. Woodward, T. Winckler, Y. Tanaka, G. Shaulsky, M. Schleicher, G. Weinstock, A. Rosenthal, E.C. Cox, R.L. Chisholm, R. Gibbs, W.F. Loomis, M. Platzer, R.R. Kay, J. Williams, P.H. Dear, A.A. Noegel, B. Barrell, and A. Kuspa. 2005. The genome of the social amoeba Dictyostelium discoideum. *Nature*. 435:43-57.

Evans, I.R., P.A. Ghai, V. Urbancic, K.L. Tan, and W. Wood. 2013. SCAR/WAVE-mediated processing of engulfed apoptotic corpses is essential for effective macrophage migration in Drosophila. *Cell Death Differ*. 20:709-720.

Freeman, J.L., A. Abo, and J.D. Lambeth. 1996. Rac "insert region" is a novel effector region that is implicated in the activation of NADPH oxidase, but not PAK65. *J Biol Chem*. 271:19794-19801.

Frieden, C. 1983. Polymerization of actin: mechanism of the Mg2+-induced process at pH 8 and 20 degrees C. *Proc Natl Acad Sci U S A*. 80:6513-6517.

Fujimoto, L.M., R. Roth, J.E. Heuser, and S.L. Schmid. 2000. Actin assembly plays a variable, but not obligatory role in receptor-mediated endocytosis in mammalian cells. *Traffic*. 1:161-171.

Fukui, Y., E. de Hostos, S. Yumura, T. Kitanishi-Yumura, and Inou. 1999. Architectural dynamics of F-actin in eupodia suggests their role in invasive locomotion in Dictyostelium. *Exp Cell Res*. 249:33-45.

Gao, Y., J.B. Dickerson, F. Guo, J. Zheng, and Y. Zheng. 2004. Rational design and characterization of a Rac GTPase-specific small molecule inhibitor. *Proc Natl Acad Sci U S A*. 101:7618-7623.

Goldschmidt-Clermont, P.J., M.I. Furman, D. Wachsstock, D. Safer, V.T. Nachmias, and T.D. Pollard. 1992. The control of actin nucleotide exchange by thymosin beta 4 and profilin. A potential regulatory mechanism for actin polymerization in cells. *Mol Biol Cell*. 3:1015-1024.

Goley, E.D., S.E. Rodenbusch, A.C. Martin, and M.D. Welch. 2004. Critical conformational changes in the Arp2/3 complex are induced by nucleotide and nucleation promoting factor. *Mol Cell*. 16:269-279.

Gomez, T.S., and D.D. Billadeau. 2009. A FAM21-containing WASH complex regulates retromer-dependent sorting. *Dev Cell*. 17:699-711.

Gottlieb, T.A., I.E. Ivanov, M. Adesnik, and D.D. Sabatini. 1993. Actin microfilaments play a critical role in endocytosis at the apical but not the basolateral surface of polarized epithelial cells. *J Cell Biol*. 120:695-710.

Grassart, A., V. Meas-Yedid, A. Dufour, J.C. Olivo-Marin, A. Dautry-Varsat, and N. Sauvonnet. 2010. Pak1 phosphorylation enhances cortactin-N-WASP interaction in clathrin-caveolin-independent endocytosis. *Traffic*. 11:1079-1091.

Gudima, G.O., I.A. Vorobjev, and S. Chentsov Yu. 1988. Centriolar location during blood cell spreading and motion in vitro: an ultrastructural analysis. *J Cell Sci*. 89 (Pt 2):225-241.

Haataja, L., J. Groffen, and N. Heisterkamp. 1997. Characterization of RAC3, a novel member of the Rho family. *J Biol Chem*. 272:20384-20388.

Hacker, U., R. Albrecht, and M. Maniak. 1997. Fluid-phase uptake by macropinocytosis in Dictyostelium. *J Cell Sci*. 110 (Pt 2):105-112.

Hailey, D.W., A.S. Rambold, P. Satpute-Krishnan, K. Mitra, R. Sougrat, P.K. Kim, and J. Lippincott-Schwartz. 2010. Mitochondria supply membranes for autophagosome biogenesis during starvation. *Cell*. 141:656-667.

Han, J.W., L. Leeper, F. Rivero, and C.Y. Chung. 2006. Role of RacC for the regulation of WASP and phosphatidylinositol 3-kinase during chemotaxis of Dictyostelium. *J Biol Chem*. 281:35224-35234.

Han, S.I., K. Friehs, and E. Flaschel. 2004. Improvement of a synthetic medium for Dictyostelium discoideum. *Process Biochemistry*. 39:925–930.

Hanson, J.a.L., J. 1963. The Structure of F-Actin and of Actin Filaments Isolated from Muscle. *J. Mol. Biol.*:46-60.

Hao, Y.H., J.M. Doyle, S. Ramanathan, T.S. Gomez, D. Jia, M. Xu, Z.J. Chen, D.D. Billadeau, M.K. Rosen, and P.R. Potts. 2013. Regulation of WASH-dependent actin polymerization and protein trafficking by ubiquitination. *Cell*. 152:1051-1064.

Hara, T., K. Nakamura, M. Matsui, A. Yamamoto, Y. Nakahara, R. Suzuki-Migishima, M. Yokoyama, K. Mishima, I. Saito, H. Okano, and N. Mizushima. 2006. Suppression of basal autophagy in neural cells causes neurodegenerative disease in mice. *Nature*. 441:885-889.

Hart, M.J., Y. Maru, D. Leonard, O.N. Witte, T. Evans, and R.A. Cerione. 1992. A GDP dissociation inhibitor that serves as a GTPase inhibitor for the Ras-like protein CDC42Hs. *Science*. 258:812-815.

Haugh, J.M., F. Codazzi, M. Teruel, and T. Meyer. 2000. Spatial sensing in fibroblasts mediated by 3' phosphoinositides. *J Cell Biol*. 151:1269-1280.

Hoeller, O., and R.R. Kay. 2007. Chemotaxis in the absence of PIP3 gradients. *Curr Biol*. 17:813-817.

Hoffman, G.R., N. Nassar, and R.A. Cerione. 2000. Structure of the Rho family GTP-binding protein Cdc42 in complex with the multifunctional regulator RhoGDI. *Cell*. 100:345-356.

Holmes, K.C., D. Popp, W. Gebhard, and W. Kabsch. 1990. Atomic model of the actin filament. *Nature*. 347:44-49.

Holt, M.R., and A. Koffer. 2001. Cell motility: proline-rich proteins promote protrusions. *Trends Cell Biol*. 11:38-46.

Houk, A.R., A. Jilkine, C.O. Mejean, R. Boltyanskiy, E.R. Dufresne, S.B. Angenent, S.J. Altschuler, L.F. Wu, and O.D. Weiner. 2012. Membrane tension maintains cell polarity by confining signals to the leading edge during neutrophil migration. *Cell*. 148:175-188.

Huss, M.J. 1989. Dispersal of Cellular Slime Molds by Two Soil Invertebrates. *Mycologia*. 81:677-682.

Ichimura, Y., T. Kumanomidou, Y.S. Sou, T. Mizushima, J. Ezaki, T. Ueno, E. Kominami, T. Yamane, K. Tanaka, and M. Komatsu. 2008. Structural basis for sorting mechanism of p62 in selective autophagy. *J Biol Chem*. 283:22847-22857.

Insall, R.H., and O.D. Weiner. 2001. PIP3, PIP2, and cell movement--similar messages, different meanings? *Dev Cell*. 1:743-747.

Itoh, R.E., K. Kurokawa, Y. Ohba, H. Yoshizaki, N. Mochizuki, and M. Matsuda. 2002. Activation of rac and cdc42 video imaged by fluorescent resonance energy transfer-based single-molecule probes in the membrane of living cells. *Mol Cell Biol*. 22:6582-6591.

Jantsch-Plunger, V., P. Gonczy, A. Romano, H. Schnabel, D. Hamill, R. Schnabel, A.A. Hyman, and M. Glotzer. 2000. CYK-4: A Rho family gtpase activating protein (GAP) required for central spindle formation and cytokinesis. *J Cell Biol*. 149:1391-1404.

Jia, D., T.S. Gomez, Z. Metlagel, J. Umetani, Z. Otwinowski, M.K. Rosen, and D.D. Billadeau. 2010. WASH and WAVE actin regulators of the Wiskott-Aldrich syndrome protein (WASP) family are controlled by analogous structurally related complexes. *Proc Natl Acad Sci U S A*. 107:10442-10447.

Johansen, T., and T. Lamark. 2011. Selective autophagy mediated by autophagic adapter proteins. *Autophagy*. 7:279-296.

Jones, L.J., R. Carballido-Lopez, and J. Errington. 2001. Control of cell shape in bacteria: helical, actin-like filaments in Bacillus subtilis. *Cell*. 104:913-922.

Jones, R.A., Y. Feng, A.J. Worth, A.J. Thrasher, S.O. Burns, and P. Martin. 2013. Modelling of human Wiskott-Aldrich syndrome protein mutants in zebrafish larvae using in vivo live imaging. *J Cell Sci*. 126:4077-4084.

Jost, M., F. Simpson, J.M. Kavran, M.A. Lemmon, and S.L. Schmid. 1998. Phosphatidylinositol-4,5-bisphosphate is required for endocytic coated vesicle formation. *Curr Biol*. 8:1399-1402.

Kabeya, Y., N. Mizushima, T. Ueno, A. Yamamoto, T. Kirisako, T. Noda, E. Kominami, Y. Ohsumi, and T. Yoshimori. 2000. LC3, a mammalian homologue of yeast Apg8p, is localized in autophagosome membranes after processing. *EMBO J*. 19:5720-5728.

Kabsch, W., H.G. Mannherz, D. Suck, E.F. Pai, and K.C. Holmes. 1990. Atomic structure of the actin:DNase I complex. *Nature*. 347:37-44.

Kaksonen, M., Y. Sun, and D.G. Drubin. 2003. A pathway for association of receptors, adaptors, and actin during endocytic internalization. *Cell*. 115:475-487.

Kanki, T., K. Wang, Y. Cao, M. Baba, and D.J. Klionsky. 2009. Atg32 is a mitochondrial protein that confers selectivity during mitophagy. *Dev Cell*. 17:98-109.

Kasai, M., S. Asakura, and F. Oosawa. 1962. The G-F equilibrium in actin solutions under various conditions. *Biochim Biophys Acta*. 57:13-21.

Kast, D.J., and R. Dominguez. 2017. The Cytoskeleton-Autophagy Connection. *Curr Biol*. 27:R318-R326.

Kast, D.J., A.L. Zajac, E.L. Holzbaur, E.M. Ostap, and R. Dominguez. 2015. WHAMM Directs the Arp2/3 Complex to the ER for Autophagosome Biogenesis through an Actin Comet Tail Mechanism. *Curr Biol*. 25:1791-1797.

Katayama, M., M. Kawata, Y. Yoshida, H. Horiuchi, T. Yamamoto, Y. Matsuura, and Y. Takai. 1991. The posttranslationally modified C-terminal structure of bovine aortic smooth muscle rhoA p21. *J Biol Chem*. 266:12639-12645.

Kessin, R.H., G.G. Gundersen, V. Zaydfudim, M. Grimson, and R.L. Blanton. 1996. How cellular slime molds evade nematodes. *Proc Natl Acad Sci U S A*. 93:4857-4861.

Kim, A.S., L.T. Kakalis, N. Abdul-Manan, G.A. Liu, and M.K. Rosen. 2000. Autoinhibition and activation mechanisms of the Wiskott-Aldrich syndrome protein. *Nature*. 404:151-158.

King, J.S., A. Gueho, M. Hagedorn, N. Gopaldass, F. Leuba, T. Soldati, and R.H. Insall. 2013. WASH is required for lysosomal recycling and efficient autophagic and phagocytic digestion. *Mol Biol Cell*. 24:2714-2726.

King, J.S., D.M. Veltman, and R.H. Insall. 2011. The induction of autophagy by mechanical stress. *Autophagy*. 7:1490-1499.

Kircher, P., C. Hermanns, M. Nossek, M.K. Drexler, R. Grosse, M. Fischer, A. Sarikas, J. Penkava, T. Lewis, R. Prywes, T. Gudermann, and S. Muehlich. 2015. Filamin A interacts with the coactivator MKL1 to promote the activity of the transcription factor SRF and cell migration. *Sci Signal*. 8:ra112.

Kirkin, V., T. Lamark, Y.S. Sou, G. Bjorkoy, J.L. Nunn, J.A. Bruun, E. Shvets, D.G. McEwan, T.H. Clausen, P. Wild, I. Bilusic, J.P. Theurillat, A. Overvatn, T. Ishii, Z. Elazar, M. Komatsu, I. Dikic, and T. Johansen. 2009. A role for NBR1 in autophagosomal degradation of ubiquitinated substrates. *Mol Cell*. 33:505-516.

Klebe, C., H. Prinz, A. Wittinghofer, and R.S. Goody. 1995. The kinetic mechanism of Ran--nucleotide exchange catalyzed by RCC1. *Biochemistry*. 34:12543-12552.

Kochubey, O., A. Majumdar, and J. Klingauf. 2006. Imaging clathrin dynamics in Drosophila melanogaster hemocytes reveals a role for actin in vesicle fission. *Traffic*. 7:1614-1627.

Kollmar, M., D. Lbik, and S. Enge. 2012. Evolution of the eukaryotic ARP2/3 activators of the WASP family: WASP, WAVE, WASH, and WHAMM, and the proposed new family members WAWH and WAML. *BMC Res Notes*. 5:88.

Komatsu, M., S. Waguri, T. Ueno, J. Iwata, S. Murata, I. Tanida, J. Ezaki, N. Mizushima, Y. Ohsumi, Y. Uchiyama, E. Kominami, K. Tanaka, and T. Chiba. 2005. Impairment of starvation-induced and constitutive autophagy in Atg7-deficient mice. *J Cell Biol*. 169:425-434.

Kopitz, J., G.O. Kisen, P.B. Gordon, P. Bohley, and P.O. Seglen. 1990. Nonselective autophagy of cytosolic enzymes by isolated rat hepatocytes. *J Cell Biol*. 111:941-953.

Kuma, A., M. Matsui, and N. Mizushima. 2007. LC3, an autophagosome marker, can be incorporated into protein aggregates independent of autophagy: caution in the interpretation of LC3 localization. *Autophagy*. 3:323-328.

Kunda, P., G. Craig, V. Dominguez, and B. Baum. 2003. Abi, Sra1, and Kette control the stability and localization of SCAR/WAVE to regulate the formation of actin-based protrusions. *Curr Biol*. 13:1867-1875.

Kupfer, A., D. Louvard, and S.J. Singer. 1982. Polarization of the Golgi apparatus and the microtubule-organizing center in cultured fibroblasts at the edge of an experimental wound. *Proc Natl Acad Sci U S A*. 79:2603-2607.

Kwon, T., D.Y. Kwon, J. Chun, J.H. Kim, and S.S. Kang. 2000. Akt protein kinase inhibits Rac1-GTP binding through phosphorylation at serine 71 of Rac1. *J Biol Chem*. 275:423-428.

Laevsky, G., and D.A. Knecht. 2001. Under-agarose folate chemotaxis of Dictyostelium discoideum amoebae in permissive and mechanically inhibited conditions. *Biotechniques*. 31:1140-1142, 1144, 1146-1149.

Lamaze, C., T.H. Chuang, L.J. Terlecky, G.M. Bokoch, and S.L. Schmid. 1996. Regulation of receptor-mediated endocytosis by Rho and Rac. *Nature*. 382:177-179.

Lammers, M., S. Meyer, D. Kuhlmann, and A. Wittinghofer. 2008. Specificity of interactions between mDia isoforms and Rho proteins. *J Biol Chem*. 283:35236-35246.

Lebensohn, A.M., and M.W. Kirschner. 2009. Activation of the WAVE complex by coincident signals controls actin assembly. *Mol Cell*. 36:512-524.

Lee, E., and D.A. Knecht. 2002. Visualization of actin dynamics during macropinocytosis and exocytosis. *Traffic*. 3:186-192.

Lee, S., J.W. Han, L. Leeper, J.S. Gruver, and C.Y. Chung. 2009. Regulation of the formation and trafficking of vesicles from Golgi by PCH family proteins during chemotaxis. *Biochim Biophys Acta*. 1793:1199-1209.

Lenzen, C., R.H. Cool, H. Prinz, J. Kuhlmann, and A. Wittinghofer. 1998. Kinetic analysis by fluorescence of the interaction between Ras and the catalytic domain of the guanine nucleotide exchange factor Cdc25Mm. *Biochemistry*. 37:7420-7430.

Leonard, D., M.J. Hart, J.V. Platko, A. Eva, W. Henzel, T. Evans, and R.A. Cerione. 1992. The identification and characterization of a GDP-dissociation inhibitor (GDI) for the CDC42Hs protein. *J Biol Chem*. 267:22860-22868.

Lewis, A.K., and P.C. Bridgman. 1992. Nerve growth cone lamellipodia contain two populations of actin filaments that differ in organization and polarity. *J Cell Biol*. 119:1219-1243.

Li, A., Y. Ma, X. Yu, R.L. Mort, C.R. Lindsay, D. Stevenson, D. Strathdee, R.H. Insall, J. Chernoff, S.B. Snapper, I.J. Jackson, L. Larue, O.J. Sansom, and L.M. Machesky. 2011. Rac1 drives melanoblast organization during mouse development by orchestrating pseudopod- driven motility and cell-cycle progression. *Dev Cell*. 21:722-734.

Li, F., and H.N. Higgs. 2003. The mouse Formin mDia1 is a potent actin nucleation factor regulated by autoinhibition. *Curr Biol*. 13:1335-1340.

Li, Z., M. Hannigan, Z. Mo, B. Liu, W. Lu, Y. Wu, A.V. Smrcka, G. Wu, L. Li, M. Liu, C.K. Huang, and D. Wu. 2003. Directional sensing requires G beta gamma-mediated PAK1 and PIX alpha-dependent activation of Cdc42. *Cell*. 114:215-227.

Linardopoulou, E.V., S.S. Parghi, C. Friedman, G.E. Osborn, S.M. Parkhurst, and B.J. Trask. 2007. Human subtelomeric WASH genes encode a new subclass of the WASP family. *PLoS Genet*. 3:e237.

Loomis, W.F., and D.W. Smith. 1990. Molecular phylogeny of Dictyostelium discoideum by protein sequence comparison. *Proc Natl Acad Sci U S A*. 87:9093-9097.

Lorenz, M., H. Yamaguchi, Y. Wang, R.H. Singer, and J. Condeelis. 2004. Imaging sites of N-wasp activity in lamellipodia and invadopodia of carcinoma cells. *Curr Biol*. 14:697-703.

Machesky, L.M., S.J. Atkinson, C. Ampe, J. Vandekerckhove, and T.D. Pollard. 1994. Purification of a cortical complex containing two unconventional actins from Acanthamoeba by affinity chromatography on profilin-agarose. *J Cell Biol*. 127:107-115.

Machesky, L.M., and R.H. Insall. 1998. Scar1 and the related Wiskott-Aldrich syndrome protein, WASP, regulate the actin cytoskeleton through the Arp2/3 complex. *Curr Biol*. 8:1347-1356.

Macro, L., J.K. Jaiswal, and S.M. Simon. 2012. Dynamics of clathrin-mediated endocytosis and its requirement for organelle biogenesis in Dictyostelium. *J Cell Sci*. 125:5721-5732.

Madania, A., P. Dumoulin, S. Grava, H. Kitamoto, C. Scharer-Brodbeck, A. Soulard, V. Moreau, and B. Winsor. 1999. The Saccharomyces cerevisiae homologue of human Wiskott-Aldrich syndrome protein Las17p interacts with the Arp2/3 complex. *Mol Biol Cell*. 10:3521-3538.

Madaule, P., and R. Axel. 1985. A novel ras-related gene family. *Cell*. 41:31-40.

Malecz, N., P.C. McCabe, C. Spaargaren, R. Qiu, Y. Chuang, and M. Symons. 2000. Synaptojanin 2, a novel Rac1 effector that regulates clathrin-mediated endocytosis. *Curr Biol*. 10:1383-1386.

Marchand, J.B., D.A. Kaiser, T.D. Pollard, and H.N. Higgs. 2001. Interaction of WASP/Scar proteins with actin and vertebrate Arp2/3 complex. *Nat Cell Biol*. 3:76-82.

Mari, M., J. Griffith, E. Rieter, L. Krishnappa, D.J. Klionsky, and F. Reggiori. 2010. An Atg9-containing compartment that functions in the early steps of autophagosome biogenesis. *J Cell Biol*. 190:1005-1022.

McCarrol, R., G.J. Olsen, Y.D. Stahl, C.R. Woese, and M.L. Sogin. 1983. Nucleotide Sequence of the Dictyostelium discoideum Small-Subunit Ribosomal Ribonucleic Acid Inferred from the Gene Sequence: Evolutionary Implications. *Biochemistry*. 22:5858-5868.

Meijering, E., O. Dzyubachyk, and I. Smal. 2012. Methods for cell and particle tracking. *Methods Enzymol*. 504:183-200.

Meijerman, I., W.M. Blom, H.J. de Bont, G.J. Mulder, and J.F. Nagelkerke. 1999. Changes of G-actin localisation in the mitotic spindle region or nucleus during mitosis and after heat shock: a histochemical study of G-actin in various cell lines with fluorescent labelled vitamin D-binding protein. *Biochim Biophys Acta*. 1452:12-24.

Meili, R., C. Ellsworth, S. Lee, T.B. Reddy, H. Ma, and R.A. Firtel. 1999. Chemoattractant-mediated transient activation and membrane localization of Akt/PKB is required for efficient chemotaxis to cAMP in Dictyostelium. *EMBO J*. 18:2092-2105.

Melendez, A., Z. Talloczy, M. Seaman, E.L. Eskelinen, D.H. Hall, and B. Levine. 2003. Autophagy genes are essential for dauer development and life-span extension in C. elegans. *Science*. 301:1387-1391.

Merrifield, C.J., M.E. Feldman, L. Wan, and W. Almers. 2002. Imaging actin and dynamin recruitment during invagination of single clathrin-coated pits. *Nat Cell Biol*. 4:691-698.

Merrifield, C.J., B. Qualmann, M.M. Kessels, and W. Almers. 2004. Neural Wiskott Aldrich Syndrome Protein (N-WASP) and the Arp2/3 complex are recruited to sites of clathrin-mediated endocytosis in cultured fibroblasts. *Eur J Cell Biol*. 83:13-18.

Michaelson, D., J. Silletti, G. Murphy, P. D'Eustachio, M. Rush, and M.R. Philips. 2001. Differential localization of Rho GTPases in live cells: regulation by hypervariable regions and RhoGDI binding. *J Cell Biol*. 152:111-126.

Michiels, F., G.G. Habets, J.C. Stam, R.A. van der Kammen, and J.G. Collard. 1995. A role for Rac in Tiam1-induced membrane ruffling and invasion. *Nature*. 375:338-340.

Miki, H., K. Miura, and T. Takenawa. 1996. N-WASP, a novel actin-depolymerizing protein, regulates the cortical cytoskeletal rearrangement in a PIP2-dependent manner downstream of tyrosine kinases. *EMBO J*. 15:5326-5335.

Miki, H., T. Sasaki, Y. Takai, and T. Takenawa. 1998a. Induction of filopodium formation by a WASP-related actin-depolymerizing protein N-WASP. *Nature*. 391:93-96.

Miki, H., S. Suetsugu, and T. Takenawa. 1998b. WAVE, a novel WASP-family protein involved in actin reorganization induced by Rac. *EMBO J*. 17:6932-6941.

Milburn, M.V., L. Tong, A.M. deVos, A. Brunger, Z. Yamaizumi, S. Nishimura, and S.H. Kim. 1990. Molecular switch for signal transduction: structural differences between active and inactive forms of protooncogenic ras proteins. *Science*. 247:939-945.

Miralles, F., G. Posern, A.I. Zaromytidou, and R. Treisman. 2003. Actin dynamics control SRF activity by regulation of its coactivator MAL. *Cell*. 113:329-342.

Missy, K., V. Van Poucke, P. Raynal, C. Viala, G. Mauco, M. Plantavid, H. Chap, and B. Payrastre. 1998. Lipid products of phosphoinositide 3-kinase interact with Rac1 GTPase and stimulate GDP dissociation. *J Biol Chem*. 273:30279-30286.

Mizutani, K., H. Miki, H. He, H. Maruta, and T. Takenawa. 2002. Essential role of neural Wiskott-Aldrich syndrome protein in podosome formation and degradation of extracellular matrix in src-transformed fibroblasts. *Cancer Res*. 62:669-674.

Moissoglu, K., B.M. Slepchenko, N. Meller, A.F. Horwitz, and M.A. Schwartz. 2006. In vivo dynamics of Rac-membrane interactions. *Mol Biol Cell*. 17:2770-2779.

Monastyrska, I., C. He, J. Geng, A.D. Hoppe, Z. Li, and D.J. Klionsky. 2008. Arp2 links autophagic machinery with the actin cytoskeleton. *Mol Biol Cell*. 19:1962-1975.

Moreau, V., F. Frischknecht, I. Reckmann, R. Vincentelli, G. Rabut, D. Stewart, and M. Way. 2000. A complex of N-WASP and WIP integrates signalling cascades that lead to actin polymerization. *Nat Cell Biol*. 2:441-448.

Muinonen-Martin, A.J., O. Susanto, Q. Zhang, E. Smethurst, W.J. Faller, D.M. Veltman, G. Kalna, C. Lindsay, D.C. Bennett, O.J. Sansom, R. Herd, R. Jones, L.M. Machesky, M.J. Wakelam, D.A. Knecht, and R.H. Insall. 2014. Melanoma cells break down LPA to establish local gradients that drive chemotactic dispersal. *PLoS Biol*. 12:e1001966.

Mullins, R.D., J.A. Heuser, and T.D. Pollard. 1998. The interaction of Arp2/3 complex with actin: nucleation, high affinity pointed end capping, and formation of branching networks of filaments. *Proc Natl Acad Sci U S A*. 95:6181-6186.

Myers, S.A., J.W. Han, Y. Lee, R.A. Firtel, and C.Y. Chung. 2005. A Dictyostelium homologue of WASP is required for polarized F-actin assembly during chemotaxis. *Mol Biol Cell*. 16:2191-2206.

Myers, S.A., L.R. Leeper, and C.Y. Chung. 2006. WASP-interacting protein is important for actin filament elongation and prompt pseudopod formation in response to a dynamic chemoattractant gradient. *Mol Biol Cell*. 17:4564-4575.

Nagasaki, A., E.L. de Hostos, and T.Q. Uyeda. 2002. Genetic and morphological evidence for two parallel pathways of cell-cycle-coupled cytokinesis in Dictyostelium. *J Cell Sci*. 115:2241-2251.

Nassar, N., G.R. Hoffman, D. Manor, J.C. Clardy, and R.A. Cerione. 1998. Structures of Cdc42 bound to the active and catalytically compromised forms of Cdc42GAP. *Nat Struct Biol*. 5:1047-1052.

Navarro-Lerida, I., S. Sanchez-Perales, M. Calvo, C. Rentero, Y. Zheng, C. Enrich, and M.A. Del Pozo. 2012. A palmitoylation switch mechanism regulates Rac1 function and membrane organization. *EMBO J*. 31:534-551.

Niswonger, M.L., and T.J. O'Halloran. 1997. Clathrin heavy chain is required for spore cell but not stalk cell differentiation in Dictyostelium discoideum. *Development*. 124:443-451.

Nobes, C.D., and A. Hall. 1999. Rho GTPases control polarity, protrusion, and adhesion during cell movement. *J Cell Biol*. 144:1235-1244.

Noda, N.N., Y. Ohsumi, and F. Inagaki. 2010. Atg8-family interacting motif crucial for selective autophagy. *FEBS Lett*. 584:1379-1385.

Nolan, K.M., K. Barrett, Y. Lu, K.Q. Hu, S. Vincent, and J. Settleman. 1998. Myoblast city, the Drosophila homolog of DOCK180/CED-5, is required in a Rac signaling pathway utilized for multiple developmental processes. *Genes Dev*. 12:3337-3342.

Nomanbhoy, T.K., J.W. Erickson, and R.A. Cerione. 1999. Kinetics of Cdc42 membrane extraction by Rho-GDI monitored by real-time fluorescence resonance energy transfer. *Biochemistry*. 38:1744-1750.

Oberoi, T.K., T. Dogan, J.C. Hocking, R.P. Scholz, J. Mooz, C.L. Anderson, C. Karreman, D. Meyer zu Heringdorf, G. Schmidt, M. Ruonala, K. Namikawa, G.S. Harms, A. Carpy, B. Macek, R.W. Koster, and K. Rajalingam. 2012. IAPs regulate the plasticity of cell migration by directly targeting Rac1 for degradation. *EMBO J*. 31:14-28.

Okamoto, K., N. Kondo-Okamoto, and Y. Ohsumi. 2009. Mitochondria-anchored receptor Atg32 mediates degradation of mitochondria via selective autophagy. *Dev Cell*. 17:87-97.

Okrut, J., S. Prakash, Q. Wu, M.J. Kelly, and J. Taunton. 2015. Allosteric N-WASP activation by an inter-SH3 domain linker in Nck. *Proc Natl Acad Sci U S A*. 112:E6436-6445.

Onesto, C., A. Shutes, V. Picard, F. Schweighoffer, and C.J. Der. 2008. Characterization of EHT 1864, a novel small molecule inhibitor of Rac family small GTPases. *Methods Enzymol*. 439:111-129.

Onodera, J., and Y. Ohsumi. 2005. Autophagy is required for maintenance of amino acid levels and protein synthesis under nitrogen starvation. *J Biol Chem*. 280:31582-31586.

Otto, G.P., M.Y. Wu, N. Kazgan, O.R. Anderson, and R.H. Kessin. 2004. Dictyostelium macroautophagy mutants vary in the severity of their developmental defects. *J Biol Chem*. 279:15621-15629.

Pai, E.F., U. Krengel, G.A. Petsko, R.S. Goody, W. Kabsch, and A. Wittinghofer. 1990. Refined crystal structure of the triphosphate conformation of H-ras p21 at 1.35 A resolution: implications for the mechanism of GTP hydrolysis. *EMBO J*. 9:2351-2359.

Palamidessi, A., E. Frittoli, M. Garre, M. Faretta, M. Mione, I. Testa, A. Diaspro, L. Lanzetti, G. Scita, and P.P. Di Fiore. 2008. Endocytic trafficking of Rac is required for the spatial restriction of signaling in cell migration. *Cell*. 134:135-147.

Palazzo, A.F., H.L. Joseph, Y.J. Chen, D.L. Dujardin, A.S. Alberts, K.K. Pfister, R.B. Vallee, and G.G. Gundersen. 2001. Cdc42, dynein, and dynactin regulate MTOC reorientation independent of Rho-regulated microtubule stabilization. *Curr Biol*. 11:1536-1541.

Pan, P., E.M. Hall, and J.T. Bonner. 1972. Folic acid as second chemotactic substance in the cellular slime moulds. *Nat New Biol*. 237:181-182.

Pankiv, S., T.H. Clausen, T. Lamark, A. Brech, J.A. Bruun, H. Outzen, A. Overvatn, G. Bjorkoy, and T. Johansen. 2007. p62/SQSTM1 binds directly to Atg8/LC3 to facilitate degradation of ubiquitinated protein aggregates by autophagy. *J Biol Chem*. 282:24131-24145.

Papayannopoulos, V., C. Co, K.E. Prehoda, S. Snapper, J. Taunton, and W.A. Lim. 2005. A polybasic motif allows N-WASP to act as a sensor of PIP(2) density. *Mol Cell*. 17:181-191.

Parent, C.A., B.J. Blacklock, W.M. Froehlich, D.B. Murphy, and P.N. Devreotes. 1998. G protein signaling events are activated at the leading edge of chemotactic cells. *Cell*. 95:81-91.

Pawlowski, R., E.K. Rajakyla, M.K. Vartiainen, and R. Treisman. 2010. An actin-regulated importin alpha/beta-dependent extended bipartite NLS directs nuclear import of MRTF-A. *EMBO J*. 29:3448-3458.

Pelkmans, L., D. Puntener, and A. Helenius. 2002. Local actin polymerization and dynamin recruitment in SV40-induced internalization of caveolae. *Science*. 296:535-539.

Pellegrin, S., and H. Mellor. 2005. The Rho family GTPase Rif induces filopodia through mDia2. *Curr Biol*. 15:129-133.

Pirone, D.M., D.E. Carter, and P.D. Burbelo. 2001. Evolutionary expansion of CRIB-containing Cdc42 effector proteins. *Trends Genet*. 17:370-373.

Pollard, T.D. 1986. Rate constants for the reactions of ATP- and ADP-actin with the ends of actin filaments. *J Cell Biol*. 103:2747-2754.

Pollard, T.D., and M.S. Mooseker. 1981. Direct measurement of actin polymerization rate constants by electron microscopy of actin filaments nucleated by isolated microvillus cores. *J Cell Biol*. 88:654-659.

Polson, H.E., J. de Lartigue, D.J. Rigden, M. Reedijk, S. Urbe, M.J. Clague, and S.A. Tooze. 2010. Mammalian Atg18 (WIPI2) localizes to omegasome-anchored phagophores and positively regulates LC3 lipidation. *Autophagy*. 6:506-522.

Prehoda, K.E., J.A. Scott, R.D. Mullins, and W.A. Lim. 2000. Integration of multiple signals through cooperative regulation of the N-WASP-Arp2/3 complex. *Science*. 290:801-806.

Pring, M., M. Evangelista, C. Boone, C. Yang, and S.H. Zigmond. 2003. Mechanism of formin-induced nucleation of actin filaments. *Biochemistry*. 42:486-496.

Qualmann, B., and M.M. Kessels. 2009. New players in actin polymerization--WH2-domain-containing actin nucleators. *Trends Cell Biol*. 19:276-285.

Qualmann, B., J. Roos, P.J. DiGregorio, and R.B. Kelly. 1999. Syndapin I, a synaptic dynamin-binding protein that associates with the neural Wiskott-Aldrich syndrome protein. *Mol Biol Cell*. 10:501-513.

Raper, K.B. 1935. DICTYOSTELIUM DISCOIDEUM, A NEW SPECIES OF SLIME MOLD FROM DECAYING FOREST LEAVES. *Journal of Agricultural Research*. VO:135-147.

Raper, K.B. 1940. The Communal Nature of the Fruiting Process in the Acrasieae. *American Journal of Botany*. 27:436-448.

Raper, K.B., and N. Smith. 1939. The growth of Dictyostelium discoideum upon pathogenic bacteria. *Journal of bacteriology*. 38:431-445.

Ravikumar, B., K. Moreau, L. Jahreiss, C. Puri, and D.C. Rubinsztein. 2010. Plasma membrane contributes to the formation of pre-autophagosomal structures. *Nat Cell Biol*. 12:747-757.

Ridley, A.J., H.F. Paterson, C.L. Johnston, D. Diekmann, and A. Hall. 1992. The small GTP-binding protein rac regulates growth factor-induced membrane ruffling. *Cell*. 70:401-410.

Riedl, J., A.H. Crevenna, K. Kessenbrock, J.H. Yu, D. Neukirchen, M. Bista, F. Bradke, D. Jenne, T.A. Holak, Z. Werb, M. Sixt, and R. Wedlich-Soldner. 2008. Lifeact: a versatile marker to visualize F-actin. *Nat Methods*. 5:605-607.

Rivero, F., H. Dislich, G. Glockner, and A.A. Noegel. 2001. The Dictyostelium discoideum family of Rho-related proteins. *Nucleic Acids Res*. 29:1068-1079.

Robinson, M.S. 2015. Forty Years of Clathrin-coated Vesicles. *Traffic*. 16:1210-1238.

Robinson, R.C., K. Turbedsky, D.A. Kaiser, J.B. Marchand, H.N. Higgs, S. Choe, and T.D. Pollard. 2001. Crystal structure of Arp2/3 complex. *Science*. 294:1679-1684.

Rodal, A.A., O. Sokolova, D.B. Robins, K.M. Daugherty, S. Hippenmeyer, H. Riezman, N. Grigorieff, and B.L. Goode. 2005. Conformational changes in the Arp2/3 complex leading to actin nucleation. *Nat Struct Mol Biol*. 12:26-31.

Rohatgi, R., L. Ma, H. Miki, M. Lopez, T. Kirchhausen, T. Takenawa, and M.W. Kirschner. 1999. The interaction between N-WASP and the Arp2/3 complex links Cdc42-dependent signals to actin assembly. *Cell*. 97:221-231.

Rohatgi, R., P. Nollau, H.Y. Ho, M.W. Kirschner, and B.J. Mayer. 2001. Nck and phosphatidylinositol 4,5-bisphosphate synergistically activate actin polymerization through the N-WASP-Arp2/3 pathway. *J Biol Chem*. 276:26448-26452.

Rohr, G., and H.G. Mannherz. 1978. Isolation and characterization of secretory actin . DNAase I complex from rat pancreatic juice. *Eur J Biochem*. 89:151-157.

Sander, E.E., J.P. ten Klooster, S. van Delft, R.A. van der Kammen, and J.G. Collard. 1999. Rac downregulates Rho activity: reciprocal balance between both GTPases determines cellular morphology and migratory behavior. *J Cell Biol*. 147:1009-1022.

Schaefer, A., N.R. Reinhard, and P.L. Hordijk. 2014. Toward understanding RhoGTPase specificity: structure, function and local activation. *Small GTPases*. 5:6.

Schell, C., L. Baumhakl, S. Salou, A.C. Conzelmann, C. Meyer, M. Helmstadter, C. Wrede, F. Grahammer, S. Eimer, D. Kerjaschki, G. Walz, S. Snapper, and T.B. Huber. 2013. N-wasp is required for stabilization of podocyte foot processes. *J Am Soc Nephrol*. 24:713-721.

Schindelin, J., I. Arganda-Carreras, E. Frise, V. Kaynig, M. Longair, T. Pietzsch, S. Preibisch, C. Rueden, S. Saalfeld, B. Schmid, J.Y. Tinevez, D.J. White, V. Hartenstein, K. Eliceiri, P. Tomancak, and A. Cardona. 2012. Fiji: an open-source platform for biological-image analysis. *Nat Methods*. 9:676-682.

Schirenbeck, A., T. Bretschneider, R. Arasada, M. Schleicher, and J. Faix. 2005. The Diaphanous-related formin dDia2 is required for the formation and maintenance of filopodia. *Nat Cell Biol*. 7:619-625.

Servant, G., O.D. Weiner, P. Herzmark, T. Balla, J.W. Sedat, and H.R. Bourne. 2000. Polarization of chemoattractant receptor signaling during neutrophil chemotaxis. *Science*. 287:1037-1040.

Shikama, N., C.W. Lee, S. France, L. Delavaine, J. Lyon, M. Krstic-Demonacos, and N.B. La Thangue. 1999. A novel cofactor for p300 that regulates the p53 response. *Mol Cell*. 4:365-376.

Shintani, T., and D.J. Klionsky. 2004. Cargo proteins facilitate the formation of transport vesicles in the cytoplasm to vacuole targeting pathway. *J Biol Chem*. 279:29889-29894.

Snapper, S.B., F. Takeshima, I. Anton, C.H. Liu, S.M. Thomas, D. Nguyen, D. Dudley, H. Fraser, D. Purich, M. Lopez-Ilasaca, C. Klein, L. Davidson, R. Bronson, R.C. Mulligan, F. Southwick, R. Geha, M.B. Goldberg, F.S. Rosen, J.H. Hartwig, and F.W. Alt. 2001. N-WASP deficiency reveals distinct pathways for cell surface projections and microbial actin-based motility. *Nat Cell Biol*. 3:897-904.

Srinivasan, S., F. Wang, S. Glavas, A. Ott, F. Hofmann, K. Aktories, D. Kalman, and H.R. Bourne. 2003. Rac and Cdc42 play distinct roles in regulating PI(3,4,5)P3 and polarity during neutrophil chemotaxis. *J Cell Biol*. 160:375-385.

Steffen, A., M. Ladwein, G.A. Dimchev, A. Hein, L. Schwenkmezger, S. Arens, K.I. Ladwein, J. Margit Holleboom, F. Schur, J. Victor Small, J. Schwarz, R. Gerhard, J. Faix, T.E. Stradal, C. Brakebusch, and K. Rottner. 2013. Rac function is crucial for cell migration but is not required for spreading and focal adhesion formation. *J Cell Sci*. 126:4572-4588.

Suetsugu, S., M. Hattori, H. Miki, T. Tezuka, T. Yamamoto, K. Mikoshiba, and T. Takenawa. 2002. Sustained activation of N-WASP through phosphorylation is essential for neurite extension. *Dev Cell*. 3:645-658.

Suetsugu, S., and T. Takenawa. 2003. Translocation of N-WASP by nuclear localization and export signals into the nucleus modulates expression of HSP90. *J Biol Chem*. 278:42515-42523.

Suthers, H.B. 1985. Ground-feeding migratory songbirds as cellular slime mold distribution vectors. *Oecologia*. 65:526-530.

Swanson, J.A., M.T. Johnson, K. Beningo, P. Post, M. Mooseker, and N. Araki. 1999. A contractile activity that closes phagosomes in macrophages. *J Cell Sci*. 112 (Pt 3):307-316.

Takeshige, K., M. Baba, S. Tsuboi, T. Noda, and Y. Ohsumi. 1992. Autophagy in yeast demonstrated with proteinase-deficient mutants and conditions for its induction. *J Cell Biol*. 119:301-311.

Tal, T., D. Vaizel-Ohayon, and E.D. Schejter. 2002. Conserved interactions with cytoskeletal but not signaling elements are an essential aspect of Drosophila WASp function. *Dev Biol*. 243:260-271.

Tang, H., A. Li, J. Bi, D.M. Veltman, T. Zech, H.J. Spence, X. Yu, P. Timpson, R.H. Insall, M.C. Frame, and L.M. Machesky. 2013. Loss of Scar/WAVE complex promotes N-WASP- and FAK-dependent invasion. *Curr Biol*. 23:107-117.

Taunton, J., B.A. Rowning, M.L. Coughlin, M. Wu, R.T. Moon, T.J. Mitchison, and C.A. Larabell. 2000. Actin-dependent propulsion of endosomes and lysosomes by recruitment of N-WASP. *J Cell Biol*. 148:519-530.

Tomasevic, N., Z. Jia, A. Russell, T. Fujii, J.J. Hartman, S. Clancy, M. Wang, C. Beraud, K.W. Wood, and R. Sakowicz. 2007. Differential regulation of WASP and N-WASP by Cdc42, Rac1, Nck, and PI(4,5)P2. *Biochemistry*. 46:3494-3502.

Torres, E., and M.K. Rosen. 2006. Protein-tyrosine kinase and GTPase signals cooperate to phosphorylate and activate Wiskott-Aldrich syndrome protein (WASP)/neuronal WASP. *J Biol Chem*. 281:3513-3520.

Tweedy, L., D.A. Knecht, G.M. Mackay, and R.H. Insall. 2016. Self-Generated Chemoattractant Gradients: Attractant Depletion Extends the Range and Robustness of Chemotaxis. *PLoS Biol*. 14:e1002404.

van den Ent, F., L.A. Amos, and J. Lowe. 2001. Prokaryotic origin of the actin cytoskeleton. *Nature*. 413:39-44.

Veltman, D.M., G. Akar, L. Bosgraaf, and P.J. Van Haastert. 2009a. A new set of small, extrachromosomal expression vectors for Dictyostelium discoideum. *Plasmid*. 61:110-118.

Veltman, D.M., G. Auciello, H.J. Spence, L.M. Machesky, J.Z. Rappoport, and R.H. Insall. 2011. Functional analysis of Dictyostelium IBARa reveals a conserved role of the I-BAR domain in endocytosis. *Biochem J*. 436:45-52.

Veltman, D.M., and R.H. Insall. 2010. WASP family proteins: their evolution and its physiological implications. *Mol Biol Cell*. 21:2880-2893.

Veltman, D.M., I. Keizer-Gunnink, and P.J. Haastert. 2009b. An extrachromosomal, inducible expression system for Dictyostelium discoideum. *Plasmid*. 61:119-125.

Veltman, D.M., J.S. King, L.M. Machesky, and R.H. Insall. 2012. SCAR knockouts in Dictyostelium: WASP assumes SCAR's position and upstream regulators in pseudopods. *J Cell Biol*. 198:501-508.

Veltman, D.M., M.G. Lemieux, D.A. Knecht, and R.H. Insall. 2014. PIP(3)-dependent macropinocytosis is incompatible with chemotaxis. *J Cell Biol*. 204:497-505.

Wang, J., V.C. Virta, K. Riddelle-Spencer, and T.J. O'Halloran. 2003. Compromise of clathrin function and membrane association by clathrin light chain deletion. *Traffic*. 4:891-901.

Wang, P., C. Richardson, C. Hawes, and P.J. Hussey. 2016. Arabidopsis NAP1 Regulates the Formation of Autophagosomes. *Curr Biol*. 26:2060-2069.

Wegner, A. 1976. Head to tail polymerization of actin. *J Mol Biol*. 108:139-150.

Welch, H.C., W.J. Coadwell, C.D. Ellson, G.J. Ferguson, S.R. Andrews, H. Erdjument-Bromage, P. Tempst, P.T. Hawkins, and L.R. Stephens. 2002. P-Rex1, a PtdIns(3,4,5)P3- and Gbetagamma-regulated guanine-nucleotide exchange factor for Rac. *Cell*. 108:809-821.

Worthylake, D.K., K.L. Rossman, and J. Sondek. 2000. Crystal structure of Rac1 in complex with the guanine nucleotide exchange region of Tiam1. *Nature*. 408:682-688.

Worthylake, R.A., S. Lemoine, J.M. Watson, and K. Burridge. 2001. RhoA is required for monocyte tail retraction during transendothelial migration. *J Cell Biol*. 154:147-160.

Xia, P., S. Wang, Y. Du, Z. Zhao, L. Shi, L. Sun, G. Huang, B. Ye, C. Li, Z. Dai, N. Hou, X. Cheng, Q. Sun, L. Li, X. Yang, and Z. Fan. 2013. WASH inhibits autophagy through suppression of Beclin 1 ubiquitination. *EMBO J*. 32:2685-2696.

Xu, X., D.C. Barry, J. Settleman, M.A. Schwartz, and G.M. Bokoch. 1994. Differing structural requirements for GTPase-activating protein responsiveness and NADPH oxidase activation by Rac. *J Biol Chem*. 269:23569-23574.

Yamamoto, H., S. Kakuta, T.M. Watanabe, A. Kitamura, T. Sekito, C. Kondo-Kakuta, R. Ichikawa, M. Kinjo, and Y. Ohsumi. 2012. Atg9 vesicles are an important membrane source during early steps of autophagosome formation. *J Cell Biol*. 198:219-233.

Yla-Anttila, P., H. Vihinen, E. Jokitalo, and E.L. Eskelinen. 2009. 3D tomography reveals connections between the phagophore and endoplasmic reticulum. *Autophagy*. 5:1180-1185.

Yumura, S., and Y. Fukui. 1985. Reversible cyclic AMP-dependent change in distribution of myosin thick filaments in Dictyostelium. *Nature*. 314:194-196.

Zang, J.H., G. Cavet, J.H. Sabry, P. Wagner, S.L. Moores, and J.A. Spudich. 1997. On the role of myosin-II in cytokinesis: division of Dictyostelium cells under adhesive and nonadhesive conditions. *Mol Biol Cell*. 8:2617-2629.

Zeller, R., L. Jackson-Grusby, and P. Leder. 1989. The limb deformity gene is required for apical ectodermal ridge differentiation and anteroposterior limb pattern formation. *Genes Dev*. 3:1481-1492.

Zhao, J., R.K. Mialki, J. Wei, T.A. Coon, C. Zou, B.B. Chen, R.K. Mallampalli, and Y. Zhao. 2013. SCF E3 ligase F-box protein complex SCF(FBXL19) regulates cell migration by mediating Rac1 ubiquitination and degradation. *FASEB J*. 27:2611-2619.

Zhu, W.L., M.S. Hossain, D.Y. Guo, S. Liu, H. Tong, A. Khakpoor, P.J. Casey, and M. Wang. 2011. A role for Rac3 GTPase in the regulation of autophagy. *J Biol Chem*. 286:35291-35298.

Zhu, Z., Y. Chai, Y. Jiang, W. Li, H. Hu, W. Li, J.W. Wu, Z.X. Wang, S. Huang, and G. Ou. 2016. Functional Coordination of WAVE and WASP in C. elegans Neuroblast Migration. *Dev Cell*. 39:224-238.

Zuchero, J.B., A.S. Coutts, M.E. Quinlan, N.B. Thangue, and R.D. Mullins. 2009. p53-cofactor JMY is a multifunctional actin nucleation factor. *Nat Cell Biol*. 11:451-459.